A FIELD STUDY OF BEACHING BEHAVIOUR AND THE IN–SITU MOISTURE REGIME OF TAILINGS DURING ACTIVE DEPOSITION

Charles John MacRobert

A dissertation submitted to the Faculty of Engineering and the Built Environment, of the University of the Witwatersrand, in fulfilment of the requirements for the degree of Master of Science in Civil Engineering.

Johannesburg 2012

Candidate Declaration

I declare that this dissertation is my own unaided work. It is being submitted to the Degree of Masters of Science to the University of the Witwatersrand, Johannesburg. It has not been submitted before for any degree or examination to any other University. The information used in the thesis was obtained whilst under the employment of Anglo Operations Limited.

…………………………………………………………….
(Signature of Candidate)

……9…..day of……October……………………year……2012………..

Abstract

This research investigated the in-situ beaching and drying behaviour of platinum tailings in relation to proposed mechanisms described in literature and predicted from laboratory behaviour. Successive field depositions allowed the impact of finer grinds, slurry density and beach length to be investigated and compared to flume tests, indicating beach length to be a key parameter. By monitoring gravimetric water contents following deposition the quantity of water released during sedimentation showed that the beach acts as a natural "machine" thickener. After sedimentation the water content was observed to decrease, at a rate correlated with Reference Evapotranspiration, reaching a steady state condition. Field capacity values determined from laboratory experimentation and numerical modelling correlated closely with this steady state condition; restricting further moisture loss due to the relative abundance of moisture to replenish deficits. Liquidity indices demonstrated that as a result only the head of the beach dries sufficiently to impound the waste.

Synopsis

A common method to dispose tailings in semi-arid environments, such as South Africa, is to thicken the waste stream and deposit it in such a way that it self-impounds. Increased quantities of tails are being produced as a consequence of improved milling and extraction process making lower grade ore bodies attractive. Geotechnical engineers are faced with a number of questions regarding the behaviour of the tailings upon deposition. Of particular interest to this research was the in-situ beaching and drying behaviour of platinum tailings in relation to various proposed mechanisms described in literature and predicted from laboratory behaviour.

Increasingly finer grinds are required to fully liberate minerals from ore bodies as was the case with the tailings investigated. Successive field depositions allowed the impact of the finer grind, slurry density and beach length to be investigated and compared to flume tests. By monitoring the water contents following deposition the quantity of water released during sedimentation was determined giving an indication of the amount of water recovery possible. Following sedimentation, samples recovered by auger along the beach and with depth were used to determine the gravimetric water content regime. Climatic data were also obtained to determine the impact of changing reference evapotranspiration over the investigation period on the rate of drying. A geotechnical model based on laboratory tests and numerical models was then used to interpret the water contents. This was to determine the degree of moisture loss during active deposition and the distribution of strength along the beach.

Very little segregation was observed due to the finer grind; however any coarse material appeared to settle shortly after deposition. A flume test adequately predicted the segregation along the beach however; the profile was not well predicted. The material in the flume appeared to be prematurely arrested predicting a convex up beach whereas a concave beach typical of most platinum facilities was observed. Lower slurry densities did result in more material being deposited on the lower course however no definite relationship with chord slope was found. Rather it was shown that the longer the beach the flatter the chord angle. The beach was observed to act as a natural thickener with the water content after sedimentation comparable to what machine thickening was proposed to achieve. After sedimentation the water content was observed to decrease to a steady state condition. The rate at which this drying occurred was shown to be related to reference evapotranspiration. A method is therefore proposed to monitor the rate of drying so as to manage the rate of rise of a facility. A range of field capacity values, as a consequence of varying particle sizes, was shown to correlate with the steady state condition. Although further along the beach the water

contents were higher due to equilibrium with the phreatic surface. As such it was only at the head of the beach that significant drying occurred, Liquidity Indices showed that it was only here that considerable consolidation occurred. The majority of the interior appeared to remain an essentially viscous semi-solid.

Acknowledgments

Woe to him who strives with him who formed him,
a pot among earthen pots!
Does the clay say to him who forms it, 'What are you making?'
But now, O LORD, you are our Father;
we are the clay, and you are our potter;
we are all the work of your hand.

Isaiah 45:9 and 64:8

A number of individuals are hereby acknowledged for their various contributions to making this thesis possible. Andrew Copeland who at the start of my working career at Anglo American got me involved in the task of sifting through the seeming mire of data obtained from the water-saving investigation. Geoff Blight my supervisor is acknowledged for helping to guide my thoughts and providing information used to analyse the collected field data. No field work would have been possible if it was not for Anglo American Platinum Mogalakwena Mine allowing its tailings facility to be studied. Richard Pilkington, Barry Davis and Ashina Buddu are therefore acknowledged for making it possible for the research to be carried out. Thanks also go to Elizabeth Marsden and Neville Plint of Anglo American Platinum for providing approval for the use of monitoring data collected by SRK Consulting to be used in this study. The dedicated work of the Fraser Alexander Tailings staff at Mogalakwena made this study feasible. In particular Michael Knight, Dingaan Botsane, Ofentse Phete and Shaun Anderson are recognized as having put up with my often relentless queries regarding the veracity of the collected data. The South African Weather Service is credited for providing climatic data used in the study. A great number of informal discussions with a number of different people during my analysis helped to formulate and sharpen my understanding of the subject. Although not specifically named their contributions are greatly appreciated. Finally I am extremely grateful to my wife Jani for encouraging me and providing the impetus to finish the work.

Table of Contents

Candidate Declaration	i
Abstract	ii
Synopsis	iii
Acknowledgments	v
Table of Contents	vi
List of Figures	viii
List of Tables	xii
Abbreviations and Symbols	xiii
Chapter 1 General Introduction	1.1
1.1 Background and Justification	1.1
1.2 Scope and Objectives	1.1
1.3 Structure of Dissertation	1.2
Chapter 2 Literature Review	2.1
2.1 Historical Overview	2.1
2.2 Tailings Properties	2.5
2.3 Management Key	2.6
2.4 Beaching Behaviour	2.7
2.5 Moisture Loss and Strength Gain	2.12
Sedimentation	2.13
Drying	2.15
2.6 Reference Evapotranspiration	2.24
Evaporation, Transpiration and Evapotranspiration	2.24
Measuring Evapotranspiration	2.25
FAO-56 Methods	2.26
Application in Tailings Management	2.31
Chapter 3 Methodology	3.1
3.1 Experimental Rationale	3.1
3.2 Test Site	3.1
3.3 Data Capture	3.2
Climatic Data	3.2
Slurry Feed	3.3
Laboratory Data	3.4
Test Strips	3.5
3.4 Data Analysis	3.7
Slurry Feed	3.7
Beaching Behaviour	3.7
Reference Evapotranspiration	3.7
Moisture Loss	3.9
Chapter 4 Results and Analysis	4.1
4.1 Basic Geotechnical Properties	4.1

	Particle Size Distribution	4.1
	Atterberg Limits	4.4
	Particle Specific Gravity	4.5
4.2	Settling Behaviour	4.6
4.3	Beaching Behaviour	4.8
	Predicted Beaching Behaviour	4.8
	Master Profile	4.1
	Chord Slope	4.11
4.4	Drying Behaviour	4.17
	Laboratory Behaviour	4.17
	Field Behaviour	4.21
	Reference Evapotranspiration	4.3
	Relationship between Field Drying and Reference Evapotranspiration	4.35
	Steady State Stage	4.36
Chapter 5 Conclusions and Recommendations		5.1
5.1	Conclusions	5.1
	Beaching Behaviour	5.1
	Drying Behaviour	5.2
5.2	Recommendations	5.5
	Beaching Behaviour	5.5
	Drying Behaviour	5.5
References		R.1
Appendix A: Historical Development of Tailings Management		A.1
Appendix B: The Classification of Tailings		B.1
Appendix C: Failures		C.1
Appendix D: Factors Influencing Evaporation		D.1
Appendix E: FAO 56 Method		E.1
Appendix F: Interpretation of Climatic Data		F.1
Appendix G: Beach Profile Regression		G.1
Appendix H: Drying Iterative Regression Methodology		H.1

List of Figures

Figure 2.1: Definition of master profile 2.7
Figure 2.2: Sample master profiles (Blight and Bentel, 1983) 2.8
Figure 2.3: Particle segregation along a hydraulic fill beach (Blight, 1987) 2.10
Figure 2.4: Chord slope as a function of solids concentration; left Fly Ash (Blight, 1987) and right Gold (CMSA, 1996) 2.12
Figure 2.5: Forms of the β constitutive relationship (Pane and Schiffman, 1985) 2.13
Figure 2.6: Sedimentation Moisture Loss 2.14
Figure 2.7. Hjulstom diagram, relating stream velocity to particle size for conditions of erosion, transportation and deposition (Kehew, 2006) 2.15
Figure 2.8: Water content continuum showing the various stages of a soil as well as the generalized stress-strain response (Holtz and Kovacs, 1981) 2.16
Figure 2.9: Schematic illustration of the shrinkage and desaturation phases in different planes: (a) e-w relationship; (b)e-ψ volumetric shrinkage curve; and (c) water retention curve expressed as w-ψ and Sr-ψ (after Mbonimpa et al., 2006) 2.20
Figure 2.10: Change in dry density as a consequence of moisture loss 2.23
Figure 2.11: Sedimentation and drying moisture loss 2.23
Figure 2.12: Basis of FAO 56 (after Allen et al., 1998) 2.27
Figure 2.13: Comparison of evapotranspiration methods (Benli et al., 2010) 2.30
Figure 3.1: Test site layout 3.2
Figure 3.2: Beach access; winch on left and catamaran on right 3.6
Figure 4.1: South plant tails particle grading (Tailings Dam 1) 4.1
Figure 4.2: North plant tails particle grading (Tailings Dam 2) 4.2
Figure 4.3: PSD on Tailings Dam 1 4.2
Figure 4.4: PSD on Tailings Dam 2 4.3
Figure 4.5: Laboratory study PSD relative to field PSD 4.4
Figure 4.6: Distribution of percentage clay in field samples 4.5
Figure 4.7: Histogram of particle specific gravities determined during field testing 4.5
Figure 4.8: Settling Behaviour 4.6
Figure 4.9: Relationship between slurry density and settled moisture content 4.7
Figure 4.10: Relationship between particle size and settled moisture content 4.7
Figure 4.11: Flume test PSD 4.8
Figure 4.12: Comparisson of small-scale and full-scale beaching behaviour 4.9
Figure 4.13: Particle segregation along respective beaches 4.10
Figure 4.14: Scatter plot comparing Blight and Bentel (1983) to the current 4.11

study
Figure 4.15: Successive beach profiles on Tailings Dam 1 4.12
Figure 4.16: Successive beach profiles on Tailings Dam 2 4.13
Figure 4.17: Variation of chord slope with slurry density 4.14
Figure 4.18: Relationship between chord slope and beach length 4.14
Figure 4.19: Relationship between settlement and distance along beach 4.15
Figure 4.20: Tailings Dam 1 baseline moisture regime 4.16
Figure 4.21: Tailings Dam 1 moisture regime during active deposition 4.16
Figure 4.22: Laboratory determined water retention curves 4.17
Figure 4.23: Laboratory determined volumetric shrinkage curve 4.18
Figure 4.24: Flux based field capacity values 4.20
Figure 4.25: Drying time 4.21
Figure 4.26: Steady state differences 4.23
Figure 4.27: Deposition 1 drying curves 4.25
Figure 4.28: Deposition 1 scatter plot 4.25
Figure 4.29: Deposition 2 drying curves 4.27
Figure 4.30: Deposition 2 scatter plot 4.27
Figure 4.31: Deposition 3 drying curves 4.29
Figure 4.32: Deposition 3 scatter plot 4.29
Figure 4.33: Regional calibration of Hargreaves method 4.30
Figure 4.34: Daily ETo values based on SAWS Mokopane data 4.31
Figure 4.35: Scatter plot comparing average daily ETo values for based on monthly time steps 4.31
Figure 4.36: Daily ETo values based on Mogalakwena data 4.32
Figure 4.37: Scatter plot comparing Mokopane and Mogalakwena ETo values 4.32
Figure 4.38: Mogalakwena daily pan evaporation 4.33
Figure 4.39: Scatter plot comparing monthly pan evaporation 4.33
Figure 4.40: Scatter plot comparing ETo values to A-Pan values 4.34
Figure 4.41: Histogram of Coefficients 4.34
Figure 4.43: Days to dry for outer 150 m 4.36
Figure 4.44: All water content samples over period of investigation 4.37
Figure 4.45: Histogram of all water contents determined 4.37
Figure 4.46: Comparison of field water contents to the laboratory determined volumetric shrinkage curve 4.38
Figure 4.47: Field drying behaviour - Dam 1, Deposition 1, Position 0 m 4.39
Figure 4.48: Field drying behaviour - Dam 2, Deposition 1, Position 0 m 4.39
Figure 4.49: Dam 1 water contents plotted against beach position 4.41
Figure 4.50: Dam 1 water content distributions along beach 4.42
Figure 4.51: Dam 2 water contents plotted against beach position 4.42
Figure 4.52: Dam 2 water content distributions along beach 4.43
Figure 4.53: Dam 1 liquidity indices with beach; based on minimum, 4.45

average and maximum Atterberg limits
Figure 4.54: Dam 2 liquidity indices with beach; based on minimum, average and maximum Atterberg limits 4.46
Figure 4.55: Dam 1, 0 m depth trend 4.47
Figure 4.56: Dam 2, 0 m depth trend 4.48
Figure 4.57: Liquidity indices with depth at 0 m; based on average Atterberg limits, Dam 1 on left and Dam 2 on right 4.49
Figure A.1: Modern paddock construction, note the two day walls (Robinson, 2010) A.3
Figure A.2: Plan and section through typical single deposition point tailings dam (Cooper, 1988) A.3
Figure A.3: Plan and section through a typical ring main spigot tailings dam (Cooper, 1988) A.4
Figure A.4: Schematic of a cyclone (www.scielo.br) A.5
Figure A.5: Section through a wall constructed upstream (CMSA, 1996) A.5
Figure A.6: Section through a wall constructed downstream (CMSA, 1996) A.6
Figure A.7: Section through a wall constructed centreline (CMSA, 1996) A.6
Figure A.8: Conventional thickener (WesTech, 2008a) A.7
Figure A.9: Paste thickener (WesTech, 2008b) A.8
Figure A.10: Conceptual scheme for a belt filter press modified with EK (Kalumba et al., 2009) A.10
Figure B.1: Simplified schematic of a mining operation (Robinson, 2008) B.1
Figure B.2: Tailings phase relationships B.2
Figure B.3: Robinson (2008) particle size classification B.5
Figure B.4: Sample Gold tailing PSD B.6
Figure B.5: Sample Platinum tailings PSD B.7
Figure B.6: Sample Copper tailing PSD B.8
Figure B.7: Sample Coal tailings PSD B.9
Figure B.8: Sample Iron Ore tailings PSD B.10
Figure B.9: Samples of various other tailings PSD B.11
Figure B.10: Prediction of phreatic surface due to particle sorting along beach (Blight et al., 1985) B.16
Figure B.11: Void ratio versus saturated hydraulic conductivity (Qiu and Sego, 2001) B.17
Figure B.12: Phreatic surface for down stream embankment (Vick, 1983) B.18
Figure D.1: Variation in solar radiation at the top of the atmosphere as a function of latitude and season (http://oso.tamucc.edu/labs/lab6/lab6.htm) D.2
Figure D.2: Solar radiation balance (after Allen et al., 1998) D.4
Figure E.1: Two cases of evaporation pan siting and their environment (after Allen et al., 1998) E.10
Figure F.1: Comparison of Mogalakwena and Mokopane air temperature data F.1

Figure F.2: Air temperature linear regression	F.1
Figure F.3: Interpolation of maximum temperature	F.2
Figure F.4: Interpolation of relative humidity values	F.2
Figure G.1: Dam 1 surveyed beach profile	G.1
Figure G.2: Illustrative regression for Deposition 2 on Dam 1	G.1
Figure G.3: Approximated Dam 1 beach profiles	G.2
Figure G.4: Dam 2 surveyed beach profile	G.2
Figure G.5: Illustrative regression for Deposition 1 on Dam 2	G.3
Figure G.6: Approximated Dam 2 beach profiles	G.3
Figure H.1: Raw Data	H.1
Figure H.2: Deposition 1 Sedimentation trend along Beach	H.2
Figure H.3: Rate of Sedimentation along Beach	H.2
Figure H.4: Drying Iterative Step 1	H.3
Figure H.5: Steady State Water Contents	H.4
Figure H.6: Determination of Drying Period	H.4
Figure H.7: Drying Period trend for Deposition 1	H.5
Figure H.8: Final Sedimentation and Drying Lines	H.5
Figure H.9: Raw Data fitted with Regression Model	H.6

List of Tables

Table 2.1: Methods of tailings management	2.3
Table 2.2: Methods of wall construction	2.4
Table 2.3: Liquefaction susceptibility of silty soils (Andrews and Martin, 2000)	2.18
Table 2.4: Techniques for measuring evapotranspiration	2.25
Table 3.1: SAWS Mokopane Weather Station Data	3.4
Table 3.2: Deposition details	3.6
Table 3.3: Mokopane FAO-56 ETo	3.9
Table 4.1: Laboratory PSD sample details	4.3
Table 4.2: Atterberg limits	4.4
Table 4.3: Field slurry densities	4.8
Table 4.4: Tailings Dam 1 beach profile details	4.12
Table 4.5: Tailings Dam 2 beach profile details	4.13
Table 4.6: VSC data source and designation	4.18
Table 4.7: SEEP/W input data	4.19
Table 4.8: Comparison of field capacity values	4.20
Table 4.9: Summary of drying results from laboratory tests	4.21
Table 4.10: Summary of drying results from field tests	4.23
Table 4.11: Developed Empirical Relationship	4.35
Table 4.12: Summary of liquidity indices at 0 m	4.44
Table B.1: Specific Gravity values quoted in literature	B.12
Table B.2: Approximate values of specific surface and activity for clay minerals (Atkinson, 2007)	B.13
Table B.3: Sample of PI, clay fractions and activity (Vick, 1983)	B.13
Table D.1: Types of scattering (after Tyson and Preston-Whyte, 2004)	D.3
Table D.2: Some typical albedo values (after Tyson and Preston-Whyte, 2004 and Blight, 2010)	D.4
Table E.1: Reference Evapotranspiration for different time steps	E.1
Table E.2: General classes of monthly wind speed data	E.10
Table E.3: Pan coefficient for A-pan for different pan siting and environment and different levels of mean relative humidity and wind speed (after Allen et al., 1998)	E.11
Table G.1: Respective Dam 1 r^2 values	G.2
Table G.2: Respective Dam 2 r^2 values	G.3
Table H.1: Settled Water Contents for all Depositions	H.3

Abbreviations and Symbols

AEV – Air Entry Value
ASCE – American Society of Civil Engineers
CMSA – Chamber of Mines of South Africa
EPA – United States of America Environmental Protection Agency
FAO – Food and Agriculture Organization of the United Nations
FAO 56 – PM – FAO 56 Penman Monteith
PGM – Platinum group minerals
PSD – Particle Size Distribution
SAWS – South African Weather Service
UN – United Nations
VSC – Volumetric Shrinkage Curve
WMO – World Meteorological Organization
WRC – Water Retention Curve
Δ - Slope of the vapour pressure versus temperature, kPa $^{\circ}C^{-1}$
$^{\circ}C$ – Degree Celsius
μm – Micrometre, m × 10^{-6}
A – Activity, no unit
A – Arbitrary relationship to define the dominant particle size, no unit
A – Instrument specific psychrometric constant, no unit
A – Power constant for relating permeability to void ratio, no unit
a – Solar absorptivity, no unit
α – Solar albedo, no unit
a_s – Angstrom equation regression constant for overcast conditions, no unit
B – Power constant for relating permeability to void ratio, no unit
b_s – Angstrom equation regression constant for clear conditions, no unit
C_a – Specific heat of air, MJ kg^{-1} $^{\circ}C^{-1}$
c_s – Soil heat capacity, MJ m^{-3} $^{\circ}C^{-1}$
D – Dominant particle size, mm
D_{10} – Particle size below which 10% by mass are smaller in size, mm
D_{15} – Particle size below which 15% by mass are smaller in size, mm
D_{50} – Particle size below which 50% by mass are smaller in size, mm
d_r – Inverse relative Earth-Sun distance, no unit
e – Base of the natural logarithm, 2.7183
e – Void Ratio, no unit
e°(T) – Vapour pressure at the air temperature T, kPa
e_a – Actual vapour pressure, kPa
e_a – Void ratio associated to the AEV, no unit
e_m– Void ratio above which a slurry behaves as a suspension, no unit
E_{pan} – Daily pan evaporation, mm day^{-1}
e_s – Saturated vapour pressure, kPa

e_s – Void ratio at true shrinkage limit, no unit
e_s – Void ratio below which a slurry behaves as a soil, no unit
ET_o – Reference evapotranspiration, mm day^{-1}
$ET_{o,\ FAO56\ -\ PM}$ – Reference evapotranspiration determined by the FAO-57 Penman Monteith equation, mm day^{-1}
$ET_{o,\ Hargreaves\ Method}$ – Reference evapotranspiration determined by the Hargreaves method, mm day^{-1}
G – Soil heat flux density, MJ $m^{-2}\ {}^{\circ}C^{-1}$
G_S – Particle specific gravity, no unit
h – Depth or height, m
H – Distance from point of deposition along the beach, m
h – Hour
i – Slope of a stream, no unit
J – Number of the day in the year between 1 (1 January) and 365 or 366 (31 December)
K – Kelvin
k – Coefficient of permeability, cm s^{-1}, m s^{-1}, mm day^{-1}
k value – Relationship between rate of water content loss and reference evapotranspiration, % mm^{-1}
K_c – Crop coefficient, no unit
km – Kilometre, m × 10^3
k_p – Pan coefficient, dimensionless
k_{rs} – Hargreaves equation humidity adjustment factor, no unit
ktpm – Kilotons per month
kW/m^2 – Kilowatt per square meter
LI – Liquidity index, no unit
LL – Liquid limit, %
m – Metre
M – Particle segregation characteristic of particular tailings, no unit
m^2 – Square metres
m^3 – Cubed metres
mm – Millimetre, m × 10^{-3}
n – Empirical tailings beaching exponent, no unit
n – Porosity, no unit
n – The actual duration of sunshine, h
N – The maximum possible duration of sunshine in a day, h
P – Atmospheric pressure at a given elevation, kPa
P – Pulp density, percentage weight of solids to total weight, %
PI – Plasticity index, no unit
PL – Plastic limit, %
Q_S – Quantity of solids, unit not specified
Q_W – Quantity of water, unit not specified

r^2 – Square of the Pearson product moment correlation coefficient, no unit
R_a – Daily radiation incident on a horizontal surface at the top of the atmosphere, MJ m^{-2} $^{\circ}C^{-1}$ (Converted to depth of water evaporated per day (mm day^{-1}) by dividing by latent heat of vaporisation and density of water)
R_n – Net radiation, MJ m^{-2} $^{\circ}C^{-1}$
R_{nl} – Net long wave radiation, MJ m^{-2} $^{\circ}C^{-1}$
R_{ns} – Net solar (short wave) radiation, MJ m^{-2} $^{\circ}C^{-1}$
R_s – Solar radiation passing through the atmosphere, MJ m^{-2} $^{\circ}C^{-1}$
R_{so} – Clear sky solar radiation value, MJ m^{-2} $^{\circ}C^{-1}$
RH – Relative humidity, %
RH_{max} – Daily maximum relative humidity, %
RH_{mean} – Daily mean relative humidity, %
RH_{min} – Daily minimum relative humidity, %
S – Degree of saturation, %
SD – Slurry density, t/m^3
SL – Shrinkage limit, %
S_o – Solar constant, 0.0820 MJ m^{-2} $^{\circ}min^{-1}$
S_r – Degree of saturation, %
$S_{r,es}$ – Degree of saturation at the onset of the no-shrinkage phase, %
T – Temperature, $^{\circ}C$
T_{dew} – Dew point temperature, $^{\circ}C$
T_{dry} – Dry-bulb temperature, $^{\circ}C$
T_{max} - Maximum 24 h temperature, $^{\circ}C$
$T_{max,K}$ – Maximum 24 h temperature, K
T_{mean} – Average of 24h minimum and maximum temperature, $^{\circ}C$
T_{min} - Minimum 24 h temperature, $^{\circ}C$
$T_{min,K}$ – Minimum 24 h temperature, K
T_{wet} – Wet-bulb temperature, $^{\circ}C$
u – Wind speed, m s^{-1}
u_2 – Wind speed at 2 m above ground surface, m s^{-1}
u_z – Wind speed at z m above ground surface, m s^{-1}
V – Volume, m^3
V_s – Volume of solids, m^3
V_v – Volume of voids, m^3
V_w – Volume of water, m^3
w – Gravimetric water content (dry solid basis), %
W – Weight, kg
w/s – Water to sediment ratio
w_0 – Initial water content, %
w_a – Water content associated to the AEV, %
w_{es} – True shrinkage limit, %
w_{es} – Water content at the onset of the no-shrinkage phase, %

w_m – Metallurgist water content (wet solids basis), %
w_n – Natural in-situ gravimetric water content, %
w_s – Shrinkage limit, %
W_s – Weight of solids, kg
W_w – Weight of water, kg
X – Distance, m
Y – Depth or height, m
z – Elevation above sea level (mAMSL), m
z – Height above ground level, m
z – Height, m
β – Bowen ratio, no unit
γ – Psychrometric constant, kPa $^{\circ}C^{-1}$
γ_s – Unit weight of solids, t/m^3
γ_w – Unit weight of water, t/m^3
δ – The solar declination, radians
Δt – Length of time, days
Δz – Effective depth, m
ε – Ratio of the molecular weight of water vapour to dry air, no unit
λ – Latent heat of vaporisation, 2.45 MJ kg^{-1}
π – Ratio of perimeter to diameter of a circle, no unit
σ – Stefan-Boltzmann constant, 4.903 MJ K^{-4} m^{-2} day^{-1}
ψ – Suction head, kPa
ψ_0 – Suction head at complete dryness ($S_r = 0$), kPa
ψ_a – Air entry value (or AEV), kPa
ψ_{es} – Suction head at the onset of the no-shrinkage phase, kPa
ω_s – The sunset hour angle, radians
Φ – Latitude, radians

Chapter 1 General Introduction

1.1 Background and Justification

This research seeks to address various issues associated with the sub-aerial deposition of platinum tailings in a semiarid environment. With the depletion of high grade ore bodies and the improvement of mineral extraction process the volume of tailings requiring storage is ever increasing. A common method is to allow the tailings to beach in a controlled manner and gain strength thus forming an impoundment for subsequent tailings. Strength is gained as the slurry is dewatered under the natural actions of gravity and evaporation. Water that bleeds from the slurry is decanted from the facility and can be reused.

The thinking world is faced with an ever growing concern of how best to utilise its mineral resources in a sustainable and justifiable manner. As populations grow the associated need for every day necessities increases and so the available mineral resources need to be extracted in the most efficient manner possible. Further population growth is resulting in increasing competition for natural resources such as water. Mining houses are therefore increasingly attempting to ensure that mining is carried out with as small an impact on the environment as possible, with this ethos increasingly being applied at all stages within a mine life cycle. It can be argued that the ill repute and environmental consequences of a tailings dam failure far outweigh any gains at other stages.

Thus a better understanding of how the process of beaching, immediate moisture loss and the longer term moisture movements influence stability is important. Increased competition for water makes it necessary to recover as much water from the tailings as possible. Hence understanding how water naturally bleeds from conventionally thickened[1] tailings is further justification for this study. To these ends a joint research and development project between Anglo American and Fraser Alexander was initiated to better understand various aspects of conventional tailings deposition by beaching.

1.2 Scope and Objectives

This dissertation does not seek to address all issues surrounding the storage of platinum tailings and therefore the scope of the study is limited by the following objectives:

- Wates et al. (1987) suggested that tailings beach profiles vary over a period of time as different depositions take place and that once-off measurements may not

[1] Conventional thickening is here defined as a mill process in which some of the water is removed (Wortmann, 2007) with the resulting pulp density (the percentage solids by mass) ranging between 30 and 50% (Palkovits, 2007).

detect the dynamic process involved. To this effect an investigation of this dynamic process was undertaken with the aim of better understanding the beach profile following successive depositions. As the tailings investigated were of a particularly fine grind the impact of this on particle segregation and beaching could be studied.

- It has long been accepted that strength gain in tailings is influenced by the desiccating influence of climate aridity (Donaldson, 1960). Extensive laboratory research has been conducted into this process; however field experiments have often been limited. The in-situ drying of platinum tailings was therefore investigated over an eleven month period on two active tailings dams. Climatic parameters were also obtained to investigate the effect of changing aridity during the course of the year on the rate of moisture loses. Of importance to strength gain is the degree of moisture loss that occurs. The extensive nature of the investigation allowed this to be explored.

All field test work was limited to the Mogalakwena Tailings facility which consisted of two dams that share a common wall. The investigation was thus limited to the tailings produced by the Anglo American Platinum Mogalakwena Mine North and South plants.

1.3 Structure of Dissertation

This dissertation is structured into 5 chapters; 1 General Introduction, 2 Literature Review, 3 Methodology, 4 Results and Discussions and 5 Conclusions and Recommendations. These chapters are then subdivided into sub chapters. Chapter 1 sets out the background, justification, objectives and scope of the study. The literature review which follows gives the basis for the research reported within. It gives a brief history of tailings management, outlines the factors influencing beaching behaviour and shows the current understandings of how moisture is lost from tailings. Chapter 3 outlines the test methodology as well as the methodology used to analyse the data captured. The analysis of the data is presented in Chapter 4 along with a discussion of the results. Finally a summary of the main findings and its implications on tailings management are presented as conclusions and recommendations in Chapter 5. A detailed list of references is given and is followed by six Appendices outlining material that is not essential for reading the dissertation.

Chapter 2 Literature Review

2.1 Historical Overview

Mankind has relied on the natural resources contained within the earth's crust to form crude stone tools to the complex electronic devices now common to our everyday lives. Many of these end products are cleanly packaged belying the fact they come from dirty processes that generate vast amounts of waste. The sought-after minerals are rarely in a free form and are most often bound to other molecules and hence are dilute and dispersed throughout the host rock (Robinson, 2008). To extract the minerals the host rock has to be crushed so extraction can take place either mechanically or chemically. Typically a mining operation will involve removing barren or over-burden rock which is then discarded. The ore body is then milled and the mineral extracted, generating waste material that has to be stored.

The type and amount of waste produced has followed the demand and available technology to extract the minerals. For instance the early recovery of copper and iron, for crude tools, was from ore bodies exposed by erosion resulting in very little waste. As demand for the metals increased, excavation to the ore bodies was required. Initially this only meant removing surface layers, but eventually required excavating shafts and adits. The main waste produced from these processes was overburden material made up of rock fragments and sand (Mason, 1982). Such waste was simply discarded as close as practically possible to the mining operation. As demand increased milling was required to extract ore from host materials. This was carried out by crude millstones from the 1500's through to the mid 1800's (Martin et al., 2002). The requirement of ample water to drive the processes meant that crushing only occurred on a small scale and often during wetter seasons. This resulted in low daily volumes of coarse free-draining waste (Cooper, 1988).

With more efficient drill and blast techniques and the introduction of steam power, greater amounts of ore could be crushed with greater efficiency. During the late 1800's the development of froth flotation and the use of cyanide for gold extraction brought about dramatic changes to the mining industry. Once uneconomical low-grade ore bodies could now be processed resulting in still larger quantities of tailings at even finer grinds. The requirement of ample water often meant that riverine disposal of waste was adopted. However with these technologies came supporting industries and the development of remote mining districts. These communities required food and water which led to a conflict of interests. Downstream irrigation channels became silted up by the accumulating tailings and agricultural land became contaminated resulting in lower yields.

The "first" generation of tailings management included little more than washing of the wastes into the nearest water course and allowing the solid material to be transported downstream as sediment load. Increasing stringency from regulators resulted in a move away from uncontrolled deposition to what can be termed "second" generation tailings management. These involve impounding tailings within hydraulic-fill structures. Deposition occurred simply by open ending slurry into the impoundment with little requirement for the tailings to gain any strength. "Third" generation tailings management was brought about by the ability to reduce the moisture in the tailings by thickening to roughly 50% solids content. Tailings could thus be "managed" to form stable, drained and consolidated waste piles. The "fourth" generation of mineral waste managements involves the application of dewatering technology to further reduce the engineering and operational risk of containment facilities. Application of "paste" and "dry" stack solutions with the possible addition of cementitious material to increase the strength can result in greater flexibility in both containment facility siting and placement methodology (Cincilla et al., 1997).

In general the historical development of tailings facilities has resulted from outside pressures requiring mining houses to change the way they dispose their waste. Various failures of impoundments led to more engineering and regulatory input. In recent years the number of agencies involved in setting prescriptive and/or rigid guidelines has increased. This has caused mining companies to no longer discard waste in the simplest manner. Rather many have set up internal programs to assess waste facilities and carefully plan future impoundments (Davies, 2002). Today's mining houses are more aware of the negative impacts that can result from not taking a proactive stance towards mining in a sustainable manner. To this effect statements are made along the lines of minimising the impact on the environment from exploration through to mine closure (Anglo American, 2010). For this to become a reality, potential areas of improvement need to be identified and investigated. Universities now provide learning environments and research projects to better understand the engineering and environmental implications of disposing mine waste. Issues surrounding the disposal of mine waste are thus increasingly influencing planning and operation decisions (Palkovits, 2007).

Table 2.1 outlines further details on the above mentioned methods of tailings management. Appendix A is a more comprehensive text on the historical development of the various tailings management methods available. Tailings facilities are not often built in one single step but are raised as production increases. This requires that tailings impoundment walls be raised and the three common methods of doing this are outlined in Table 2.2.

Table 2.1: Methods of tailings management

Method	Details
Uncontrolled Disposal	**Riverine.** Legal precedents due to the environmental degradation downstream have lead to the cessation of such deposition. **Offshore.** Studies have shown various advantages to offshore deposition away from the biologically active and sensitive shoreline zones. However significant public opposition means this is not an option that can be readily considered.
Sub-aqueous Disposal	This method developed from the need to impound riverine disposal behind embankments. Embankments are constructed of material other than the tailings, such as waste rock or earth. They are constructed of sufficient strength so that the contained tailings need not gain strength and can remain wet and saturated at low shear strengths. This method is used to prevent acidification caused by the oxidation of wastes with pyrite content, although only sustainable in water surplus climates.
Sub-aerial Deposition	In semiarid and arid environments it was soon realised tailings gained sufficient strength to form impoundments for subsequent tailings leading to a number of different disposal methods: **Paddock Construction.** In flat terrain a series of paddocks, constructed by raising low berms from previously deposited tailings, are used to form a ring dyke. During the day tailings are deposited into the paddocks in a successive fashion allowing sufficient drying to take place, at night tailings are discharged into the basin formed by the ring dyke. **Spigot Construction.** Tailings are discharged successively from a series of spigots around the perimeter of a basin and allowed to flow towards a central point. The tailings require a sufficient range of particle sizes to allow coarse particles to settle out higher along the beach. Due to the superior consolidating properties of the coarse particles they form a wall of sufficient strength to contain the finer particles further down the beach. **Cyclone Construction.** Centrifugal acceleration within a cyclone separates the coarse and fine fraction of a tailings stream with the coarse fraction being utilised to construct a wall and the fine fraction deposited within the basin.
Conventional Thickening	Most mineral processing circuits will contain a thickening step prior to disposal in which some of the process water is removed for immediate recirculation. Conventional thickening is here defined as producing slurries with a typical pulp density (the percentage solids by mass) between 30 and 50% with deposition carried out via the above mentioned methods.
Paste Thickening	Advances in conventional thickening have resulted in so called paste thickeners producing slurries with pulp densities between 60 and 65%. The ability to thicken to such densities is limited by ore body and grain size necessary for mineral extraction. At these densities tailings are non-segregating (i.e. particles cannot settle out due to higher viscosities) and so cannot be deposited in a conventional manner. They require higher energies to transport, often needing positive displacement pumps, and are then deposited from a single deposition point and allowed to flow out to form a flat sloping conical fan.

Table 2.1 Methods of Tailings Management (Continued)

Method	Details
Chemical Thickening	Speciality chemical companies are developing flocculants that can improve the compressibility and dewatering characteristics of slurries whilst reducing viscosity.
"Dry" Filtering	The development of large capacity filter and vacuum presses that can further increase pulp densities to above 80% such that the tailings are near saturation or unsaturated but not completely dry. The filter cakes produced have insufficient water to be pumped and are therefore transported by conveyor or truck, placed, spread and compacted to form an unsaturated dense stack requiring little or no impoundment walls for retention.
Backfilling Mined Areas	Due to the nature of mining a host rock at least 50% of the mined material cannot be returned to its original resting place due to the bulking that occurs. Disposal in underground mined areas is often only carried out as a consequence of the mining operation requiring stable working areas. Backfilling in open pit operations is often overlooked as it requires careful planning and can lead to environmental problems if the pit is partially below the natural water table.

Table 2.2: Methods of wall construction

Method	Description
Upstream	The wall is advanced in such a manner that the centre-line of the wall moves progressively upstream. As a consequence the outer retaining wall is constructed over previously deposited tailings and essentially remains the same thickness with increasing height.
Downstream	The wall is advanced in such a manner that the centre-line of the wall moves progressively downstream. When constructed in this fashion the wall gets progressively larger with each deposition and is constructed over foundation material. This method is often favoured when a competent wall is necessary for exceptional loading cases such as potential seismic events.
Centre-Line	This method is combination of the above two methods with the centre-line of the wall not changing with successive rises. As such, one half of the wall is raised on tailings and the other on previously deposited wall material. The downstream method requires a considerable amount of material and the centre-line method is often a trade-off when a substantial wall is necessary but material is not readily available.

2.2 Tailings Properties

A review of literature will reveal a host of geotechnical issues that have to be addressed when considering the management of mine waste. Appendix B is an extensive review of these properties however below is a summary originally put forward by Fahey and Newson (1997) and augmented here:

- The rate of sedimentation particularly in sub-aqueous tailings deposition.
- The manner in which the tailings form a beach, defined by the beach angle and segregation of coarse and fine fractions in sub-aerial deposition.
- The immediate water released within 1 or 2 days after deposition, this is dictated by the initial slurry density and the density achieved within this period.
- The long term consolidation behaviour.
- When tailings are used for wall construction the shear strength, erodibility and compaction characteristics are also important.
- For rehabilitation to take place a workable surface crust needs to develop and so the time that elapses for this to take place needs to be determined.
- The susceptibility to erosion and dust generation of the tailings surface during operation and after decommissioning needs to be assessed. Short term solutions then need to be determined along with potential long term capping solutions.
- The long term water and air movement within and through the tailings needs to also be determined.

A superficial understanding of the above geotechnical issues can be determined by determining the following criteria: (CMSA, 1996, Fahey and Newson, 1997):

- Particle size distribution
- Atterberg limits
- Particle specific gravity
- Mineralogy of the clay-sized fraction
- Shear strength characteristics
- Permeability

A more detailed understanding would require doing some of the following:

- Slurry settling tests
- Flume box beaching tests
- Rowe cell consolidation tests
- Consolidated undrained triaxial tests with measured pore pressures
- Evaporative drying tests

Increasingly, however, the environmental impacts of tailings disposal are dictating the method of disposal. The presence of potential toxins and pollutants needs to be determined as well as the longer term affects of changes in pH, weathering and oxidation on these substances. As such the following key environmental properties need to be quantified (CMSA, 1996):

- The presence of any toxic substances such as fluorine, arsenic, lead, nickel or similar toxic or heavy metal salts.
- Possible radioactivity or potential health hazards such as free asbestos.
- The potential for changes in pH, weathering and oxidation to mobilise toxins and heavy metals held in tailings or release radioactive particles. For example the oxidation of pyrites in gold tailings results in sulphates and sulphuric acid.
- The possibility of spontaneous combustion for instance in colliery residue.
- Decomposition of certain contents of the residue may produce either combustible or toxic gases which will then emanate from the deposit.
- The performance of design features of an impoundment can also be affected by chemical reactions resulting in the tailings. For example underdrains can become clogged by the precipitation of insoluble Fe_2O_3 gels and clay liners (used to reduce polluting seepage escaping) can become rigid and brittle when in contact with calcium hydroxide or phosphoric acid.

Residues with adverse chemical properties may possibly be altered by a simple pre-treatment before deposition to either eliminate or reduce any environmental impact. For example, an initially acidic residue could be neutralised before deposition.

2.3 Management Key

A review of literature shows that a number of catastrophic failures of tailings dams such as the Los Frailes, El Cobre, Barahona, Bafokeng and Merriespruit disasters (covered in Appendix C). However many tailings failures never reach main stream media outlets and go undocumented. Blight (2010) in analysing the extensive records of failures in Japan, a country not known for mining, but having a large number of failures although non major, noted the following; Tailings dams are subject to many mishaps but these seldom set of the chain of events that result in major damage. Management procedures need to be in place so that continual monitoring is undertaken to pick up any potential failure. Emergency repairs can then be undertaken and if possible the area cordoned off and deposition temporarily ceased. Many of the major disasters can be linked to mines running on a “shoe-string” budget or threatened by closure and thus management procedures were lacking. A growing list of past failures and analysis means that many reasons for failure are readily identifiable. The necessary information to eliminate such events exists (Davies, 2002) and if not available, ongoing research is giving further insight. So although studies can be made and conclusions derived, a key component to any mine tailings disposal strategy is to ensure that the correct procedures are in place, operational staff are well trained and management are willing and able to steward the facility.

2.4 Beaching Behaviour

When deposited, tailings slurry forms a beach, cone or fan as it gravitates towards a pool where excess decant water can be drawn off. The prediction of a beach profile is important when designing a tailings facility. This allows the designer to predict the position of the pool as well as assessing the storm water storage of the top of the dam. Furthermore, the tailings storage capacity can be assessed. Beaching angle can also influence the volume of compacted earthworks required when a tailings dam is commissioned. If a capping is required at closure the beach profile will also influence the quantity of material required. To this effect research has been carried out by various authors such as Blight and Bentel (1983), Blight et al. (1985), Wates et al. (1987) and Fourie (1988) following on from original work carried out by Melent'ev et al. (1973).

Through the work of these researchers various propositions have been made regarding both the change in gradient along the beach and the overall or average gradient between the point of deposition and the pool. Both these aspects are required to fully predict the beach profile. Referring to Figure 2.1 the chord slope would be Y/X and the change in gradient would be the gradient of the curve at each value of H and h. The gradient below the pool is known to increase rapidly. Studies reported here did not measure the gradient below the water. The under-water regime usually only applies a considerable distance from the outer perimeter and is therefore less important to the overall stability of tailings dams (Blight and Bentel, 1983).

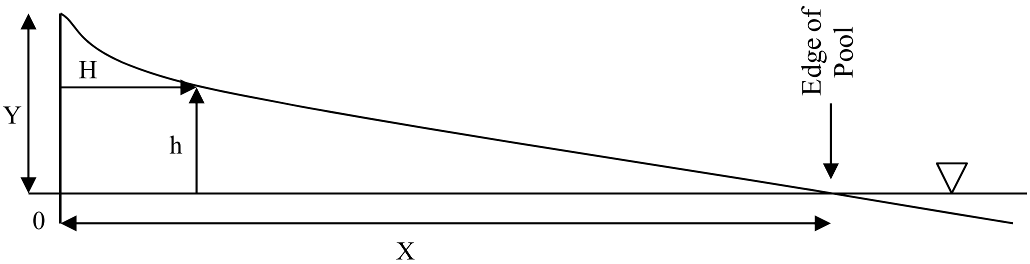

Figure 2.1: Definition of master profile

Blight and Bentel (1983) showed that for different dams constructed with the same tailings appeared to result in the same master profile approximated by the expression:

$$h/Y = (1 - H/X)^n \quad \textbf{Equation 2.1}$$

where h, Y, H and X are defined by Figure 2.1
n is an exponent that is a characteristic of the tailings

Data from various different operations and tailings minerals were analysed and showed that master profiles were repeatable for a particular tailings mineral as illustrated by Figure 2.2.

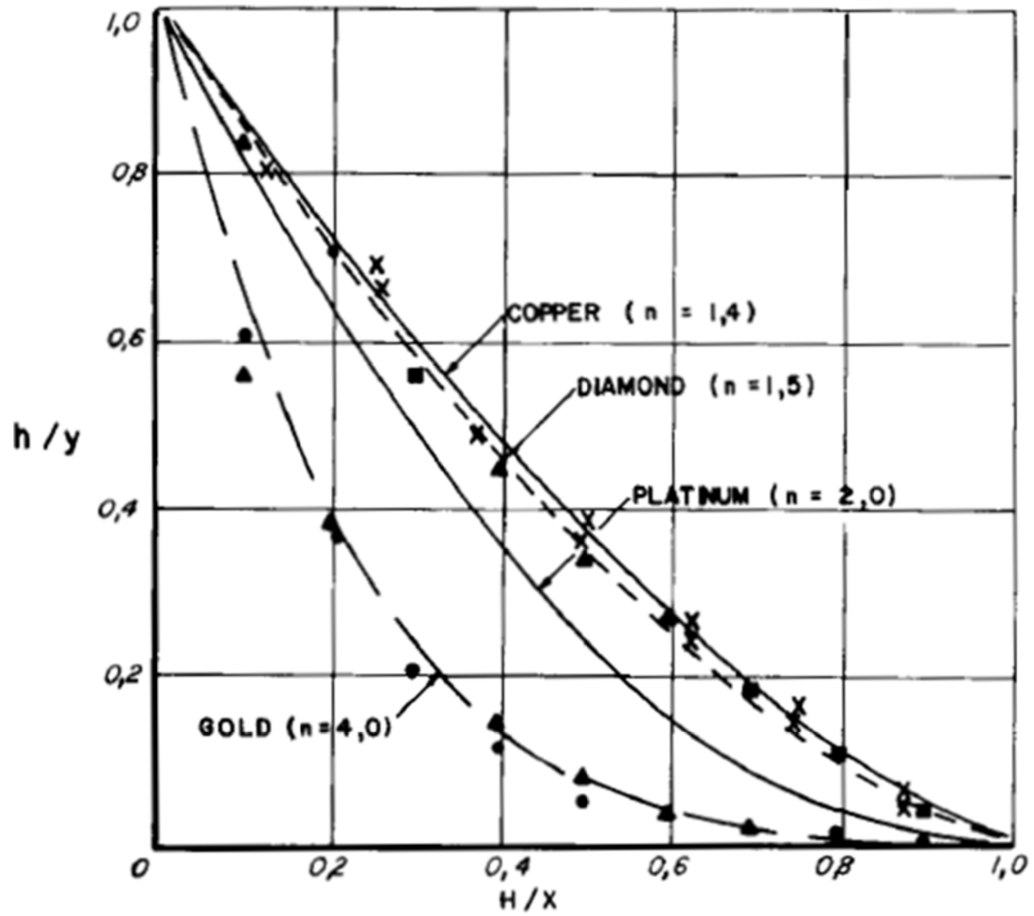

Figure 2.2: Sample master profiles (Blight and Bentel, 1983)

Blight et al. (1985) went on to show that the exponent n could be predicted by small-scale flume tests provided the same material is used and deposited at a similar solids content. This enabled investigations to be carried out into the effects of slurry density, tailings particle distribution, dispersants and particle segregation on the beach profile in a controlled environment.

Blight et al. (1985) varied the percentage solids (50%, 60% and 70%) and divided gold tailings into a coarse, fine and total fraction and investigated the resulting beach profile. They found that increasing the solids content resulted in a steeper slope at the point of discharge and shallower slopes at the end of the flume. Likewise the coarse fraction resulted in a steep slope close to the point of discharge and shallower slope at the end of the flume. However the difference in beach profile between the fine fraction and total fraction was not as pronounced as that between the total fraction and the coarse fraction.

Fourie (1988) investigated the effect of; changing slurry densities, adding dispersants and particle size distribution on the flume beaching of Bauxite tailings, Nickel ore slurry and Coal tailings. The Bauxite tailings were beached at a solids content of 32% and 27% which was reported to have a "relatively thick consistency". Surprisingly the profiles resulting had a convex upwards master profile, i.e. an n value of 0.43, which fitted both the solids content tested. However the chord slope increased for the slurry at a higher relative density. The convex upwards curve was attributed to the high initial solids content and the gap graded nature of the tailings.

Nickel ore slurries were investigated at solids contents of 42% and 35% however in flumes that were tilted at angles. The ore slurry had a relatively uniform particle size and was observed to beach in a mudflow type regime. Very little segregation occurred down the beach as expected. Again as in the case of the Bauxite tailings the master profiles were not affected by the solids concentration and resulted in convex up curves with an n value of 0.36.

Fine uniformly graded coal tailings at solids contents of 43% (Tap water), 50% (Tap water with a dispersant), 15% (Tailings water) and 48% (Tailings water) were also investigated. The two tests at similar solids contents but using tap and tailings water resulted in a slightly steeper beach for the tap water compared to the tailings water. However adding a dispersant to the tap water at high solids content resulted in an extremely flat beach which was only slightly steeper than the beach at a solids content of 15%. Although the make up of the slurries was markedly different the resulting master profile was very similar in each test. Again as in the Bauxite tailings and Nickel ores slurry the master profile was convex up. To investigate whether the n parameter was a consequence of the tailings mineral a coarse coal tailings described as silty sand was tested. This resulted in a concave upwards profile as shown by Blight and Bentel (1983). Fourie (1988) thus concludes that the exponent n is insensitive to the initial solids concentration but is very sensitive to changes in particle size distribution. Recommending further investigations be carried out into these effects.

Blight and Bentel (1983) put forward that beach profiles were dependant on the particle-size segregation that occurs along the beach. The strength that can be generated by the settling slurry determines the beaching gradient. Coarse material settles quicker and develops shear strength faster than finer material which settles out further down the beach. This results in a beach with decreasing slope from the point of deposition. Blight (1987) illustrated this particle segregation with the Figure 2.3.

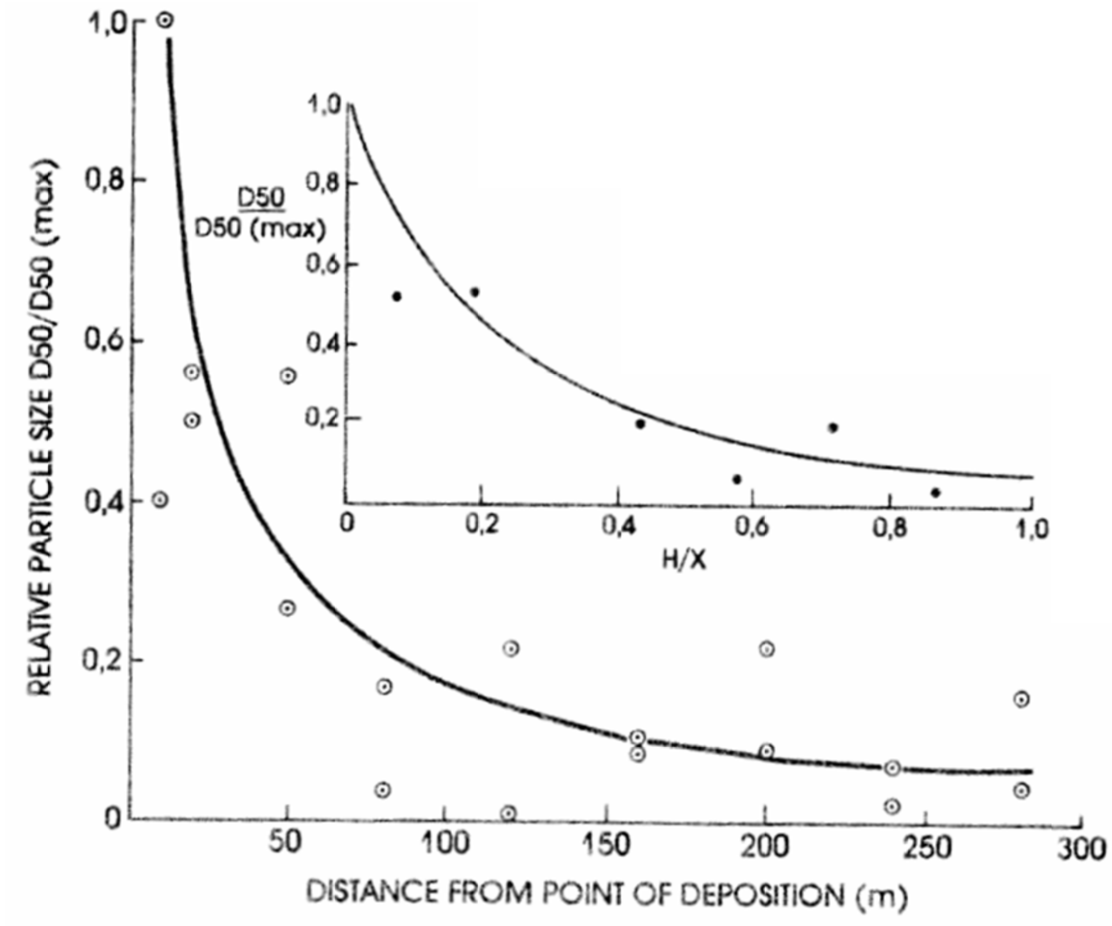

Figure 2.3: Particle segregation along a hydraulic fill beach (Blight, 1987)

Blight and Bentel (1983) tested two theoretical models to describe the particle segregation along the beach based on theories of settling by Graf and Stokes law:

$$\textit{Following Graf} \ldots D \propto \frac{1}{H} \quad \textbf{Equation 2.2}$$

$$\textit{Following Stokes Law} \ldots D \propto \frac{1}{\sqrt{H}} \quad \textbf{Equation 2.3}$$

where D is the Dominant particle size
H is the distance from the point of deposition

This analysis suggested that the particle sorting was close to the theory after Graf's theory of settling however the data exhibited a great deal of scatter.

Wates et al. (1987) set out to investigate the influence of slurry density on the chord slope for uranium tailings. Their investigations involved both field observations and controlled flume tests on the effects of slurry density. They argued that for uranium tailings particle size distribution is generally uniform and does not vary widely between operations and from year to year within one operation. Thus very little segregation can occur along the beach and thus the resulting average beach slope must mainly be influenced by the slurry relative density. The relationship put forward by Lane (1955) that relates to the equilibrium of flow conditions and deposition of sediment was used to describe the findings

$$i \propto \frac{Q_W}{Q_S \times D} \qquad \textbf{Equation 2.4}$$

where i is the slope of a stream
Q_W is the quantity of water
Q_S is the quantity of solids
D is the dominant particle size

This relationship is consistent with Blight and Bentel's (1983) observation that as the particle size increases so does the slope of the beach. However it also shows that the ratio between the quantity of water and the quantity of solids has a part to play. Wates et al. (1987) postulated that as the slurry progresses, some particles settle out leaving the slurry with an ever decreasing slurry density. This implies that as the slurry bleeds the viscosity decreases resulting in the observed decreasing beach angle. Further as the slurry relative density decreases the velocity of the slurry will increase due to the decreasing viscosity suggesting that velocity also has a role to play in flattening the beach profile. Robinsky (1975) provides argument for this proposition in that reducing the flow rate results in an increase in the slope of the beach. Increasing the number of discharge points will in effect reduce the discharge velocity for a given volume of slurry. Wates et al. (1987) noted that this effect is observed when using a spigot system of deposition.

Various field observations and flume tests are reported by Wates et al. (1987) that support the proposition that increasing slurry density results in an increasing average beach slope. However no quantitative analysis is presented as they reported the variations to be too great. They were also unable to find the parameter n suggested by Blight and Bentel (1983) for the flume data. They conclude that the beaching process is highly dynamic and that a single n value may not be appropriate and that further research be conducted for a number of successive full-scale field depositions.

Further investigation was carried out by Blight (1987) into the effect of slurry density on the average beach slope. The research showed that the average beach slope increases as the slurry density (Solids Concentration) increases. Yet as the slurry density increases the interface between particles also increases. Thus at a certain solids concentration no more sorting occurs (Particle Settling flow regime) instead a homogenous flow occurs (Mud Flow regime). When the flow regime changes there is a marked decrease in the chord slope as illustrated by Figure 2.4. Although not observed in the studies reported it was postulated that at some higher solids concentration the average beach slope may start increasing once again.

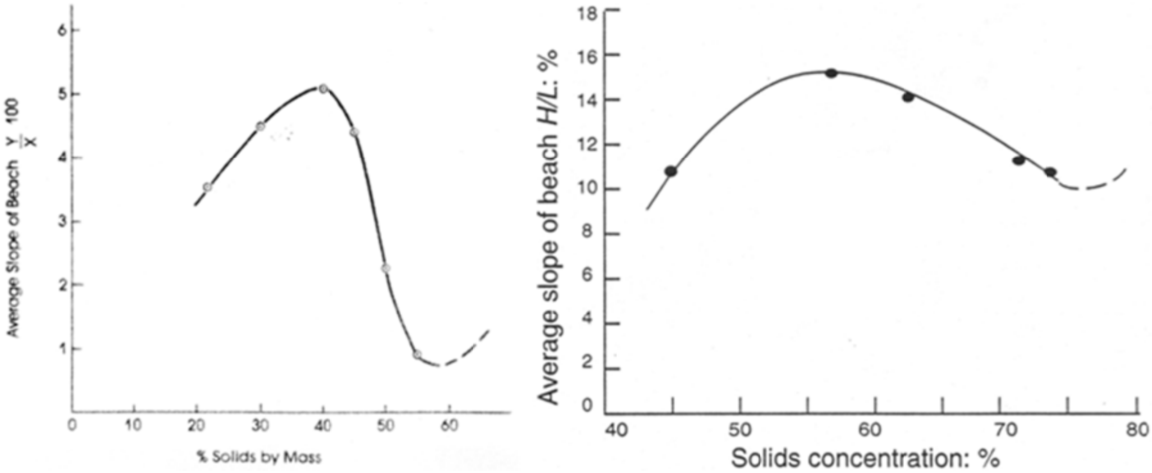

Figure 2.4: Chord slope as a function of solids concentration; left Fly Ash (Blight, 1987) and right Gold (CMSA, 1996)

Blight (1987) also proposes that as the rate of deposition increases the discontinuity between the two regimes will occur at progressively lower solids concentrations. That is higher discharge results in higher velocity and an increased depth of flow resulting in less opportunity for particle settling. This further supports the concept put forward by Wates et al. (1987) and Robinsky (1975) that increasing velocities result in shallower beaches.

2.5 Moisture Loss and Strength Gain

Strength gain is dependant on the increase of inter-particle forces as tailings undergo first sedimentation and settlement followed by some initial consolidation and finally drying. After deposition the velocity of the tailings stream decreases and the solid particles settle out as the water is unable to sustain the shear stress. An initially uniform flocculation/suspension zone is formed however this soon changes into three zones; the supernatant, sedimentation and consolidation zones. In sub-aerial deposition the supernatant runs along the sloping surface and is optimally recovered by decant penstocks (Qiu and Sego, 2006). Often this sedimentation and settlement occurs over a large area and a fan is developed. Depositional strategies are often adopted such that deposition occurs at different locations around the perimeter of the dam over time. This results in active zones in which sedimentation, settlement and initial consolidation occur and dormant zones where drying occurs. The design and operation of tailings facilities requires an understanding of how tailings behave during these various stages.

Sedimentation

The sedimentation behaviour of tailings slurry is often modelled as a pelagic deposition of a sediment column. Two stages are considered to occur simultaneously; a state of dispersion in the uppermost part and an accretion of soil as sediment particles accumulate and consolidate under self-weight. Pane and Schiffman (1985) derived an extended equation which governs the sedimentation and simultaneous consolidation of pelagic sediments. This theory linked the Kynch (1952) theory of sedimentation and the Gibson et al. (1967) theory of non-linear, finite strain consolidation of saturated clays. This was via a constitutive relationship between void ratio and effective stress as illustrated in Figure 2.5. For void ratios greater than e_m the soil-water mixture is truly a suspension and effective stresses are zero and the height of solids is determined by Kynch (1952) theory of hindered settling. For void ratios less than e_s the soil-water mixture is truly a soil and effective stresses are fully active and the interaction coefficient is equal to unity. The height of solids is therefore determined by Gibson et al. (1967) theory of consolidation as a function of permeability and effective stress. At intermediate void ratios the water mixture is no longer a suspension but is not a soil. Pore fluid velocities are still high and thus drag forces are comparable to effective stresses which start to become active. During this stage the interaction coefficient increases from zero at $e_{m,}$ to unity at $e_{s,}$ along path b, however for simplicity this is often assumed to occur along path a. As the height of solids increases the void ratio decreases and if it is assumed that the accumulating soil remains saturated simple phase relationships can be used to determine the water content.

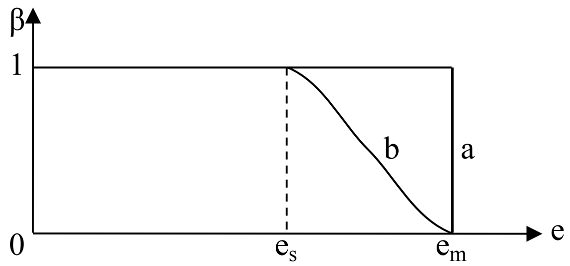

Figure 2.5: Forms of the β constitutive relationship (Pane and Schiffman, 1985)

Data presented by Welff and Wates (2004)[1] based on test work on kimberlitic tailings can be used to illustrate these various interactions during sedimentation. Figure 2.6 is an illustration of the change in water content during sedimentation. The data shows

[1] Welff and Wates (2004) investigated the sedimentation and drying of the coarse and fine fractions of kimberlitic tailings in troughs placed outdoors (but under cover) at ambient temperature. (The extraction of diamonds results in tailings with two distinct size graduations that are often discarded in a single stream. However the two fractions behave differently). Slurries of the respective coarse and fine samples were added to containers, with bleed water removed as settlement took place, and then allowed to dry over a number of days. The sample thickness was also varied during the investigation. Their results have been used to illustrate various changes during sedimentation and drying. A number of graphs are presented; these graphs are interpretations unique to this thesis and are not presented in the original paper.

that the rate and amount of moisture loss is more a function of particle size than sample thickness. The rate is also affected by electrostatic repulsions and attractions which can cause considerable hindrance to settlement when clay minerals are present (Swarbrick and Fell, 1992). However in general when tailings are deposited the coarse material will settle out first and the finer material further down the beach. Initially the rate of moisture loss is rapid as hindered settling occurs, however as the void ratio decreases and effective stresses start to develop the rate reduces. This process continues up until the soil structure has enough strength to sustain the effective stresses; however the strength required is often not significant. Further consolidation would only take place if the effective stresses are increased by for instance additional depositions.

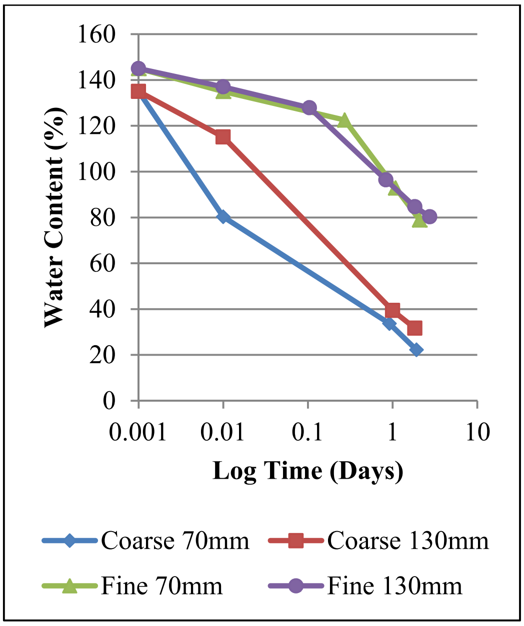

Figure 2.6: Sedimentation Moisture Loss

Tailings sedimentation however often does not occur under pelagic conditions (defined as sedimentation occurring under a large water head that does not change, for example in a marine environment) rather discharge from a deposition point forms a type of alluvial fan. The transportation and deposition of sediments is therefore more analogous to stream sheet flow. Flow along a tailings beach is often characterised by an unstable, meandering, turbulent rill flow (Blight and Bentel, 1983). This results in variations in velocity and depth of flow along the beach. The velocity and sediment size impact whether the sediment is deposited or transported further down the beach. Previously deposited sediment may also be entrained by erosion. The Hjulstom diagram (Figure 2.7) is often used to relate the velocity and particle size to the processes of deposition, transportation and sedimentation. This diagram shows that the velocity required to entrain a particle is higher than is required to transport the particle. Further the velocity required to entrain particles is not proportional to particle size. The velocity required to entrain consolidated clays and silts is comparable to the velocity required to entrain boulders, whereas sands require the least. Unconsolidated clays and silts however can be entrained at lower velocities (Southard, 2006). Most tailings fall within the clay to fine sand region and hence velocities have to reduce significantly for deposition to take place. Another factor that comes into play is the porous and often dry beach onto which deposition takes place. This can result in water rapidly infiltrating and the sediment load being deposited almost immediately. As deposition continues this moves down the beach by the various processes described above. Deposition is also controlled by the water to sediment ratio with debris type flow when the sediment load is high and stream type flow when low. Flow regimes are likely to vary considerably and therefore deposition will range between the different flow types with intermediate mixtures of both (Kehew, 2006). The deposition of tailings is therefore subject to a number of different factors resulting in an often random distribution of particles sizes and slopes along the beach.

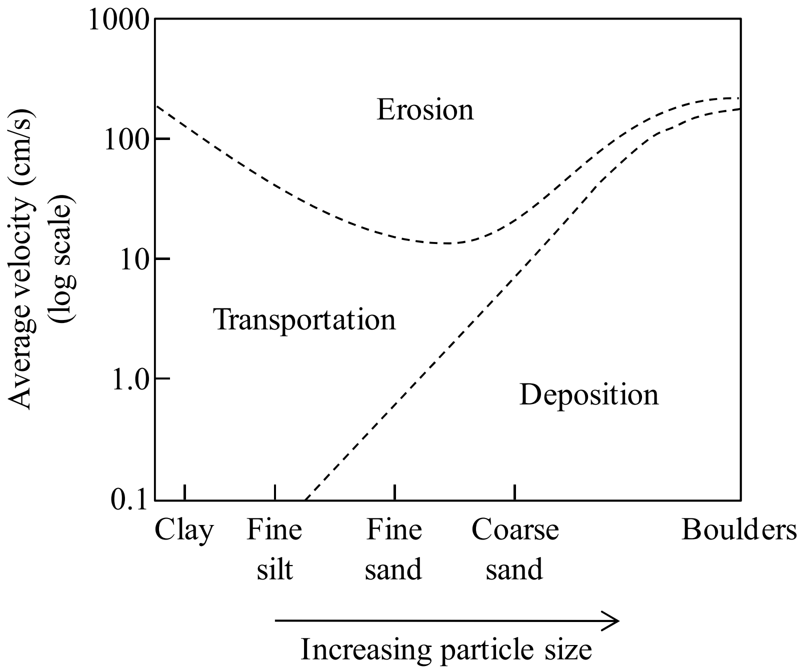

Figure 2.7. Hjulstom diagram, relating stream velocity to particle size for conditions of erosion, transportation and deposition (Kehew, 2006)

Drying

The amount of water in the voids of a fine-grained soil can have a significant influence on its engineering properties. Understanding how the consistency or strength of the tailings changes as moisture is lost is important in determining the risks of failure as the facility is raised. It is important to understand the rate at which moisture is lost (and hence strength gained) and the maximum strength that can be gained. During sedimentation, as already discussed, strength gain ceases when the soil structure can maintain the shear stresses present. Further layers could only be added at a rate sufficient to cater for the rate at which consolidation can occur under these imposed loads. If tailings are added at a higher rate, the inherent shear resistance would be insufficient to retain the deposited solids. In such cases an alternative means of impounding the tailings would be required. The rate at which this occurs is dependent on the permeability of the material and the distance the pore water has to flow to escape. Various authors have shown that Terzaghi's self weight consolidation theory (Donaldson, 1960) (Robinson, 2004) does not fully describe the observed strength gain in arid and semiarid environments. However this strength gain has been attributed to drying by evaporative forces that draw the water out; resulting in an over-consolidated state (i.e. the layer is consolidated more than can be explained by the overburden loading of the layer).

Atterberg limits are often used to describe the change in consistency of a soil on a continuum of changing water content. Atterberg limits are determined on thoroughly remoulded samples and hence any strength as a result of soil structure is lost. However they correlate with engineering properties and behaviour because both the Atterberg limits and the engineering properties are affected by the same things. Six limits were developed by A. Atterberg a Swedish soil scientist in 1911 (cited in Holtz and Kovacs, 1981):

1. Upper limit of viscous flow.
2. Liquid limit – lower limit of viscous flow.
3. Sticky limit – clay loses its adhesion to a metal blade.
4. Cohesion limit – grains cease to cohere to each other.
5. Plastic limit – lower limit of the plastic state.
6. Shrinkage limit – lower limit of volume change (caused by drying).

The liquid limit (LL), plastic limit (PL) and shrinkage limit (SL) are the only limits predominantly used in geotechnical engineering as they can be linked to a various generalised stages of stress-strain response as illustrated in Figure 2.8.

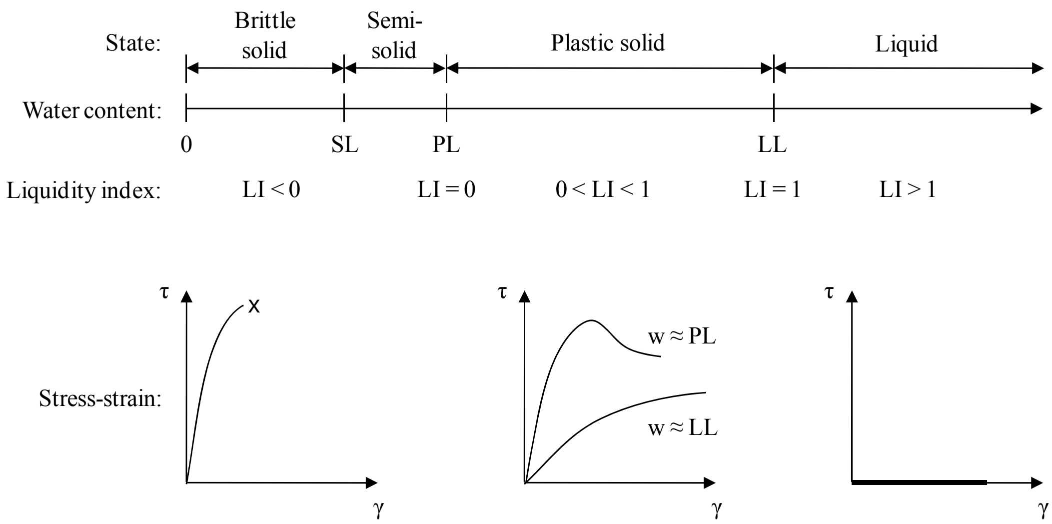

Figure 2.8: Water content continuum showing the various stages of a soil as well as the generalized stress-strain response (Holtz and Kovacs, 1981)

More generally the consistency limits of a fine grained soil can be viewed as remoulded undrained shear strengths. A review of literature by Kayabali and Tufenkci (2010) showed that the undrained shear strength at the LL ranges from 0.5 to 4.0 kPa with most researches concluding that it is around 1.6 to 1.7 kPa. Likewise literature revealed a large range in undrained strengths for remoulded soils at the plastic limit from 20 to 320 kPa. Most researchers proposed that the undrained shear strength for remoulded soils at the plastic limit is around 110 to 170 kPa, mostly towards the lower bound. Kayabali and Tufenkci (2010) investigated the relationship further by conducting a series of extrusion tests at varying water contents and thus determined the undrained shear strength of remoulded soils at the LL and PL. They concluded that the average undrained shear strength of soils at the LL was 2.3 kPa. The average undrained shear strength of remoulded soils at the PL water content was about 180 kPa. Further they proposed that the logarithm of the undrained shear strength and the water content have a linear relationship from which the undrained shear strength can be determined at intermediate water contents between the LL and PL.

The plasticity index (PI) and liquidity index (LI) are defined from these consistency limits. The PI is the numerical difference between the LL and PL, the larger the value the larger the water content range over which the soil will behave as a plastic solid. PI has been found to be empirically correlated with many engineering properties as a consequence. Clay mineral activity tends to increase the PI; unless tailings are derived from clayey weathered ore bodies they generally have low PI values (Vick, 1983). The LI is used to scale the laboratory determined behaviour to the in-situ behaviour and is defined as:

$$LI = \frac{w_n - PL}{PI}$$ **Equation 2.5**

where w_n is the in-situ water content

With reference to Figure 2.8 a soil with an LI less than zero will have brittle fracture if sheared. However this is also dependant on the average imposed stress conditions. Negative LI values are often indicative of heavily overconsolidated soil deposits (Das, 2008) and higher shear strengths (Bovis, 2003). If the LI is between zero and one the soil will behave as a plastic. If the LI is greater than one then the soil will essentially be a viscous liquid. Figure 2.8 indicates that for LI values greater than 1 no shear strength is present however this is not necessarily the case as the liquid soil will have a low degree of shear strength. This is further dependant on the rate of shearing as viscous resistance will be generated. The deposition of tails is dependant on these viscous forces to arrest the flowing stream and bring about deposition of particles. Soils in this state will be extremely sensitive to breakdown if sheared although sensitive clays may be relatively strong in an undisturbed state (Holtz and Kovacs, 1981).

Consistency limits can also be used to determine the susceptibility of tailings to liquefaction. The hydraulic deposition of tailings can result in a loose fill of saturated sandy and silty material. When subject to a large increase in strain, for example as a result of shear stresses imposed by an earthquake or steepening of clay river banks due to erosion, there is a tendency for the material to decrease in volume. This tendency causes a positive increase in pore pressure which results in a decrease in effective stresses within the soil mass. Once the pore pressure becomes equal to the effective stress, the sand/silt loses most of its strength, and it is said to be in a state of liquefaction (Holtz and Kovacs, 1981). The presence of clay minerals can decrease this tendency as the resulting Hydrogen bond and van der Waal bond forces give the material a degree of cohesion. Seed et al. (1964) (citied in Andrews and Martin, 2000) defined the liquid limit as the water content at which a soil has a shear strength of approximately 2.5 kPa. The void ratio can be viewed as a measure of the average inter-grain spacing and can be determined from the water content of a soil. The LL can therefore be viewed as a measure of the grain spacing at which the net attractive forces produce a shear strength of approximately 2.5 kPa. Consequently a silty soil with a high liquid limit will have a high net attractive force and will be less susceptible to liquefaction. Seed et al. (1964) (citied in Andrews and Martin, 2000) therefore provided the following criteria for liquefaction based on various case studies:

Clay content (defined as % finer than 0.05 mm)	<15%
and Liquid Limit (fall cone penetrometer method)	<35
and Water Content (in-situ)	>0.9 x Liquid Limit

Andrews and Martin (2000) refined this criteria based on further case studies and taking into account that clay content is more often defined as % finer than 0.02 mm and the LL determined by the Casagrande method:

Table 2.3: Liquefaction susceptibility of silty soils (Andrews and Martin, 2000)

	Liquid Limit < 32	Liquid Limit ≥ 32
Clay Content < 10%	Susceptible	Further studies required (Considering plastic non-clay sized grains – such as Mica)
Clay Content ≥ 10%	Further studies required (Considering non-plastic clay sized grains – such as mine and quarry tailings)	Not susceptible

In situ water content was excluded from the criteria as this they argued this to be difficult to accurately determine.

The preceding discussion has outlined the framework by which the water content can be used to interpret the apparent strength of tailings once it has undergone sedimentation and desiccation. However the mechanism by which moisture is lost and strength is gained during drying has yet to be defined. As moisture is lost by evaporation capillarity forces as a result of surface tension between water, mineral grains and air are generated. The magnitudes of these forces are inversely proportional to the pore size which in turn is dependant on grain size. Typically tailings particles are fine-grained and hence the capillary forces can be significant. Whilst remaining saturated the surface tension in the water will result in menisci forming at the soil air boundary. As evaporation occurs, pressure decreases and the radii become smaller. Following sedimentation the deposited tailings are still significantly loose and hence still able to compress. The increased surface tension of the reducing menisci radii causes the deposited material to shrink and increase in density. This process continues until the rigidity in the shrinking tailings is equal to the capillary forces. (Holtz and Kovacs, 1981) The water content may continue to decrease. However the rigidity will result in very little further shrinkage and air will start to enter the pore spaces and saturation will drop below unity. This evaporation driven volume change therefore results in an overconsolidated state which allows the rate of rise to exceed the rate of self weight consolidation. Robinson (2004) proposed that the induced void ratio due to evaporation-driven overconsolidation can be related to the normal odometer consolidation curve to determine the rate of rise.

The processes described above are controlled by the Water Retention Curves (WRC) and the Volumetric Shrinkage Curves (VSC). The WRC is typically a plot of (gravimetric or volumetric) water content against suction at constant (zero) total stress. It is often assumed that the void ratio remains constant during testing (enabling saturation to be determined from the water content) however for highly compressible soils this assumption cannot be made. In these cases the volumetric change is also required to determine the change in void ratio. The VSC is therefore typically a plot of volume change against suction or water content at constant (zero) total stress. Three stages of shrinkage can generally be distinguished (Mbonimpa et al., 2006) on a typical VSC and these are illustrated in Figure 2.9 from saturation to full dryness:

1. Saturated (or normal) phase,
2. A combined desaturation-shrinkage (or residual) phase, and
3. A (quasi) constant volume (or no-shrinkage) phase

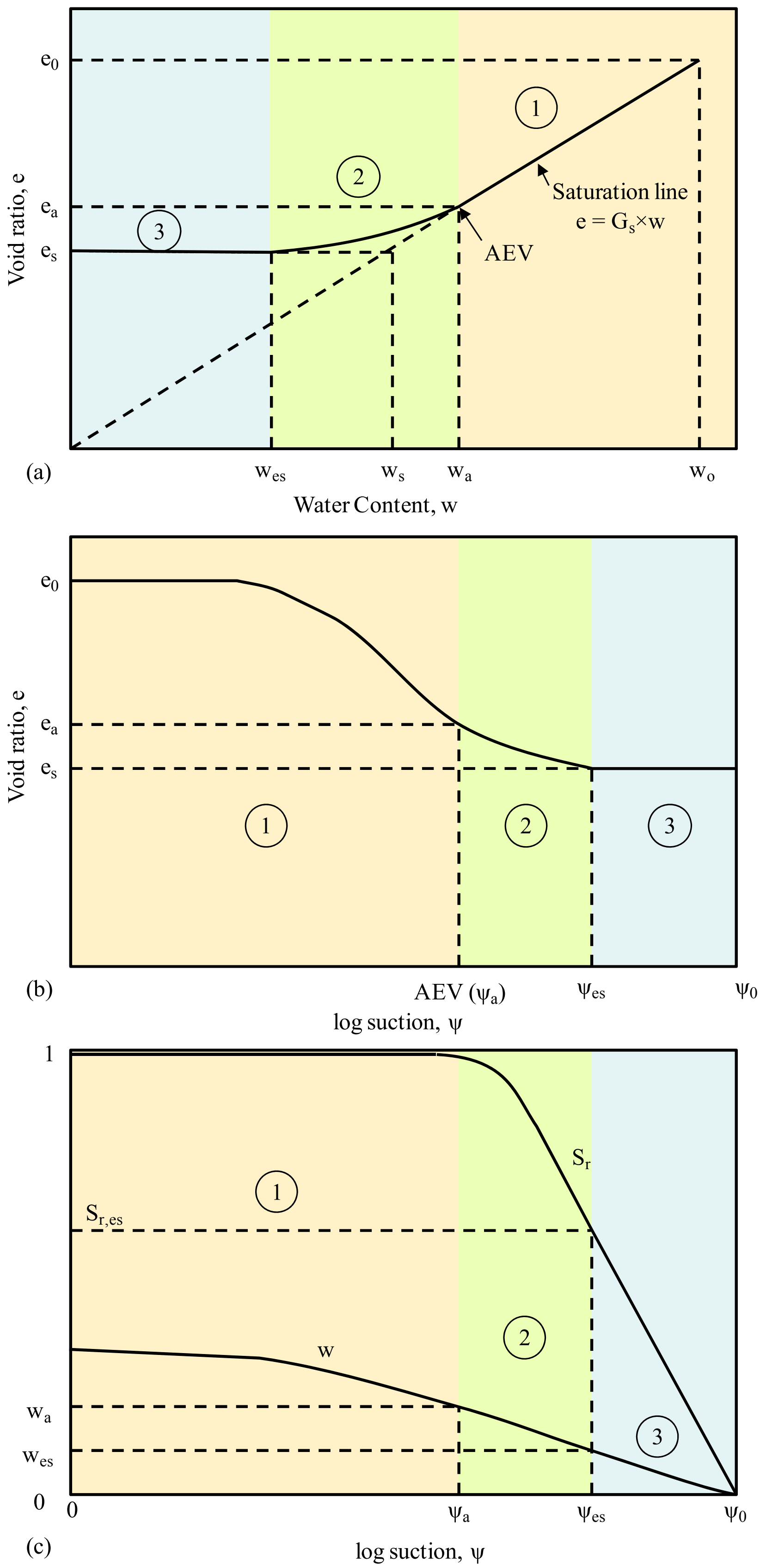

Figure 2.9: Schematic illustration of the shrinkage and desaturation phases in different planes: (a) e-w relationship; (b)e-ψ volumetric shrinkage curve; and (c) water retention curve expressed as w-ψ and S_r-ψ (after Mbonimpa et al., 2006)

In Phase 1 the volume decrease is equal to the volume of water lost as the water remains saturated. Phase 2 begins at the air entry value (AEV) and air starts to enter the voids. Desaturation tends to increase the soils resistance to deformation. In this stage the volume change is smaller than the water loss. In Phase 3 particles are in close proximity and further volume change becomes negligible. The true shrinkage limit, w_{es} (%), is the upper bound of the water content corresponding to Phase 3. However in géotechnique the shrinkage limit, w_s (%), is the water content on the saturation line at a void ratio of e_s (Mbonimpa et al., 2006).

Moisture movement within a tailings deposit is dominantly as a result of gravitational and potential gradient differences. Potential gradients are formed as suction forces are generated due to capillarity with movement from areas of low potential to areas of high potential. Initially movement is by gravitational forces as the entire profile is saturated following a deposition. However as the water content decreases due to evaporation at the surface a degree of desaturation occurs and gravitational flow becomes negligible as capillarity induced suctions induce potential differences. The water content at which this occurs is defined as field capacity (Miller and Donahue, 1990). Field capacity is important as it is the equilibrium point between gravitational and potential induced water movements, thus depending on the availability of moisture, the water content within a soil profile will be maintained at this value.

Field capacity is often thought of as an intrinsic property of a soil, however a number of methods are proposed for determining its value and these lead to various non hydraulic characteristics influencing its value (Meyer and Gee, 1999). Classically it is defined as the water content at a suction of 33 kPa although this reference is often closer to 10 to 20 kPa (Miller and Donahue, 1990). The potential at which field capacity occurs is also dependant on the groundwater regime. When this is relatively stable and at a shallow depth field capacity corresponds with hydrostatic equilibrium with the groundwater, however when the ground water table is deep field capacity generally shows suctions of 33 kPa (Koorevaar et al., 1999). Field capacity has also been defined as the water content at which drainage fluxes become negligible. Hydraulic conductivity is fairly constant when a soil is saturated however as it desaturates this conductivity reduces. Meyer and Gee (1999) proposed that field capacity is reached when fluxes are between 10^{-11} and 10^{-9} m s^{-1}, dependant on the soil texture. Ratliff et al. (1983) proposed that field capacity can be determined in the field when the water content decreases by 0.1 to 0.2 % water content per day. With this definition they defined the field capacity for 401 field soil samples and compared these to pressure determined laboratory values. They found that for morphologically similar soils minor variations in soil properties give rise to different values of field capacity. With higher values predominantly as a result of higher clay contents. For similar soil textures they found the average standard deviation of field determined values was 4.9 % and 3.6 % for laboratory determined values. They also found that for finer soils the pressure plate method under predicted the in situ field capacity with the opposite being the case for coarser soils. As a consequence they conclude that when absolute accuracy is required field determined values are to be preferred.

The decrease in water content is dependant on the availability of moisture to replenish deficits. For the potential (larger suctions) to increase past field capacity the phreatic surface needs to be sufficiently depressed to result in high capillarity forces. Within a tailings dam the phreatic regime is known to originate from the pond of supernatant water at the surface becoming depressed towards the periphery of the facility (Blight et al., 1985). This phreatic regime is constantly replenished during active deposition. The depth of the depositional surface to the phreatic surface is therefore a function of both the length of the beach and the height of the facility. The impact of this depth to the phreatic surface and the suctions that can be maintained, to the author's knowledge, has not been extensively investigated.

Evaporation from bare soil is often characterized as occurring in two distinct stages. Stage one is often termed the "energy limited" stage, during which moisture is available or transported to the near soil surface at a rate sufficient to supply the potential rate of evaporation. This rate is defined by the energy available at the surface. Stage two often termed the "falling rate" or "soil limited stage" is where the hydraulic properties of the soil are unable to supply moisture at the potential evaporation rate. During this stage the soil appears dry and a portion of the evaporation occurs from below the soil surface. The subsurface evaporation is caused by transport of heat from the soil surface into the soil profile. Allen et al. (2005b) analysed a number of soils and determined that the change from stage one to stage two evaporation occurs at a water content value between the field capacity and wilting point. The wilting point is defined as the water content at a suction of 1500 kPa (Miller and Donahue, 1990). Stage two continues until the water content is half the wilting point, which is presumed to approximate the air dry water content.

Results reported by Welff and Wates (2004) into the drying of diamond tails are presented to illustrate some of the changes outlined in the preceding discussion. A VSC of dry density on a continuum of water content from their tests is presented in Figure 2.10. A distinction is made between the values obtained during sedimentation and drying. The amount of volume change during sedimentation appears to be dependent on particle size with the coarse samples undergoing the largest change. The maximum dry density reached by drying was also dependant on the grain size. This maximum dry density is related to the point at which air entry occurs. Fredlund et al. (2002) showed that the air entry value is inversely proportional to the pore size which can be assumed to be proportional to the grain size. Thus the research by Welff and Wates (2004) illustrates this phenomenon. Once desaturation began Welff and Wates (2004) reported that the samples began to crack however no volume correction was done. This likely lead to an underestimation of the dry density and the discrepancy between the dry densities reached for the different size samples. However the larger volume of water that had to be removed from the thicker samples may have also contributed to the differences. The difference is not significant and the range of dry densities in the field is likely to exceed this laboratory difference.

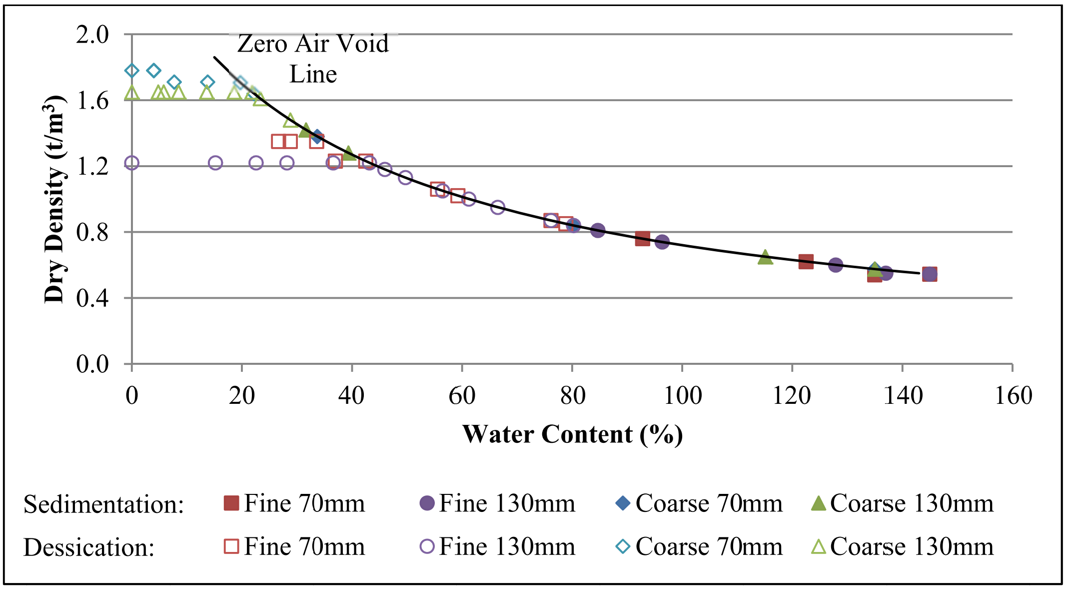

Figure 2.10: Change in dry density as a consequence of moisture loss

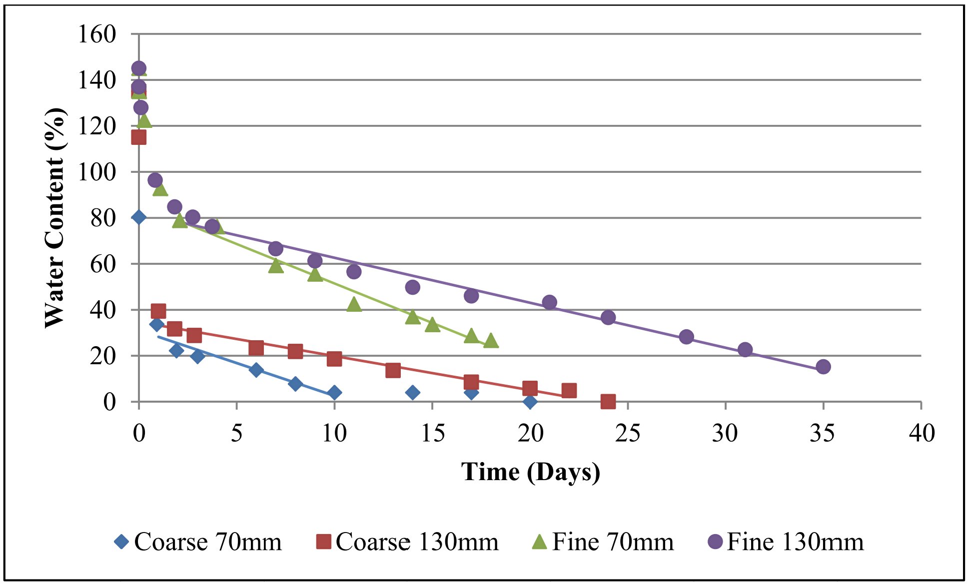

Figure 2.11: Sedimentation and drying moisture loss

Figure 2.11 illustrates that the rate at which moisture was lost appeared to remain constant for the respective samples over the entire drying period except for the 70 mm coarse sample. At a very low water content the rate decreased dramatically for the 70 mm coarse sample. This is likely the point at which stage two evaporation started which as shown by (Allen et al., 2005b) generally occurs at a low water content. Based on the change in water content it would appear that the thinner samples lost moisture faster than the thicker samples. However the rate at which the gravimetric water content decreased for the thinner samples was roughly twice the rate at which the thicker samples did. This corresponds to the fact that the thinner sample was roughly half the thickness of the thicker sample. Thus although on a mass basis the rates are different on a volumetric basis the rates are the same.

Numerical modelling allows parametric studies to be undertaken to determine the influence of variations in deposition strategies. Various models have been proposed by Swarbrick and Fell (1992), Fahey and Toh (1992) and Qiu and Sego (2006). These models employ a combination of soil physics, large strain consolidation theory, empirical relationships from laboratory work and various assumptions for the behaviour during the different deposition stages. Model parameters for platinum and gold tailings in South Africa based on the Swarbrick and Fell (1992) model that predicts water contents and dry densities have been developed by Boshoff (2002) and Wortmann (2007). Numerical modelling is not addressed further in this thesis however interested readers are referred to the above authors for further information.

2.6 Reference Evapotranspiration

Evaporation, Transpiration and Evapotranspiration

As outlined above the contributions of evaporation to strength gain in sub-aerial deposited tailings in arid climates (i.e. net annual evaporation exceeds net annual rainfall) must be taken into account. Thus knowledge of the mechanisms that control evaporation is essential if one is to predict the consolidation of tailings. Evaporation is the process whereby liquid water is transformed into the gas phase as a result of an increase in molecular energy. Direct solar radiation and, to a lesser extent, the ambient temperature of the air provide this energy. After sunset energy stored within the evaporating surface is the only remaining source of energy (Blight, 2009). The driving force to remove water vapour from the evaporating surface is the difference between the water vapour pressure at the evaporating surface and that of the surrounding atmosphere. As evaporation proceeds, the surrounding air becomes gradually saturated and the process will slow down and might stop if the moist air is not transferred to the atmosphere. The replacement of the saturated air with drier air depends greatly on wind speed. Hence, solar radiation, air humidity, air temperature and wind speed are climatological parameters to consider when assessing the evaporation process (Allen et al., 1998). Appendix D contains a more extensive review of how these various climatological parameters influence the rate of evaporation.

Transpiration is the vaporisation of liquid water contained in plant tissues and its subsequent transfer to the environment. In many natural systems water is lost from the soil by a combination of transpiration and evaporation. Due to the importance of understanding water loss from cropped soils in agricultural science transpiration and evaporation are combined and termed evapotranspiration. Factors that control transpiration are similar to the climatic factors that control evaporation. However crop type, stage of crop development and crop management influence the amount of transpiration. For instance at sowing nearly 100% of the evapotranspiration is from evaporation, while at full crop cover more than 90% of evapotranspiration is from transpiration (Allen et al., 1998).

Measuring Evapotranspiration

In general, two types of problems have characterised attempts to measure evapotranspiration. First the scientific problem of understanding the physics of evapotranspiration from which complex ideas and experimental methods have developed. The second problem is evaluating the pedological and botanical parameters contributing to evapotranspiration. Table 2.4 summaries a review of various methods by Kairu (1991).

Table 2.4: Techniques for measuring evapotranspiration

Techniques	Details
Lysiméteric Methods	A block of soil as identical as possible to the surroundings is isolated so that the changing water content can be measured by changes in mass. They are the only direct measure of water flux and consequently have often been used as a standard to which other methods are compared.
Sap-based Methods	The rate at which evapotranspiration from a plant can be measured by monitoring the flow of sap within the xylem system.
Eddy Correlation Models	Water vapour, heat, CO_2 and other atmospheric substances are transported vertically by eddies. By measuring the fluxes of these eddies and assuming that atmospheric eddies transport the above substances with equal facility evapotranspiration can be estimated.
Mass Transport Models	Such models empirically relate evaporation to the difference in vapour pressure between the evaporating surface and a reference point above it. In practice it is difficult to measure the vapour pressure at the surface unless it is saturated and so this method is often limited to open water surfaces such as lakes. Dalton in 1802 was the first to develop such a method.
Aerodynamic Models	The aerodynamic approach rests on the assumption that the upward flow of water vapour is equal to the product of the vertical gradient of specific humidity and the rate of air mixing. An example of such a method was proposed by Thornthwaite and Holzman (1942). Aerodynamic methods yield sufficiently accurate results for most applications. However, these methods have stringent requirements for adequate fetch.

Resistance Models	Resistance models are based on the premise that the transport of water vapour is directly proportional to the gradient in vapour pressure from the evaporating surface to the air and inversely proportional to the sum of the aerial and substomatal resistances to the transport of water vapour. Monteith (1963) developed such a model based on canopy (bulk stomatal) and atmospheric resistance.
Energy Balance Methods	Energy balance methods are based on the assumption that the energy received by a surface through radiation (and advection) equals the energy used for evaporation and heating of the air and soil plus advection. The Bowen ratio was proposed to simplify energy balance based methods.
Combination Methods	The Penman model (1948) combines the aerodynamic and energy balance methods and was original developed to estimate evaporation from water surfaces. Monteith (1965) modified Penman's model for application to vegetated canopies by including canopy and atmospheric resistances.
Pan Methods	Evapotranspiration can be estimated empirically from the evaporation of water from an open pan. The water evaporated gives an indication of the integrated effect of radiation, wind, temperature and humidity.
Empirical Methods	Thornthwaite (1948), Blaney and Criddle (1950) and Hargreaves and Samani (1985) developed empirical methods of estimating evapotranspiration based on air temperatures. Makkink (1957) developed a method based on a single radiation term.

FAO-56 Methods

Due to the importance of evapotranspiration to the agrarian sciences the Food and Agriculture Organisation (FAO) of the United Nations (UN) undertook to investigate and define the most suitable methods for determining reference evapotranspiration under various climatic conditions. To meet this aim a group of experts within the field were convened in 1990 to review the available methods and following 8 years of research and consultation the FAO Irrigation and Drainage Paper No. 56 was published (Allen et al., 1998).

Figure 2.1 illustrates the basis for the method presented in FAO 56. As already stated evapotranspiration is influenced by crop stage and management, thus a grass reference surface was outlined so that the reference evapotranspiration is purely a result of the climatic conditions of a site. This surface is a hypothetical grass with an assumed crop height of 0.12 m, a fixed surface resistance of 70 s m^{-1} and an albedo of 0.23. This surface closely resembles an extensive green, well watered (irrigated weekly) grass of uniform height, actively growing and completely shading the ground. Consumptive water use for a particular crop can then be obtained by the crop coefficient–reference evapotranspiration (K_c-ET_o) procedure. The K_c value as defined are therefore predominately dependent on crop characteristics. This enables the transfer of standard values and curves for K_c between locations and climates. (Allen et al., 2005b).

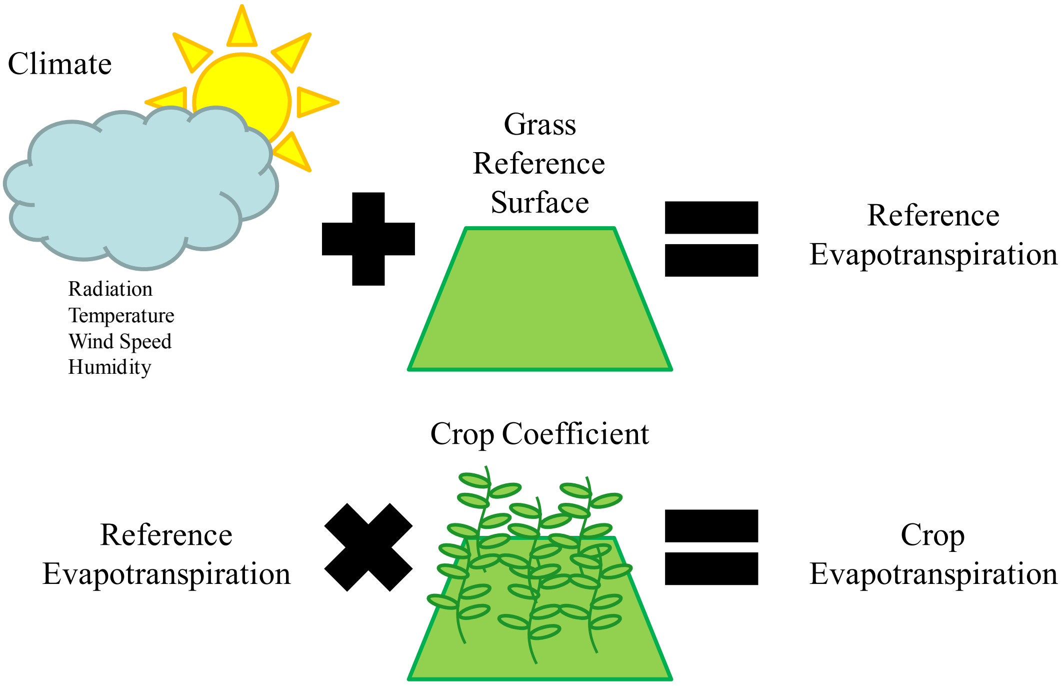

Figure 2.12: Basis of FAO 56 (after Allen et al., 1998)

Various different methods of determining reference evapotranspiration were then investigated under the auspices of the American Society of Civil Engineering (ASCE) Committee on Irrigation Water Requirements and the European Community. These studies involved comparing carefully screened lysimeter data to various other methods of determining evapotranspiration across variable climatic conditions. As a result the FAO Penman-Monteith method (referred to as FAO 56 – PM) was adopted as the sole standard method due to its relatively accurate and consistent performance under both arid and humid climates. The FAO 56 – PM equation is derived from the original Penman-Monteith equation and equations for aerodynamic and surface resistance and is presented below:

$$ET_{o,\,FAO\text{-}56PM} = \frac{0.408\Delta(R_n - G) + \gamma \frac{900}{T+273} u_2 (e_s - e_a)}{\Delta + \gamma(1 + 0.34 u_2)} \qquad \textbf{Equation 2.6}$$

where ET_o is the reference evapotranspiration in mm day^{-1}
R_n is the net radiation at the crop surface in MJ m^{-2} day^{-1}
G is the soil heat flux density in MJ m^{-2} day^{-1}
T is the air temperature at a height of 2 m in °C
u_2 is the wind speed at a height of 2 m in ms^{-1}
e_s is the saturation vapour pressure in kPa

e_a is the actual vapour pressure in kPa
$e_s - e_a$ is the vapour pressure deficit in kPa
Δ is the slope of the vapour pressure temperature curve in kPa °C^{-1}
γ is the psychrometric constant in kPa °C^{-1}

Appendix E outlines how this equation can be used to calculate the reference evapotranspiration for different time steps and includes procedures for applying the equation when climatic data is missing.

When no solar radiation, relative humidity and/or wind speed is available FAO 56 recommends that reference evapotranspiration be estimated with the Hargreaves method;

$$ET_{o,\text{ Hargreaves Method}} = 0.0023 \times (T_{mean} + 17.8) \times \sqrt{(T_{max} - T_{min})} \times R_a \quad \textbf{Equation 2.7}$$

where ET_o and R_a are expressed in mm day^{-1}
T_{mean}, T_{max} and T_{min} are expressed in °C

A regional calibration can be undertaken by comparing ET_o values calculated via the Hargreaves Method to the FAO 56 – PM method using the following relationship;

$$ET_{o,\text{ FAO-56 PM}} = a \times ET_{o,\text{ Hargreaves Method}} + b \quad \textbf{Equation 2.8}$$

where a and b are coefficients determined by linear regression

The principles behind the Hargreaves method were developed from experience gained in managing irrigation in the very arid, arid and semiarid climates of California's agricultural regions. Research was initiated in 1938 and augmented by research in various other global regions under USAID initiatives. The first Hargreaves method was proposed in 1975 and was based on eight years of daily cool season grass evapotranspiration and weather data from precision weighing lysimeters operated at Davis California. This method was updated following further investigation and data sets from various other climates leading to the current method penned in 1985. In 1993 the Hargreaves method was assessed against data from 3000 globally distributed weather stations and again in 2001 against 56 000 globally distributed sites and was found to be universally applicable. However the Hargreaves method tended to under predict in climates with high wind conditions and to over predict in climates with high relative humidity. Often a concern in estimating reference evapotranspiration is the condition of the reference grass surface which requires regular watering often not practical in arid climates. Research based on 580 globally distributed sites found that under such conditions the Hargreaves method is a better estimator of reference evapotranspiration in both arid and humid environments to the full FAO 56 – PM method. This is a consequence of the combination equation assuming steady-state and equilibrium aerodynamic conditions which rely on a well watered evaporating surface (Hargreaves and Allen, 2003).

A historical method of evaluating evaporation is the use of evaporation pans which give an indication of the integrated effect of radiation, wind, temperature and humidity. Pan evaporation is highly dependent on the microclimatic conditions surrounding the pan and the management of the pan. These factors can result in errors in the determination of evaporation. A number of different pans are used such as the Class A-Pan, Colorado Sunken Pan and Symon's pan. Evaporation from the respective pans differs as does the evaporation from non representative surfaces. As such various conversion formulae have been proposed such as those by Bosman (1990). Further conversion factors are necessary to convert pan evaporation to reference evapotranspiration. These pan coefficients take into account the class of pan, surrounding ground cover, average relative humidity and wind conditions. FAO 56 suggests pan coefficients for A-Pans and Colorado Sunken Pans which are applied according to the following equation:

$$ET_o = k_p E_{pan}$$ **Equation 2.9**

Appendix E outlines the how an appropriate pan coefficient should be chosen based on pan type, ground cover under the pan and the surroundings, as well as general wind and humidity conditions.

Benli et al. (2010) reviewed research by DehghaniSanij et al. (2004), Berengena and Gavilán (2005), López-Urrea et al. (2006) and Benli et al. (2006) in arid to semiarid climates indicating the FAO 56 – PM method to be generally superior with variable results from other methods. Benli et al. (2010) reported their own research comparing various methods of estimating evapotranspiration to carefully collected lysimeter data over a 3 year period. The lysimeter was a semielectronic weighing device that ensured high accuracy. Meteorological data was then collected along with Class A pan evaporation data. Figure 2.13 reproduced from the paper illustrates the superior performance of the FAO 56 – PM method to the Hargreaves and A-Pan methods. A disadvantage of the full FAO 56 – PM method is the requirement for temperature, relative humidity, wind speed and radiation data which are often not all available. The FAO 56 document therefore outlines methods for estimating missing data. Benli et al. (2010) instigated these various methods and found them to be acceptable for estimating evapotranspiration.

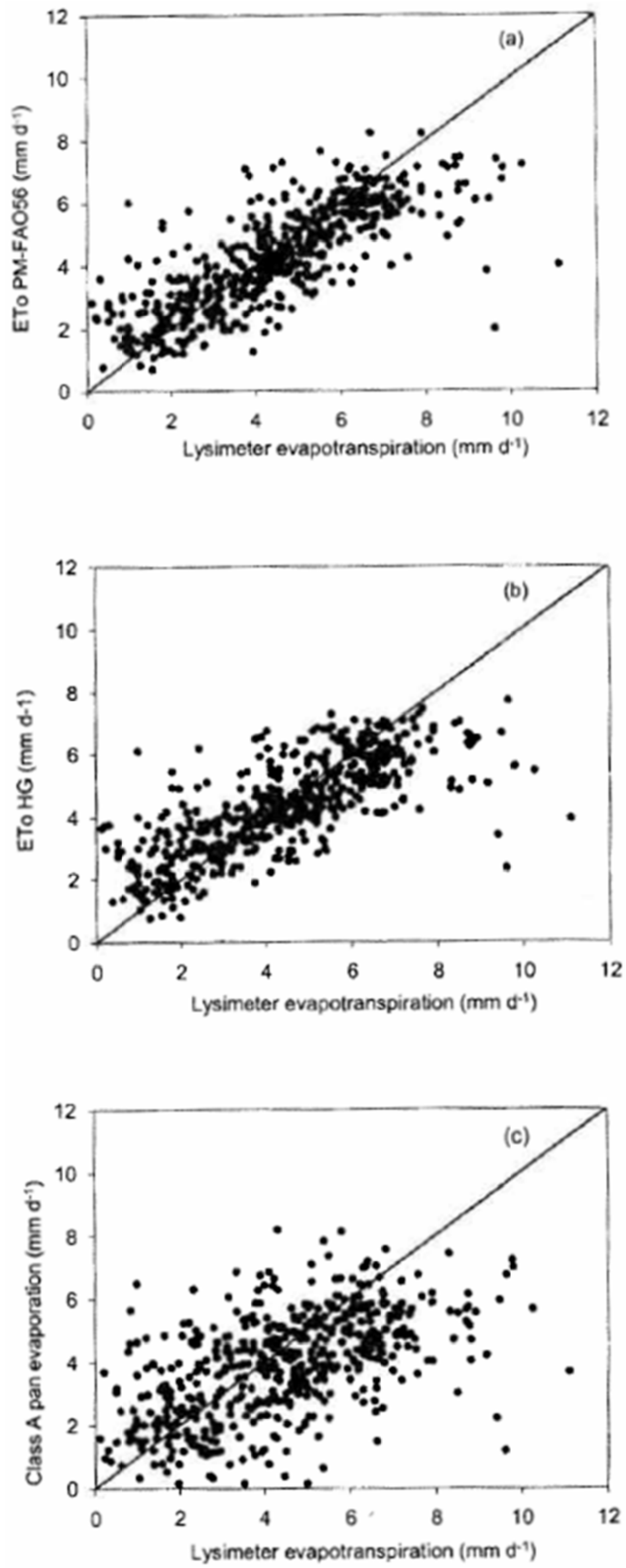

Figure 2.13: Comparison of evapotranspiration methods (Benli et al., 2010)

Application in Tailings Management

The nature of tailings facilities is that transpiration is unlikely to occur extensively on the surface of the dam however it is possible to occur on the vegetated side slopes. Which is only sustainable during construction for dams constructed by the upstream method. Furthermore in tailings management it is the expulsion of water that is critical not the point at which a soil has to be irrigated to improve crop yields. During a crop cycle initial stages are often characterised by a bare soil from which seeds emerge and hence crop coefficients have been developed for this period (Allen et al., 2005b). It is thus not unusual to apply reference evapotranspiration rates to the drying of soils as would be the case in tailings management. However to the author's knowledge reference evapotranspiration has not been used to predict the loss of moisture that leads to strength gain in tailings.

Chapter 3 Methodology

3.1 Experimental Rationale

3.2 Test Site

Test work was carried out at the Anglo American Platinum Mogalakwena Mine roughly 30 km north of Mokopane in South Africa (Latitude: 23°59'S, Longitude: 28°56'E). The Platreef ore body is mined by conventional open cast methods from 5 pits along the reef outcrop. Two plants process the ore through crushing, milling and flotation to produce a metal bearing concentrate and a disposable tailings component. Tailings Dam 1 was originally commissioned in 1991 and served the South Plant. Tailings Dam 2 was commissioned as an extension to Tailings Dam 1 in 2004 so as to split tailings from the South Plant between the two dams.

Tailings Dam 1 construction was originally planned to be done by cyclone methods however after commissioning it became apparent that the underflow was insufficient for wall construction. From this point onwards the dam was developed as a spigot dam. Tailings Dam 2 was designed and initially operated in a similar fashion to Tailings Dam 1. The Mogalakwena North Expansion project resulted in an additional North Plant commissioned in 2008. However due to land claim and social issues Tailings Dam 3 was not commissioned timeously to receive tailings from the North Plant. As a result Tailings Dam 2 was converted into an impoundment dam with walls constructed from waste rock necessary to safely contain the increased volume of tailings. Thus Tailings Dam 1 received the full 385 ktpm of tailings from South Plant and Tailings Dam 2 received the full 700 ktpm from North Plant. The Mogalakwena Tailings complex was therefore chosen for the large-scale field testing due to the two back-to-back dams receiving similar tailings at different rates of rise.

The entire tailings dam complex is underlain by pyroxenite of the Bushveld Complex which is approximately 15 m in thickness. The pyroxenite is underlain by a highly fractured rock horizon containing an aquifer. On initial commissioning of Tailings Dam 1 considerable serpentine was found in the ore body which contains higher portions of talcs and nickel. Thus the ore body has a relatively lower hardness index than the standard Merensky Reef resulting in a significant portion of fine material. This fine material has the propensity to form very fine layers with low permeability within the tailings dam. Metallurgical test work on the ore found that a considerable amount of platinum group metals (PGM) was trapped in particles less than 10 µm. As a result test work into using IsaMill technology to produce a finer grind was undertaken (Anyimadu et al., 2006). As a result a program was put in place to introduce IsaMill technology to the plants at Mogalakwena.

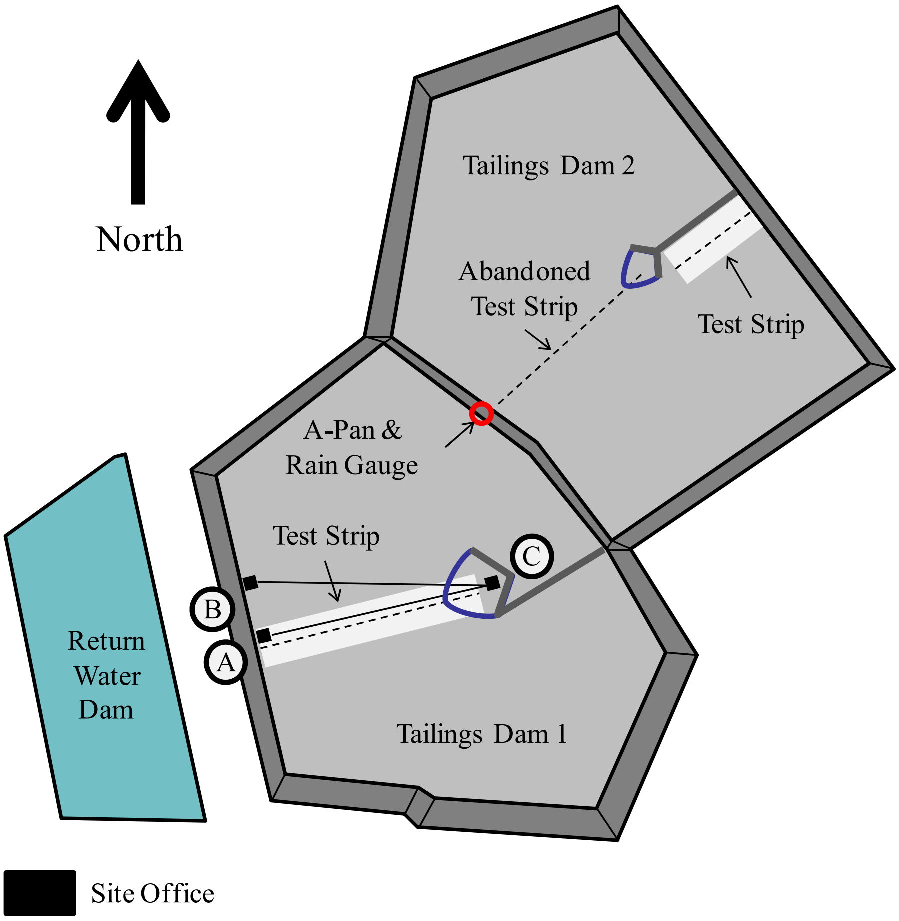

Figure 3.1: Test site layout

Figure 3.1 illustrates the various components of the large-scale field test site. Two test strips were used on each tailings dam however the envisaged test strip on Tailings Dam 2 had to be changed due to operational constraints. A rain gauge and an A-pan were placed on the dividing wall between the two dams to monitor evaporation and rainfall. A min-max mercury thermometer was located at the site offices and used to determine minimum and maximum temperatures during field work. The site office also had a small laboratory where gravimetric water contents were determined.

3.3 Data Capture

Climatic Data

1. *Site Data.* The following site climate data was collected:
    a. Maximum and minimum temperature at roughly 6:45 daily using a mercury thermometer. A possible drawback to the data was that the thermometer was not placed within a Stevenson screen. However it was attached to a large Marula tree and therefore was adequately shaded throughout the year. At the start of the study some data was not collected and therefore an interpolation was developed based on data

from the South African Weather Services station at Mokopane. Appendix F contains details of this interpolation.

b. Rainfall and evaporation data was collected with a rain gauge and an A-pan evaporation tank. Initially the A-pan was located at the crest of the dam wall. As a result a microclimate developed as wind was funnelled up the wall. This resulted in very erratic evaporation values consequently the A-pan was moved to a more central position on the facility between the two dams at the end of March 2010. During the analysis of the data it was apparent that the A-Pan had not been calibrated correctly therefore a calibration exercise was carried out in June 2011. Details of this exercise are contained within Appendix F.

2. *South African Weather Service Records.* In addition to mine temperature records meteorological data, outlined in Table 3.1, was obtained from the South African Weather Service Mokopane Station (Latitude: 24°12'18"S, Longitude: 29°00'40"E, Elevation 1107 m).

Table 3.1: SAWS Mokopane Weather Station Data

Data	Description
Temperature	Hourly Averages, Daily Averages, Daily Maximum and Minimum Values
Wind Speed	Hourly Averages, Daily Averages, Daily Maximum Value
Relative Humidity	Hourly Averages, Daily Averages, Daily Maximum and Minimum Values

The test site was roughly 25 km north and 8 km west of the weather station. Data was sourced from 1 January 2010 until 31 December 2010 however temperature and relative humidity data was missing for 20 April 2010. The method used to interpolate the data for this day is outlined in Appendix F.

Slurry Feed

1. *Field Samples.* A bulk 20 l sample of the South Plant feed to Tailings Dam 1 was taken on the final day of the first deposition on the test strip (see below for description of test strips). The particle size distribution of the sample was analysed at the University of Witwatersrand. A possible limitation to this study is that a similar sample was not taken from the North Plant feed.
2. *Plant Samples.* Tails grading data were obtained from the North and South Plants for the duration of the study. North Plant recorded grading data for particles size; 0.150 mm, 0.106 mm, 0.075 mm and 0.053 mm. Whereas South Plant recorded grading data for particles size; 0.150 mm, 0.106 mm and 0.075 mm. Plant records of the slurry density and flow rates to the tailings facilities were also obtained over the entire testing period.

Laboratory Data

1. *Current Study*. As part of the current study the following data were determined from tests at the University of Witwatersrand:
    i. Particle size distributions
    ii. Particle specific gravity
    iii. Water content-suction curves on samples dried under atmospheric conditions using calibrated gypsum blocks. A sample of tailings was placed in a small plastic bucket with a depth of 120mm and a diameter of 150mm insulated within a box by 25mm of dry wood shavings. Two gypsum block sensors were placed centrally 20mm and 100mm below the surface.
    iv. Two series of triaxial permeability tests were also carried out.
2. *SRK Consulting Reports*. The following data were obtained from studies previously done by SRK Consulting on the Mogalakwena tailings:
    a. To understand the impact of a finer grind on the geotechnical properties as well as the possible change of depositional strategy to a thickened or paste disposal the University of Witwatersrand did a number of laboratory tests. The following samples were tested to model the various anticipated grind and slurry densities:
        i. A blend of 66% of a 80% finer than 75 μm material and 33% of a 80% finer than 45 μm material by mass at a slurry density of 1.59 t m^{-3}.
        ii. 100% of a 80% finer than 45 μm material at a slurry density of 1.59 t m^{-3}.
        iii. 100% of a 80% finer than 75 μm material at a slurry density of 1.77 and 1.88 t m^{-3} respectively.
        iv. 100% of a 80% finer than 45 μm material at a slurry density of 1.77 and 1.88 t m^{-3} respectively.

    Although a number of tests were undertaken only the following information was used from these reports in the research reported here:
        i. Particle size distribution
        ii. Atterberg limits
        iii. Flume box tests
        iv. Slurry settling test
        v. Evaporative drying tests
    b. The following data were obtained from a report by SRK Consulting on the stability of Tailings Dam 1 based on test work undertaken by the University of Pretoria:
        i. Water content-suction curve using the filter paper method. The contact filter paper method was used to measure matric

suctions. Whatman no. 42 filter paper was used with the Hamblin (1981) calibration reference.

c. The following data were obtained from a report by SRK Consulting on thickened finer tails based on test work undertaken by BM Du Plessis Civil Engineering:
    i. Particle size distribution
    ii. Atterberg limits

Test Strips

1. *Sampling Points and Deposition Regimes.* Sampling points on the two deposition strips were marked out by poles set every 50 m along the beach, Tailings Dam 1 was marked from 0 to 392 m and Tailings Dam 2 was marked from 0 to 200 m. This length was determined by the beach length with the pools 130 m from the last pole on Tailings Dam 1 and 80 m from the last pole on Tailings Dam 2. Regression was used to determine the entire beach profile, Appendix G summarises the approach taken. During the testing period four depositions were made on Tailings Dam 1 and three depositions were made on Tailings Dam 2 the details of which are summarised in Table 3.2.

Table 3.2: Deposition details

Test Strip	Deposition	Dates
Tailings Dam 1	1	12 January to 17 January
	2	2 March to 10 March
	3	12 April to 23 April†
	4	8 June to 18 June
Tailings Dam 2	1	21 July to 26 July
	2	10 September to 19 September
	3	19 October to 26 October

† On the 4th of May the test strip was flooded beyond a distance of 100 m due to operational constraints however measurements were still carried out.

Access to the beach was necessary to take samples and survey the beach profile over the period of investigation. The initial solution involved a catamaran which was towed by a steel cable attached to a winch system. Cable guide pulleys were located on specifically built anchor blocks, which were located with reference to Figure 3.1 at A, B and C allowing the boat to traverse between A and C. This system was successfully used on Tailings Dam 1 however insurmountable difficulties with trying to transfer the cable across the tailings in Tailings Dam 2 without embedding it required a different solution. The solution was to use a different test strip that ran 30 m from pool wall leading to the decant penstocks of Tailings Dam 2. Test positions were accessed by laying down old conveyor belt and wooden scaffold planks which were taken up after each recording.

Figure 3.2: Beach access; winch on left and catamaran on right

2. *Beach Profile.* It was anticipated that each deposited layer would be 400 mm in thickness and so a means to survey the deposited slurry was required. The top of each pole was surveyed and the height of the slurry determined by measuring the height below the pole with a tape measure. On Tailings Dam 1 the final height immediately after deposition was ceased was measured. On Tailings Dam 2 the final height after deposition was measured and the height was recorded preceding the next deposition. This gave an indication of the settlement and consolidation of the tailings during the drying period.

3. *Beach Segregation.* At the ends of the first and third deposition on Tailings Dam 1 samples were taken to determine the particle size distribution along the beach. Three separate samples were taken after the first deposition to check the variability in grading at sampling points. Only one sample was taken after the third deposition as the variability was not significant. Single samples were also taken following the first and third depositions on Tailings Dam 2. These samples also allowed the particle specific gravity, G_S, to be determined along the beach.

4. *Moisture Loss.* Due to the constraints of working on slurries still gaining strength two methods were adopted for taking samples:
    a. *Grab Samples.* On the two days following deposition grab samples from the slurry were taken as it was undergoing sedimentation.
    b. *Auger Samples.* A hand held auger was used to take samples below the surface of the beach. However this could only be done once sufficient strength was gained to prevent collapse of the auger hole. This drying time ranged between 1 and 2 weeks depending on the season. Auger holes were always undertaken within a 5 m radius of the 50 m marker poles. Each deposition was roughly 400 mm in depth and thus the auger hole depth was increased by 500 mm after each deposition ensuring that all deposited layers were tested during the entire period.

The auger was marked every 200 mm and once this depth was reached the auger was removed. A 150 mm steel nail was used to place a sample from the auger tip into a cleaned sampling tin of known weight and labelled. The auger hole was then backfilled with subsequent auger holes avoiding previous holes.

Immediately after the field work the respective samples were returned to the on site laboratory and weighed. Samples were then dried at 110 ^{o}C in an oven for 12 h and the dry weight determined. The gravimetric water content was then determined from the various weights recorded. Finally the sample tins were cleaned and weighed ready for the next sampling.

3.4 Data Analysis

Slurry Feed

1. *Impact of IsaMilling*. Plant tailings grading data was analysed to determine the impact of the introduction of IsaMills on the overall grind. North plant had IsaMills running for the entire test period. South plant had a single IsaMill running at the start of the study however in April 2010 the two additional streams had IsaMills commissioned on them. Both plants experienced commissioning problems during the study which resulted in some anomalies.

Beaching Behaviour

1. *Beach Profile*. Both a qualitative and quantitative analysis of the beach profile was undertaken based on the data collected. A qualitative description of the observed beaching profiles after each deposition was undertaken in line with the reported research in the literature review. Further a quantitative analysis was undertaken comparing the observed beach profiles to the beach profile suggested by Blight and Bentel (1983) for platinum tailings. An analysis of the impact of plant slurry densities was also undertaken.
2. *Beach Segregation*. The grading analysis of the various samples collected was analysed to determine the impact of the finer grind on beach segregation.
3. *Comparison to Predictions*. Predictions made by SRK Consulting could be compared to the field data.

Reference Evapotranspiration

Methods outlined in the FAO Irrigation and Drainage Paper No. 56 (Allen et al 1998) were used to determine the reference evapotranspiration from different data sets.

1. *Mokopane Data Set*. Table 3.3 indicates the data used to determine the reference evapotranspiration based on a daily time step at the Mokopane site. Appendix E outlines the method used in greater detail.

Table 3.3: Mokopane FAO-56 ET_o

Data Requirements	Data Source
1. Atmospheric parameters	The elevation of the site.
2. Air temperature	Daily maximum and minimum temperatures.
3. Air humidity	Daily maximum and minimum relative humidity.
4. Solar radiation	Daily extraterrestrial radiation and the Hargreaves and Samani (1982) correlation based on daily maximum and minimum temperature.
5. Soil heat flux	Assumed to be zero as recommended for daily time steps (Allen et al 1998).
6. Wind speed	Daily average wind speed.

Results obtained were compared to ET_o values calculated by the CROPWAT program using data from the CLIMWAT data set for Pietersburg/Polokwane (± 55 km away but within in the same climatic region). CROPWAT is a program that calculates ET_o as per the FAO 56 – PM method and is accompanied by the CLIMWAT database of monthly climatic parameters for 3000 sites (Smith, 1993). Daily ET_o values were also calculated using the Hargreaves method using Equation 2.8 and then correlated with the FAO 56 - PM ET_o values as per Equation 2.9. This was used to develop a regional calibration for the Hargreaves method.

2. *Mogalakwena Data Set.* Daily ET_o values were calculated from daily maximum and minimum temperatures using the above regionally calibrated Hargreaves method. A-Pan data was checked against historical S-Pan data using a correlation proposed by Bosman (1990). The site A-Pan data was then compared to the daily ET_o values based on correlation factors outlined in FAO 56 (Allen et al., 1998).

Moisture Loss

1. *In-Situ Sedimentation and Drying.* Plant slurry densities, grab samples, and auger samples following the successive depositions on Tailings Dam 2 allowed the effects of sedimentation and evaporation on moisture loss to be investigated. It was assumed that the grab samples gave an indication of sedimentation and the first three surface auger samples gave an indication of evaporation-driven drying. The remaining surface auger samples did not vary significantly and a steady state moisture regime appeared it was thus assumed that no change in water content occurred after the initial surface drying stage.

   An iterative statistical method was used to intersect three separate linear regression curves through the sedimentation, drying and steady state condition. A number of possible alternate legs could have been taken however these were not found to be of any use to the study. An example of the iterative steps used is included in Appendix H. A scatter plot was used to test the performance of the regression model to the field water contents. Moisture loss in the field is driven by evaporation and seepage. Seepage was assumed to remain constant throughout the year however evaporation was not. The collected climatic and permeability data was therefore compared to the rate of moisture loss and a relationship between the factors developed.

2. *In-situ Moisture Regime.* The results from field water contents appeared to vary in a random fashion with no definitive change with time, barring the few samples used for the above analysis. Reasons for this apparent random behaviour were thus explored. Rather than trying to define the moisture regime by a single number, for example the average, the distributions of water content values along the beach and with depth were investigated. Field capacity water contents determined from experimentation and numerical modelling were compared to the in-situ water contents to explain these variances. The density and strength of the material was then inferred from laboratory drying tests and Atterberg limits by determining the respective liquidity indices.

Chapter 4 Results and Analysis

4.1 Basic Geotechnical Properties

Particle Size Distribution

Due to research indicating that to fully liberate PGM's finer grinds would have to be employed (Anyimadu et al., 2006) Mogalakwena Platinum Mine introduced IsaMills at its North and South Plants. During the testing period South Plant was in the process of upgrading all its streams with IsaMills. Prior to April 2010 only one stream was operational after this all three streams were operational. Figure 4.1 illustrates the impact that the IsaMills had on the overall grind with the percentage retained at the larger particle sizes reducing significantly (The solid lines indicate the median values). During the testing period all streams at the North Plant had operational IsaMills and this is illustrated by Figure 4.2. With all IsaMills operational both plants had fairly similar tails particle grading distributions and exhibited similar scatter.

During the field work a number of particle size distributions were determined from the feed and along the beach. It will be shown later that very little segregation occurred along the beach. In Figure 4.3 all the particle size distributions (PSD) obtained during the investigation on Tailings Dam 1 along with the three quartile values are presented. The median and lower quartile lines are closer together than the upper quartile line and the median line. This is a consequence of the majority of the data being collected prior to all the IsaMills being operational. The upper quartile is therefore indicative of the finer grind after the introduction of all IsaMills in the South Plant.

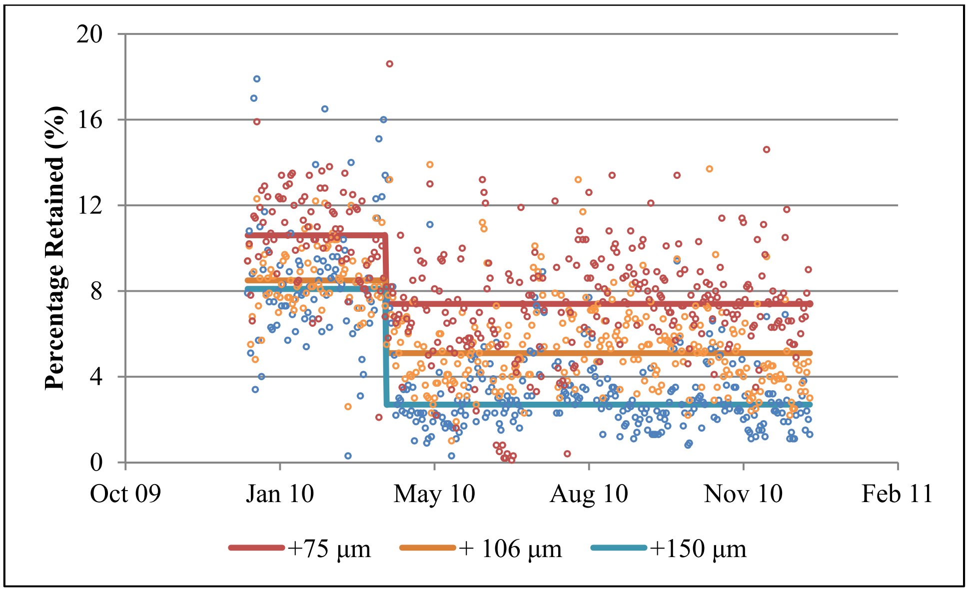

Figure 4.1: South plant tails particle grading (Tailings Dam 1)

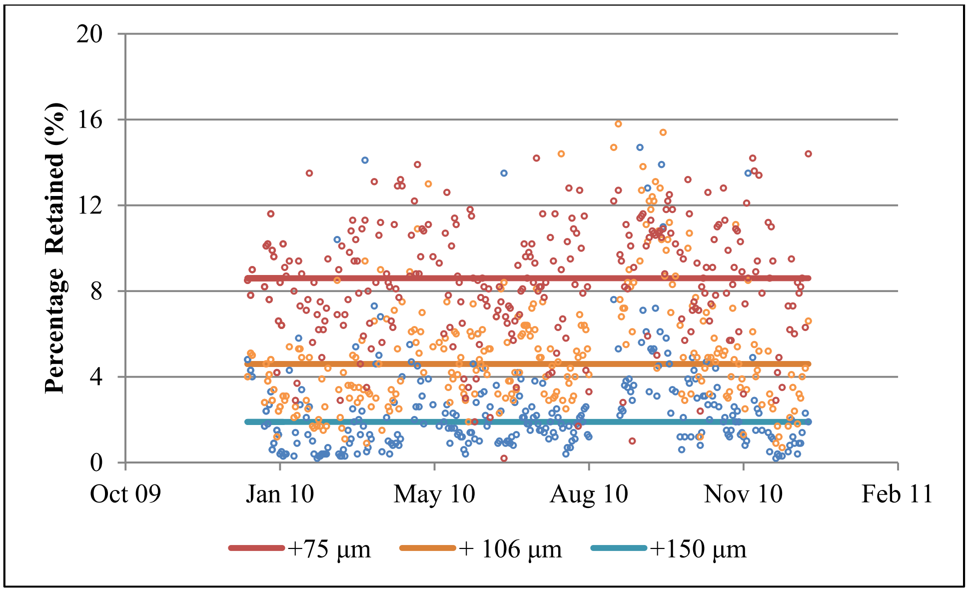

Figure 4.2: North plant tails particle grading (Tailings Dam 2)

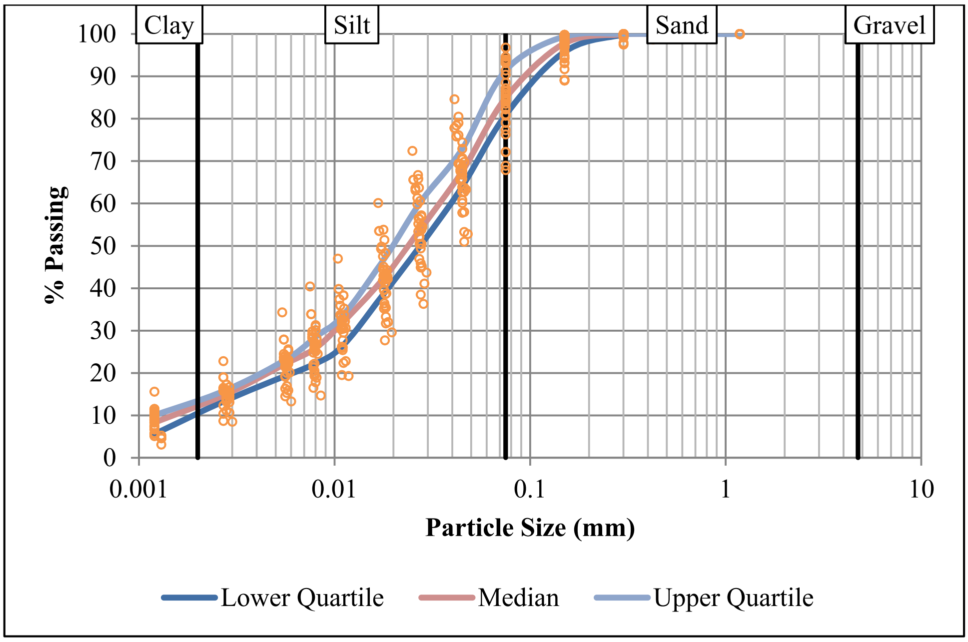

Figure 4.3: PSD on Tailings Dam 1

Figure 4.4 plots all the particle size distributions obtained during the investigation on Tailings Dam 2 along the with the three quartile values. All these samples were taken with fully operational IsaMills therefore little particle segregation along the beach was observed. This resulted in minimal scatter about the median, with the lower and upper quartile lines plotting along virtually the same line.

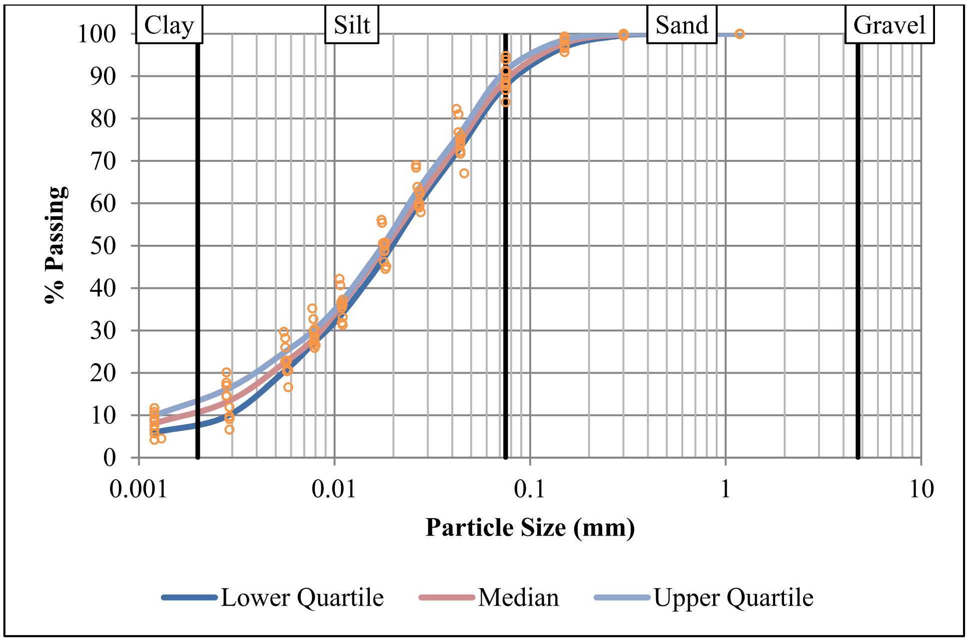

Figure 4.4: PSD on Tailings Dam 2

As indicated in the section outlining the methodology followed in this research a number of previous investigations into the Geotechnical behaviour of the Mogalakwena tailings were relied upon. Table 4.1 gives details of these previous samples and shows the designation referred to in the PSD in Figure 4.5. This illustrates that although the laboratory study particle size distributions do not fit along the median of the field samples they fit within the envelope. Results from the tests carried out on these samples will therefore represent the complete spectrum of particle size distributions encountered along the beach.

Table 4.1: Laboratory PSD sample details

Reference	Description	Study Designation
SRK Consulting (2006b)	A blend of 55 % of a 80 % finer than 75 µm material and 45 % of a 80 % finer than 45 µm material	Sample A
SRK Consulting (2006a)	100 % of a 80 % finer than 75 µm material	Sample B
	100 % of a 80 % finer than 45 µm material	Sample C
SRK Consulting (2010)	Two bulk samples taking from the South Plant tailings stream	Sample D.1 Sample D.2

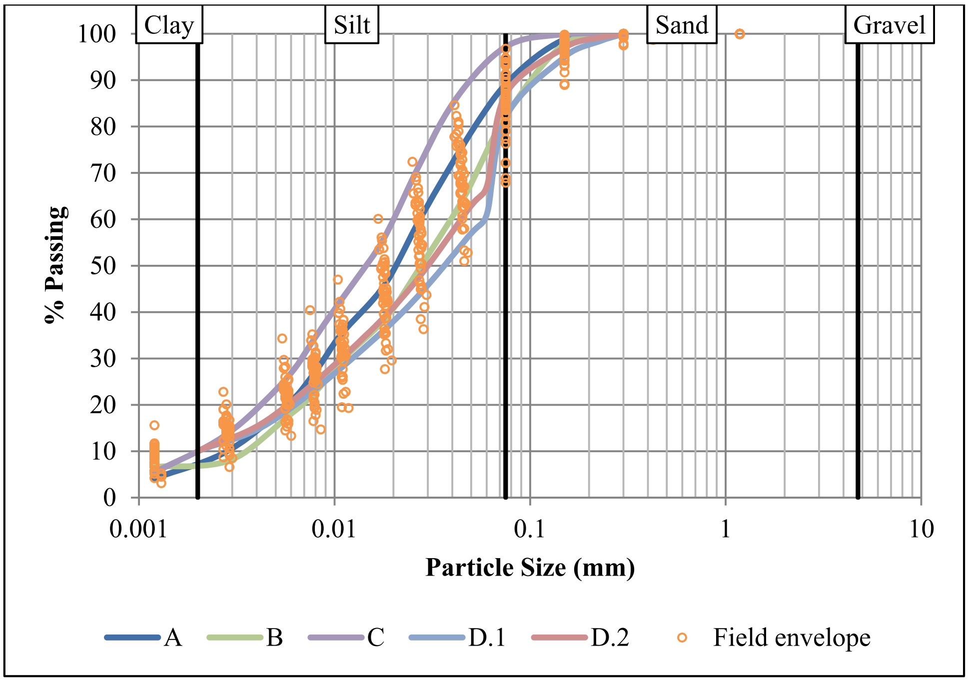

Figure 4.5: Laboratory study PSD relative to field PSD

Atterberg Limits

Along with the above PSD tests, Atterberg limits were determined from these samples, Table 4.2 below details the results. Although taken at different points in time and with slightly different particle size distributions the values are not significantly different. Later the water content samples determined during the field work are compared to these determined Atterberg limits by the liquidity index. The average as well as a worst case scenario (maximum values) and best case scenario (minimum values) are computed and presented.

Table 4.2: Atterberg limits

Study Designation	Liquid Limit	Plastic Limit	Plasticity Index	Shrinkage Limit
Sample A	22	19	3	Not determined
Sample B	20	18	2	Not determined
Sample C	24	19	5	Not determined
Sample D.1	24	21	3	1.8
Sample D.2	25	20	5	1.2
Average	23	19	4	1.5
Maximum	25	21	5	
Minimum	20	18	2	

The liquid limit determined was less than 32 in all cases. Figure 4.6 illustrates that the majority of the samples had a percentage clay size greater than 10%. Andrews and Martin (2000) criteria deem such a material possibly susceptible to liquefaction depending on the mineralogy of the clay size fraction. Based on the average plasticity index and average clay fraction the activity at 0.3 is very low. This indicates that the clay sized fraction is unlikely to contain any clay minerals and the material is likely susceptible to liquefaction.

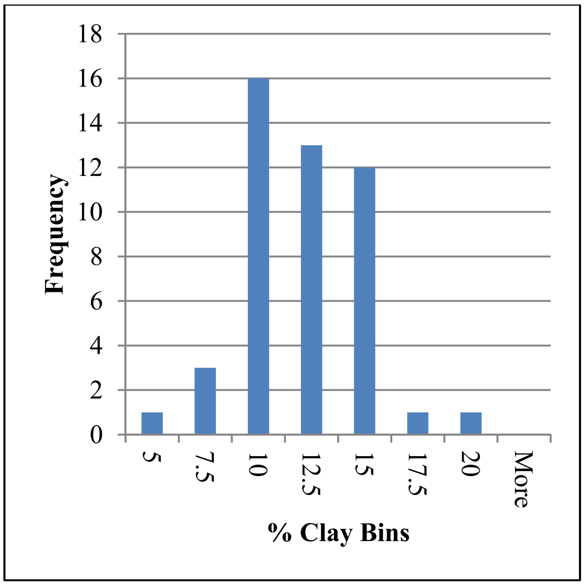

Figure 4.6: Distribution of percentage clay in field samples

Particle Specific Gravity

Particle specific gravity can have a significant impact on calculated values therefore a number of samples were taken. The histogram of the values in Figure 4.7 shows a slight right skew about the average of 3.10. However the standard deviation was relatively small at 0.03 justifying the use of the average for all further calculations.

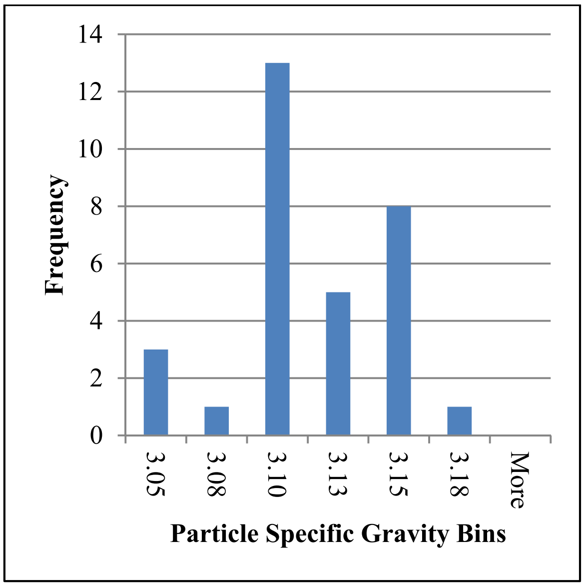

Figure 4.7: Histogram of particle specific gravities determined during field testing

4.2 Settling Behaviour

Different samples were tested under laboratory conditions to determine the settling behaviour. Tailings from the Mogalakwena operation were blended to anticipate the change in behaviour due to changes in the grinding regime. Coupled to this the slurry density was changed to determine the impact of increased thickening. Figure 4.8 shows the settling behaviour with time of the various samples. In all cases settling occurred within roughly 2 to 3 day after which very little change in water content[1] was observed. Samples set up at higher slurry densities (i.e. lower water content) exhibited the least change in water content.

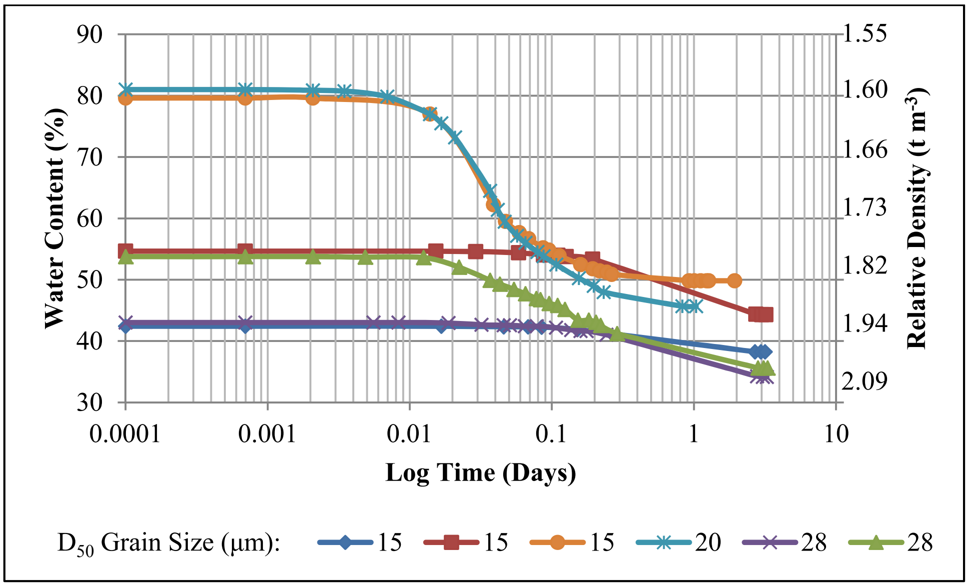

Figure 4.8: Settling Behaviour

The results from these laboratory experiments could be compared to field values. A regression method was used to determine the intersection of the settling curve and the drying curve as outlined in the methodology. The results from this analysis will be explained fully later in the thesis, however at this point the settled water contents will be analysed. On average the settled field water content was obtained after 2.7 days (Standard deviation of 7 hours) which was similar to the trend observed in the laboratory. It is thus emphasised that for laboratory investigations to be realistic of field conditions settling tests need to be carried out over a number of days.

The impact of slurry density on the settled water content as illustrated in Figure 4.8 is investigated in Figure 4.9. This shows that for the laboratory determined values higher slurry densities prior to settling resulted in slightly lower settled water contents. Values obtained from the field are also plotted to give a comparison. It is assumed that the median slurry density recorded at the plant during deposition is representative of the initial slurry density prior to sedimentation; however the quartile range is also

[1] Water contents are used here as the samples are assumed to be saturated and so density and void ratio are related by simple phase relationships.

given. Using these values is conservative as the slurry density at deposition is often lower than the value recorded after the thickener. Interestingly the settled field water contents are lower than the settled laboratory water contents at similar slurry densities. No apparent relationship between increasing slurry density and settled water content was apparent from the field results.

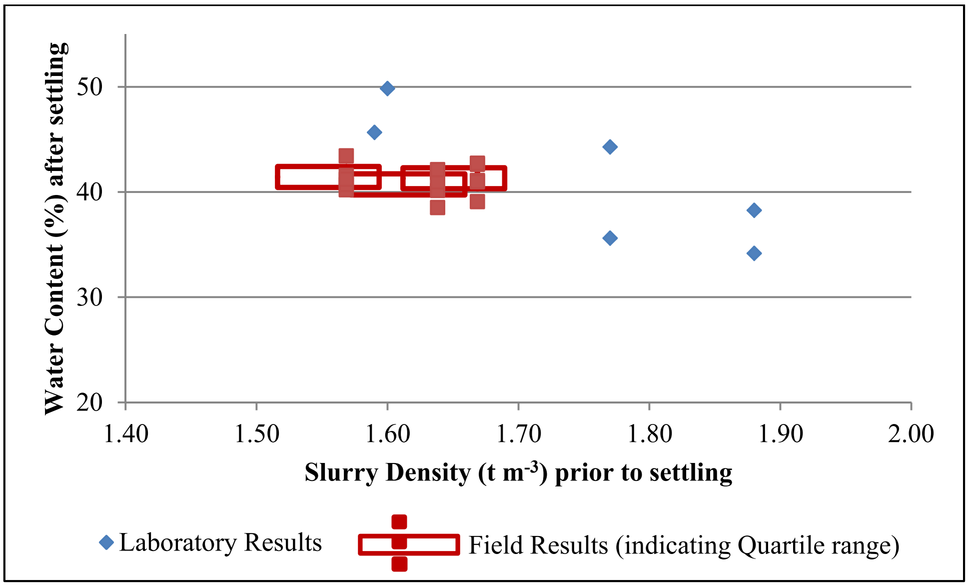

Figure 4.9: Relationship between slurry density and settled moisture content

Figure 4.10 illustrates that, albeit with a degree of scatter, increasing the slurry particle size increases the settled water contents slightly. This was observed for both the field tests and the laboratory tests. Laboratory settling tests are done under pelagic conditions whereas settling in the field occurs over a large fan. As such difference between the results can be expected.

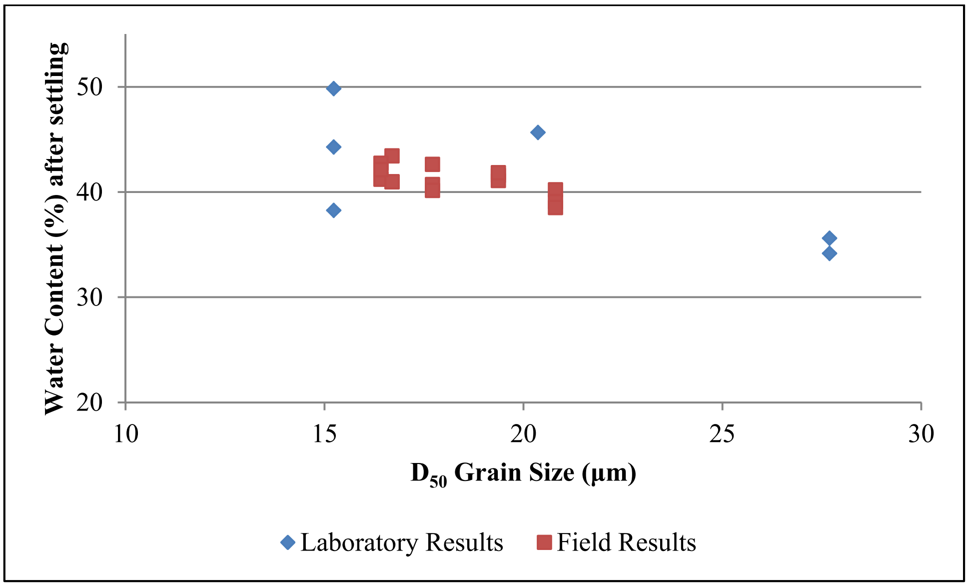

Figure 4.10: Relationship between particle size and settled moisture content

Mechanical thickening of tailings, at a higher cost, is often promoted as a means of recovering a larger volume of water. Optimally all water released during sedimentation can be recovered, subject to various operational requirements (Blight, 2010). The results indicate that it was anticipated that the slurry could be thickened to a slurry density of roughly 1.88 t m^{-3}, this equates to a water content of roughly 45 %. When compared to the average settled field water content of 41 % it is apparent that very little water saving is obtained by mechanical thickening at the plant.

4.3 Beaching Behaviour

Predicted Beaching Behaviour

SRK Consulting (2006b) reported the predicted beaching behaviour of the Mogalakwena tailings as a consequence of the proposed finer grind. The PSD of the slurry used in the flume test is illustrated in Figure 4.11 showing that it was representative of the average field PSD's obtained. The sample was beached at a slurry density of 1.59 t m^{-3} which is fairly representative of the field values, albeit at the higher end of the reported values in Table 4.3.

Table 4.3: Field slurry densities

Dam	1				2		
Deposition	1	2	3	4	1	2	3
Average Slurry Density (t m^{-3})	1.61 ± 0.06	1.48 ± 0.08	1.39 ± 0.13	1.53 ± 0.09	1.55 ± 0.09	1.61 ± 0.09	1.59 ± 0.05

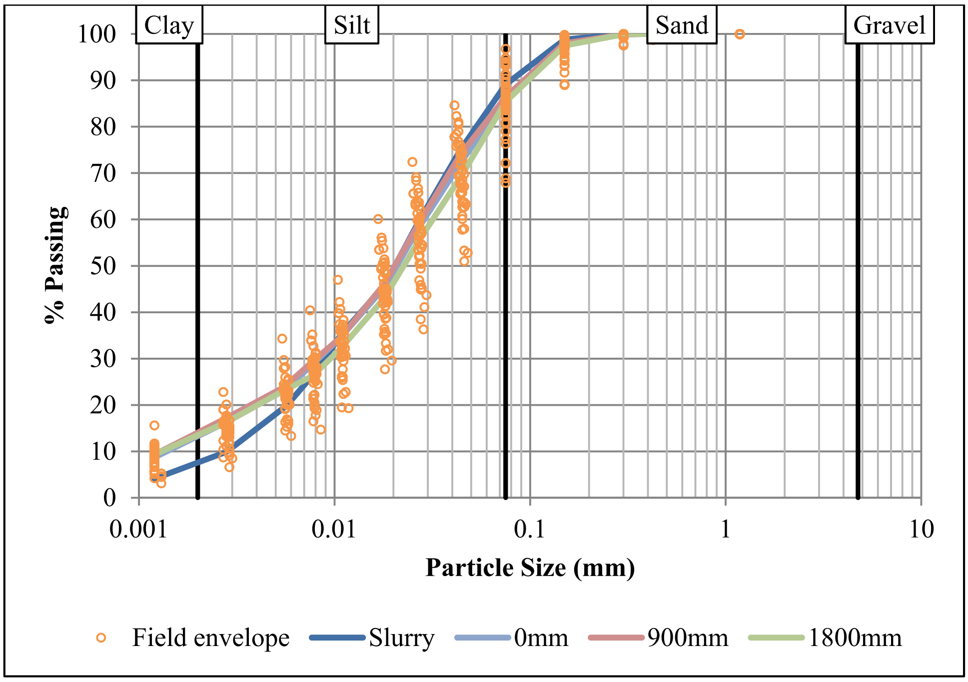

Figure 4.11: Flume test PSD

Blight et al (1985) reported that small-scale models could adequately predict the full-scale behaviour provided the slurry was made up of the same material at a similar slurry density. However Figure 4.12 below illustrates that the flume test, Prediction 1, failed to adequately predict the full scale beach. The predicted beach appeared to have two parts a shallow upper course and then a steep lower course. This type of behaviour in a flume was reported by Fourie (1988) for slurries with a "thick consistency". In these cases the slurry had insufficient available energy to beach, in that the manner in which the slurry was deposited into the flume may have prematurely arrested the flow, although the slurry density was similar to field conditions. If the upper course is used to predict the beach, Prediction 2 as indicated, the profile appears to be better a representation of the field conditions. It is suggested that further work be carried out to better understand flume tests especially at higher slurry densities.

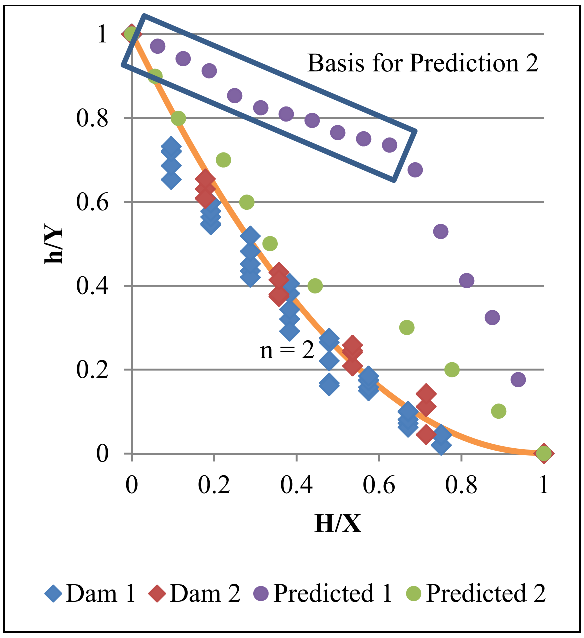

Figure 4.12: Comparisson of small-scale and full-scale beaching behaviour

Samples at positions; 0 mm, 900 mm and 1800 mm were recovered from the flume and the grading of the samples determined. Figure 4.11 illustrates that very little segregation occurred along the beach. Interestingly the percentage of material finer than 10 μm was higher in all the beach samples than in the slurry sample. It is proposed that during the flume test settling occurred with larger particles settling to the bottom of the flume. The samples tested were then recovered from the surface and so had slightly higher percentages of finer material.

A comparison between the particle segregation in the flume tests is compared to the particle segregation observed in the field in Figure 4.13. A distinction between the different grinding regimes during the field tests has been made in this figure. A fairly good agreement between the small-scale and full-scale segregation is observed. An inverse relationship as per Blight (1987) has been forced through the data however there is a large degree of scatter. Any coarse material appeared to settle out within the first 50 m although this was observed more so on Dam 1 and mainly prior to the full introduction of the finer grind. With reference to Figure 2.3 the results presented by Blight (1987) for Diamond tailings also exhibited this rapid settling of coarse particles within the first 50 m of the beach. However the range in particle sizes along the beach was much smaller for the platinum tailings studied. This has an important bearing on the overall stability of facilities constructed by the spigot method as it is this outer perimeter that provides the strength necessary to impound the finer material within.

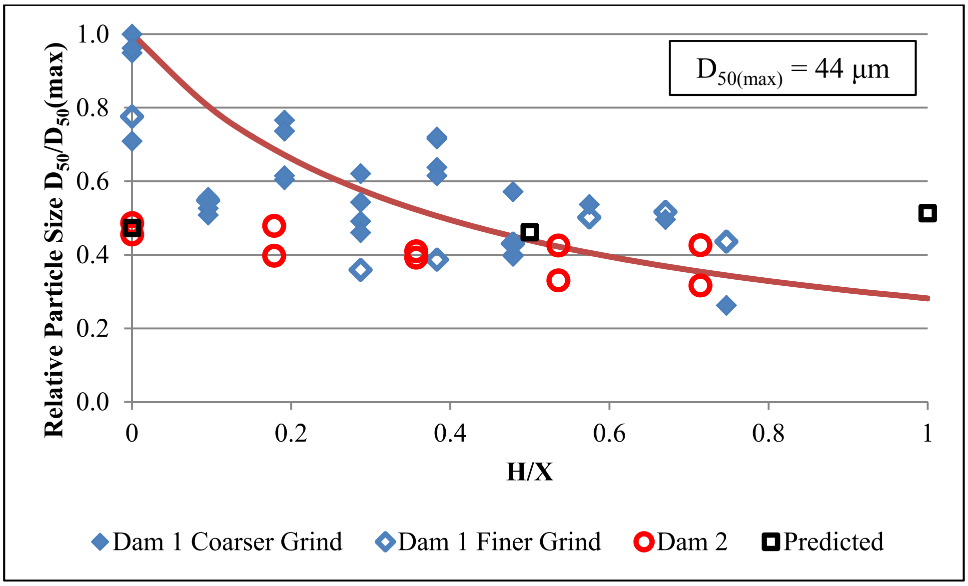

Figure 4.13: Particle segregation along respective beaches

Master Profile

Wates et al (1987) brought into question whether a once-of measurement could be used to define a "master" beach profile. The current study allowed the comparison of a number of successive depositions on two separate tailings dams to the original platinum tailings "master" profile proposed by Blight and Bentel (1983). A "master profile" with an n value of 2 was plotted in Figure 4.12 above as proposed by Blight and Bentel (1983). The field data showed similar scatter at each sampling point, however the scatter about the "master" profile differs from the original. The current study data points plot below the proposed profile higher up the beach but it is more consistent further down the beach. This suggests that the two beaches from the current study are less concave than the original beaches reported. This anomaly will be explored further in the following sections. Figure 4.14 shows the correlation between the Blight and Bentel (1983) "master" profile and the data obtained from the current study by means of a scatter plot. Whilst some differences have been highlighted above, the overall correlation between the original study and the current study is not that statistically large.

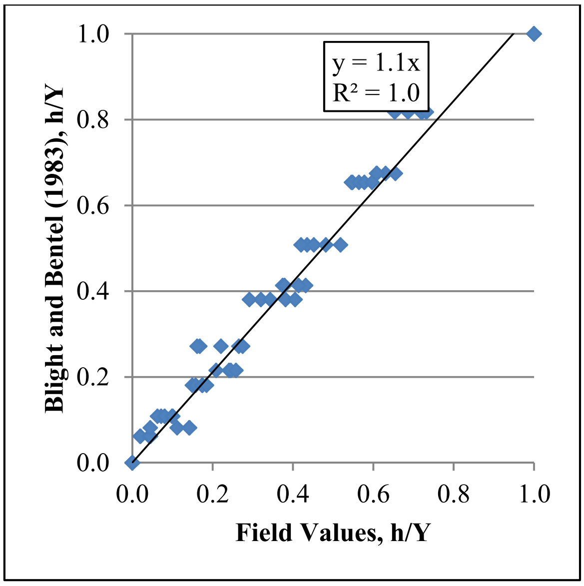

Figure 4.14: Scatter plot comparing Blight and Bentel (1983) to the current study

Chord Slope

As indicated the "master" profile deduced from the current field studies correlated fairly well with the platinum beaches studied by Blight and Bentel (1983). A shortcoming of the "master" profile is that alone it cannot be used to predict the profile of a full-size tailings beach. The chord slope is required so that the overall dimension of the beach can be determined to which the "master" profile can then be "draped". The literature review presented a number of mechanisms that affect the beaching of tailings and these shall be explored with relation to the field results. Survey results of the four successive depositions on Tailings Dam 1 and the three successive depositions on Tailings Dam 2 were analysed to establish how the chord slope changes during active deposition. An important factor that must be kept in mind is that surveying occurred at every 50 m along the beach. Thus a large percentage of the beach was not surveyed and assumptions had to be made about the profile in between the sampling points. Further it has been assumed that flow around the poles used to mark the sampling positions did not result in abnormal deposition to free flow conditions.

Successive depositions on Tailings Dam 1 are illustrated in Figure 4.15 and some of the pertinent details about the depositions are listed in Table 4.4. The initial beach on Dam 1 consisted of a steep upper section (0 – 50 m) and a relatively flat section along the rest of the beach albeit with a slight depression at 250 m. This profile became more pronounced with subsequent depositions. The first deposition appeared to hang up on the beach whereas the subsequent two depositions reached the lower courses. After deposition 3 had ceased a brief cross deposition occurred from an adjoining active depositional area. As this interfered with the test strip the spigots on this active depositional area were closed and deposition occurred further away from the test strip. It is suggested that a similar cross deposition prior to test work may have been the reason for the non uniform initial profile. The final deposition deposited material along the entire beach length however not as much material reached the lower course as was the case with depositions 2 and 3. As a consequence of these tapered depositions the depth of material on the upper reaches was 5 times greater than the depth of material on the lower reaches, with the majority of the material deposited within the first 200 m. Due to the length of the beach however the chord slope only increased slightly following these depositions.

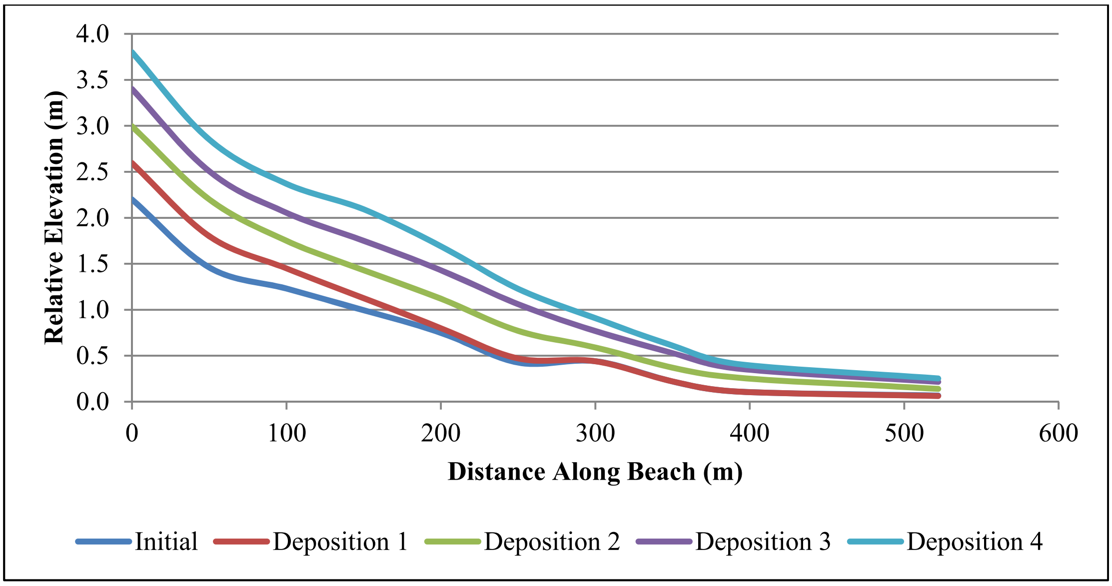

Figure 4.15: Successive beach profiles on Tailings Dam 1

Table 4.4: Tailings Dam 1 beach profile details

		Deposition			
	Initial	1	2	3	4
Days to Deposit	-	5	8	11	10
Average Slurry Density (t m^{-3})	-	1.61 ± 0.06	1.48 ± 0.08	1.39 ± 0.13	1.53 ± 0.09
Chord Slope (%)	0.41	0.49	0.55	0.61	0.68

Successive depositions on Tailings Dam 2 are illustrated in Figure 4.16 and some of the pertinent details about the depositions are listed in Table 4.5. The test strip on Dam 2 was roughly half the length of the test strip on Dam 1 and this appeared to influence the beaching behaviour. The test strip on Dam 2 was adjacent to the pool wall and prior to test work, deposition had occurred from this wall and not from the dam perimeter as was the case during testing. Thus the initial beach profile had been formed by cross deposition and this resulted in an irregular profile with a "bulge" nearly half way down the beach. The first deposition on this beach corrected this irregular profile resulting in a uniform profile along its length. The tapering of deposited material observed on Dam 1 was not apparent on Dam 2 rather the difference in deposited material on the lower and upper course varied between depositions. Consequently after the three depositions the depth of material along the entire beach was relatively constant. Similarly to Dam 1 the beach on Dam 2 consisted of a steep upper section (0 – 50 m) and a relatively flat section along the rest of the beach.

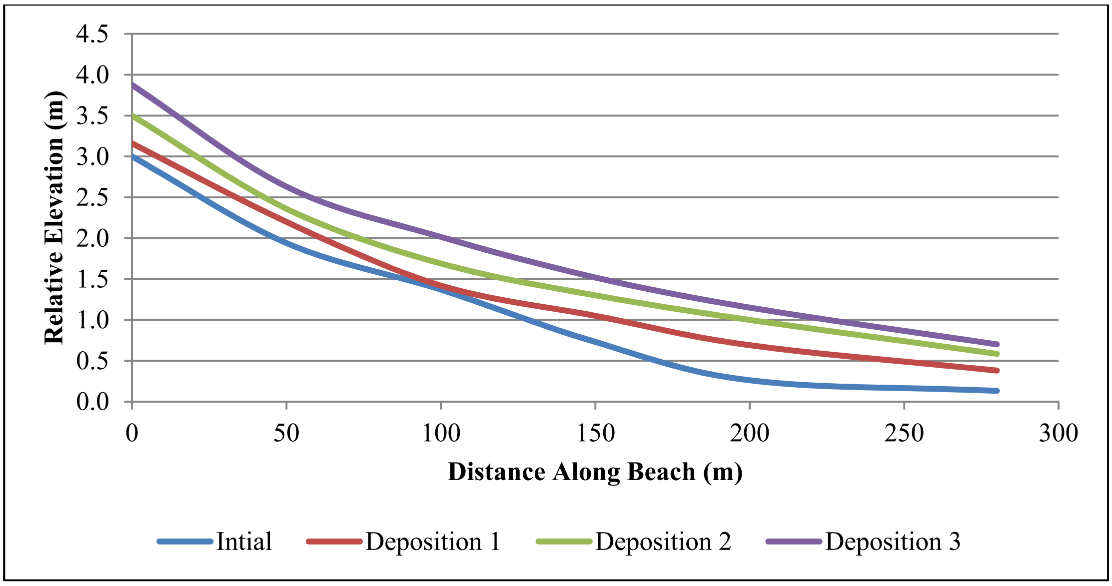

Figure 4.16: Successive beach profiles on Tailings Dam 2

Table 4.5: Tailings Dam 2 beach profile details

		Deposition		
	Initial	1	2	3
Days to Deposit	-	6	10	6
Average Slurry Density (t m^{-3})	-	1.55 ± 0.09	1.61 ± 0.09	1.59 ± 0.05
Chord Slope (%)	1.02	0.99	1.04	1.13

Blight (1987) suggested that the chord slope is dependant on the slurry density, in that higher slurry densities have less available energy to beach with material predominantly deposited on the upper course. Slurry density delivered to Dam 2 was better controlled hence the chord slope remained fairly constant. On Dam 1 the slurry density did vary with lower slurry densities resulting in more material being deposited further along the beach. However Figure 4.17 illustrates that the chord slope was not significantly influenced by the slurry density but rather appeared to be dam specific. Wates et al (1987) suggested that the energy available upon deposition changes as the slurry water/sediment ratio changes along the beach. In that as sediment is deposited the viscosity decreases resulting in less impedance to flow. The slope of the proceeding layer also influences how the available energy is utilised, in that slurry deposited on a steep beach will required less energy to flow. Thus although a high slurry density may result in a steep beach subsequent depositions will erode and entrain this material to maintain the flatter lower course. This explains why the field results indicated that regardless of beach length the beaches consisted of a steep upper 50 m with the rest of the beach being much flatter.

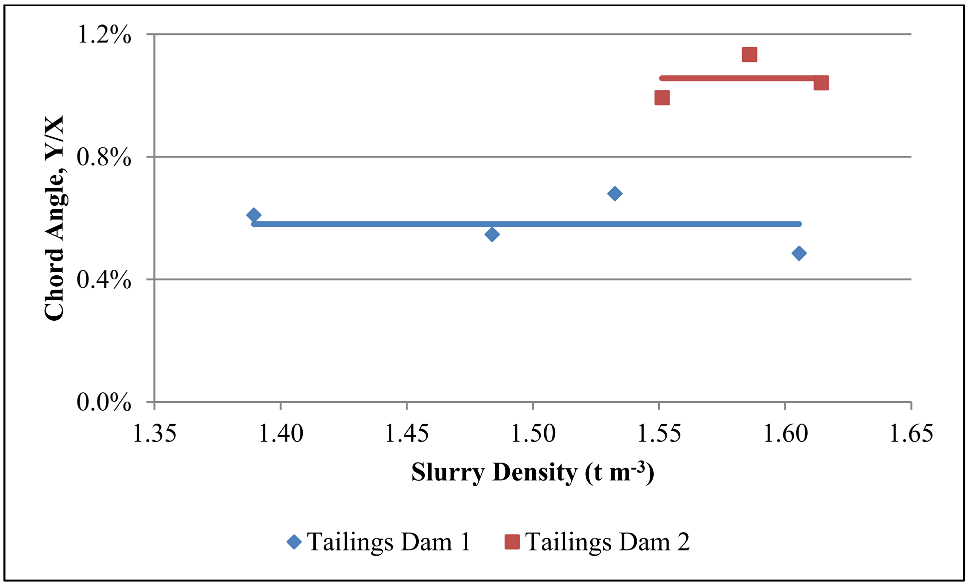

Figure 4.17: Variation of chord slope with slurry density

The relationship between beach length and chord slope was investigated further by comparing the original beaches studied by Blight and Bentel (1983) to the current study. Figure 4.18 illustrates, albeit with a degree of scatter, that the longer the beach the flatter the chord angle. This is further evidence that particles settle out rapidly decreasing the impedance to slurry flow along the beach enabling material to be entrained and deposited further along. It is often suggested that higher slurry densities can result in steep chord slopes. The results presented here suggest that the manner in which the beach is allowed to develop has an even greater influence.

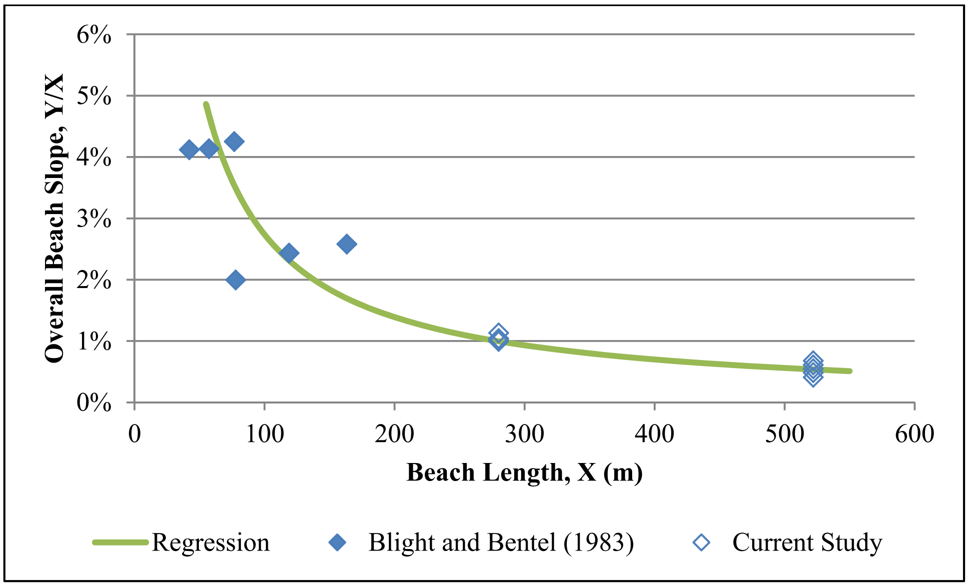

Figure 4.18: Relationship between chord slope and beach length

On Tailings Dam 2 due to easier access to the test strip sampling points it was possible to measure the beach profile immediately after deposition had ceased and again prior to the next deposition[1]. Blight (1987) reported that appreciable settlement can occur with very fine tailings after it has come to rest and this can flatten the beach. The difference in the surveys could be used to give an indication of the settlement along the beach. Percentage settlement was determined by dividing the difference between the successive surveys by the height of material deposited at each point and here plotted against beach length in Figure 4.19. Recalling Figure 4.13 it is apparent that more settlement occurred further along the beach where the particle size was slightly smaller. The settlement at 0 m was on average 21 % whereas the settlement along the rest of the beach was on average 33% which corresponds to the observed steep initial 50 m and shallower lower course. Further research is necessary to fully determine the impact of this settlement on the beach profile.

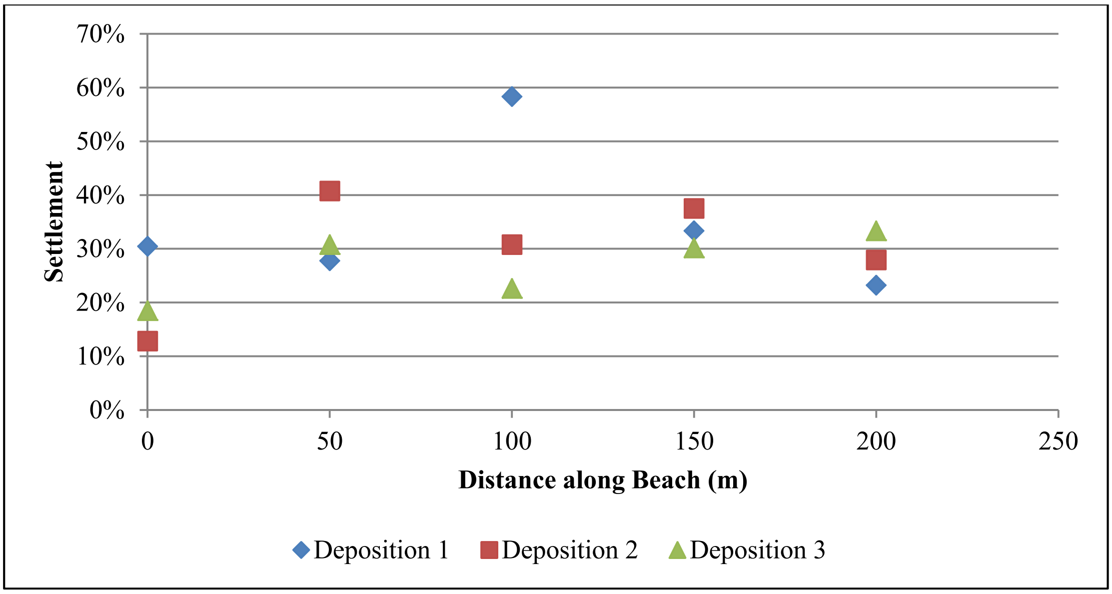

Figure 4.19: Relationship between settlement and distance along beach

An apparently anomalous deposition was alluded to in the preceding discussions in that the first deposition on Tailings Dam 1 appeared to hang up. Due to operational constraints deposition on Tailings Dam 1 was preceded by an approximately 6 month period of inactivity. This resulted in a drier than usual outer section of the beach, illustrated in Figure 4.20 compared to active deposition conditions illustrated by Figure 4.21. The initial dry conditions appeared to result in a shorter and steeper beach profile as illustrated by Figure 4.15 compared to successive depositions. Kehew (2006) indicated that in alluvial depositions dry beds can result in rapid infiltration and almost immediate sediment deposition. This appeared to be the case with the observed tailings deposition. Further research is necessary to fully determine the impact of this dry beach infiltration on the beach profile.

[1] Figure 4.15 and Figure 4.16 are both produced from survey data prior to the next deposition.

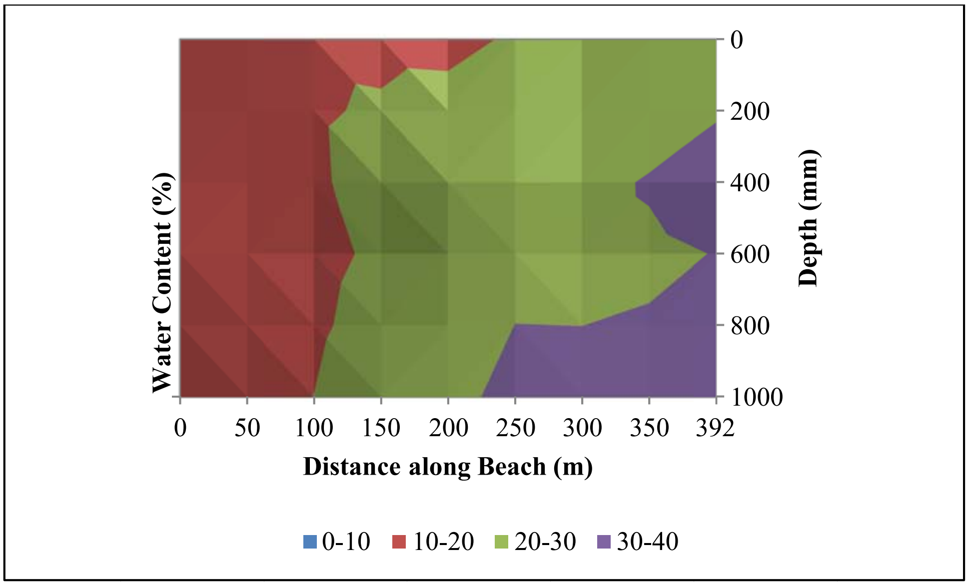

Figure 4.20: Tailings Dam 1 baseline moisture regime

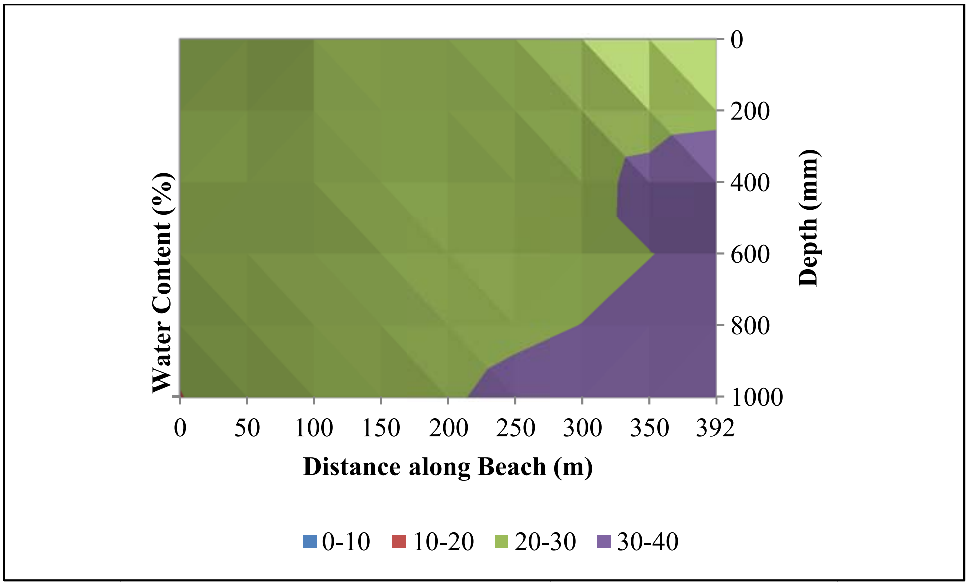

Figure 4.21: Tailings Dam 1 moisture regime during active deposition

4.4 Drying Behaviour

Laboratory Behaviour

1. *Water Retention Curves*. Three separate WRC's were established; two drying and subsequent wetting curves determined with calibrated gypsum blocks and a drying curve determined by the filter paper method. The computer program RETC (van Genuchten et al., 1991) was used to estimate the WRC from the raw data based on the van Genuchten model and these are illustrated in Figure 4.22. Air entry occurs at roughly the field capacity value (here defined as the water content at a suction head of 33 kPa) for all the tests however the corresponding water contents are different. These water contents are likely to under predict the in-situ field capacity values due to the fine material tested (Ratliff et al., 1983). The difference between the various tests is likely due to variations in particle size distributions (Fredlund et al., 2002) and test procedures. The difference between the drying and wetting curves is a consequence of hysteresis. l of the different test procedures. All tests indicate that suctions begin to develop below a water content of 26 % with significant suction below 20 % and extremely high suctions below 10%.

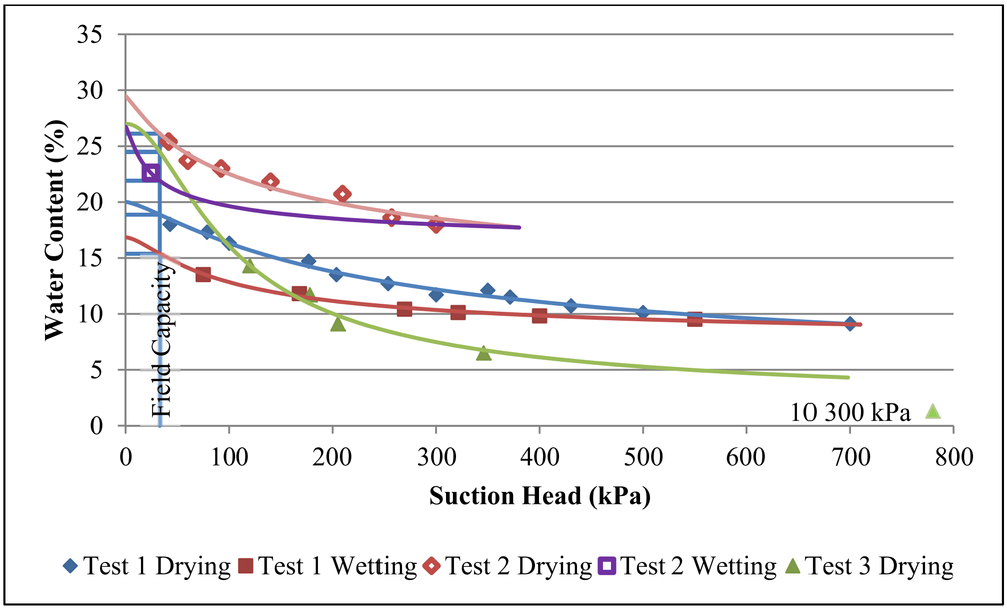

Figure 4.22: Laboratory determined water retention curves

2. *Volume Shrinkage Curves*. VSC in terms of increasing dry density with decreasing water content are presented in Figure 4.23. Table 4.6 details the source of data used to plot the VSC as well as the sample designations used to easily identify which data points correspond to which test.

Table 4.6: VSC data source and designation

Reference	Description	Initial Slurry Density (t m^{-3})	Study Designation
SRK Consulting (2006b)	A blend of 55 % of a 80 % finer than 75 µm material and 45 % of a 80 % finer than 45 µm material was dried under ambient conditions	1.59	Sample A
SRK Consulting (2006a)	100 % of a 80 % finer than 75 µm material was dried under ambient conditions	1.88	Sample B.1
		1.77	Sample B.2
	100 % of a 80 % finer than 45 µm material was dried under ambient conditions	1.88	Sample C.1
		1.77	Sample C.2
SRK Consulting (2009)	Filter paper suction test on a sample of material taken from the South Plant thickener underflow	Not applicable	Sample E

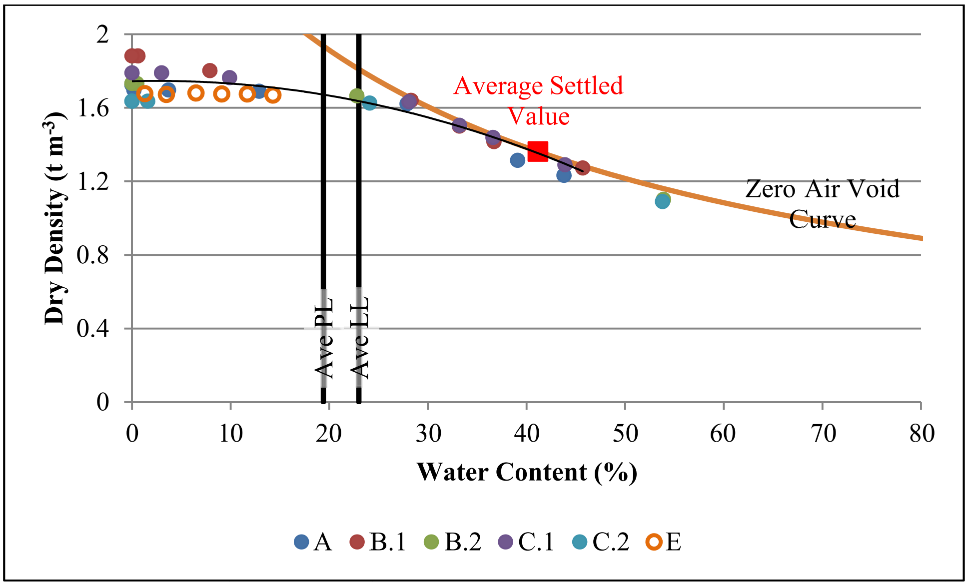

Figure 4.23: Laboratory determined volumetric shrinkage curve

All the samples dried in a similar manner, following the zero air void curve to a water content of roughly 30% after which air entry can be assumed to have occurred. It is likely that the tailings will remain essentially saturated to a water content of 23% which was the average liquid limit. The water content at which air entry occurred in the drying tests was higher than was determined from the first gypsum block WRC. However it correlated better with the second gypsum block WRC and the filter paper WRC. Furthermore the dry densities interpreted from the filter paper suction tests correlated well with the drying test results. After air entry dry density did not increase appreciably and remained roughly constant at a value of 1.7 t m^{-3}. This behaviour was also shown for data on diamond tailings presented by Welff and Wates (2004). The dry densities after a water content of 10 % exhibited a greater degree of scatter. One difficulty reported by the laboratory staff was that cracking occurred and the sample volume was difficult to accurately determine. Resulting in an under estimation of the volume and dry density. The observed scatter can thus be attributed to these difficulties. No considerable difference between the density at the liquid limit and plastic limit was observed. The plastic limit however is roughly the water content at which considerable suctions started to develop (referring to Figure 4.22).

3. *Water Content Permeability Relationship*. Meyer and Gee (1990) proposed that field capacity is reached when fluxes are between 10^{-11} and 10^{-9} m s^{-1} depending on soil texture. The SEEP/W (GeoStudio, 2007) numerical modelling computer program was used to estimate the hydraulic conductivity on a continuum of gravimetric water contents for the entire envelope of field particle sizes. Table 4.7 details the parameters used in the analysis as well as the various assumptions made. The range in field capacity water contents, as a consequence of the variations in particles sizes, is illustrated in Figure 4.24.

Table 4.7: SEEP/W input data

Parameter		Sample				
		1	2	3	4	5
Volumetric Water Content Function	Saturated Water Content	0.48[a]				
	Estimation Method	Grain-size data				
	D_{10} (mm)[b]	0.0012	0.0015	0.0019	0.0022	0.0027
	D_{60} (mm)[c]	0.022	0.027	0.033	0.042	0.059
	Liquid Limit (%)	23[d]				
Hydraulic Conductivity Function	Estimation Method	van Genuchten				
	Saturated Hydraulic Conductivity (m s^{-1})	7.5×10^{-8} [e]				
	Residual Water Content	0.048[f]				

[a] Assumed to be the porosity when saturation fell below 1 as per Figure 4.23
[b] Minimum, maximum and quartile D_{10} values from field PSD's
[c] Corresponding minimum, maximum and quartile D_{60} values from field PSD's
[d] Average Liquid Limit see Table 4.2
[e] Average triaxial permeability tests which gave values of 6 and 9×10^{-8} m s^{-1}
[f] Assumed to be 10 % of the saturated water content
Gravimetric water contents were obtained by the ratio between the gravimetric water content at saturation and the volumetric water content at saturation

Upper and lower bounds are defined by the coarse and fine samples modelled whereas the quartile values fall within a narrow band. Field capacity water contents at the quartile values for a given hydraulic conductivity of 1×10^{-9} m s^{-1} range between 20 and 24 %. These values correlate well with the laboratory determined field capacity values, as shown in Table 4.8, giving further evidence of the impact of particle size distribution on the water retention characteristics. As the differences due to particle size distribution are greater than the differences due to hysteresis, the effects of hysteresis are not considered in further analysis. The field capacity values at 1 × 10^{-11} m s^{-1} range between 10 and 15 % which are lower than the laboratory determined values and therefore may not be realistic.

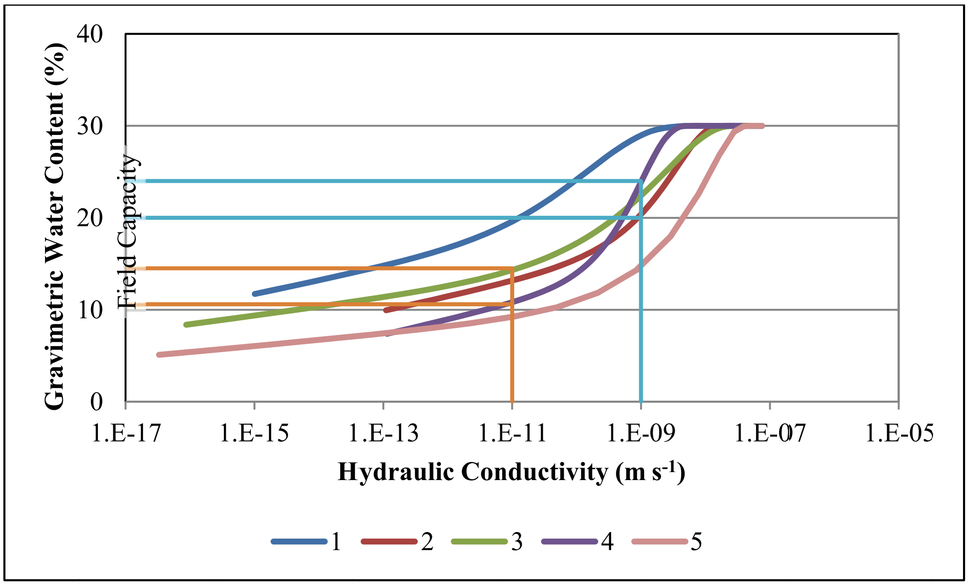

Figure 4.24: Flux based field capacity values

Table 4.8: Comparison of field capacity values

	Numerical Modelling	Laboratory Results†
Minimum	15	15
First Quartile	20	19
Third Quartile	24	24
Maximum	29	26

† Includes field capacity values after hysteresis.

4. *Drying Time*. The time taken to reach the respective water contents, under ambient temperatures, was also recorded as part of the experimental procedure. Figure 4.25 illustrates the observed drying behaviour. Similarly to the results presented by Welff and Wates (2004) drying occurred rapidly at first and then at a low water content the rate abruptly slowed. It can therefore be assumed that stage one evaporation occurs during the majority of the drying process and only after considerable suctions have developed does stage two begin. With reference to Table 4.9 it would appear that the rate of moisture loss was related to the period when the test was done rather than the grading. Samples A, B.2 and C.2 which were tested during late October and early November had very similar rates. Although the drying time was determined by

the amount of water in the sample at the beginning of the experiment. Samples B.1 and C.1 tested at the end of November and beginning of December dried at a slower rate. All the tests were undertaken during the summer months however cloud cover is considerably more during the later parts of the year (the period when samples B.1 and C.1 were tested). It is suggested that the reference evapotranspiration was thus lower for the tests that results in slower drying behaviour. However no climatic information was available to substantiate this assumption and other factors may have affected the results.

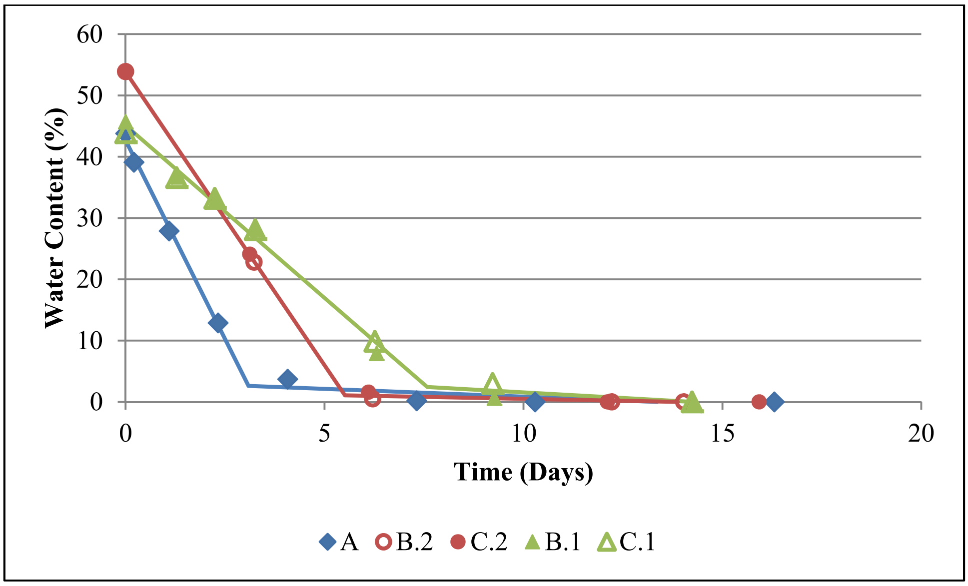

Figure 4.25: Drying time

Table 4.9: Summary of drying results from laboratory tests

Study Designation	Test Start	Stage Change	Test End	Drying Time (Days)	Final Water Content (%)
Sample A	24 Oct	27 Oct	9 Nov	3.1	3
Sample B.2	28 Oct	3 Nov	11 Nov	5.5	1
Sample C.2	28 Oct	3 Nov	13 Nov	5.5	1
Sample B.1	29 Nov	7 Dec	13 Dec	7.6	2
Sample C.1	29 Nov	7 Dec	13 Dec	7.6	2

Field Behaviour

Grab samples taken on the two days following deposition on Dam 2 as well as surface auger samples taken once the surface had gained sufficient strength were used to determine the moisture loss regime following active deposition. Figure 4.27, Figure 4.29 and Figure 4.31 illustrate the result of the regression analysis undertaken on the respective data sets. The performance of the regression analysis to the values obtained in the field was checked by means of scatter plots these are given in Figure 4.28, Figure 4.30 and Figure 4.32. The legend includes the respective, Pearson product moment correlation coefficient, r^2 values at each sampling point and a single line is plotted indicating the average correlation for each deposition. It is evident that the regression analysis fitted the first and third deposition with better accuracy with the average r^2 value above 0.9. The average r^2 value for the second deposition was however above 0.85. The following discussions are based on the results of the regression analysis illustrated in Figure 4.27, Figure 4.29 and Figure 4.31:

1. *Sedimentation.* Sedimentation behaviour was found to not vary considerably along the beach for each deposition. The final water content following sedimentation was found to be very similar for all the depositions along the entire beach. With the calculated p-value being greater than 0.05 at 0.15 indicating the probability of a zero slope was high and hence no significant relationship with beach position. Likewise the time for sedimentation to occur appeared independent of beach position. The p-value in this case was 0.39 indicating the probability of a relationship with beach position to be low. The average water content after sedimentation was therefore 41.2 % with a standard deviation of 1.3 %. The average time for sedimentation to occur was 2.7 days with a standard deviation of 7 hours.

2. *Drying.* The drying behaviour was only determined from a limited number of water contents recorded towards the end of the drying period. An iterative statistical method was therefore required to predict values at the start of the drying period after sedimentation. Consequently a number of assumptions were relied upon. The first was that the water content after sedimentation was the same along the entire beach for each respective deposition. Based on the above this assumption is valid. Secondly the water content after drying was assumed to be the median of the n + 3 surface auger samples. This was justified as the average p-value for the slope of water content with time was found to be 0.41 for this period indicating the probability of a relationship with time to be low. This apparent steady state moisture regime will be further explored. The third assumption was that a linear relationship based on these upper and lower boundaries and the first three auger samples defined the drying behaviour. Based on the exhibited linear laboratory behaviour this assumption was reasonable. Fourthly the rate of drying was assumed to be related to the available reference evapotranspiration during the period as the rate of moisture loss due to seepage was assumed constant for each deposition.

   Table 4.10 summaries the field results and can be compared to the summarised laboratory behaviour in Table 4.9. It is clear that both the rate and amount of moisture lost in the laboratory overestimated the realities in the field. Results for deposition 3 were obtained at roughly the same time as the laboratory values however the in situ tailings required almost twice as long to dry out. Further the lowest water content obtained in the field was 24 % whereas all the laboratory experiments were practically desaturated at the end of the drying period. Reference evapotranspiration did increase over the investigation period and consequently the number of days required for drying decreased. Another interesting factor is that not all samples exhibited the same degree of drying and in general the water content after drying increased towards the pool.

Table 4.10: Summary of drying results from field tests

Deposition	Position	Test Start	Stage Change	Drying Time (Days)	Final Water Content (%)
1	0	28-Jul	15-Aug	18	25
	50	28-Jul	16-Aug	19	32
	100	28-Jul	14-Aug	17	29
	150	29-Jul	10-Aug	13	33
	200	29-Jul	07-Aug	9	36
2	0	20-Sep	05-Oct	15	23
	50	21-Sep	06-Oct	15	27
	100	21-Sep	09-Oct	18	28
	150	21-Sep	10-Oct	19	30
	200	22-Sep	14-Oct	22	33
3	0	25-Oct	07-Nov	13	28
	50	26-Oct	09-Nov	14	25
	100	26-Oct	10-Nov	14	29
	150	27-Oct	08-Nov	12	32
	200	27-Oct	09-Nov	13	28

3. *Steady State.* Following the drying period the moisture content appeared to remain steady. Figure 4.26 is a histogram of the differences between the respective assumed water content (i.e. median value) for this steady state and the actual water contents. The left skew suggests that the average (2.6 %) is influenced by the obvious outliers and the median value of 1.5 % is a better estimate of this difference. Although higher than the 0.1 to 0.2 % water content change per day assumed by Ratliff et al. (1983) as indicative of field capacity it is suggested this steady state is field capacity. The larger variation with time is then attributed to variations in particle size distribution.

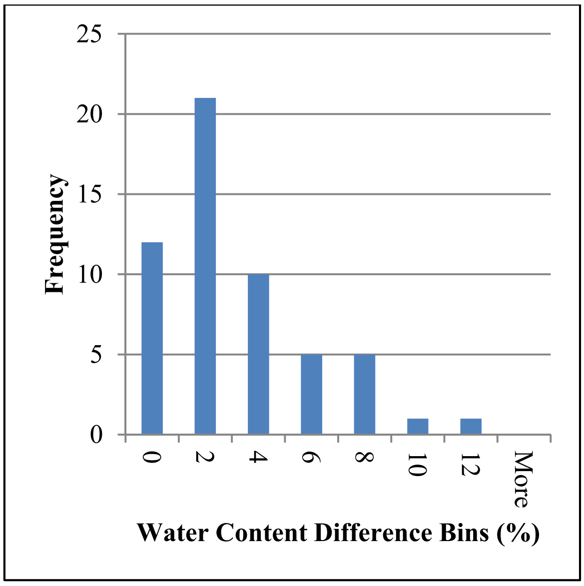

Figure 4.26: Steady state differences

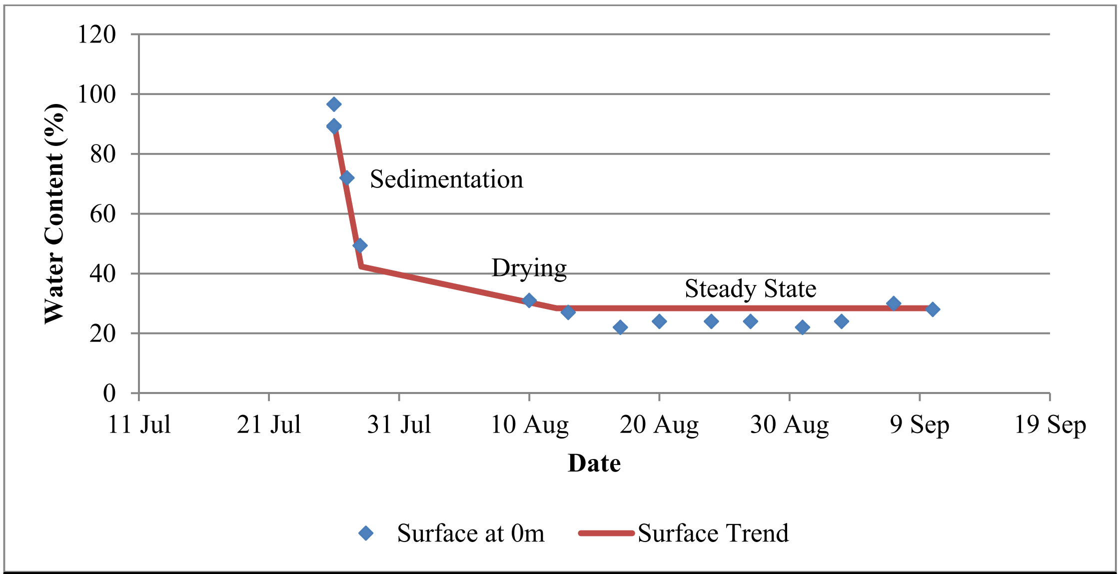

Water Content (%)
Sedimentation
Drying
Steady State
Date
Surface at 0m
Surface Trend

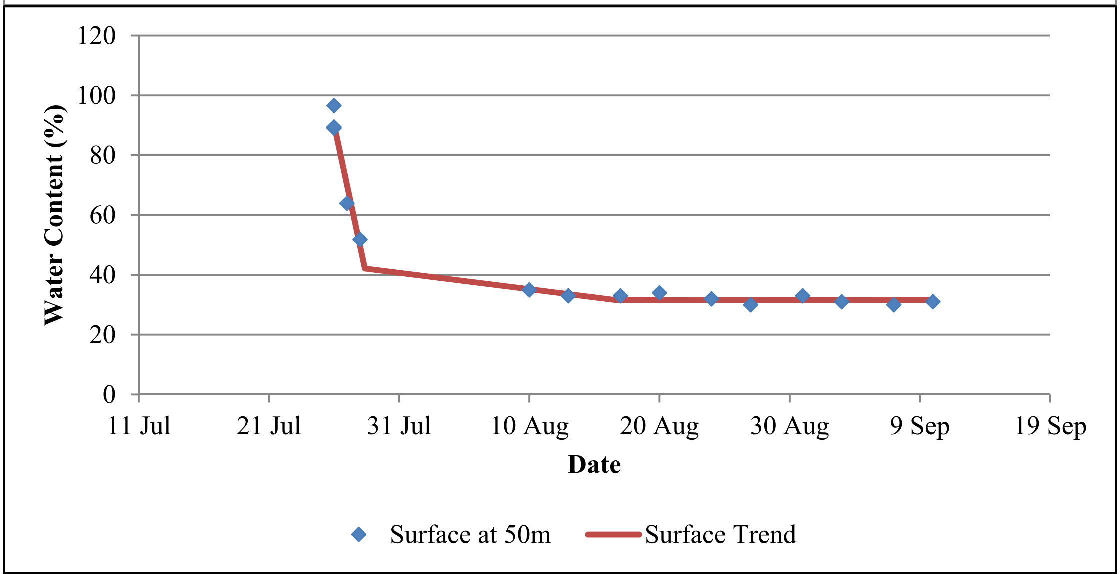

Water Content (%)
Date
Surface at 50m
Surface Trend

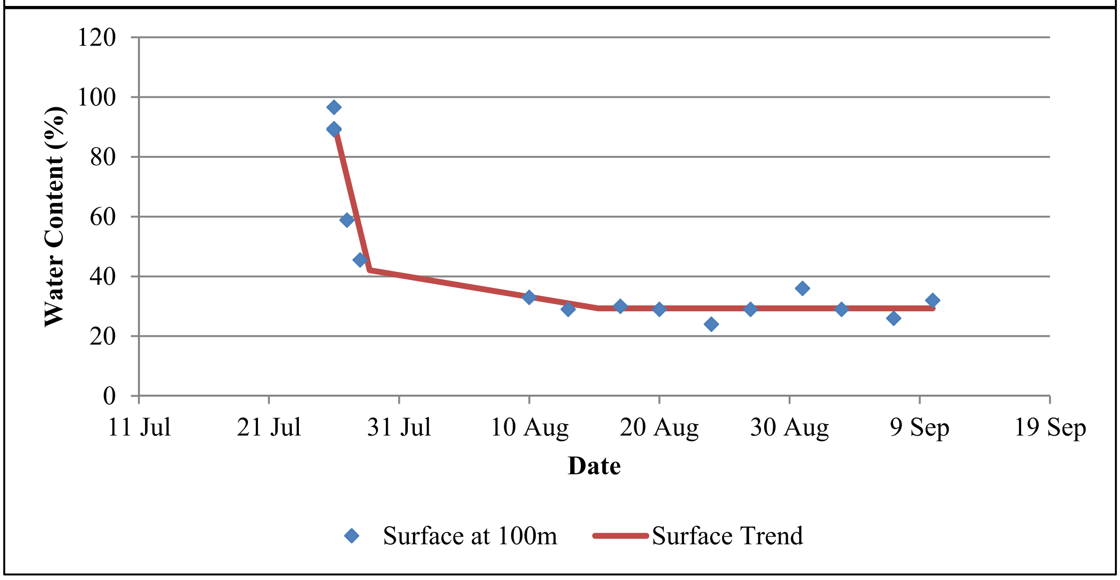

Water Content (%)
Date
Surface at 100m
Surface Trend

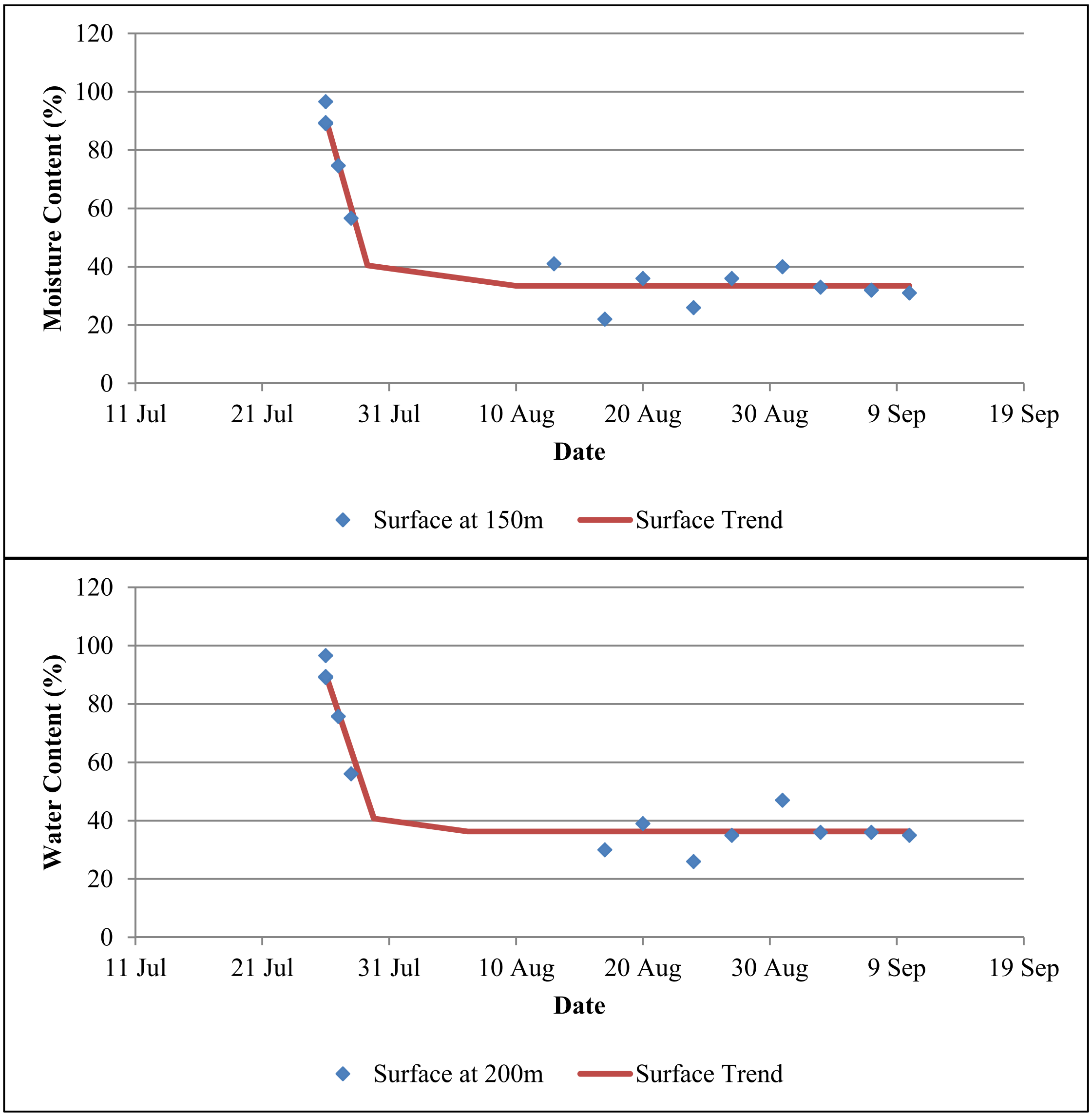

Figure 4.27: Deposition 1 drying curves

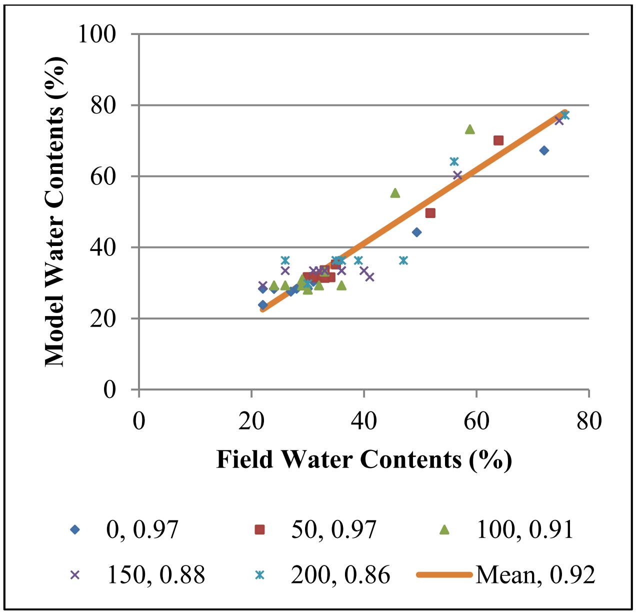

Figure 4.28: Deposition 1 scatter plot

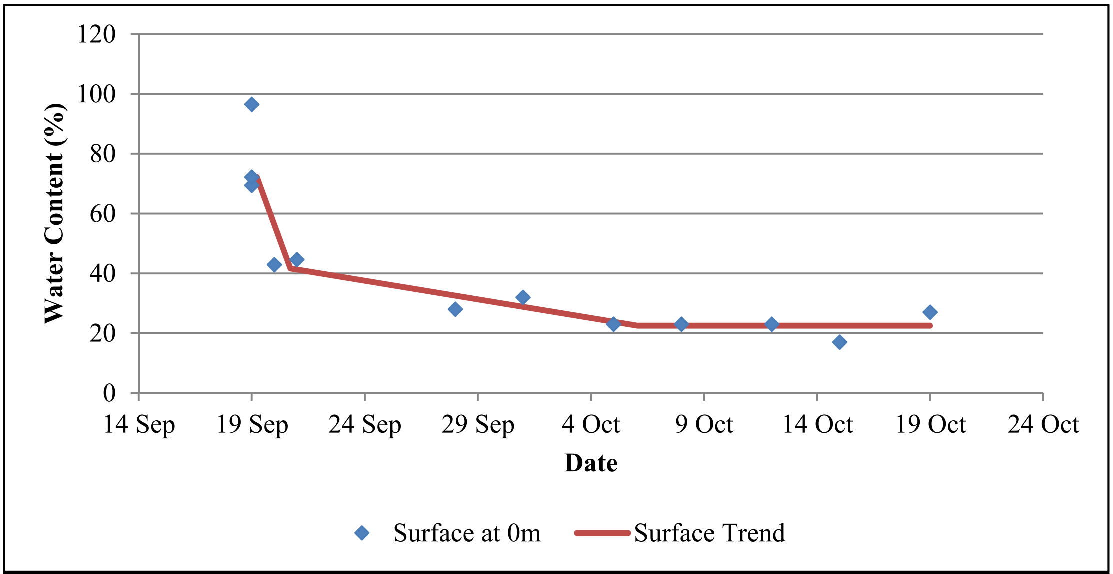
120
100
80
60
40
20
0
Water Content (%)
14 Sep
19 Sep
24 Sep
29 Sep
4 Oct
9 Oct
14 Oct
19 Oct
24 Oct
Date
Surface at 0m
Surface Trend

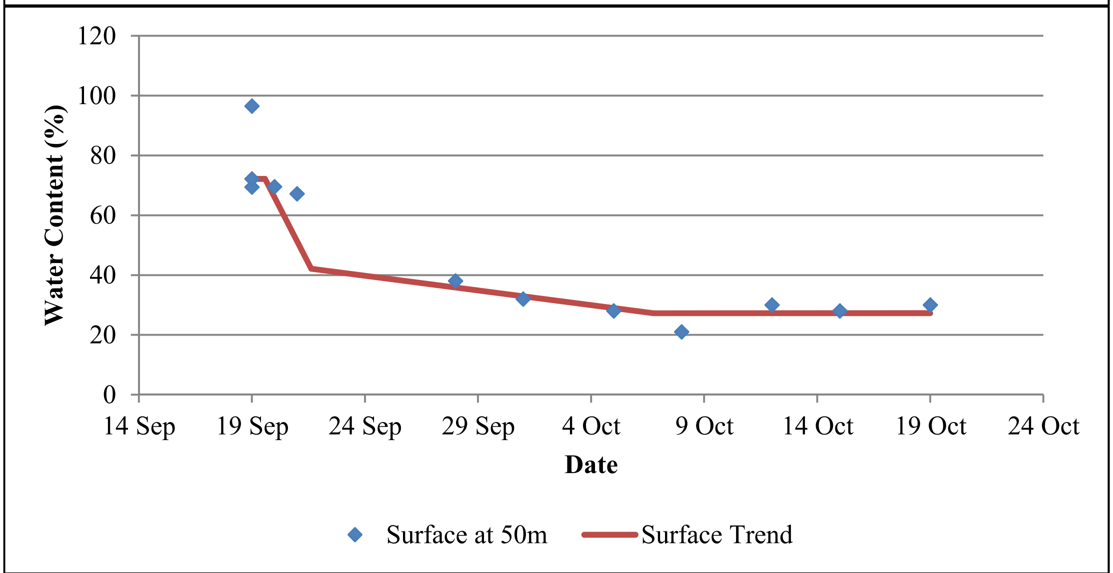
120
100
80
60
40
20
0
Water Content (%)
14 Sep
19 Sep
24 Sep
29 Sep
4 Oct
9 Oct
14 Oct
19 Oct
24 Oct
Date
Surface at 50m
Surface Trend

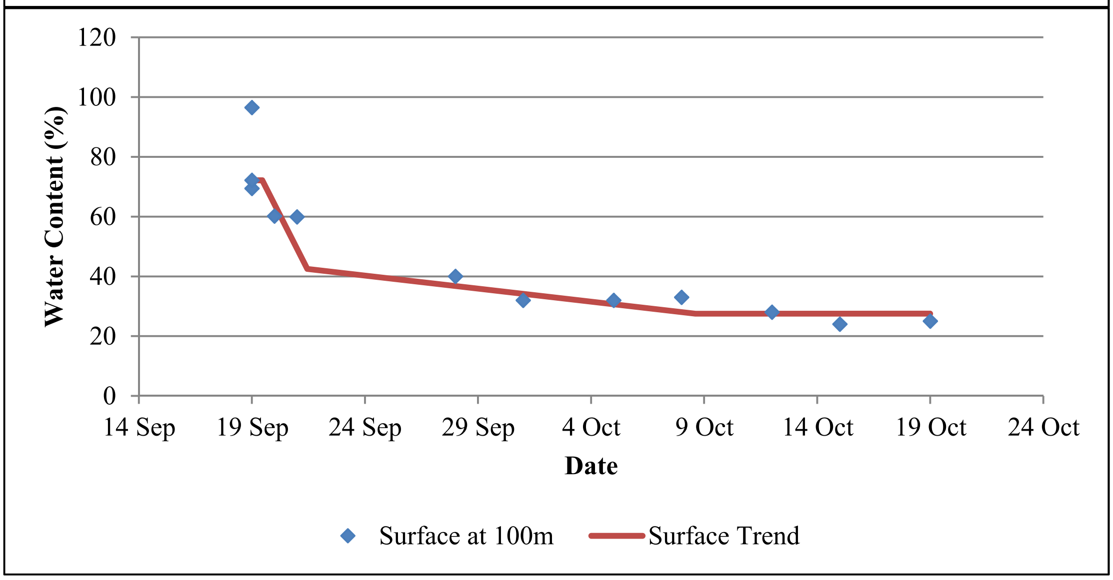
120
100
80
60
40
20
0
Water Content (%)
14 Sep
19 Sep
24 Sep
29 Sep
4 Oct
9 Oct
14 Oct
19 Oct
24 Oct
Date
Surface at 100m
Surface Trend

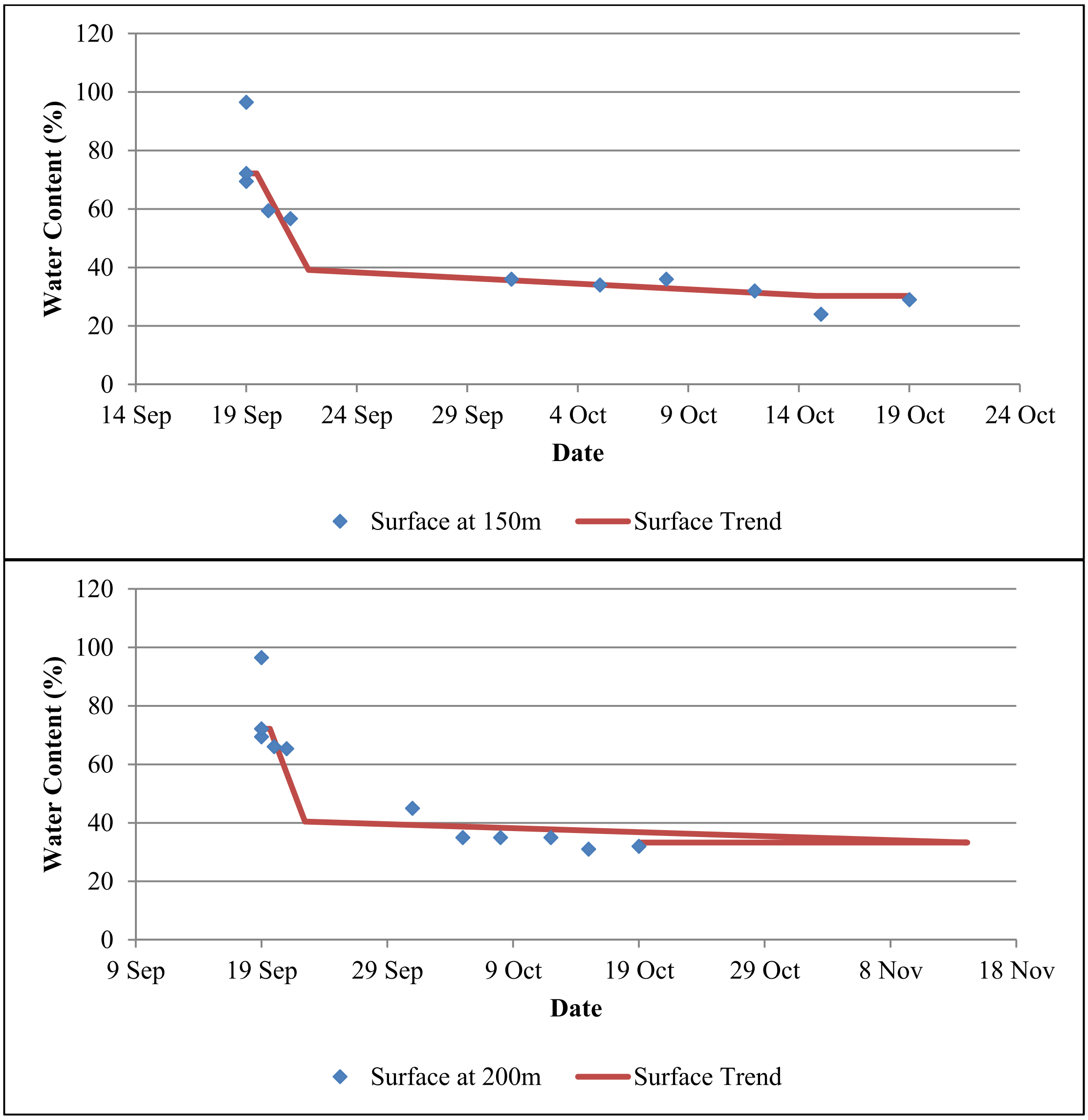

Figure 4.29: Deposition 2 drying curves

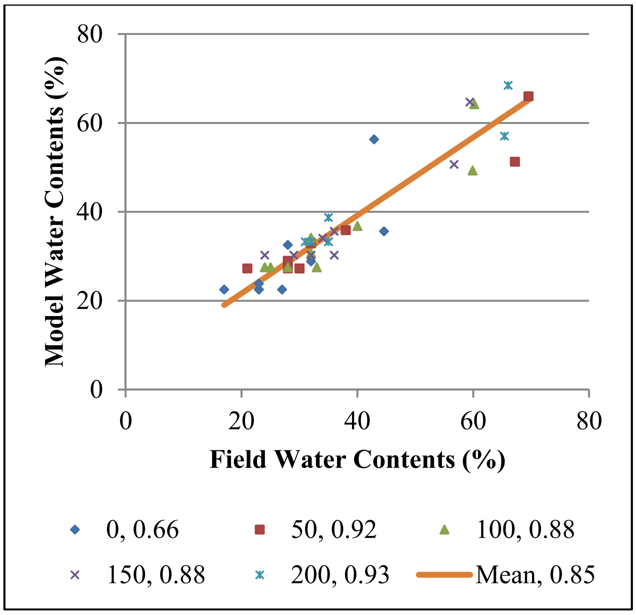

Figure 4.30: Deposition 2 scatter plot

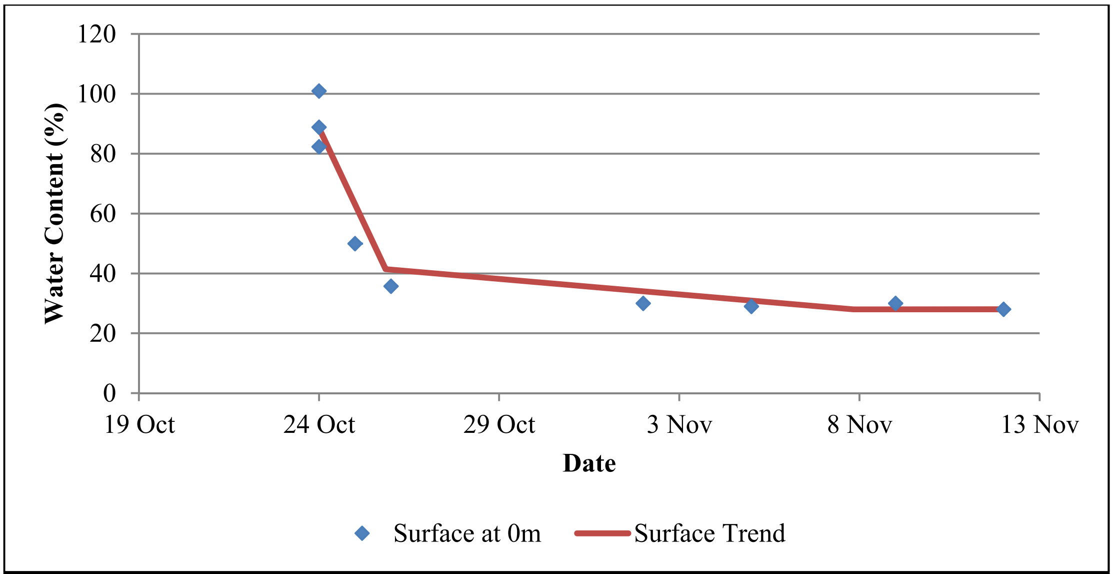
120
100
80
60
40
20
0
Water Content (%)
19 Oct
24 Oct
29 Oct
3 Nov
8 Nov
13 Nov
Date
Surface at 0m
Surface Trend

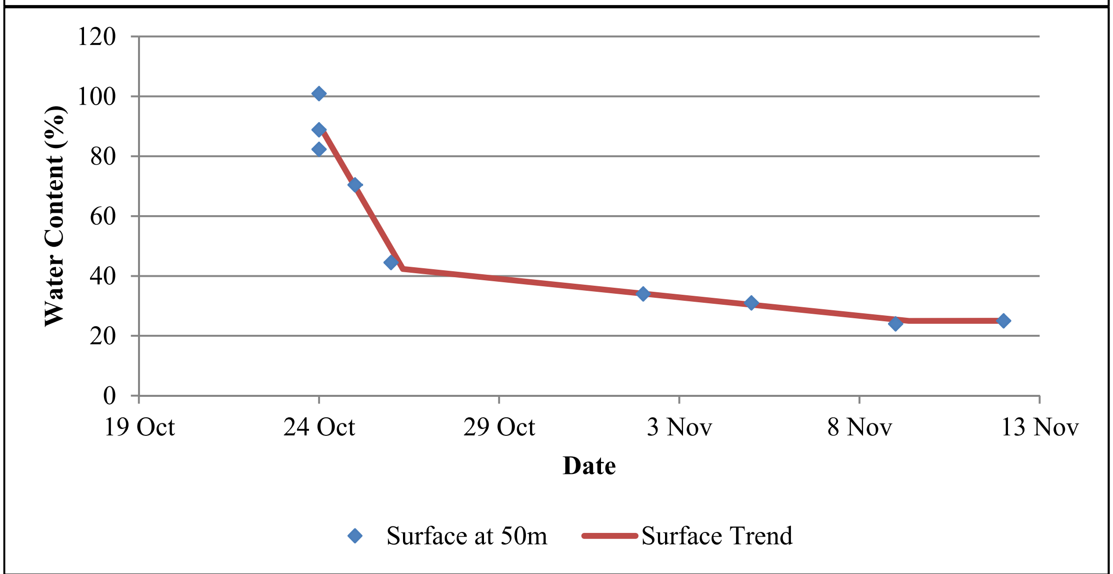
120
100
80
60
40
20
0
Water Content (%)
19 Oct
24 Oct
29 Oct
3 Nov
8 Nov
13 Nov
Date
Surface at 50m
Surface Trend

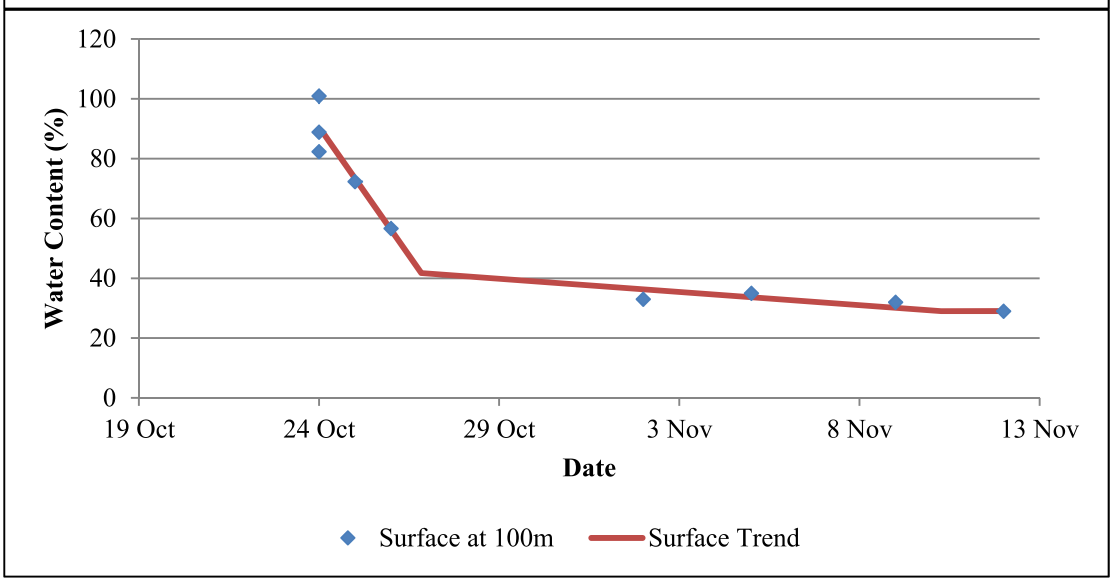
120
100
80
60
40
20
0
Water Content (%)
19 Oct
24 Oct
29 Oct
3 Nov
8 Nov
13 Nov
Date
Surface at 100m
Surface Trend

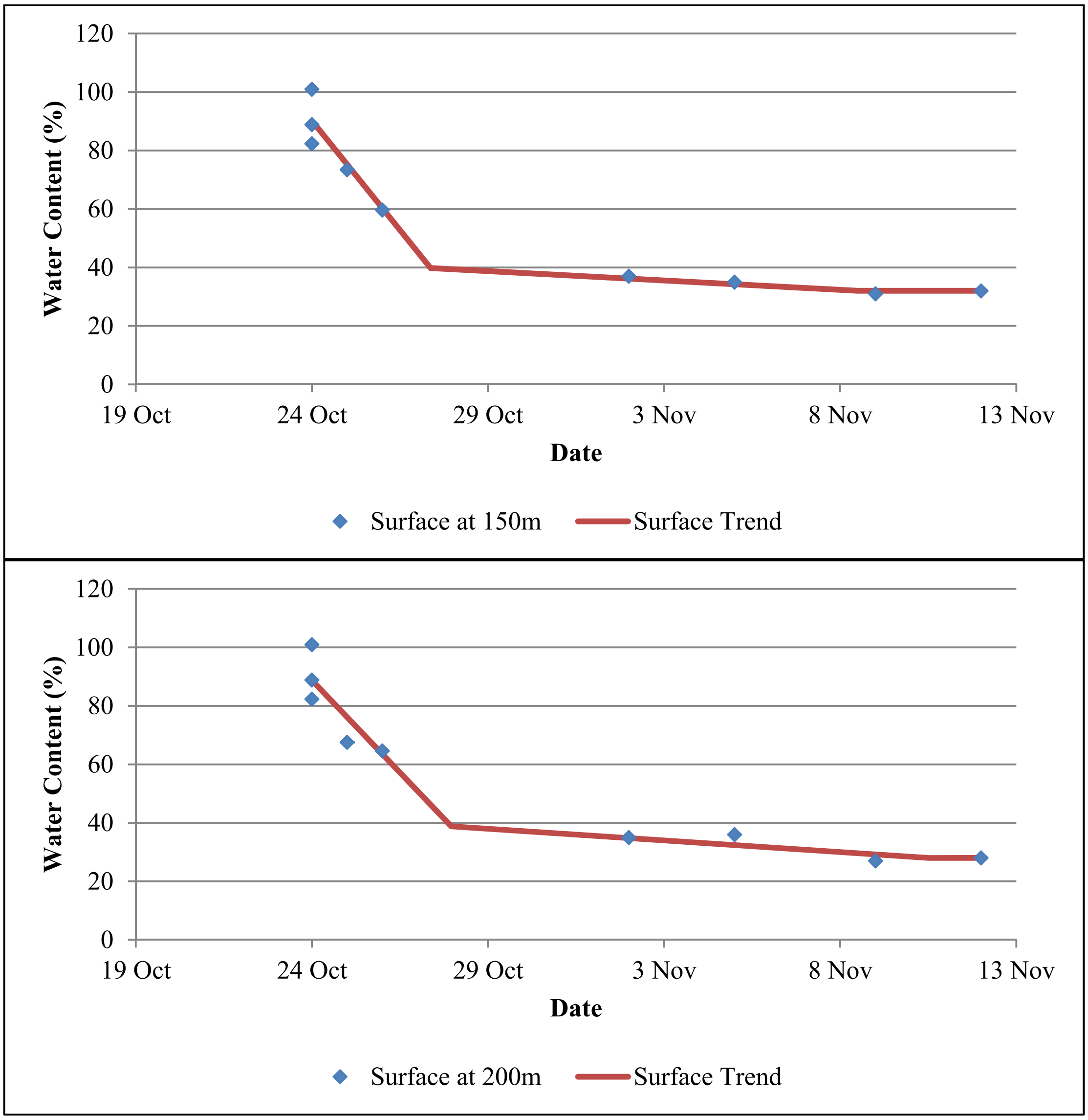

Figure 4.31: Deposition 3 drying curves

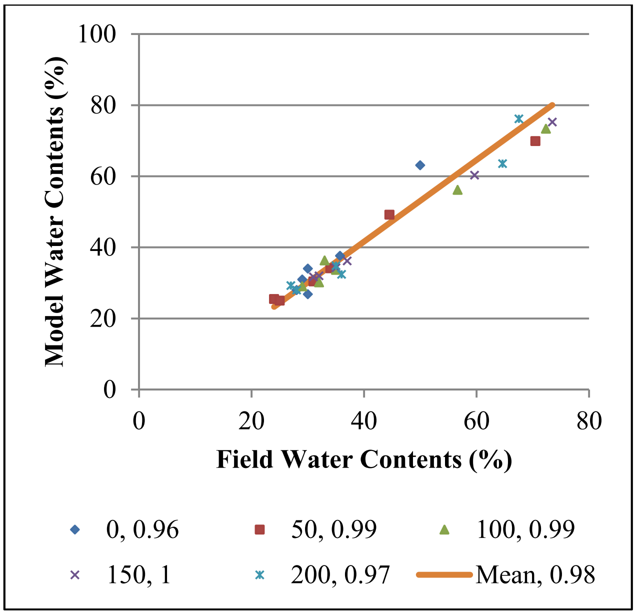

Figure 4.32: Deposition 3 scatter plot

Reference Evapotranspiration

The accuracy of meteorological variables is an important issue in evapotranspiration studies. The veracity of the evapotranspiration data was therefore compared between both regional sites during the investigation period and with historical data.

1. *Mokopane Data Set.* Daily minimum and maximum temperature, minimum and maximum relative humidity and wind speed data collected from the South African Weather Service (SAWS) Mokopane Station was used to calculate reference evapotranspiration values for the entire year of the investigation. The veracity of this data was assumed to be of a high standard as it was collected by means of a digitally controlled weather station by SAWS. This data set was therefore used to locally calibrate the Hargreaves model so that it could be applied to the Mogalakwena data set. Figure 4.33 shows the result of the local calibration as outlined in FAO 56 (Allen et al., 1998). ET_o values by the FAO 56 – PM method and by the regionally calibrated Hargreaves method are compared in Figure 4.34 for the entire year. The scatter of reference evapotranspiration is most during the summer months due to rainfall and cloud cover reducing the potential for evaporation. During winter cloud cover is minimal and therefore the full potential evaporating energy of the sun is available. The graph also illustrates that during the winter months the reference evapotranspiration is almost half that during the summer months and this should have an impact on the rate of drying during the course of the year.

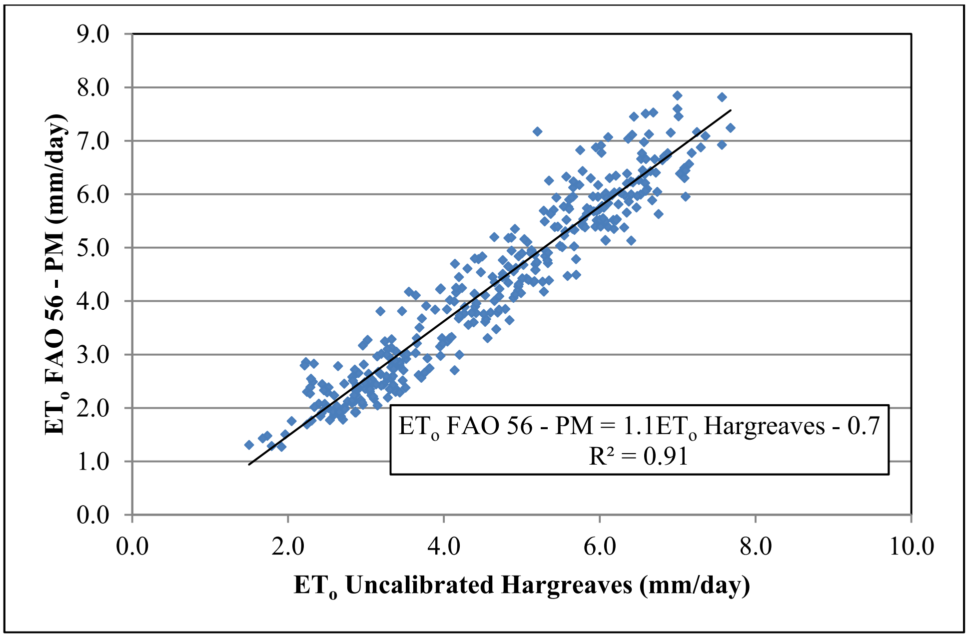

Figure 4.33: Regional calibration of Hargreaves method

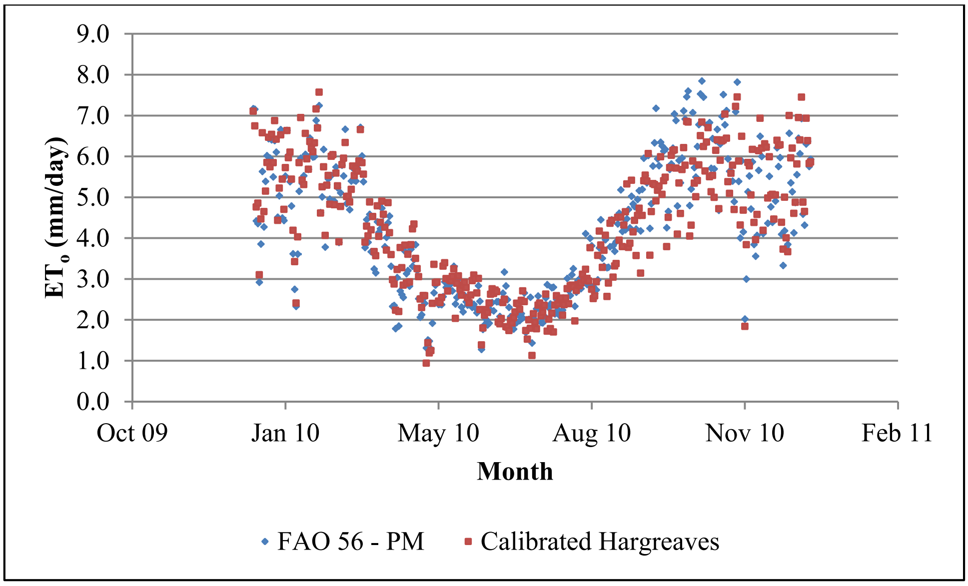

Figure 4.34: Daily ET$_o$ values based on SAWS Mokopane data

The Mokopane data set was compared to historical data for Polokwane from the CLIMWAT (Smith, 1993) database. Daily average ET$_o$ values on monthly intervals based on the SAWS Mokopane site are compared to values from the CROPWAT program for Polokwane in the scatter plot in Figure 4.35. This figure illustrates that the data collected at Mokopane during the study period correlated fairly well with historical data from the same region albeit with a degree of expected scatter.

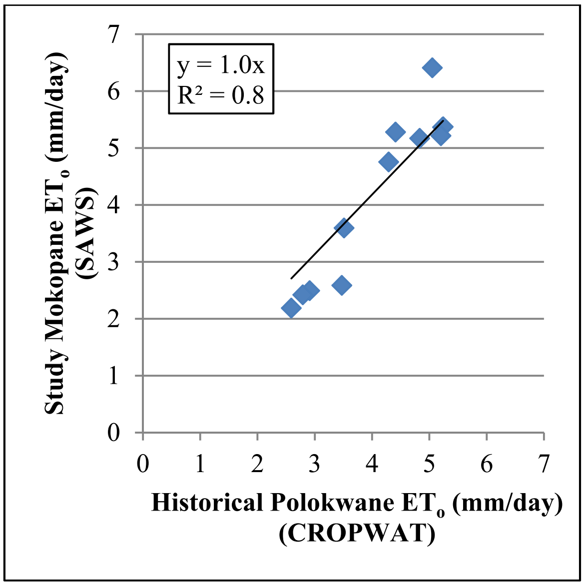

Figure 4.35: Scatter plot comparing average daily ET$_o$ values for based on monthly time steps

2. *Mogalakwena Data Set.* The calibrated Hargreaves equation based on the Mokopane data set was used to calculate the daily ET$_o$ values based on the Mogalakwena minimum and maximum daily temperatures. Similar seasonal scatter of ET$_o$ values was observed for the Mogalakwena site, however the scatter in January is larger than the scatter in December. This is as a result of

difficulties in record taking at the onset of the investigation. Figure 4.37 is a scatter plot comparing the respective ET_o values calculated from the SAWS Mokopane data set and those calculated from the Mogalakwena data set. As expected due to the sites falling in similar climatic areas there is a close correlation between the two data sets albeit with a degree of expected scatter.

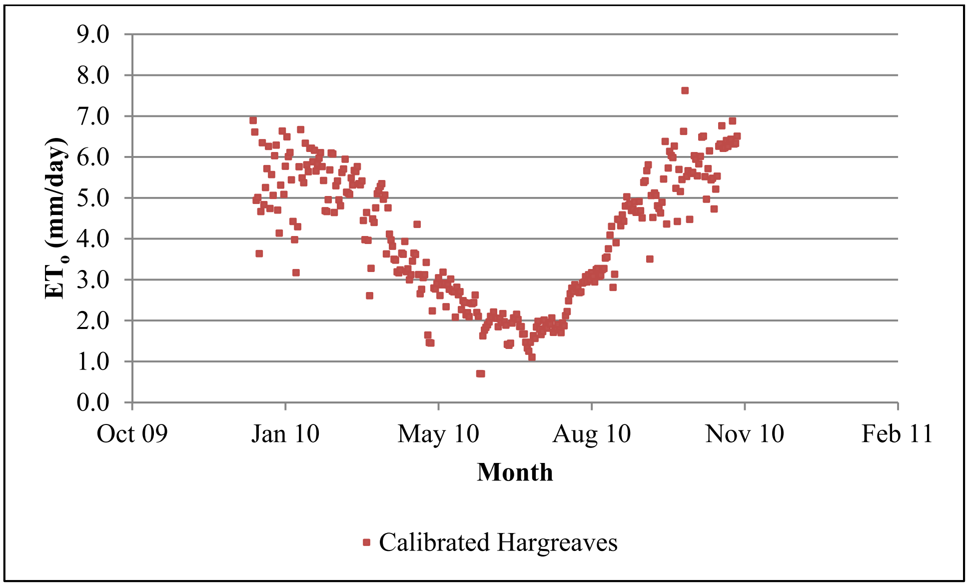

Figure 4.36: Daily ET_o values based on Mogalakwena data

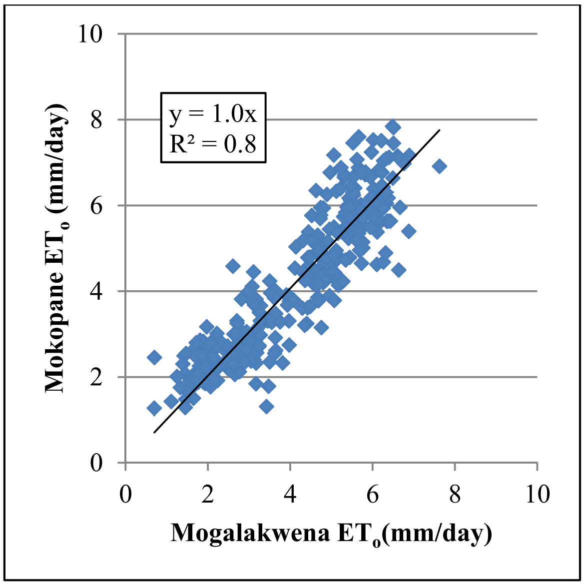

Figure 4.37: Scatter plot comparing Mokopane and Mogalakwena ET_o values

Pan evaporation from a class A-Pan was also recorded during the study and this is summarised in Figure 4.38. At the start of the study the A-Pan was located on the crest of the wall and the resulting micro climate from wind funnelling up the side of the wall is likely responsible for the observed scatter during this period. The A-Pan was moved towards the end of March to a more central position and this is the likely reason the scatter reduced after this.

However an incorrectly calibrated scale that was only picked up post the study may have compounded some errors although an attempt was made to make the necessary correction. Historical S-Pan data from the SAWS Mokopane site was converted to equivalent A-Pan evaporation based on the correlation proposed by Bosman (1988) (S-Pan on grass to A-Pan on bare soil). Figure 4.39 is a scatter plot comparing the data collected during the study to the historical data. This illustrates that although some difficulties during the investigation resulted in questionable results at times, the overall correlation with historical data was satisfactory.

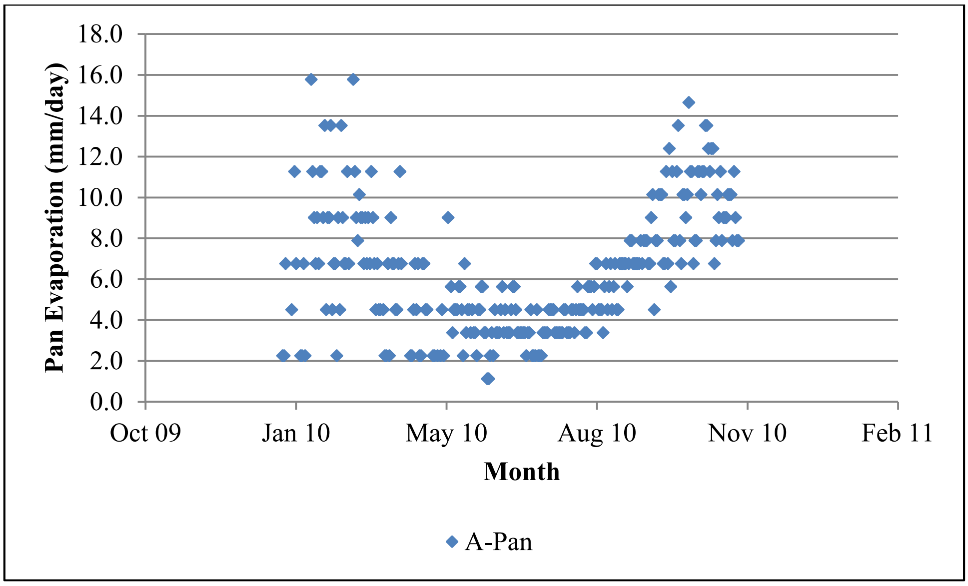

Figure 4.38: Mogalakwena daily pan evaporation

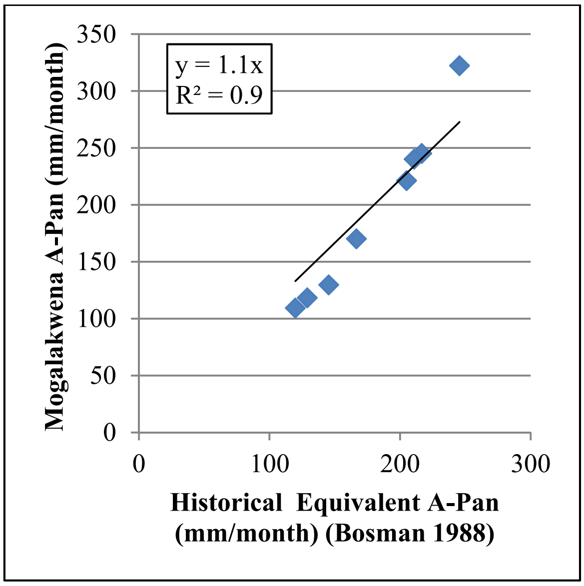

Figure 4.39: Scatter plot comparing monthly pan evaporation

The collected A-Pan data was also compared to the ET_o values computed from the Mogalakwena temperature data by means of a scatter plot. As outlined in the literature review a coefficient is required to convert A-Pan data to ET_o values, Appendix E outlines how these coefficients are determined. Based on the data obtained from Mokopane the average wind speed was 1.3 ± 0.5 m s^{-1} and the average relative humidity was 58 ± 14%. The wind speed is unlikely to be considerably higher than this on the tailings dam however the relative humidity could be higher due to the two pools and wet beaches. No vegetation was in close proximity to the A-Pan and therefore the pan would be classified as being located in a fallow area. With this information the suggested coefficient should lie between 0.6 and 0.7. The scatter plot in Figure 4.40 indicates that the average coefficient is 0.6 however the scatter is considerable.

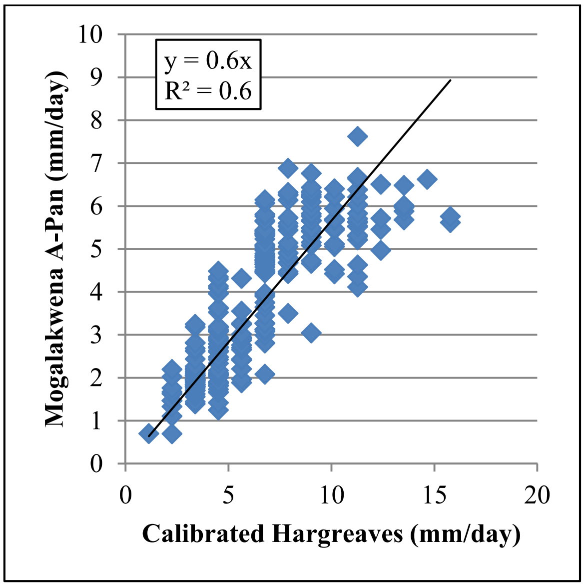

Figure 4.40: Scatter plot comparing ET_o values to A-Pan values

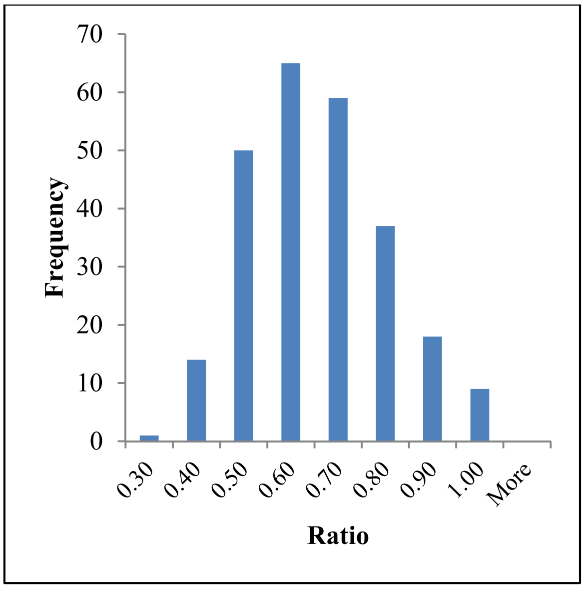

Figure 4.41: Histogram of Coefficients

A histogram of the coefficients, Figure 4.41, illustrates that the values are skewed to the right. Coefficients are generally above 0.7 for climates with relative humidities above 70 %. The right skew therefore is likely a consequence of periods when active deposition was adjacent to the A-Pan leading to a micro climate of higher humidity than those reported for the regional climate. The large scatter however is likely result of the various errors during the collection of the A-Pan data. Further as outlined in the literature review ET_o values obtained from A-Pan data are often less reliable than those based on climatic methods.

Relationship between Field Drying and Reference Evapotranspiration

An empirical correlation between the change in water content per day from sedimentation to steady state for the outer 150 m and ET_0 was developed as shown in Table 4.11. The change in water content per day was determined from the regression analysis presented above. To enable the coefficient to be compared with other sites it was felt prudent to correlate the rate of drying with a macroclimatic measure of evaporative energy independent of the dam surface microclimate that resulted in scattered A-Pan data. It is clear that the rate of drying is slower during the winter periods when evaporative energy is low and high during the summer period. The steady state reached, as shown later, is field capacity when seepage losses become negligible. Thus up to this point water loss is due to both evaporation and seepage.

Table 4.11: Developed Empirical Relationship

Deposition	Average Change in Water Content per Day	Average ET_0	k - Value	Average k - value
1	0.7	3.0	0.25	0.21
2	1.0	5.3	0.20	
3	1.1	5.9	0.18	

Evaporative energy varies throughout the year; however the rate of seepage is controlled by the materials permeability which remains essentially constant. During winter as the drying period is longer more moisture maybe lost by seepage with the opposite being the case during summer. However it is also likely that this water bleeds up to the surface as the material consolidates and is recovered. Although illustrated by the k – values being slightly higher during winter and lower during summer a longer study would be required to quantify this variation. The relationship would need to be developed taking into account evaporation, seepage and bleed water. Using the average k – value and Equation 4.1 below, Figure 4.42 illustrates the number of days to reach steady state based on daily ET_0 values.

$$\text{Days to steady state} = \frac{\text{Settled Water Content - Steady State Water Content}}{ET_0 \times \text{k-value}} \qquad \text{Equation 4.1}$$

By finding the k – value for a particular tailings it could be possible to develop a management tool to carefully control the time required for drying to maximise a facilities rate of rise.

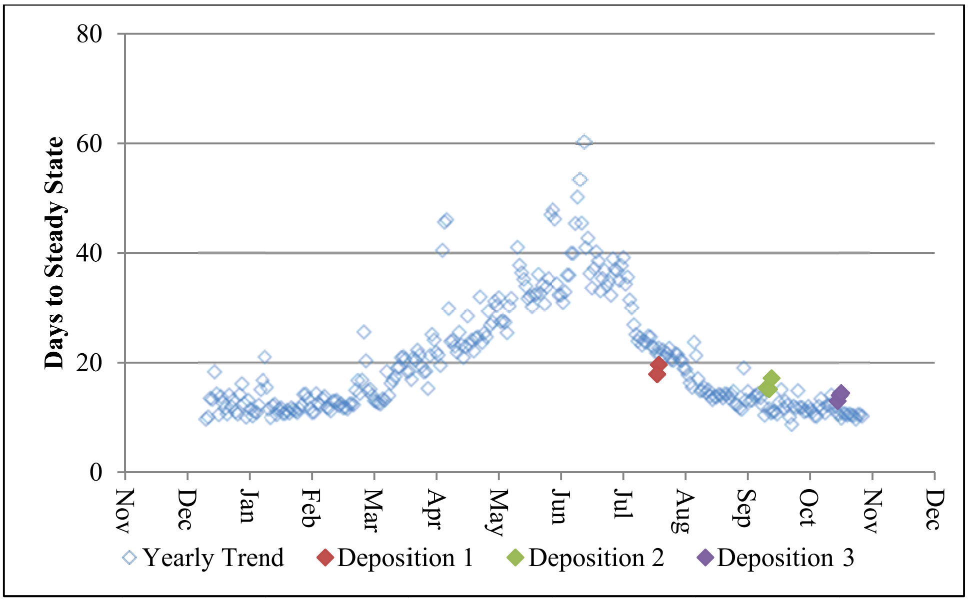

Figure 4.42: Days to dry for outer 150 m

Steady State Stage

All auger samples were taken once sufficient strength was available within the tailings to prevent the auger hole collapsing as the incremental samples were retrieved. It has already been highlighted that the surface auger samples did not exhibit any substantial change in water content with time. As such it was not possible to determine a relationship between water content and time for this stage. However a number of observations are made by looking at the distribution of water contents determined with beach position and depth. The water contents are then related to the observed geotechnical behaviour in the laboratory. These findings are presented in the following paragraphs.

1. *Time Independence*. Although it shall be shown that the water contents did vary with depth and along the beach the entire data set is plotted in Figure 4.43 against the date when the samples were taken. The range in water contents varied considerably during the investigation period with no apparent relationship with time. Water content samples were taken at progressively deeper levels over the testing period on each dam. It was found that water contents generally got higher with depth. Consequently an increasing number of higher water contents made up the samples with time. This is proposed as a possible reason for the quartile range being at higher water contents later on in the course of the experiment. However it is also possible that during the winter months less evaporation took place and that lead to a slightly wetter profile.

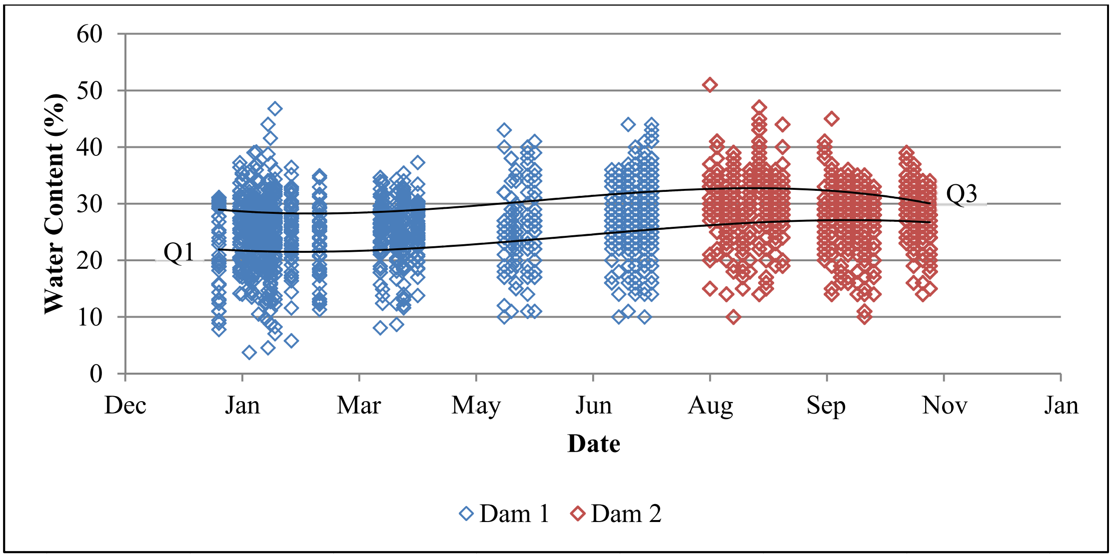

Figure 4.43: All water content samples over period of investigation

A histogram of all the water contents displayed in Figure 4.43 is presented in Figure 4.44. The distribution of values is essentially bell shaped as per the normal distribution. Results from Dam 1 were skewed slightly to the left with the quartile values in a narrow band at 23, 27 and 30 % respectively. Results from Dam 2 were skewed slightly to the right with the quartile values in a narrow band at 27, 29 and 32 % respectively. Dam 2 was therefore on average 3 % moister than Dam 1.

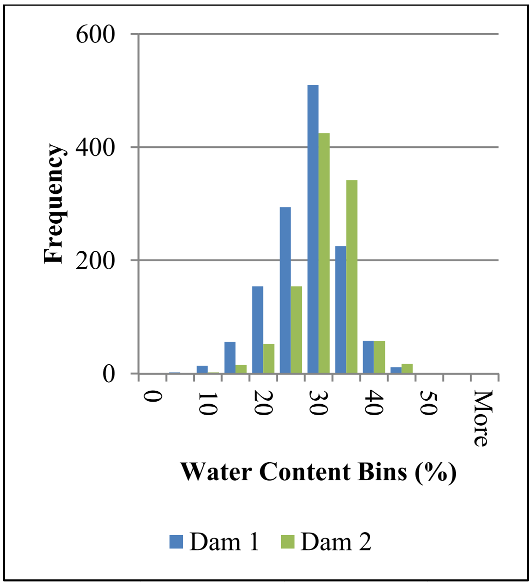

Figure 4.44: Histogram of all water contents determined

The in-situ dry densities can be inferred from the laboratory determined volumetric shrinkage curve as is done in Figure 4.45. All water contents obtained during the investigation are presented by box plots. It would appear that some samples were taken prior to peak dry density being reached at air entry. Roughly 25 % of the samples taken on Dam 1 and Dam 2 respectively were therefore saturated, whereas 75 % of the samples were at varying degrees of desaturation and had reached peak dry density. Drying in the field leads to cracks forming which are filled by subsequent depositions. This can lead to a less dense state to that illustrated by the laboratory drying tests.

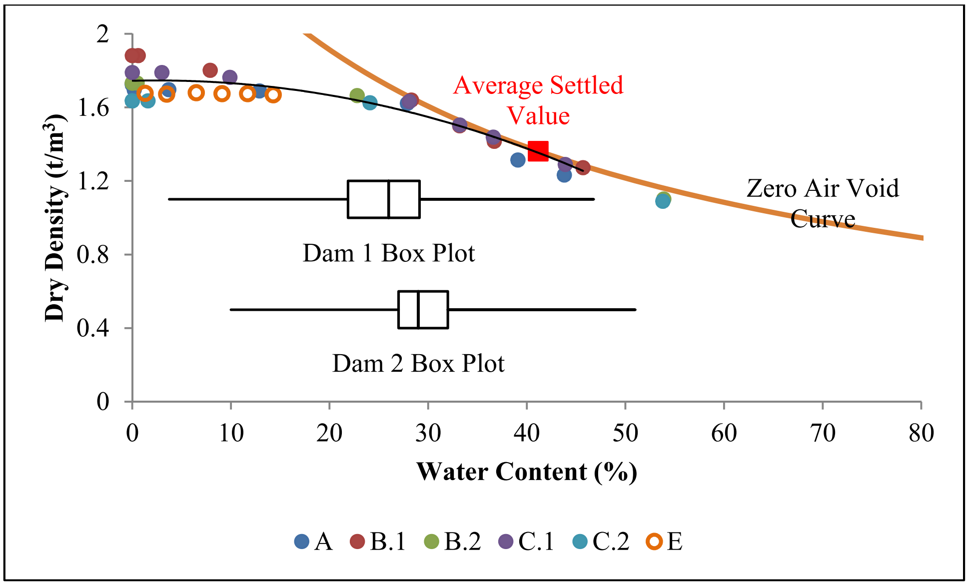

Figure 4.45: Comparison of field water contents to the laboratory determined volumetric shrinkage curve

Some of the general drying trends are illustrated in Figure 4.46 and Figure 4.47. The water contents displayed for Dam 1 varied considerably between roughly 10 and 30 % whereas on Dam 2 the values varied between 15 and 30 %. Dam 1 also exhibited a larger degree of scatter than Dam 2. It is proposed that these variations are a result of grain size and available evaporative energy. Generally the finer a material the greater its affinity for water, as was shown earlier the range in particle sizes was greater for Dam 1 than Dam 2. Further from the segregation results; Dam 1 generally was coarser at position 0 m than Dam 2. The lower water contents on Dam 1 can therefore be attributed to this difference in particle sizes. The results presented for Dam 1 also show that the reference evapotranspiration was nearly double that for the results presented for Dam 2.

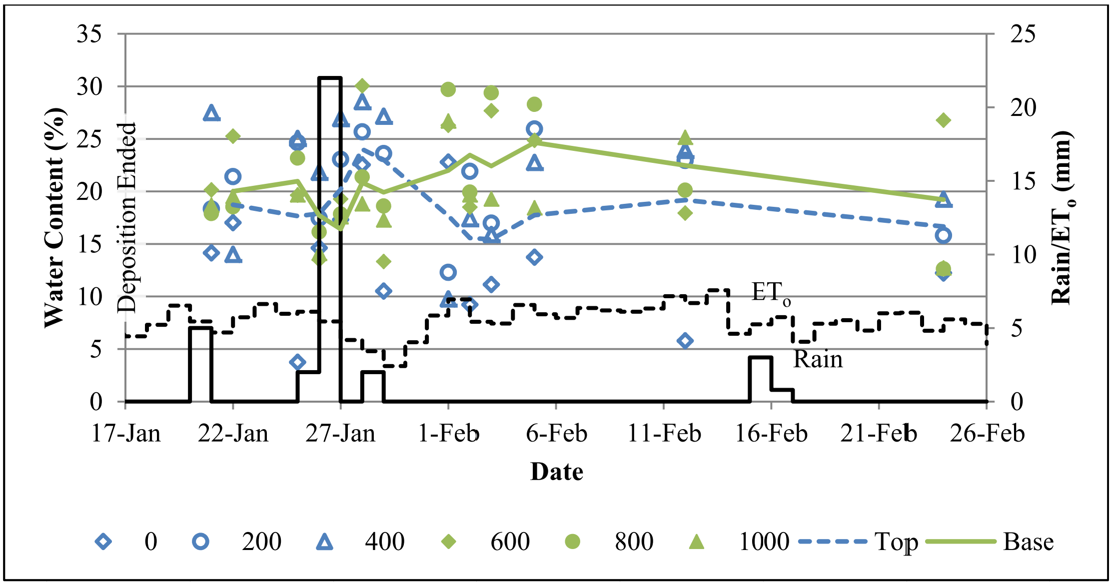

Figure 4.46: Field drying behaviour - Dam 1, Deposition 1, Position 0 m

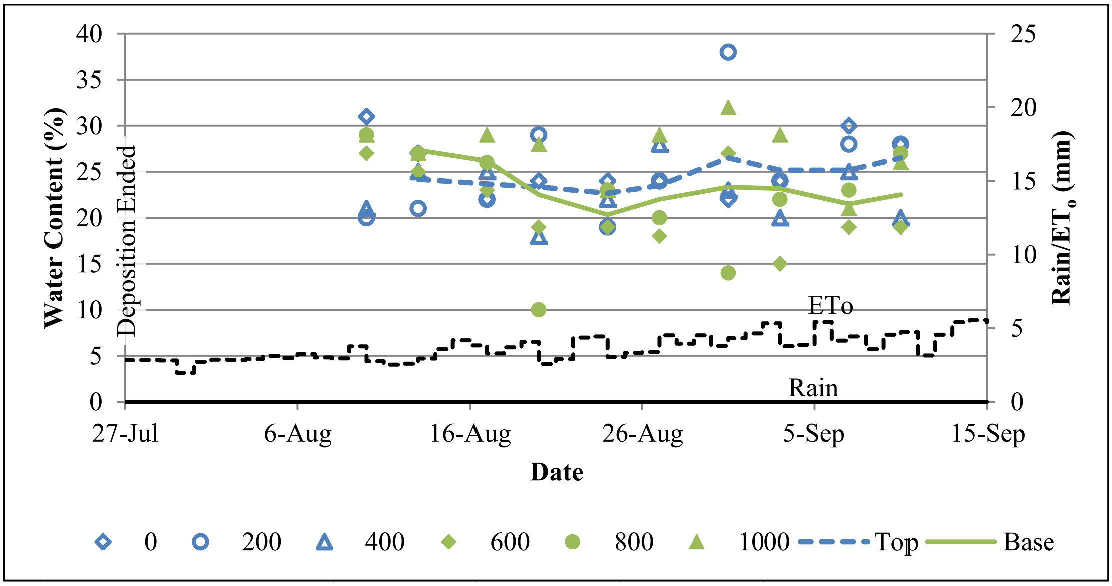

Figure 4.47: Field drying behaviour - Dam 2, Deposition 1, Position 0 m

The impact of rain on the drying behaviour is also shown by Figure 4.46. Prior to the major rainfall event on 26 January, the base layer was slightly wetter than the surface layer[3]. Following the rainfall the top layer became substantially moister however after 6 days the moisture had seeped into the lower layer. Both layers subsequently dried; with the top layer remaining slightly drier than the base layer. Due to the lower evaporative energy available during the test deposition on Dam 2 a longer period of time elapsed between the end of deposition and when sampling could commence. No rainfall was recorded during the testing period as is illustrated in Figure 4.47.

[3] The top layer curve is a 2 point moving average of the average water content of the samples taken at 0, 200 and 400 mm at each time step. Likewise the base layer curve is a 2 point moving average of the average water content of the samples taken at 600, 800 and 1000 mm at each time step.

Although the base layer initially was at a higher water content than the top layer the trend reversed for the remainder of the experimental period. However the difference between the two curves was essentially insignificant.

The behaviour during the depositions not reported here and further along the beach displayed a similar random change in water content with time. Similarly to the surface samples the average behaviour of the water samples determined did not vary considerably with time. The average water content on Dam 1 for the displayed period was 20 % with a standard deviation of 5.7 % and the respective values on Dam 2 were 24% and 4.7 %. It therefore appears that the moisture regime of the entire profile is influenced by the field capacity value. If it is assumed that the majority of samples are at field capacity and lower then moisture transfer is dominated by movements due to moisture deficits. The magnitude of these moisture deficits is governed by natural and random processes as is the transfer of moisture to replenish them. As such predicting a definitive change with time is difficult during active deposition.

Substantial drying appears to only occur after a long period of inactivity. The discussion on beaching behaviour highlighted that the test strip on Dam 1 was left dormant in excess of 6 months. Figure 4.20 illustrated that as a result the outer 100 m of the profile was at much lower water contents than the average behaviour illustrated in Figure 4.21. As the dams were operational during the investigation leaving areas dormant for long periods was not feasible and thus the long term drying was not investigated.

2. *Beach Position Relationship.* When the water contents obtained during the investigations are plotted against beach position it becomes apparent that the moisture regime becomes progressively wetter towards the pool. This is clearly shown in Figure 4.48 which plots all the water contents irrespective of depth obtained on Dam 1. At 0 m the water contents ranged between 5 and 35 % with the quartile range being between 16 and 25%. Along the rest of the beach the values ranged from 5 to 45 % with the quartile range at progressively higher water contents further along.

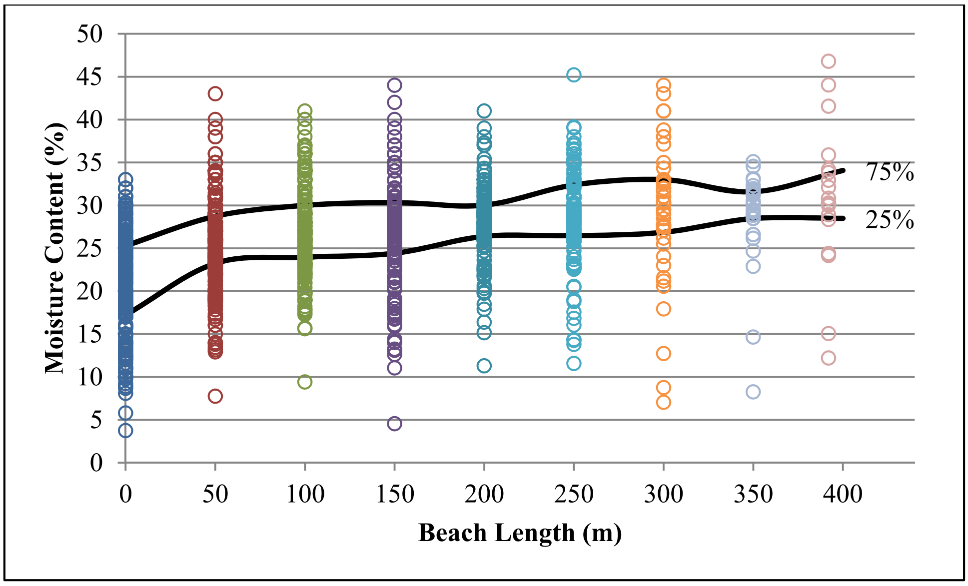

Figure 4.48: Dam 1 water contents plotted against beach position

Figure 4.49 plots the respective histograms of water contents determined along the beach. The upper and lower bound field capacities as well as the inter quartile values determined by the numerical modelling based on grain size are also shown. All the distributions are essentially normal with the peak occurring at progressively higher water contents with increasing distance along the beach. Some of the distributions have a second smaller peak at higher water contents. These are likely water content samples prior to field capacity being reached. Interestingly it is only at the 0 m position were the distribution of values exhibits a large degree of dispersion whereas the other distributions have a central tendency. This distribution of values at 0 m is across the entire range of field capacity values. The average water content at this position falls within the narrower field capacity band defined by the inter quartile range of grain sizes. The distributions further along the beach become progressively moister. It is proposed that the field capacity values are higher as a consequence the material becoming finer and the phreatic surface being closer to the surface. Further the majority of water contents after 250 m are essentially saturated (see Figure 4.23) suggesting the material is at hydrostatic equilibrium with the phreatic surface. This is consistent with Koorevaar et al (1999) who indicated that field capacity values can be higher when the moisture regime is in equilibrium with ground water.

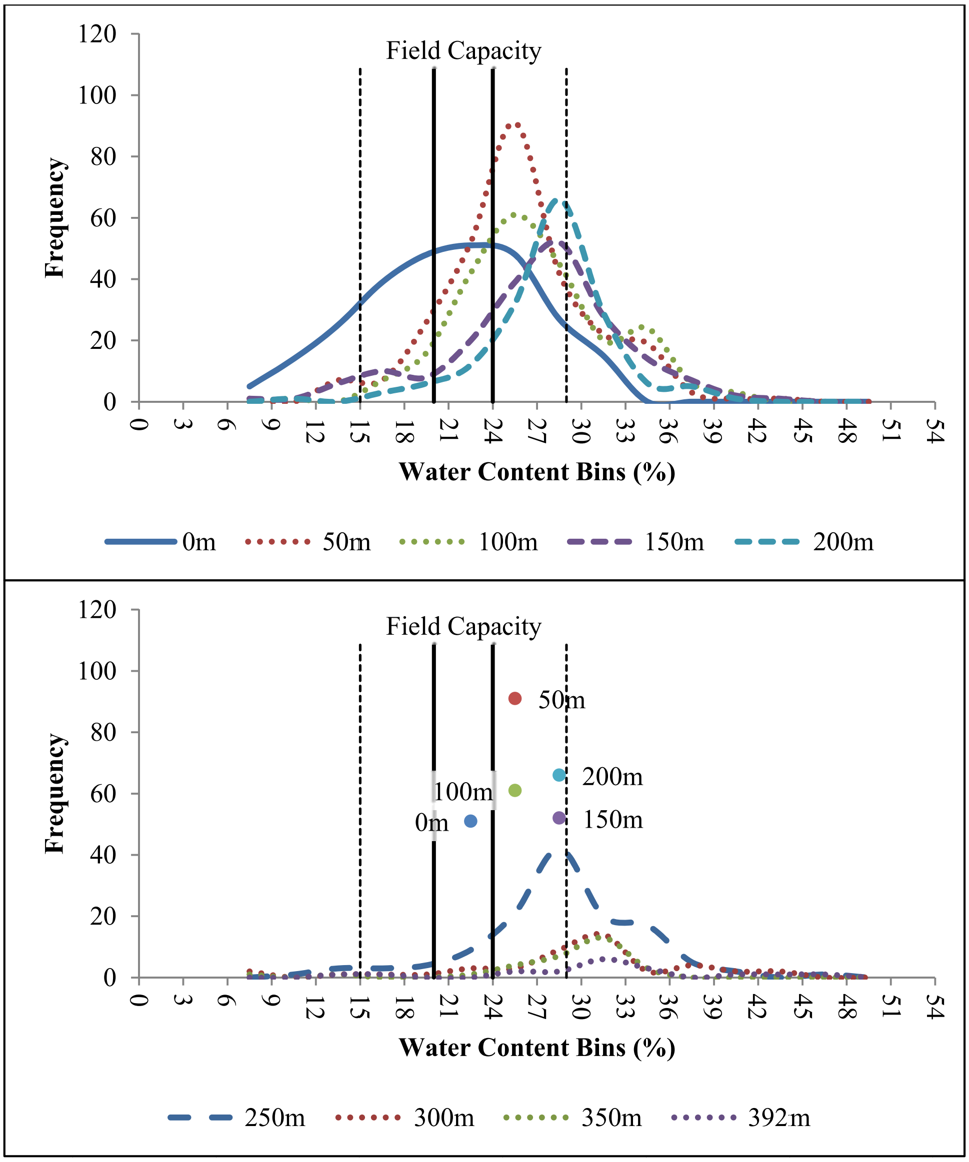

Figure 4.49: Dam 1 water content distributions along beach

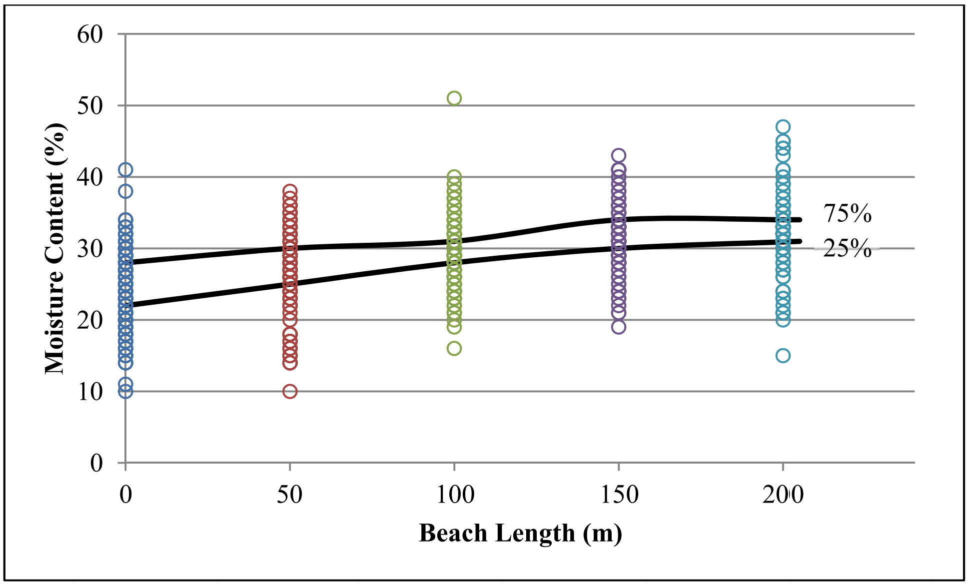

Figure 4.50: Dam 2 water contents plotted against beach position

Figure 4.50 shows that a similar trend with beach length was observed on Dam 2. At 0 m the water contents ranged between 10 and 40 % with the quartile range being between 21 and 28%. Along the rest of the beach the values ranged from 10 to 45 % with the quartile range at progressively higher water contents further along. Figure 4.51 plots the histograms of water contents determined along the beach showing the distribution of values displayed in Figure 4.50. A similar distribution of water contents to Dam 1 is also apparent.

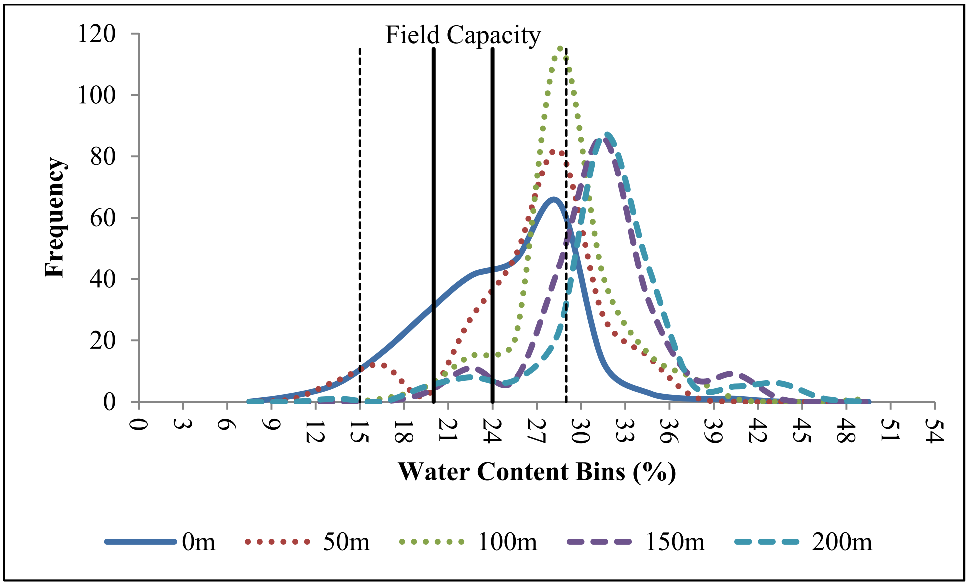

Figure 4.51: Dam 2 water content distributions along beach

All the distributions, excepting the values at 0 m are essentially normal with the peak occurring at progressively higher water content with increasing distance along the beach. At the 0 m position the peak occurs at the same class interval as the 50 and 100 m peaks, however the distribution of values exhibits a large degree of dispersion as well as left skew. Figure 4.44 showed that on the whole Dam 2 was roughly 3 % moister than Dam 1 and here it is shown that this behaviour was indeed exhibited along the entire beach. Two reasons are suggested for this; the shorter beach length and the depositional strategy. It is suggested that as the beach is shorter the phreatic surface does not become as depressed as in the case of the longer beach. Consequently a larger portion of the beach is in equilibrium with the phreatic surface leading to the higher field capacity values. Indeed a large portion of the water contents after the 100 m position are above a water content of 30 % indicating that the material is most likely saturated. Prior to test work the rate of rise on Dam 2 was almost twice the rate at which Dam 1 was being raised (During test work the rate of rise on each dam was essentially the same). This necessitated that a rock impoundment be constructed to provide a stable embankment. It is suggested that insufficient drying had taken place and the underlying tailings contained more moisture to replenish drying induced deficits.

By calculating the Liquidity Index (LI) the laboratory stress-strain relationship could be scaled to the in-situ behaviour. To take into account the variation in Atterberg limits determined for the tailings the minimum, average and maximum liquidity indices are calculated. The percentage of samples exhibiting brittle, plastic and liquid stress-strain behaviour along the beach were computed and are displayed in Figure 4.52 and Figure 4.53. It is apparent that the majority of the samples suggest that the in-situ material is a viscous mass. Holtz and Kovacs (1982) indicated that material with liquidity indices higher than 1 maybe relatively strong however if sheared can easily flow. Further the tailings have already been shown to have a propensity to liquefy. These high liquidity indices would suggest that the majority of the deposited tailings do not contribute substantially to the strength of the facility. It must be kept in mind that the material had sufficient strength to resist the weight of a man and prevent the auger hole collapsing. Thus substantial shear would be required to cause flow of the material.

Greater dispersion of water content values at the 0 m position results in a larger portion of LI values lower than 1 as indicated in Table 4.12. Due to the lower water contents on Dam 1 (reasons for which have been given earlier) a larger portion of the samples are at lower LI values than Dam 2. The percentage of samples falling in the brittle, plastic and liquid classes are thus only roughly equal at the minimum and maximum Atterberg limits for Dam 1 and Dam 2 respectively. LI values less than 0 are indicative of overconsolidated material (Das, 2008) and high shear strength (Bovis, 2000). It would thus appear that it is only the outer section that undergoes sufficient drying to result in an overconsolidated material that has sufficient shear strength to impound the viscous tailings. The higher phreatic surface as a consequence of a shorter beach may however retard this drying process and require lower rates of rise to ensure stability. Consequently it is suggested that research be focused on the drying of the outer section as it is this section that contributes significantly to the strength of the facility.

Table 4.12: Summary of liquidity indices at 0 m

Location	Liquidity Index Range	Reference Atterberg Limits			Behaviour
		Minimum	Average	Maximum	
Dam 1 0 m	LI < 0	31%	40%	48%	Brittle
	0 < LI < 1	18%	22%	26%	Plastic
	LI > 1	52%	38%	26%	Liquid
Dam 2 0 m	LI < 0	11%	15%	24%	Brittle
	0 < LI < 1	13%	22%	25%	Plastic
	LI > 1	76%	64%	52%	Liquid

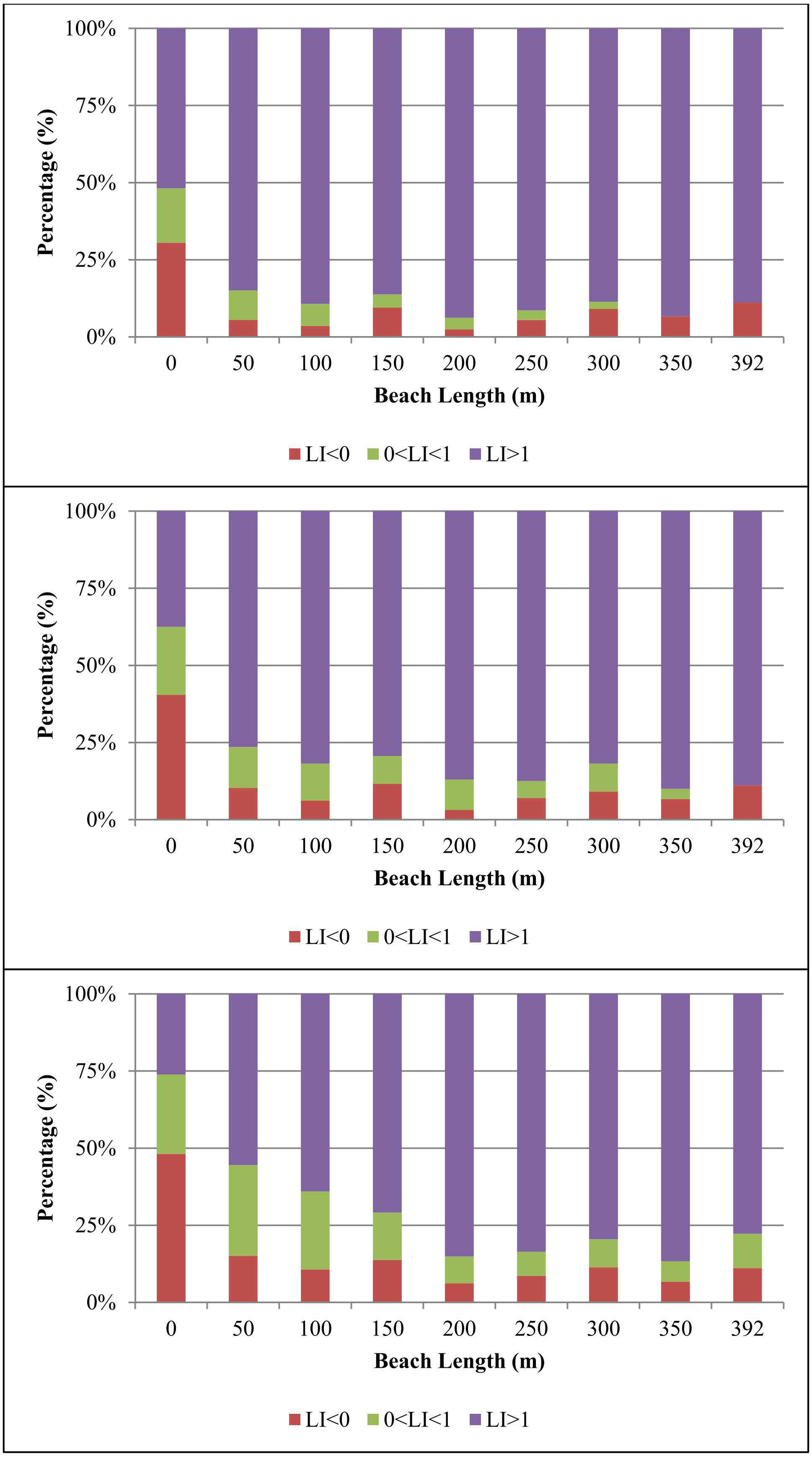

Figure 4.52: Dam 1 liquidity indices with beach; based on minimum, average and maximum Atterberg limits

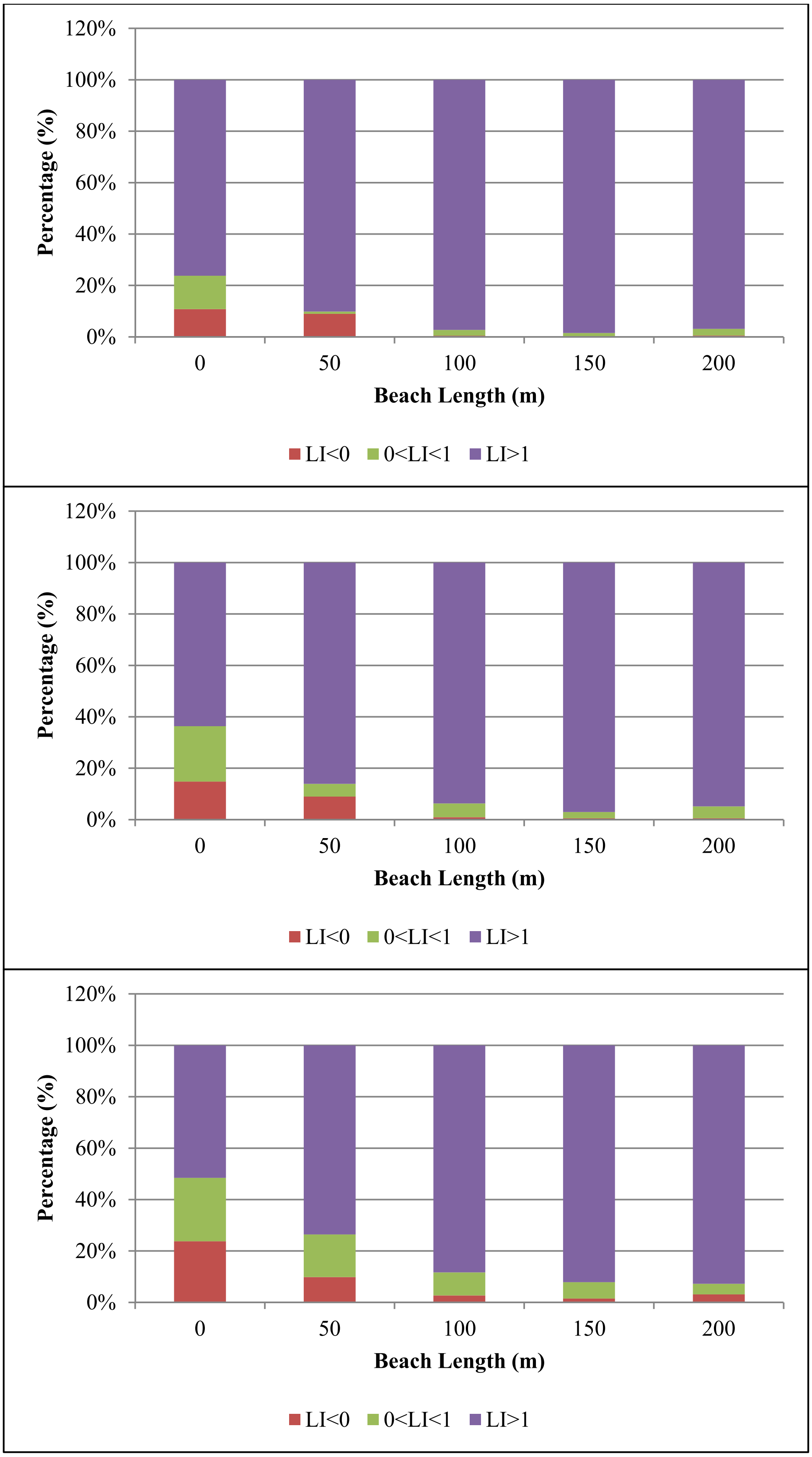

Figure 4.53: Dam 2 liquidity indices with beach; based on minimum, average and maximum Atterberg limits

3. *Depth Relationship*. The moisture regime with depth has only been explored at the 0 m beach position. It has been shown that water contents determined along the rest of the beach had a central tendency. Therefore no significant distribution of values can be expected with depth. The distribution of water contents with depth at 0 m on Dam 1 are given in Figure 4.54. The upper and lower bound field capacities determined by the numerical modelling based on grain size as well as the quartile range values are also shown. A number of the distributions are atypical of normal behaviour exhibiting a large amount of dispersion and skew both to the right and to the left. A portion of the results are at water contents lower than field capacity however this does decrease with depth. However the majority of the water contents are within the range of expected field capacity values. Very few results are above the field capacity values. This behaviour suggests that the phreatic surface is further enough from the sampling position to not influence the field capacity values and drying beyond the field capacity values could occur.

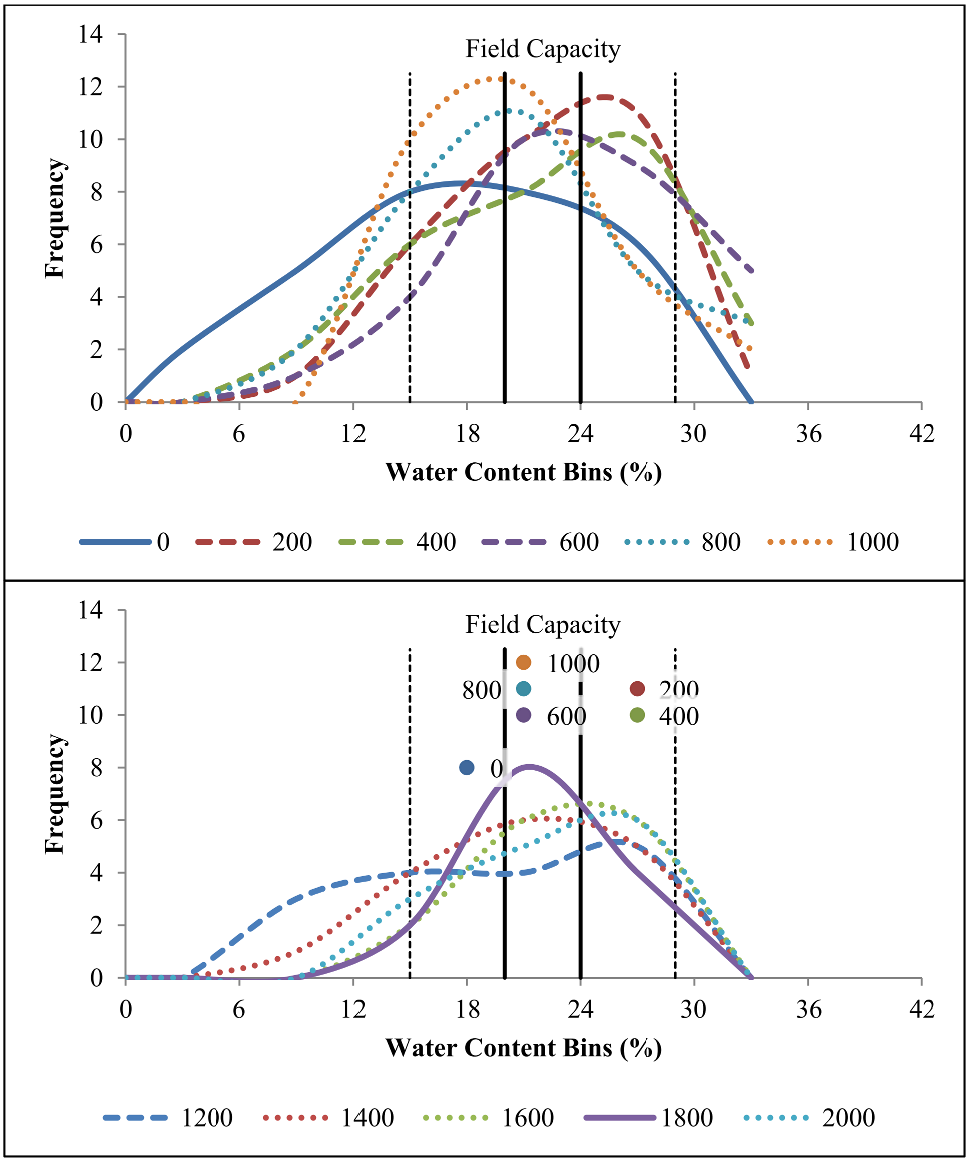

Figure 4.54: Dam 1, 0 m depth trend

The distribution of water contents with depth at 0 m on Dam 2 are given in Figure 4.55. Conversely to Dam 1 the distributions exhibit typical normal behaviour with two distinct layers within the profile. An upper layer that appears to have undergone more drying with the range of water contents similar to the range on Dam 1 at the same position. And a lower layer, although within the field capacity bounds, that did not appear to have undergone as much drying. Earlier it was highlighted that prior to test work this dam has been raised at a higher rate. During test work roughly 1 m of material was deposited in successive depositions which correlate with this drier layer. It would therefore appear that at the higher rate of rise less moisture was lost and this was trapped in by the subsequent depositions.

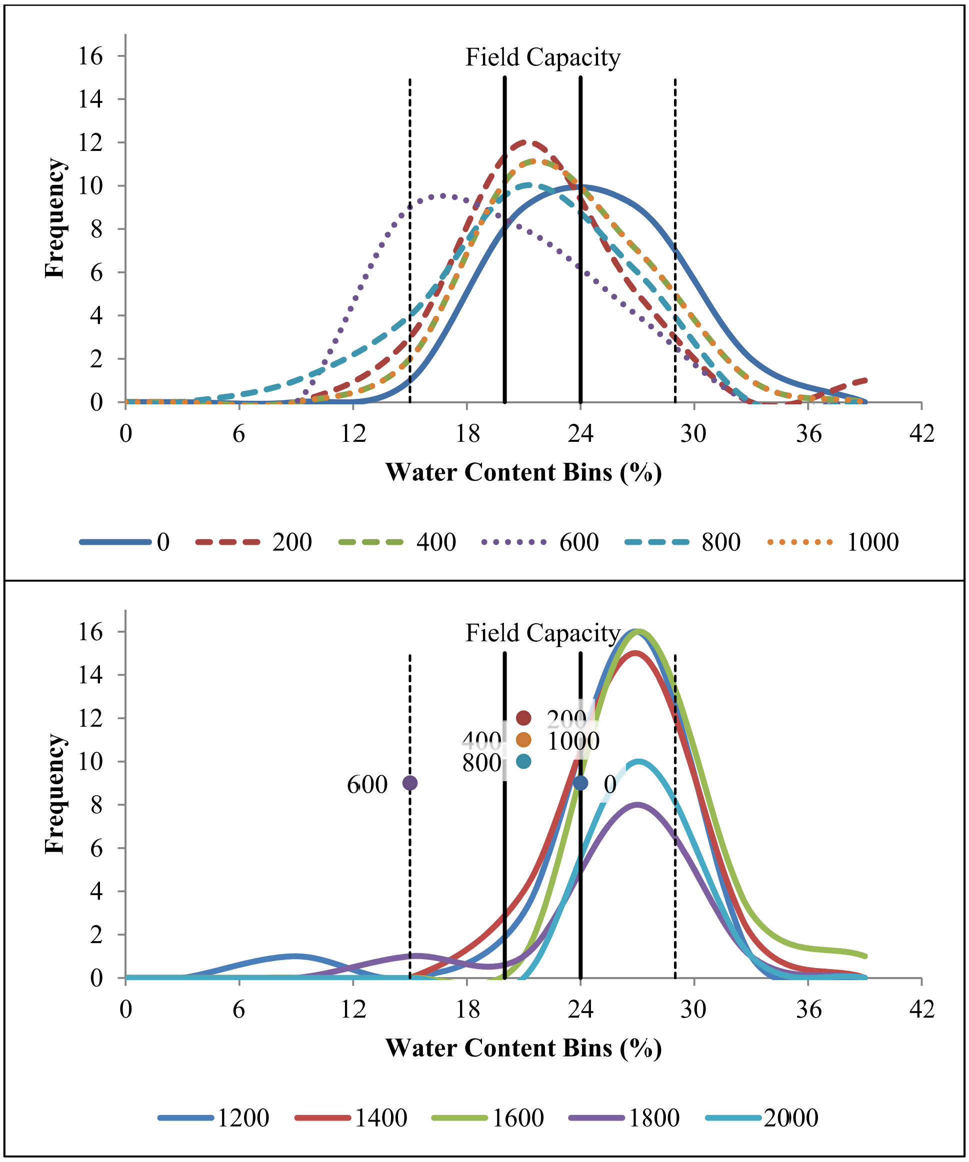

Figure 4.55: Dam 2, 0 m depth trend

The percentage of LI values falling into the brittle, plastic and liquid stress-strain behaviour classes with depth are plotted in Figure 4.56. As expected the distribution of LI values with depth does not vary considerably on Dam 1. There is a slight decrease in samples with LI values less than 0 however the number of samples with LI values less than 1 remains fairly constant with depth. This suggests that the strength gained during exposed drying is not lost when the material is rewetted by subsequent depositions. The dichotomous moisture profile on Dam 2 translates to a lower layer with LI values indicating effectively viscous material and an upper layer with some apparent strength. Thus although the upper layer dries out this did not extend to the lower layer. This suggests that if a layer does not undergo sufficient drying the moisture can be trapped resulting in a potentially weak layer that could cause failure of the facility at a later stage (However in this case a rock impoundment is provided to cater for the higher rate of rise during normal operation).

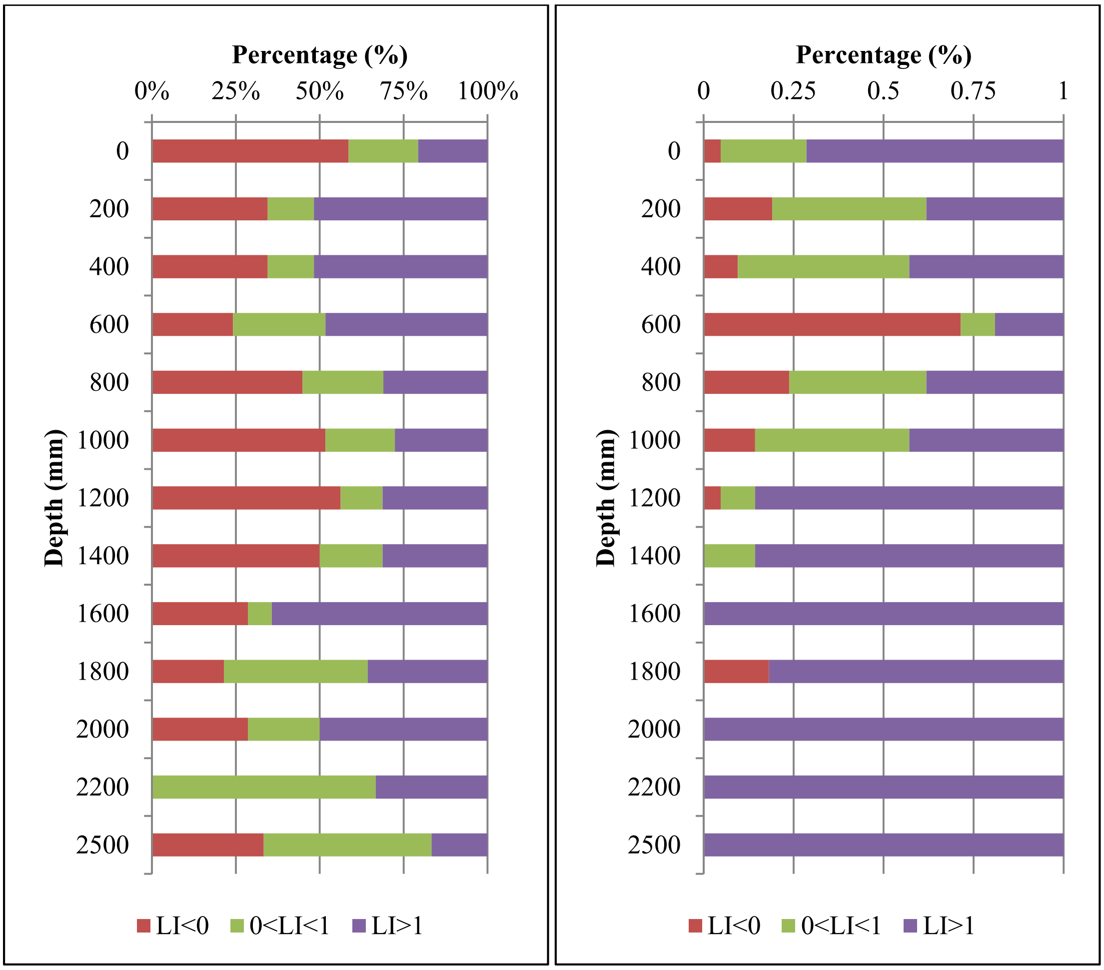

Figure 4.56: Liquidity indices with depth at 0 m; based on average Atterberg limits, Dam 1 on left and Dam 2 on right

Chapter 5 Conclusions and Recommendations

To ensure mining houses can dispose of their ever increasing volume of tailings in an environmentally efficient manner they are posed with a number of questions as to the behaviour of tailings. This dissertation reported on extensive field and laboratory work that set out to answer a few of these questions for platinum tailings. In this final chapter some of the conclusions made are presented as well as some recommendations to guide further research.

5.1 Conclusions

Beaching Behaviour

The following conclusions can be made about the beaching behaviour of platinum tailings:

- The introduction of more efficient grinding technology in the respective plants at Mogalakwena was shown to result in a very narrow envelope of particle sizes. Consequently very little segregation was observed along the beach although any coarser particles appeared to settle out within the first 50 m. Segregation observed in a flume beach adequately modelled the observed field behaviour.
- Although the segregation observed in the flume beach was similar to field conditions the resulting profile did not match field observations. A convex up beach was predicted however the field beach was concave. Further the observed beach profile resulted in a similar master profile to that originally proposed by Blight and Bentel (1983) for platinum tailings.
- Beaching was observed to be a dynamic process and no two depositions resulted in exactly the same profile. Cross depositions from adjacent sections can cause non uniform profiles which are corrected by subsequent flows. Dry beaches can result in short steep depositions as tailings loose water rapidly and “hang up.”
- Beach length appeared to have a significant impact on chord slope. The resulting profile on the 522 m long beach exhibited a significant amount of tapering. In that more material was deposited on the upper course than on the lower course. Although lower slurry densities resulted in slightly more material being deposited on the lower course no significant relationship with chord slope was found.
- This tapering was not observed on the 280 m long beach and the maximum depth of material varied between the upper and lower course for the depositions. Though each deposition resulted in a similar depth of material along the beach the chord slope was higher than the longer beach.

- When the beaches surveyed by Blight and Bentel (1983) were compared to the beaches from the current study a strong inverse relationship between chord slope and beach length was observed. That is longer beaches appear to be flatter.
- On both the 522 m and 280 m beach an initial steep 50 m section was observed after which the profile became significantly flatter. Thus although the tailings would appear to have a low amount of available energy when deposited, as determined by the flume test, the steep initial section and decreasing viscosity as solids are deposited enables the slurry to flow further. With less impedance to flow previously deposited material on steep sections can be entrained and deposited further along the beach to maintain the flatter lower course.
- Measurements of settlement post deposition showed that further along the beach more settlement occurred, assumedly due to the slightly finer material.
- The alluvial field sedimentation appeared to take place within 2.7 days which was similar to the time period taken by pelagic sedimentation laboratory samples. However the water content reached in the field was slightly lower than was observed for laboratory samples at similar slurry densities.
- Interestingly, the settled water content was essentially equal to the water content that it was proposed mechanically thickening the tailings could achieve. Optimally, all the water released during sedimentation should be recovered. The beach would appear to be a natural thickener at a significantly lower cost.

Drying Behaviour

The following conclusions can be made about the drying behaviour of platinum tailings:

- Based on laboratory experimentation and numerical modelling a geotechnical model was developed to interpret the in-situ water contents. Ambient drying tests in which dry density was measured as moisture was lost showed the dry density to increase along the zero air voids curve until desaturation occurred at the air entry value. This was found to be roughly at a water content of 30 % after which very little change in the dry density was observed. The relationship between suctions and water content were investigated via calibrated gypsum blocks in samples allowed to dry under ambient conditions as well as by the filter paper method. The air entry value determined from the ambient air drying tests correlated better with the value predicted by the filter paper method. However all tests showed that significant suctions develop at a water content of roughly 20 % and less with asymptotic behaviour between a water content of 10 and 5 %. Atterberg tests showed that the plastic limit ranged between 18 and 21 % which is the water content at which substantial suctions started to develop. Field capacity, the water content at which seepage becomes negligible, was observed to vary between water contents of 15 and 26 % assuming a suction of 33 kPa to be indicative of field capacity. Numerical modelling was used to determine the impact of grain size variations on the field capacity values. Using values obtained from various laboratory experiments the relationship between hydraulic conductivity and gravimetric water content was determined for the envelope of particle size distributions obtained from the field samples. Assuming field capacity to occur at a hydraulic conductivity of 1×10^{-9} m/s indicated field capacity would range between 15 and 29 % with the quartile range between water contents of 20 and 24 %. The range in laboratory determined values can therefore be inferred to be as a result of variations in particle size distributions within the samples.

- Of importance to tailings management is the rate and quantity of moisture lost as this determines how strength is gained which governs the rate of rise of a facility. The ambient drying tests referred to above showed the water content to decrease rapidly in a linear fashion until the samples were practically desaturated. The drying periods which ranged between 3 and 8 days were influenced by the weather conditions under which the test was done and the initial water content of the sample. Field drying behaviour appeared to take a longer period, between 14 and 22 days, with the water content following drying ranging between 24 and 36 %. Different weather as a consequence of different location and season for the laboratory and field experiments were not sufficiently large to account for the different drying behaviour.
- Various sources of climatic data were used to determine the impact of varying weather over the course of the year on evaporative energy. A regional calibration of the Hargreaves method was formulated so that minimum and maximum daily temperatures recorded on site could be converted to ET_o values. Historical and regional data was shown to verify the values obtained. An A-Pan placed on the facility was also used to determine the evaporative energy over the course of the year. However questionable results were obtained due to micro-climate impacts as well as calibration and reading errors. Steps were taken to remedy these faults although a great deal of scatter especially at the start of the experiment remained. A-Pan values can be correlated with ET_o values by published factors based on wind speed, relative humidity and pan siting. The regional wind and relative humidity values were shown to adequately account for the difference between the A-Pan values, located on the dry fallow tailings dam, and ET_o values.
- The rate of moisture loss was shown to be related to the available evaporative energy and the final water content dependant on field capacity. When the evaporative energy was low a longer time was required to reach field capacity which then increased the time over which seepage took place. It was proposed that the ratio between ET_o and the rate of drying, k – value, can be used to manage the drying cycle over the course of the year. Due to the limited data

set it was assumed that this value is constant throughout the year and was thus determined to be 0.21. However the contribution of seepage and increased bleed water to moisture loss during winter will most likely cause the ratio to be higher during winter.

- Once field capacity was reached very little change in water content with time was observed. Low water contents indicative of significant suctions were only recorded on Dam 1 for the outer 100 m at the start of the field work as the test section had been inactive in excess of 6 months. Thus during active deposition, field capacity is key to determining the strength that can be reached. Due to the relative abundance of moisture within the deposit any moisture deficits are replenished which was not the case for the laboratory experiments. The moisture within the laboratory drying troughs was not sufficient to maintain the water content at field capacity as was the case in the field. It is proposed that complete desaturation would only occur within a tailings dam after an extremely long period. This factor needs to be taken into cognisance when a dormant facility is recommissioned for although the phreatic surface may appear to be low the material will most likely contain a large amount of water. After a short period the moisture deficits can be meet and the material reach saturation and consequently result in a rapid build up of the phreatic surface. The rapid build up in the phreatic surface that lead to the failure of the Simmergo facility, referred to in Appendix C, is a classic example of this phenomenon.
- Field capacity, although a material property sensitive to particle size distribution, is also influenced by the phreatic surface. As such the dominant water content increased away from the edge of the facility towards the pool. Furthermore the longer 522 m beach was found to be ± 3 % drier than the shorter 280 m beach. It was suggested that the as a consequence of the shorter beach the phreatic surface was closer to the surface and hence more moisture was available within the deposit to replenish deficits.
- The distribution of water contents sampled at each testing position revealed an interesting factor about the strength of the facility. It was found that, on both the longer Dam 1 and shorter Dam 2 it was, only at the outer position that the water content had a large degree of dispersion. The distribution of water contents from the interior had a central tendency about the average water content which increased towards the pool. This average was also generally at the higher end of the field capacities estimated from the numerical modelling. It would thus appear that it is only the outer portion of a tailings dam where the phreatic surface is sufficiently depressed to allow significant drying to take place.
- By computing the Liquidity Indices it was also apparent that it was only the samples from the outer section that indicated a significant amount of consolidation to have occurred. The majority of the interior water contents indicated the material to be an essentially viscous mass albeit able to support

the mass a man and prevent the auger hole collapsing. This was more so on Dam 1 and was also found to be the case with depth at this outer 0 m position. On Dam 2 this behaviour was only exhibited in the upper 1 m of the profile (which was roughly the depth of material deposited during the experiment) with the lower 1 m essentially viscous. Prior to test work the rate of rise of this facility had been higher than during test work. It is suggested that insufficient time had been provided for the underlying layers to dry out and this moisture was trapped in. This drying history may impact the future stability of facilities (although in this case a rock impoundment had been provided to facilitate the high rate of rise).

5.2 Recommendations

The scope of this dissertation was limited so that a final product could be produced; however a number of questions were left unanswered. These recommendations serve to guide interested parties to further the understanding of tailings behaviour.

Beaching Behaviour

The following recommendations can be made about the beaching behaviour of tailings:

- Flume tests are an easy way to predict beaching behaviour however the manner in which, especially high density, slurries are deposited needs to be refined so that they are not prematurely arrested leading to falsely steep beaches.
- Whether flat beaches are a result of longer distances over which tailings flow needs to be explored further especially for other minerals and ore bodies.
- Importantly however as it has been shown that the beach acts as a natural thickener therefore means by which the recovery of water can be improved from the impoundment need to be understood. However this is not often in the hands of the tailings facility operators but rather an apparent reluctance of plant operators to use return water. With increasing restrictions on water for industrial purposes this ethos will change.

Drying Behaviour

The following recommendations can be made about the drying behaviour of tailings:

- With increasing volumes of tails being produced it is essential that the rate and degree of drying that takes place after deposition be understood. The laboratory based ambient drying tests were shown to over predict the rate and the degree of drying which was observed to take place in the field. Analysis of field data suggested that the rate of drying varies throughout the year with seepage and evaporation contributing different percentages as a consequence. If the rate of seepage is assumed to be constant then the rate of drying can be correlated to the available evaporative energy. However the ratio will vary thorough the year as a consequence and this relationship needs to be explored. The relationship can then be used to adequately manage the drying cycle on a tailings dam.

- An iterative method was used to establish the drying behaviour following active deposition. The assumptions used were shown to be valid based on the various observations. However to confirm the assumptions used the change in water content after sedimentation needs to be monitored by taking surface grab samples and not simply waiting for sufficient strength for auger samples to be taken.
- The study found the A-Pan based evaporation measurements to be fraught with various inaccuracies. Reference Evapotranspiration measurements based on minimum and maximum daily temperatures were found to be easier to determine and subject to less error. However the volumetric changes in water due to evaporation and seepage were not determined. Further research should therefore be undertaken to understand these aspects.
- The degree of in-situ drying was shown to be a function of the range in field capacity values of the material due to variation in particle sizes. As such the strength inherent within the material at this range of water contents is key to determining the stability of a facility. However it was found that it was only at the outer test positions that water contents were dispersed across the entire range of proposed field capacity values. Further research should therefore concentrate on this outer section so as to determine the length over which strength is allowed to develop. Although no apparent relationship with time was observed once field capacity was reached it is proposed that the distribution may change. Should more samples be taken on this outer section it is suggested that the distributions may progressively become drier with time. A probabilistic analysis of this data could then be used to fully define the rate and degree of drying during this apparent steady state stage.
- The veracity of the assumptions used in the numerical model to determine the range in field capacity as a result of grain size difference may require validating. This would require laboratory test work to determine the relationship between hydraulic conductivity and water content for samples with different particle size distributions.
- The impact of the phreatic surface on the field capacity value needs to be explored especially for shorter beaches as this could impact the rate of rise of such facilities.

References

Allen R.G., Pereira, L.S., Raes, D., Smith, M. (1998). Crop evapotranspiration - guidelines for computing crop water requirements. FAO, Rome.

Allen, G.A, Pruitt, W.O., Raes, D., Smith M., Pereira, L.S. (2005b). “Estimating evaporation from bare soil and the crop coefficient for the initial period using common soils information.” *Journal of Irrigation and Drainage Engineering*, ASCE, 131(1), 14-23.

Allen, R.G., Pereira, L.S., Smith, M., Raes M., Wright, J.L. (2005a). “FAO-56 Dual Crop Coefficient Method for Estimating Evaporation from Soil and Application Extensions.” *Journal of Irrigation and Drainage Engineering.* ASCE, 131(1), 2-13.

Andrews, C. A. A., Martin, G. R. (2000). “Criteria for Liquefaction of Silty Soils.” *Proc. of the 12th World Conf. on Earthquake Engineering.* Auckland, New Zealand.

Anglo American (2010). *Good Citizenship: Business Principles*, (Company brochure), Anglo American plc, London.

Anyimadu, A.K., Rule, C.M., Knopjes, L. (2006). “The development of ultra-fine grinding at Anglo Platinum.” *In proc. of International Platinum Conference Platinum Surges Ahead.* The South African Institute of Mining and Mettallurgy.

Atkinson, J. (2007). *The Mechanics of Soils and Foundations 2nd Edition*, Taylor and Francis, Oxon.

Baier, W. (1963) “Studies on Estimating Potential Evapotranspiration from Empirical Relationships” *South African Journal of Agricultural Science,* 6(1963):455-474

Benli, B., Bruggeman, A., Oweis, T., Üstün, H. (2010). “Performance of Penman-Monteith FAO56 in a Semiarid Highland Environment.” *Journal of Irrigation and Drainage Engineering*, ASCE, 136(11), 757-765.

Benzaazoua, M., Perez, P., Belem, T., Fall, M. (2004). “A Laboratory Study of the Behaviour of Surface Paste Disposal.” *In Proceedings of the 8th International Symposium on Mining with Backfill.”* The Nonferrous Metals Society of China, Beijing, 180–192.

Blight, G.E. (1987). “The Concept of the Master Profile for Tailings Dams.” *Proceedings of the International Conference on Mining and Industrial Waste Management Johannesburg.* SAICE.

Blight, G.E. (1988). “Some less familiar aspects of hydraulic fill structures.” *Hydraulic Fill Structures,* D.J.A. Van Zyl, and S.G. Vick, eds., American Society of Civil Engineering, New York., 1000-1027.

Blight, G.E. (2002). “Measuring evaporation from soil surfaces for environmental and geotechnical purposes.” *Water SA.* 28(4):381-394

Blight, G.E. (2009). “Solar heating of the soil and evaporation from a soil surface.” *Géotechnique.* ICE, 59(4), 355-363.

Blight, G.E. (2010). *Geotechnical Engineering for Mine Waste Storage Facilities*. CRC Press/Balkema: Leiden.

Blight, G.E., Bentel, G.M. (1983). “The Behaviour of mine tailings during hydraulic deposition.” *Journal of the South African Institute of Mining and Metallurgy,* April.

Blight, G.E., Steffen, O.K.H. (1979). “Geotechnics of gold mining waste disposal.” *In Current geotechnical practice in mine waste disposal.* Edited by The Committee on Embankments Dams and Slopes of the Geotechnical Division. American Society of Civil Engineering, New York., 1-52.

Blight, G.E., Thomson, R.R., Vorster, K. (1985). “Profiles of hydraulic-fill tailings beaches, and seepage through hydraulically sorted tailings.” *Journal of the South African Institute of Mining and Metallurgy,* May.

Blyth, F.G.H. (1960). *A Geology for Engineers.* Edward Arnold: London.

Boshoff, J.C.J. (2002). “Prediction of the desiccation and sedimentation behaviour of a typical platinum tailings.” *In Proceedings of Tailings and Mine Waste ‘02.* Swets & Zeitlinger.

Bosman, H.H. (1990). “Methods to convert American Class A-pan and Symon’s tank evaporation to that of a representative environment.” *Water SA*, 16(4), 227-236.

Bovis, M.J. (2003). “Atterberg Limits.” *Encyclopaedia of Sediments & Sedimentary Rocks,* Middleton, G.V. ed. Kluver Academic Publishers, Dordrecht, 22 – 24.

Bristow, K.L. (1992) “Prediction of daily mean vapour density from daily minimum air temperature” *Agricultural and Forest Meteorology.* Elsevier Science Publishers: Amsterdam. 59(1992):309-317.

Bristow, K.L., Campbell, G.S. “On the relationship between incoming solar radiation and daily maximum and minimum temperature.” *Agricultural and Forest Meteorology.* Elsevier Science Publishers: Amsterdam. 31(1984):159-166.

British Broadcasting Corporation, BBC. (2002). “Spain fines toxic spill firm $45m.” *BBC News,* <http://news.bbc.co.uk/2/hi/europe/2170020.sym> (Jun. 30, 2010).

Bru, K., Guezennec, A-G., Bourgeois, F. (2008). “Numerical Simulation: a Performing Tool for Water Management in Tailings Impoundments.” *Proceedings of the 10th International Mine Water Association Congress.* Karlsbad, Czech Republic. Paper 224.

Buck, A.L. (1981). “New Equations for Computing Vapour Pressure and Enhancement Factor.” *Journal of Applied Meteorology*. 20: 1527-1532

Chamber of Mines of South Africa, CMSA. (1996). "Guidelines for Environmental Protection" Chamber of Mines of South Africa, Johannesburg.

Ciba (2004a). "Ciba © RHEOMAX™ DR." *Product Brochure.* Ciba Speciality Chemicals Inc. Pub. No. W/2/E/06/04/2.

Ciba (2004b). "Ciba © RHEOMAX™ ETD." *Product Brochure.* Ciba Speciality Chemicals Inc. Pub. No. W/2/E/06/04/3.

Cincilla, W.A, Landriault, D.A., Verburg, R. (1997) "Application of paste technology to surface disposal of mineral wastes." *Tailings and Mine Waste '97.* Balkema: Rotterdam. Pp343-356

Cooper, D. (1988). "Tailings management in Australia." *Hydraulic Fill Structures*, D.J.A. Van Zyl, and S.G. Vick, eds., American Society of Civil Engineering, New York., 130-141.

Das, B.M. (2008). *Fundamentals of Geotechnical Engineering.* Thomson Learning, Toronto.

Davies, M., Martin, T., Lighthall, P. (2000). "Mine Tailings Dams: When Things go Wrong." *Proc. Tailings Dams 2000.* Assoc. State Dam Safety Officials Inc. Kentucky, March 2000, p. 261-274.

Davies, M.P. (2002). "Tailings Impoundment Failures: Are Geotechnical Engineers Listening?" *Geotechnical News.* September 2002, pp31-36

Deates, M.J. (1971). "A follow-up report on longwall coal mining at Durban Navigation Collieries (Pty.) Limited." *The Journal of the South African Institute of Mining and Metallurgy."* April.

Donaldson, G.W. (1960). "An Investigation into the stability of Slimes Dams." *Masters Thesis.* UCT.

Fahey, M and Fujiyasu, Y. (1994). "The influence of evaporation on the consolidation behaviour of gold tailings." *Proc. 1st Int. Congress on Environmental Geotechnics,* Edmonton, 10-15 July, 481-486

Fahey, M., Newson, T.A. (1997). "Aspects of the geotechnics of mining wastes and tailings dams." *In Proceedings of GeoEnvironment 97. Edited by* Bouazza, Kodikara and Parker. Balkema: Rotterdam. pp. 115–134.

Fahey, M., Toh, S.H. (1992). "Physical and numerical modelling of consolidation of mine tailings." *Australian Geomechanics*, July.

Fourie, A. (1988). "Beaching and Permeability Properties of Tailings." *Hydraulic Fill Structures*, D.J.A. Van Zyl, and S.G. Vick, eds., American Society of Civil Engineering, New York., 142-154.

Fredlund, M.D., Wilson, G.W., Fredlund, D.G. (2002). "Use of the grain-size distribution for estimation of the soil-water characteristic curve." *Canadian Geotechnical Journal.* NRC Canada, 39, 1103-1117

GeoStudio (2007), (computer software), Geo-Slope International, Calgary, Alberta.

Gibson, R.E., England, G.L., Hussey, M.J.L. (1967). "The theory of one-dimensional consolidation of saturated clays, 1: finite non-linear consolidation of thin homogeneous layers. *Géotechnique.* 17: 261-273

Hamblin, A.P. (1981). "Filter paper method for routine measurement of field water potential." *Journal of Hydrology,* 53: 355-360

Hargreaves, G. H., Samani, Z.A. (1982) "Estimating Potential Evapotranspiration" *Journal of the Irrigation and Drainage Division,* ASCE 108(IR3):225-230.

Hargreaves, G.H., Allen, R.G. (2003). "History and Evaluation of the Hargreaves Evapotranspiration Equation." *Journal of Irrigation and Drainage Engineering.* ASCE, 129(1), 53-63.

Hochreiter, R.C., Kennedy, D.C., Muir, W., Wood, A.I. (1985). "Platinum in South Africa." The *Journal of the South African Institute of Mining and Metallurgy."* June.

Holtz, R. D., Kovacs, W.D. (1982). *An Introduction to Geotechnical Engineering.* Prentice Hall, New Jersey.

Kairu, E.N. (1991). "A Review of Methods for Estimating Evapotranspiration." *GeoJournal*. 25(4), 371-376

Kalumba, D., Glendinning, S., Rogers, I.E., Tyrer, M., Boardman, DID. (2009). "Dewatering of Tunnelling Slurry Waste Using Electrokinetic Geosynthetics." *Journal of Environmental Engineering.* ASCE.

Kayabali, K., Tufenkci, O. O. (2010). "Shear strength of remoulded soils at consistency limits." *Canadian Geotechnical Journal.* NRC Canada, 47, 259-266

Kealy, C., Busch, R. (1971). "Determining Seepage Characteristics of Mill-Tailings Dams by the Finite-Element Model." *Report of Investigations 7477,* United States Department of the Interior. Bureau of Mines.

Kehew, A.E. (2006). *Geology for Engineers & Environmental Scientists.* Pearson Prentice Hall, New Jersey.

Kimball, J.S., Running, S.W., Nemani, R. (1997) "An improved method for estimating surface humidity from daily minimum temperature" *Agricultural and Forest Meteorology.* Elsevier Science Publishers: Amsterdam. 85(1997):97-98.

Koorevaar, P., Menelik, G., Dirksen, C. (1999). *Elements of Soil Physics.* Elsevier Science B.V., Amsterdam.

Kynch, G.J. (1952). "A theory of sedimentation." *Trans. Faraday Soc.* 48:166-176

Lane, E.W. (1955) "The importance of fluvial morphology in hydraulic engineering" *Proceedings, American Society of Civil Engineers,* No. 745, July.

Lloyd P.J. (2000). "The potential of coal wastes in South Africa." *The Journal of the South African Institute of Mining and Metallurgy."* January/February.

Manson, R.J. (1982). "Prehistoric mining in South Africa, and Iron Age copper mines in the Dwarsberg, Transvaal." *Journal of the South African Institute of Mining and Metallurgy.* 82, 131-141.

Martin, T.E., Davies, M.P., Rice, S., Higgs, T., and Lighthall, P.C. (2002). "Stewardship of Tailings Facilities." *Mining, Minerals and Sustainable Development Report No. 20,* International Institute for Environment and Development.

Mbonimpa, M., Aubertin, M., Maqsoud, A., Bussière, B. (2006). "Predictive Model for the Water Retention Curve of Deformable Clayey Soils." *Canadian Geotechnical Journal.* NRC Canada, 132, 1121-1132

Meyer, P.D., Gee, G.W. (1999). "Flux-Based Estimation of Field Capacity." *Journal of Geotechnical and Geoenvironmental Engineering,* ASCE, 125(7), 595-599.

Miller, R.W., Donahue, R.L. (1990). *Soils, An Introduction to Soils and Plant Growth.* Prentice Hall, New Jersey.

Mittal, H.K., Morgenstern, N.R. (1976). "Seepage control in tailings dams." *Canadian Geotechnical Journal.* NRC Canada, 13, 277-293.

Nalecki, P., Gowan, M. (2008). "Mine Water Management – Dynamic, Probabilistic Modelling Approach." *Proceedings of the 10th International Mine Water Association Congress.* Karlsbad, Czech Republic. Paper 85.

Nelson, J., Shepherd, T., Charlie, W. (1977). "Parameters Affecting the Stability of Tailings Dams." *Proceedings of the Conference on Geotechnical Practice for Disposal of Solid Waste materials,* ASCE, Michigan, p444-460

Palkovits, F. (2007). "How the mining sector is responding to change in the disposal of tailings and waste rock." *Engineering and Mining Journal.* December 2007.

Pane, V., Schiffman, R.L. (1985). "A note on sedimentation and consolidation." *Géotechnique.* 35(1):69 – 72.

Perales, A.B. (1998). "Los Frailes Tailings Dam Incident." Report published by the Mining Environment Research Network, School of Management, University of Bath.

Princeton University "About WordNet." WordNet. Princeton University. 2010. <http://wordnet.princeton.edu>

Qiu, Y., Sego, D. (2006). "Optimum deposition for sub-aerial tailings disposal: concepts and theories." *International Journal of Mining, reclamation and Environment,* 20(4), 272-285.

Qiu, Y., Sego, D.C. (2001). "Laboratory properties of mine tailings." *Canadian Geotechnical Journal.* NRC Canada, 38, 183-190.

Ratliff, L.F., Ritchie, J.T., Cassel, K. (1983). "Field-Measured Limits of Soil Water Availability as Related to Laboratory-Measured Properties." *Soil Science Society of America Journal,* 47: 770 – 775.

Reddick, J.F., Blottnitz, H. von, Kothuis, B. (2007). “A cleaner production assessment of the ultra-fine coal waste generated in South Africa.” *The Journal of the South African Institute of Mining and Metallurgy.”* December.

Robertson, A. MacG. (1987). “The Influence of the Depositional Methods on the Engineering Properties of Tailings Deposits.” *Proceedings of the International Conference on Mining and Industrial Waste Management Johannesburg.* SAICE.

Robinsky, E.I. (1975,). "Thickened Discharge - A New Approach to Tailings Disposal", *Canadian Mining and Metallurgical Bulletin,* (68)794:47-53.

Robinson, B.C.S. (2004). “Tailings Dam Rate of Rise – A Closer Look.” *Proceedings, 3rd International Mining and Industrial Waste Management Conference.*, Johannesburg.

Robinson, B.C.S. (2008). “Tailings Fundamentals, Tailings Disposal Systems and Tailings Dam Components.” *Tailings Disposal Course,* Frazer Alexander, Whitfield.

Robinson, B.C.S. (2010). *Tailings Disposal Course Slides,* Frazer Alexander, Whitfield.

Rule, C.M., Anyimadu, A.K. (2007). “Flotation cell technology and cell design – an Anglo Platinum Perspective.” *The Journal of the South African Institute of Mining and Metallurgy.”* October.

Schouwstra, R.P., Kinloch, E.D., Lee, C.A. (2000). “A Short Geological Review of the Bushveld Complex.” *Platinum Metals.* 44(1):33-39

Seneviratne, N.H., Fahey, M., Newson, T.A., Fujiyasu, Y. (1996) “Numerical modelling of consolidation and evaporation of slurried mine tailings.” *International journal for numerical and analytical methods in geomechanics,* John Wiley & Sons, 20, 647-671

Shepherd, P., Breytenbach, R., Hodgkinson, A. (1999). “Water balance for a tailings dam.” *Mining World.* November 1999, 27 and 29.

Sherard, J.L, Dunnigan, L.P, Talbot, J.R. (1984). “Basic Properties of Sand and Gravel Filters.” *Journal of Geotechnical Engineering,* ASCE 110(6):684-700

Sivakugan, N., Das, B.M. (2010). *Geotechnical Engineering: A Practical Problem Solving Approach.* J. Ross Publishing: Fort Lauderdale.

Smith, M. (1993). “CLIMWAT for CROPWAT.” *Irrigation and Drainage Paper No. 49,* Food and Agriculture Organization, Rome.

Southard, J. (2006) “12.090 Special Topics: An Introduction to Fluid Motions, Sediment Transport, and Current-generated Sedimentary Structures”, Fall 2006. (Massachusetts Institute of Technology: MIT OpenCouseWare), http://ocw.mit.edu (Accessed February 2, 2012). License: Creative Commons BY-NC-SA

Stickler G. (1990). “Solar Radiation and the Earth System.” *NASA*, < http://edmall.gsfc.nasa.gov/inv99Project.Site/Pages/science-briefs/ed-stickler/ed-irradiance.html> (13 Jan 2011).

Swarbrick G.E., Fell, R. (1992). “Modelling Desiccating Behaviour of Mine Tailings.” *Journal of Geotechnical Engineering*, ASCE 118(4):540-557.

Theriault, J., Frostiak, J., and Welch, D. (2003). “Surface disposal of paste tailings at the Bulyanhulu gold mine, Tanzania.” *In Proceedings of Sudbury 2003, Mining and the Environment, Sudbury, Ont., 26–28 May 2003*. *Edited by* G. Spiers, P. Beckett, and H. Conroy. Laurentian University Centre for Continuing Education, Sudbury, Ont. pp. 265–269.

Tyson, P.D., Preston-Whyte, R.A. (2000). *The Weather and Climate of Southern Africa*. Oxford University Press Southern Africa, Cape Town.

U.S. Environmental Protection Agency, EPA. (1994). “Design and evaluation of tailings dams.” U.S. Environmental Protection Agency, Office of Solid Waste, Special Waste Branch, Washington DC.

Ulrich, B.F., Fourie, A.B. (2003). “Assessment of the potential for static liquefaction of a tailings dam using laboratory and field testing.” *In Proceedings of Tailings and Mine Waste ‘03.* Swets & Zeitlinger: Lisse. pp. 137–147.

van Genuchten, M. Th., F. J. Leij, S. R. Yates. (1991). *The RETC Code for Quantifying the Hydraulic Functions of Unsaturated Soils, Version 1.0*. EPA Report 600/2-91/065, U.S. Salinity Laboratory, USDA-ARS, Riverside, California.

Vick, S.G. (1983). *Planning, Design, and Analysis of Tailings Dams,* John Wiley & Sons.

Voges, H.C. (1975). “The use of heavy-medium separation in the processing of iron ores.” *The Journal of the South African Institute of Mining and Metallurgy.”* June.

Warner, B. (2004). “Temperature Scales.” *Goddard Space Flight Centre Cryogenics and Fluids*, <http://cryo.gsfc.nasa.gov/introduction/temp_scales.html> (Mar. 30, 2011).

Wates, J.A., Stevenson, C., Purchase, A.R. (1987). “The effect of relative densities on beaching angles and segregation on gold and uranium tailings dams.” *Proceedings of the International Conference on Mining and Industrial Waste Management Johannesburg.* SAICE.

Wates, J.A., Strayton, G., Swardt, G de. (1999). “Long-term integrity of residue deposits.” *Geotechnics for Developing Africa. Edited by* Wardle, Blight and Fourie. Balkema, Rotterdam.

Welff, R., Wates, J. (2004). “Fine Residue Disposal Facility Rate of Rise Determination.” *3rd International Mining and Industrial Waste Management Conference Johannesburg.*

Wels, C., Robertson, A.M. (2003). "Conceptual model for estimating water recovery in tailings impoundments." *Tailings and Mine Waste '03.* Sweets & Zeitinger, Lisse.

WesTech (2008a). "HiFlo ™ Thickeners." *Product Brochure.* WesTech, Salt Lake City.

WesTech (2008b). "Paste and High Density Thickeners." *Product Brochure.* WesTech, Salt Lake City.

WesTech (2010). "Horizontal Vacuum Belt Filters." *Product Brochure.* WesTech, Salt Lake City.

Wimpey Laboratories Ltd. (1972). "Review of Research on Properties of Spoil Tip Materials." National Coal Board, Hayes, Middlesex.

World Meteorological Organisation. (2008) "Guide to Meteorological Instruments and Methods of Observation." *WMO-No. 8. 7th Edition*, World Meteorological Organization, Geneva

Wortmann, H. (2007). "Sedimentation and Desiccation of Gold Mine Tailings." MEng Dissertation. University of Pretoria.

Appendix A: Historical Development of Tailings Management

From the onset of history mankind has recovered mineral resources from the earth. Initially the recovery was crude with copper and iron being recovered from ore bodies exposed by erosion resulting in very little waste. As demand for the metals increased excavation to the ore bodies was required. Initially this only meant removing surface layers but eventually required excavating shafts and adits. The main waste produced from these processes was overburden material made up of rock fragments and sand (Mason, 1982). Such waste was simply discarded as close as practically possible to the mining operation. Indeed waste rock disposal has not changed much in that it is still typical tipped in a convenient location albeit with trucks and not by hand. Being en-tipped the rock lies at its natural angle of repose which is often flatter than its angle of shearing resistance – rock being highly frictional and free-draining. Thus the failure of rock dumps are rare and only occur if built on unfavourable foundation soils or become very high (Blight and Steffen, 1979).

Uncontrolled Riverine Disposal

As demand increased milling was required to extract ore from host materials. This was carried out by crude millstones in the New World from the 1500’s through to the mid 1800’s (Martin et al., 2002). The requirement of ample water to drive the processes meant that crushing only occurred on a small scale and often during wet seasons. This resulted in low daily volumes of coarse free-draining waste (Cooper, 1988). With more efficient drill and blast techniques and the introduction of steam power greater amounts of ore could be crushed with greater efficiency. This meant that mining operations become continuous operations. As mining operations were often in close proximity to rivers a convenient medium to carry the tailings away from the operations was available. This meant that no storage was required and tailings simply flowed away through the streams eventually into lakes and oceans.

During the late 1800’s the development of froth flotation and the use of cyanide for gold extraction brought about dramatic changes to the mining industry. Once uneconomical low-grade ore bodies could now be processed resulting in still larger quantities of tailings at even finer grinds. However riverine disposal was still much the norm. With these technologies came supporting industries and the development of remote mining districts. These communities required food and water which led to a conflict of interests. Downstream irrigation channels became silted up by the accumulating tailings and agricultural land became contaminated resulting in lower yields. Various legal precedents resulted in the need for mine waste management eventually leading to the cessation of uncontrolled riverine disposal of tailings by about 1930 in the western world.

Uncontrolled Offshore Disposal

One method that has survived from this period is the offshore disposal of tailings. If the chemical composition of the mill effluent is relatively innocuous and the tailings are relatively coarse and sufficiently flocculated to settle rapidly without excessive turbidity, little effect on water quality can be expected. Tailings deposition has to occur deep and far away from the shoreline to avoid biologically productive and sensitive shallow-water and shoreline zones. Research has shown minimal biological and water quality consequences of offshore disposal and suggests that the areas become rehabilitated quickly after deposition. Other studies have also revealed that deposition can occur over an unexpectedly large area with significant turbidity problems. Although technical arguments can be made for offshore disposal no other method generates as much public concern and thus it is often only considered as a last resort (Vick, 1983).

Sub-aqueous Disposal

With the need to impound tailings simple dams build across stream channels with little regard for the provision of freeboard for flood events were used. This was a result of very little engineering or regulatory input and hence few survived large rainfall events. Much of the dam building was undertaken by hand as mechanized earth-moving equipment was not developed yet (Martin et al., 2002). Embankment walls are now construct using similar methods to those used to build water impoundment dams. These walls are sufficiently strong to allow slurry to be continually discharged forming a fan sloping away from the discharge point. Although water is released and can be decanted the slurry essentially remains wet and saturated with low shear strength. After decommissioning the mass slowly dries, resulting in large settlements and shrinking potentially causing considerable cracking. This method of disposal is referred to as wet or sub-aqueous disposal (CMSA, 1996). Mining in featureless flat terrain without valleys in which to impound tailings required a different solution. Placement of slimes was done within similar impoundment walls constructed in a ring dyke. The height of these impoundments was limited by the ability to lift slurry which in turn was limited by the diameter of slurry wheels leading to a series of “add on” compartments (Robinson, 2004).

Sub-aerial Deposition – Paddock Construction

Soon it was realised that the impoundment walls were prohibitively expensive and the tailings soon dried out. The dried out tailings could be used to construct a dyke, then incrementally raised by constructing low berms above and behind the previous dyke. Each paddock in turn is filled and allowed to dry to form the “daywall”. Once the settled slurry was dry it was raked up from the floor of the daywall to form the berms for the next paddocks. Enough time was insured between depositing in the same paddock to insure complete drying and draining resulting in strength gain. When tailings were not used for wall building they would be directed into the basin within the daywall and allowed to beach towards a pool. This method is still used on many mines however it is now almost always mechanized and is referred to as semi-dry or sub-aerial disposal (CMSA, 1996).

Figure A.1: Modern paddock construction, note the two day walls (Robinson, 2010)

Sub-aerial Deposition – Spigot Construction

Another method developed to deposit tailings sub-aerially was the use of spigots. Earlier when the ore grind was relatively coarse, the tailings stream was delivered by a single pipe and sandbags used to direct the stream. The stream would break up into smaller streams resulting in a velocity drop. This caused the coarse material to settle out first and the finer fraction further along the forming beach. Released water was recovered through a simple over flow pipe protected by sandbags. The perimeter embankments were raised using dried tailings. This resulted in stable outer sections comprising free draining well consolidated coarse tailings (Cooper, 1988).

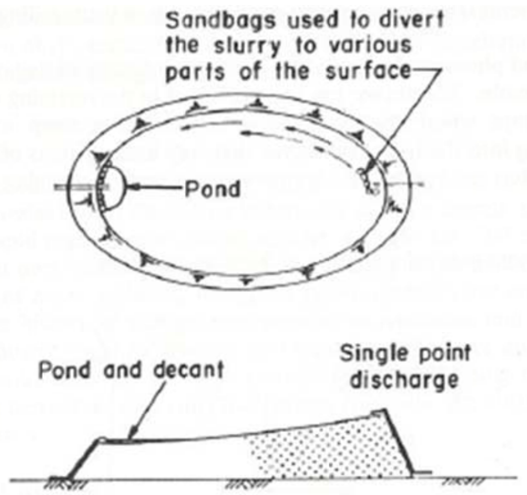

Figure A.2: Plan and section through typical single deposition point tailings dam (Cooper, 1988)

As mining and grinding technologies advanced the volume and quantity of fines reporting to the tailings facility increased. Discharging from a single point became difficult to manage as did the deposition cycle to ensure adequate drying of the tailings for wall construction. To ensure that enough coarse material was available around the perimeter, slurry was distributed via a ring main around the perimeter. This enabled easier management of deposition cycles and ensured efficient segregation. A consequence of the ring main spigotting slurry towards the centre the water released and rain water accumulated in the middle forming a pond. This was often simply left to evaporate and so for the first time operators were faced with the possibility of a phreatic surface developing which could compromise stability. As this method was predominately used in semi-arid areas, combined with ample surface areas and low rates of rise meant that high phreatic surface did not readily develop (Cooper, 1988). This method is still used however bull-dozers, front-end loaders, backactors and scrap-loaders are now used to build walls (CMSA, 1996).

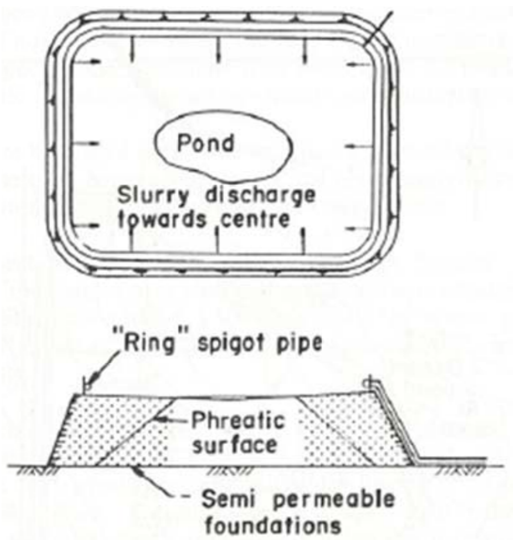

Figure A.3: Plan and section through a typical ring main spigot tailings dam (Cooper, 1988)

Sub-aerial Deposition – Cyclone Construction

The development of cyclones provided a means of harnessing centrifugal acceleration to split coarse and fine fractions in tailings streams more efficiently than merely spigotting. A cyclone, illustrated in Figure A.4, is a device designed so that the slurry under pressure moves in such away that it is subject to centrifugal forces (EPA, 1994). The coarse fraction at a lower water content spirals downwards through the conical section and exits the bottom as an underflow. The finer fraction along with most of the water moves upwards and exits the cyclone as an overflow (CMSA, 1996). The coarse underflow is in most cases relatively uniform and free draining so can gain strength rapidly without necessarily undergoing desiccation. This property of the underflow also enables it to act in a similar manner to a filter acting as a preferential drainage path and thus drawing down the phreatic surface (Vick, 1983). Thus cycloning can be used in a cost effective manner to rapidly build up the outer walls of an impoundment. The overflow has a high water content and abundant fine material giving it a lower permeability and is deposited within the walls. One of the first departures from the traditional means of dam construction to cycloning was most likely after the 1928 earthquake in Chile which resulted in the catastrophic failure of the Barahona tailings dam (Martin et al., 2002). This was necessitated to construct stable perimeter walls to contain the potentially liquefiable slimes in the seismically active region.

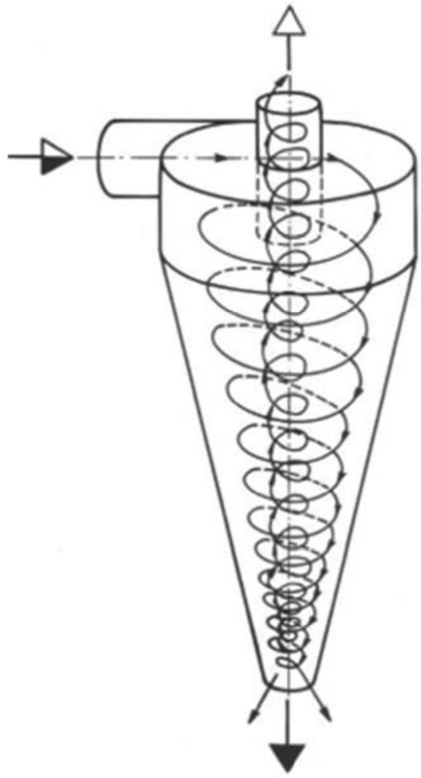

Figure A.4: Schematic of a cyclone (www.scielo.br)

Sub-aerial Deposition – Embankment Raising

Early methods of constructing tailings dams using dried out tailings as construction material involved raising the perimeters walls by stepping in the paddocks over deposited slimes. This method is what is now referred to as the upstream method as the centre-line of the embankment moves progressively upstream as illustrated by Figure A.5 (CMSA, 1996).

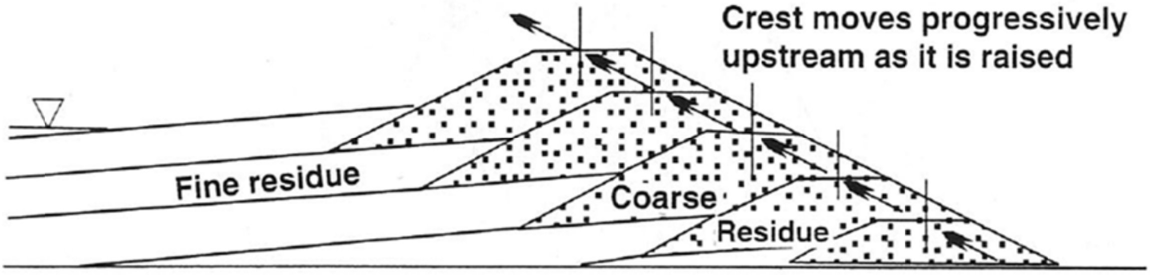

Figure A.5: Section through a wall constructed upstream (CMSA, 1996)

Since the beach forms the foundation for subsequent embankments it has to provide a reasonable degree of support. Vick (1983) states that as rule of thumb the tailings stream needs to contain a sand fraction of between 40 – 60 % to provide this strength. The upstream method is effective in rapidly increasing the height of the embankment as minimal volumes of fill are required. This has added cost savings as less machinery is required in the process. However the method results in a relatively insubstantial outer shell and an irregular contact between coarse and fine material. The Barahona tailings dam failure highlighted this shortcoming as the wall was easily breached during the earthquake and the contained finer material liquefied and flowed out (Martin et al., 2002). Consequently this most probably marked the point at which the downstream method gained significance. The method involves constructing the wall in such a fashion that the centreline of the embankment moves progressively downstream as illustrated in Figure A.6. Downstream construction is now widely adopted however upstream construction is still widely used in South Africa (CMSA, 1996).

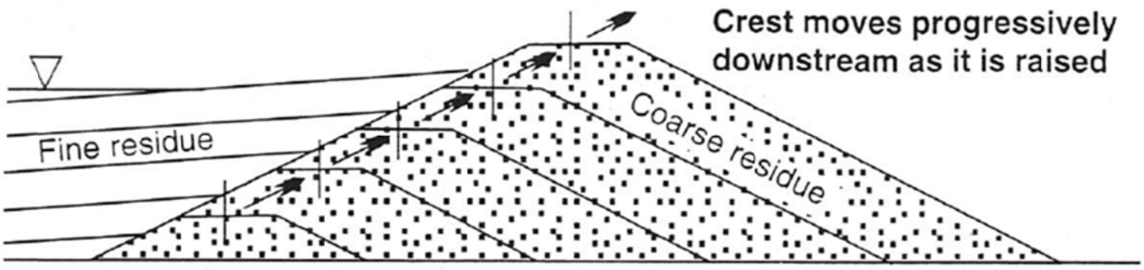

Figure A.6: Section through a wall constructed downstream (CMSA, 1996)

Downstream construction requires careful planning to ensure sufficient space is available as the toe advances outwards as the dam is raised. Further the material required to construct the outer walls increases exponentially as the embankment height increases. These two factors often result in the downstream method becoming unsustainable or prohibitive from the outset. The centreline method is therefore a compromise of the two methods in many respects. In this method the centreline remains in the same position throughout the embankment construction (Vick, 1983).

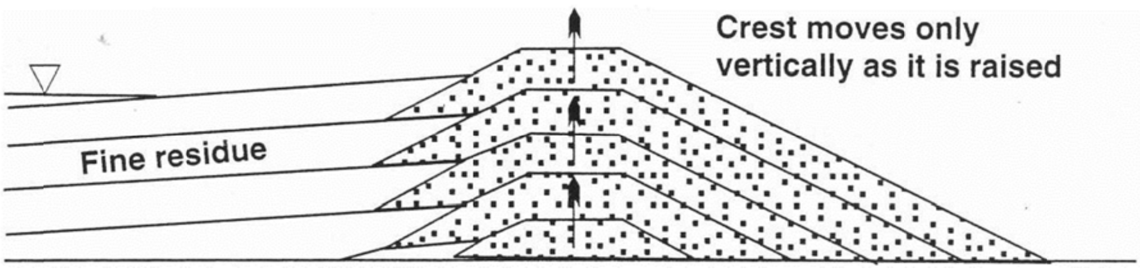

Figure A.7: Section through a wall constructed centreline (CMSA, 1996)

A combination of all three methods is used in some instances; at the onset it may be necessary to raise walls rapidly by the upstream method but later on to build a substantial wall by the centreline or downstream method (CMSA, 1996). In other cases when the material required to continue a downstream embankment at high elevations becomes prohibitive the centreline or upstream method can be used (Robinson, 2010).

Engineered Tailings – Conventional Thickening

All the above methods required very little alteration of the tailings after the mineral extraction process barring simple conventional thickening. Conventional thickening in this context is a mill process in which some of the process water is removed (Wortmann, 2007). Recently focus has been placed on further reducing the water content of the tailings such that the sophisticated depositional strategies described above are not required. The possible negative consequences of the water both structurally and environmentally on tailings disposal have driven the research into such methods (Robertson, 2008).

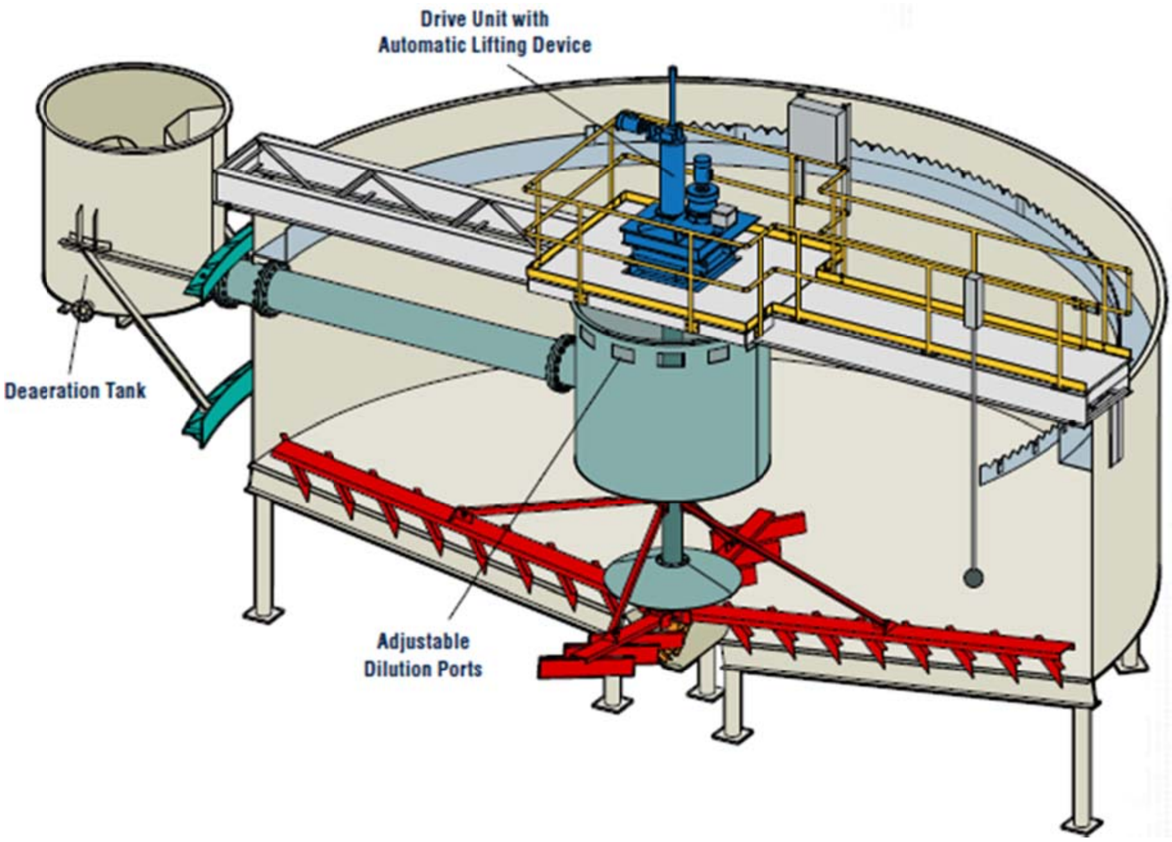

Figure A.8: Conventional thickener (WesTech, 2008a)

Engineered Tailings – Paste Thickening

Conventional thickeners consist of a shallow tank with rotating arms that convey the settled tailings to the centre of the tank, where they are collected and pumped to the disposal area (Vick, 1983). The concept of deep cone thickeners, i.e. a large height to diameter ratio, was developed in the 1960's using a steep angled cone and a thickener bed to increase underflow densities. Over the years the concept has evolved such that non-segregating slurries can be produced (WestTech, 2008b). Such thickeners are commonly referred to as paste thickeners. Conventional thickeners produce slurry that segregates, that is once it reaches the impoundment the velocity drops and the solids particles no longer remain in suspension and segregate out. On the other hand when non-segregating slurries are deposited the tailings do not beach over a long distance and the different particle sizes do not separate out. This behaviour of the slurry also influences the way in which it has to be conveyed. Segregating slurries are less viscous and so centrifugal pumps can be used whereas non-segregating slurries are more viscous and often require positive displacements pumps. This limits the distance over which paste tailings can be economically transported (Theriault et al., 2003). The capital cost and operating costs of a paste thickener can also be higher than a conventional thickener. Another factor is that not all mines produce tailings that can be thickened, as the grain size required for ore recovery may not be optimal for thickening (Palkovits, 2007).

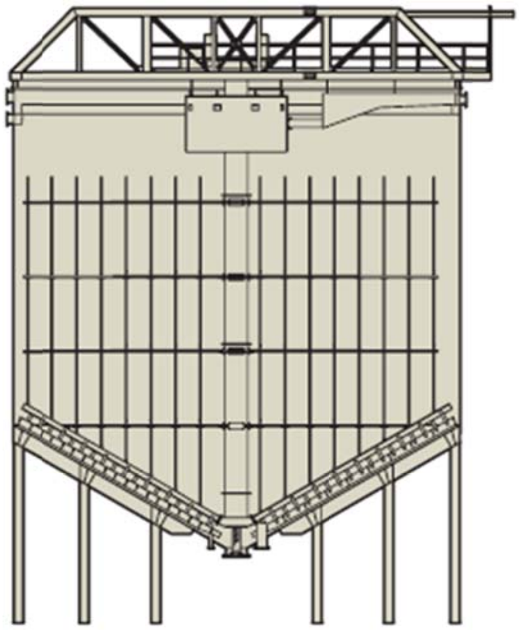

Figure A.9: Paste thickener (WesTech, 2008b)

Partially or completely removing moisture from waste streams can easily be shown to reduce the geotechnical problems associated with disposal. Reducing the moisture content also removes the most mobile source of potential groundwater and surface water pollutants. These two factors contribute to paste tailings been seen as having a better environmental performance to conventional tailings (Cincilla et al., 1997).

In most applications of thickened non-segregating tailings systems, above ground, involve conically shaped stacks formed around deposition towers. However before the paste comes to a stop it needs to gain strength which in most cases comes from desiccation which in turn is dependent on layer thickness. A limited number of deposition towers can negatively impact the depositional cycle resulting in thick layers that do not gain strength quickly. This can result in paste flowing over longer distances resulting in flatter beaches and requiring containment berms.

Considerable debate surrounds the susceptibility of paste to seismic events however research by Jayapalan in 1982 showed that thickened tailings are susceptible to liquefaction and flow sliding under moderate to high levels of seismic shacking (cited in Vick, 1983). However the addition of a hydraulic binder such as Portland cement or fly ash increases its strength, durability, and acid neutralisation potential. Cementation can also stabilise contaminants in the paste backfill (Benzaazoua et al., 2004). Not all ores can be successfully cemented for instances kimberlite ores tend to flash-set when mixed with cementitious products (Palkovits, 2007).

Engineered Tailings – Chemical Thickening

Another development has been the advancement in flocculent technology by various speciality chemical companies. Few papers have been published on the performance of these chemicals and information discussed here was obtained from product brochures. Modern flocculants can form flocs that are more robust than those produced by conventional flocculants and are thus more tolerant to fluctuations in plant and feedwell conditions. This improves the compression and dewatering characteristics resulting in higher underflow densities without compromising yield stresses. As a result the amount of water recovered at the thickening stage can be improved without compromising pumpability (Ciba, 2004a). The rheology of slurry, or the physical process accompanying the deformation and flow of slurry (WordNet, 2010), can also be altered by the addition of specialized chemicals. Thickeners produce a highly structured underflow however during the pumping stage this is broken down resulting in poor handling characteristics at disposal. Adding a rheology modifier just before disposal can restore this structure. Sedimentation occurs faster with improved water release resulting in a structure made up of both coarse and fine particles. This also aides the rate at which strength is gained and hence steeper stacking angles can be attained (Ciba, 2004b). The cost of the continued use of such chemicals is often an inhibiting factor to their application in many mining operations.

Engineered Tailings – "Dry" Filtering

Dewatering technology has been available for a considerable amount of time for industrial purposes for example in the food processing industry. Their application to tailings dewatering has been limited due to the large flow rates required. With the expertise gained from these relatively small scale operations dewatering can now be applied to demanding production rates (WesTech, 2010). Filtering takes place using pressure or vacuum force. Drums, horizontally or vertically stacked plates and horizontal belts are the most common filtration plant configurations. Belt filtration however is the most appropriate method for large scale operations (Davies and Rice, 2001). Research by Kalumba et al (2009) showed that by applying a potential difference across the filter belt improved dewatering can be achieved. The nature of the tailings is an important consideration when considering filtration. Grading and mineralogy are important factors; high percentages of fine clay minerals can result in ineffective filtration. Residual bitumen (e.g. oil sand tailings) can create difficulties in a filtration plant.

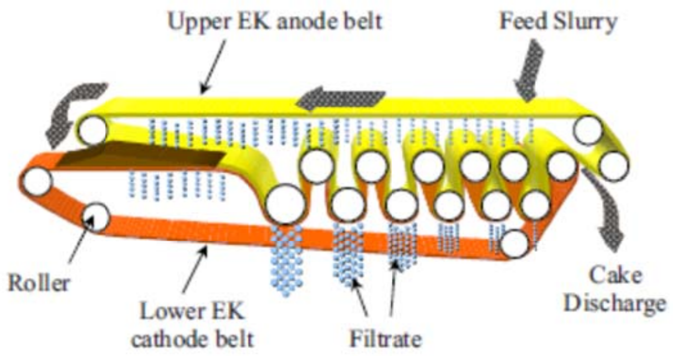

Figure A.10: Conceptual scheme for a belt filter press modified with EK (Kalumba et al., 2009)

Two types of filter cake have been defined, wet cake tailings and dry cake tailings. Wet cake tailings are near or at saturation whereas "dry" cake tailings are unsaturated but not completely dry. With so little water filtered tailings cannot be pumped and are therefore transported by conveyor or truck, placed, spread and compacted to form an unsaturated dense stack requiring little or no dam for retention. Filtered tailings are often produced at or slightly above optimum moisture content (OMC) for compaction and so compaction management can be critical. If the moisture content rises above OMC the stack can become untrafficable resulting in serious placement restrictions. In seismically active areas it is often a requirement that the outer perimeter be compacted to a higher density to act as a structural component. To cater for filter plant break downs and climatic changes considerable flexibility has to be provided for stacking the filtered tailings depending on residual moisture content. Residual water in the filtered tailings may also cause considerable seepage. Considerable debate over the economy, feasibility and advantages of filtering tailings is an ongoing topic. In most cases economic consideration mean that "Dry" stack disposal only becomes an option if filtering is an integral processing step in removing the mineral value (Vick, 1983).

Backfilling Mined Areas

The disposal of tailings in surface impoundments is the most commonly used method however returning tailings to underground mines has long been practiced. Often the backfilling of mined out areas is more a consequence of the mining operation and not reducing the amount requiring disposal at surface. In most cases up to 50 % of the mined tailings will have to be stored at surface due to the bulking that occurs upon crushing an ore body (Benzaazoua et al., 2004). Vein-type deposits are often mined from the bottom of the stope and tailings used to backfill forming a stable floor as mining progresses upwards. Mining deep deposits result in high in situ stresses being applied to remaining pillars or rock walls which can then fail violently. Backfill can be successfully used to reduce the stresses on the pillars. Tailings used in such cases needs to have high permeability, low compressibility and high stiffness. Often this can only be attained with a coarser sand fraction separated by cycloning at the surface and the addition of a cementitious material. In some cases it may be possible that once a stope is backfilled pillars can be mined out. Underground disposal below the water table may be of particular advantage for tailings high in pyrite. By keeping the tailings permanently saturated underground, oxidation that could otherwise produce sever pH and heavy metal contamination problems on the surface can be reduced. Underground disposal requires careful planning to ensure space is available in mined out areas. Backfilled tailings may also preclude the recovery of marginal value at a later date (Vick, 1983).

Open pits left from surface mining may also be used to deposit tailings, a cost effective method when backfilling is required by regulatory bodies or simply to reduce surface impoundments. Pit disposal is most suited to mining operations that have several separate pits that become worked out at different stages. Tailings can then be open ended at a single point or from several peripheral points around the empty pit. Surface area restrictions can often restrict the area available for a decant pond and water has to be pumped to the surface and used accordingly. Mining and tailings disposal simultaneously in the same pit is often proposed but seldom implemented. Pits resulting from linear ore bodies can be progressively backfilled however due to the depth of excavation the volume required for impoundment walls can become greater than the volume available for tailings. Often considerable artesian water seeps through the walls of the pits and this can result in considerable pore pressures on dam abutments and foundations. The instability resulting has been linked to the failure of at least one in-pit tailings embankment (Vick, 1983).

Appendix B: The Classification of Tailings

When considering a tailings disposal system two fundamental questions that require answering are; how much tailings will be produced and how will the tailings behave? The amount of tailings produced is directly linked to the size of the anticipated ore body and the rate at which it will be mined. In many cases the mineral value is between 0.1 and 3 % of the ore body and so the tons mined will essentially be equal to the tons requiring disposal (Robinson, 2008). The behaviour of tailings at disposal is a function of the engineering properties. The characteristics of the ore body combined with the various crushing, grinding, concentrating, leaching and heating processes determine the tailings engineering properties (Vick, 1983). However both these aspects can change as the life of mine is extended and mineral extraction processes evolve. A tailings disposal system therefore has to be flexible enough to cater for such unpredictable scenarios. Mine planners need to consider the impacts of new or proposed modifications to mining and processing steps on tailings disposal.

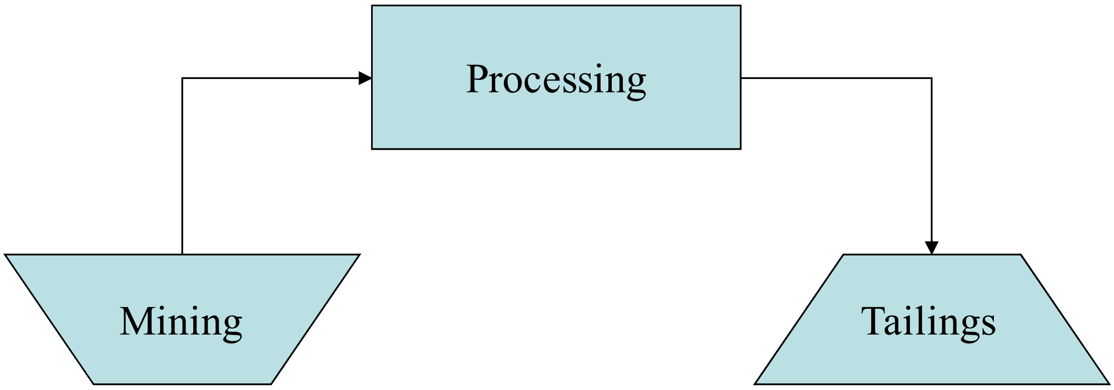

Figure B.1: Simplified schematic of a mining operation (Robinson, 2008)

Life of Mine

During mine planning it is essential to determine whether the ore body is large or small, finite or indeterminate. This determines how long a tailings facility will be required to be in operation. In most cases it is uneconomical to plan to sustain a tailings facility for more than 20 to 25 years. If the ore body is well defined and activities are expected to last for less than this period then a single design could be provided for the life of mine. However if this is not the case it may be necessary to specify a number of possible deposition areas and keep these aside for future designs. Mining operations often begin in undeveloped areas which then attract urbanization and thus long term planning is most advisable.

A facility cannot be designed until the monthly production rate and overall life of mine requirements have been specified. Once this is known conservative estimates of the required volume can be determined and the topography of the area scrutinized for possible locations. In most cases the tailings volume requiring storing can be determined by estimating an in-situ dry density and multiplying this by the anticipated run of mine tons. Tailings disposal systems cannot readily accommodate great and/or frequent fluctuations from the steady state. The range of tailings quantities expected therefore needs to be defined as closely as possible (Robinson, 2008).

Of particular importance when considering how to dispose tailings is what keeps the deposited tailings in place. Tailings are not actually "disposed of" but they often or should remain in place long after mining has ceased. It would be ideal if tailings disposal could actually improve the natural environment. Tailings disposal after the extraction of mineral sands has in one case improved the environment. The poor water retention characteristics of land in Western Australia was improved by the re-distribution of previously concentrated clay layers throughout the profile improving the agricultural productivity of the land. However this is not often the case and keeping the tailings in one place is crucial. Due to the forces of gravity, tailings stored above ground have the potential to "fall down" and fail. Thus an understanding of the geotechnical aspects of the behaviour of tailings is important for all stages of the design, operation and rehabilitation of the waste disposal area. In general, the geotechnical aspects cannot be considered in isolation from the broader environmental aspects (Fahey and Newson, 1997).

Phase Relationships

An essential element of the physical characterisation of tailings is the quantities of solid, liquid and air phases of the mass of material, whether slurry or settled form. Figure B.2 shows an idealised representation of the three phases, and then a break down of the various components by volume and weight. The liquid and solid phases are always present; however air may or may not be present depending on the degree of saturation. A number of parameters are defined from these phase relationship. (Vick, 1983)

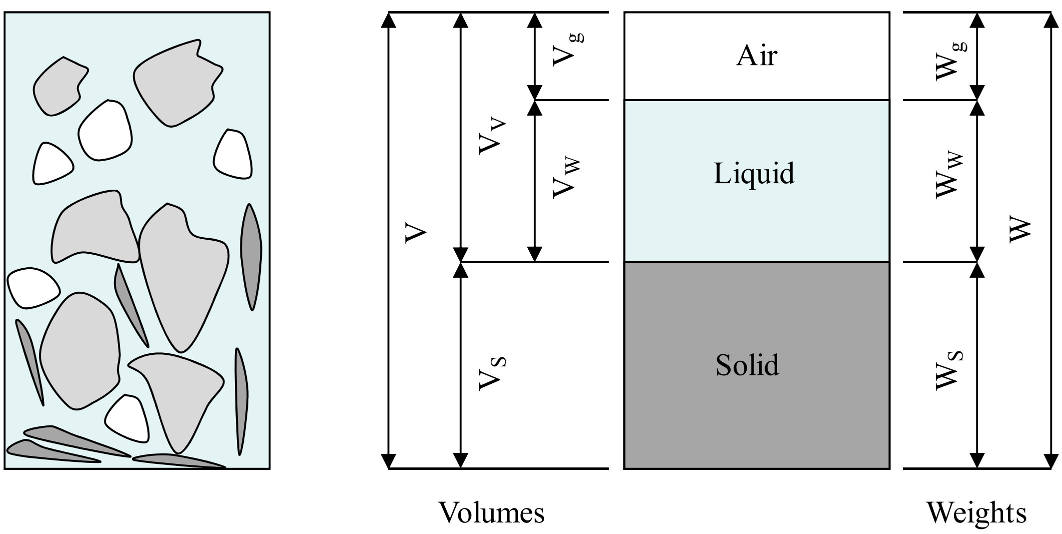

Figure B.2: Tailings phase relationships

Void Ratio $e = \frac{V_V}{V_S}$ **Equation B.1**

Degree of Saturation $S = \frac{V_W}{V_V}$ **Equation B.2**

Porosity $n = \frac{V_V}{V}$ **Equation B.3**

Specific Gravity $G_S = \frac{\gamma_S}{\gamma_W}$ **Equation B.4**

$$where \ \gamma_S = unit \ weight \ of \ solids = \frac{W_S}{V_s}$$

$$and \ \gamma_W = unit \ weight \ of \ water = \frac{W_W}{V_W}$$

Water Content $w = \frac{W_W}{W_S}$ **Equation B.5**

Pulp Density $P = \frac{W_S}{W}$ **Equation B.6**

Slurry Density $SD = \frac{W}{V}$ **Equation B.7**

It is important to note that civil engineers and metallurgists have different definitions for water content (or moisture content). Not clarifying which water content is being quoted can result in wrong calculations (Robinson, 2008).

Metallurgist Water Content $w_m = \frac{W_W}{(W_w + W_S)}$ **Equation B.8**

The equation $G_S w = Se$ follows from the above definitions. From this equation, expressions can be derived to relate the various tailings relationships (Vick, 1983).

Particle Size Distribution

The particle size distribution is the single most significant parameter affecting the behaviour and performance of the tailings at disposal (Robinson, 2008). The relative proportions of the different grain sizes in tailings are quantified in the form of a particle size distribution (PSD). The coarse grain portion is determined by sieve analysis and the fine grained portion by hydrometer analysis. Various national standards define the exact procedure that should be followed to ensure repeatability. Sieve analysis involves passing a sample through a series of sieves with decreasing aperture size and weighing the mass left behind on each sieve. In general the sieve apertures are; 9.5 mm, 4.75 mm, 0.425 mm, 0.150 mm and 0.075 mm. Below this grain size hydrometer analysis is used. A hydrometer measures the density of a suspension of fine material with time. As the grains settle the density changes and this can be converted to particle sizes using Stoke's law. The particle size distribution is generally presented in the form of a particle size distribution curve (Sivakugan and Das, 2010).

A residues particle size distribution is a function of the various process steps including the fineness to which the ore is milled, the degree of weathering of the ore, the type of milling process, the separation or extraction processes (CMSA, 1996). Traditionally soils are described as well-graded if they contain a roughly equal range of coarse and fine particles sizes and poorly graded if not. Further soils are described as uniformly graded if they contain a small envelope of grain sizes and gap-graded if there are no grains in a specific size range. A classification system proposed by Robinson (2008) is particularly defined for tailings and can be used to predict the most likely depositional strategy. The classification defines tailings according to four categories based on the general tail positions of the curves:

1. Fine-Fine: Particle sizes predominantly fall into the silt and clay ranges
2. Coarse-Coarse: Particle sizes predominantly fall into the sand and gravel ranges
3. Fine-Coarse: Particles sizes are very uniform over a small range between sand and silt sized particles.
4. Coarse-Fine: Particles sizes are well distributed across the gravel, sand, silt and clay sized particles.

Figure B.3 below illustrates the concepts of the above classification. Obviously the tailings particle distribution curves will not fall exactly onto one of these classification curves and some interpretation needs to be made.

Fine-Fine tailings are often the most problematic tailings to dispose. As will be shown in following sections the grading has a significant impact on most of the geotechnical properties at disposal. Fine-Fine tailings have poor beaching characteristics as they do not segregate and take a long time to settle. Permeability is reduced and this negatively affects the consolidation or strength gain characteristics. As such Fine-Fine tailings take too long a time to gain strength to be used in any significant way for impoundment construction and are predominantly disposed off within a preconstructed impoundment.

Coarse-Coarse tailings on the other hand beach very well and result in steep beaches as they settle fast. Increased permeability results in rapid strength gain. Coarse-Coarse tailings can therefore be used to form impoundment walls with greater ease. In many cases mining operations that produce Coarse-Coarse tailings will also produce a finer waste stream. In such cases the finer waste stream is often contained within an impoundment formed from the coarse stream. The Coarse-Coarse tailings can be deposited by spigotting or alternatively by cycloning if rapid dewatering of the fraction is required for rapid wall construction for downstream or centreline construction.

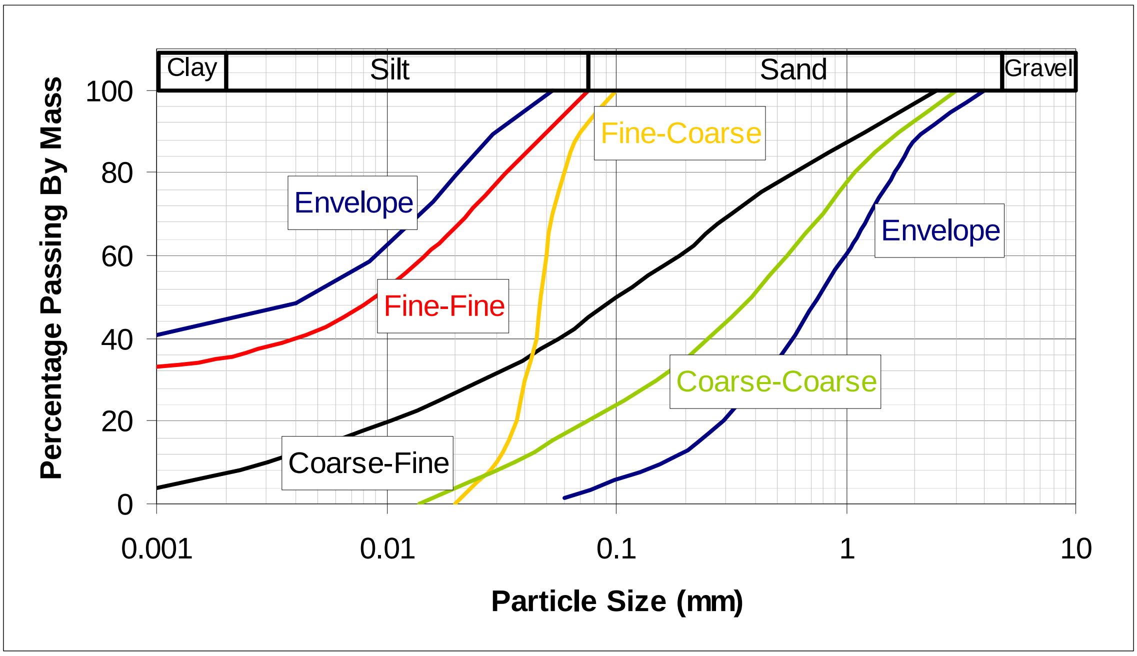

Figure B.3: Robinson (2008) particle size classification

Fine-Coarse tailings are often by-products of process circuits that require a hard-rock mineral to be finely ground to below 75 µm such as gold extraction circuits. Geotechnical properties are not significantly better than Fine-Fine tailings. However they do drain albeit slowly and can beach at a relatively flat angle. As such the paddocking method of construction is often adopted as it provides sufficient time for consolidation of the outer day walls under a negative water balance (i.e. arid areas). This is because sun drying is required to desiccate and thus consolidate the outer sections. Although these tailings only have a very small coarse sand fraction cycloning can sufficiently separate the two fractions. Further more the significant dewatering that occurs, results in the coarse fraction reaching a substantial degree of consolidation fairly rapidly. As such outer wall constructed by cyclones can safely contain tailings at high rates of rise up to 20 m/year (Robinson, 2008).

The geotechnical properties of the fine and coarse particles in Coarse-Fine tailings can be used advantageously to construct tailings facilities. By spigotting the tailings in a ring-dyke fashion segregation occurs and a well draining outer embankment forms. The finer particles gravitate towards the centre of the facility and thus the poorer geotechnical properties of this material will not significantly affect the stability. Although coarse particles have good geotechnical properties they can pose significant problems to pumping. They can cause greater wear to pipes and cause blockages as they tend to settle rapidly. This will have to be taken into account when determining the tailings disposal solution.

Following are some sample particle size distribution for various tailings minerals; however it must be kept in mind that the grading is significantly influenced by the mill process.

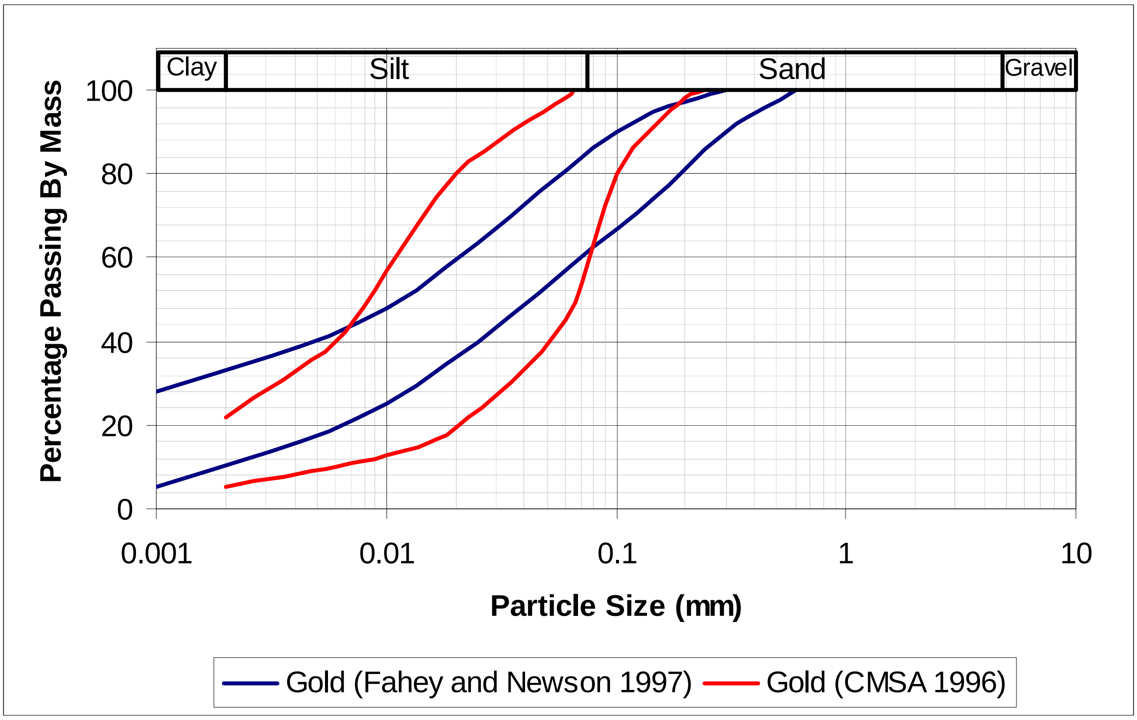

Figure B.4: Sample Gold tailing PSD

Figure B.4 illustrates they wide range of tailings particles sizes inherent to gold mining operations. This is a reflection of the fact that the gold extraction process is dependent on the particles specific area. The ore grade determines how efficient a processing circuit has to be for economic recovery of the mineral. Finer grinds are more costly to process due to higher operating costs and flotation inefficiencies. Rich ore tailings will thus often be coarser than poor ore tailings. Gold can however also be found in placer (alluvial) deposits and thus rely on gravitational rather than grinding and concentration for extraction. Such operations result in separate gravel and cobble-sized tailings and are often simply stacked in piles (Vick, 1983).

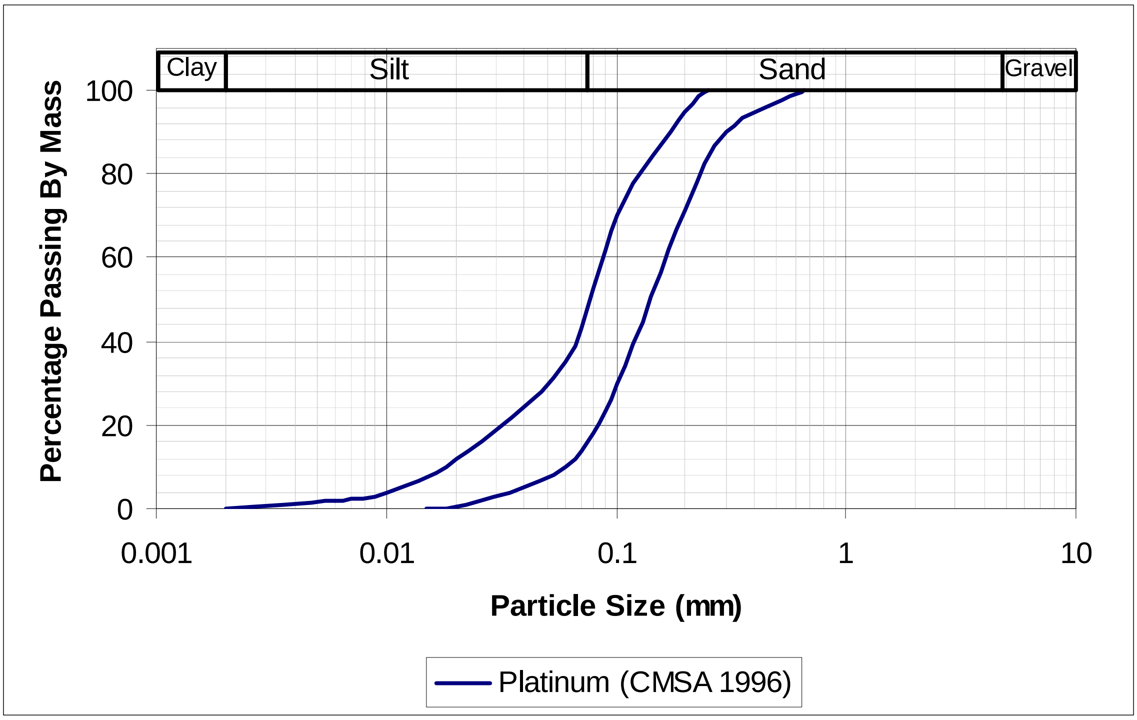

Figure B.5: Sample Platinum tailings PSD

Platinum ore bodies tend to much harder than gold ore bodies however they contain an extreme range of particle specific gravities; 2.7 for talc to between 16.0 and 17.0 for ferrous platinum (Hochreiter et al., 1985). The particle size distribution of platinum tailings is influenced significantly by the ore body which contains the platinum group minerals (PGM). In South Africa the Bushveld Complex contains three reefs that are exploited; the Merensky reef, the UG2 reef and the Platreef. The Merensky reef comprises iron-magnesium silicate minerals and calcium-aluminium-sodium silicate minerals under and overlain by discontinuous chromite concentrations. This body contains base metal sulphide grains and platinum group minerals. Coarse and dense PGM can be separated from the Merensky reef thus negating the need for a fine grind on the whole run of mine for flotation. This results in a well graded tailings product. The UG2 and Platreef bodies were not at first exploited as they do not contain as significant deposits of base metals as the Merensky reef. The UG2 reef consists of platiniferous chromite layer with the PGM predominantly present as sulphides. These sulphides are fine grained and therefore require grinding and flotation for recovery of the PGM. The Platreef is a complex assemblage of pyroxenites, serpentines and calc-silicates. The pyroxenites are associated with PGM sulphides often enclosed or on the grain boundary and the serpentines with sperrylite ($PtAs_2$). High association of PGM with silicate minerals also occurs (Schouwstra et al., 2000). The Platreef ores also require flotation for liberation of the PGM concentrate for further processing. Ongoing research is showing that to fully liberate these PGM finer grinds have to be employed; this along with improvements in flotation technology (Rule and Anyimadu, 2007) is likely to result in tailings with a very limited particle size distribution.

Due to the wide range of particle sizes, see Figure B.5, platinum tailings have largely been disposed of by means of spigotting and forming a ring dyke dam. However the increasing need for finer grinding is influencing the depositional strategies with either the need for cycloning or preconstructed impoundments to cater for increased production rates.

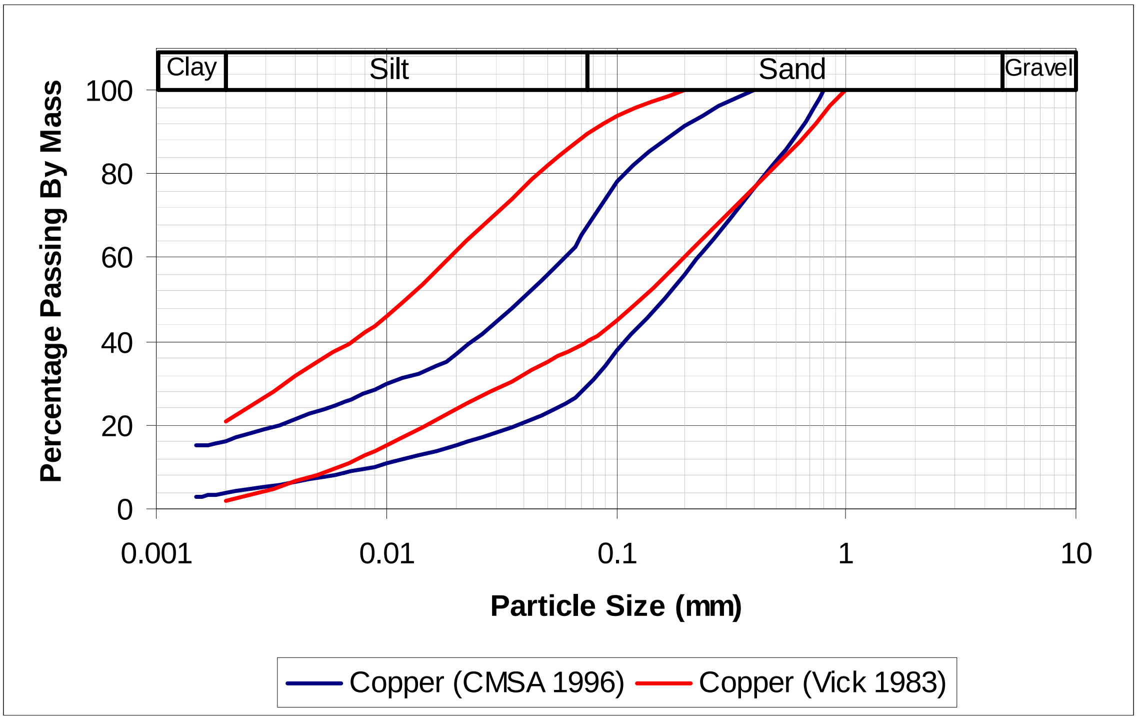

Figure B.6: Sample Copper tailing PSD

Copper is mined predominantly from hard-rock ore bodies by large-scale open-pit methods, which is then milled and concentrated by froth flotation. As a result particle size distribution for various copper tailings falls within a narrow range. Copper tailings are generally well graded and can be classified as Coarse-Fine tailings, see Figure B.6. Shale related ore bodies can result in high clay contents and finer grinds may be employed if minerals such as silver or zinc can be recovered from the same ore body (Vick, 1983). The majority of copper tailings can therefore be spigotted. However many copper deposits are contained in the Chilean Andes and are disposed of in valleys with dams built in a downstream fashion from the coarse fraction extracted by cyclone.

Coal formed from lush sub-tropical forest that became buried by incoming sediment. The vegetation was thus compressed between layers of sediment that today is predominantly shales and sandstones (Blyth, 1960). Near surface seams are mined in an open cast fashion with deeper seams mined by underground operations typically in a process called mechanized longwalling (Deates, 1971). Thermal energy is released by the combustion of coal with the production of ash as a by product. The need for low ash producing coal necessitates the washing or dense medium separation of mined coal (Lloyd, 2000). This results in a coarse stream comprising of shales, sandstones and considerable carbonaceous material. A fine stream is also produced and is also disposed. The particle size distribution of coal wastes are shown in Figure B.7. The low particle specific gravity of coal washery fines results in them having very poor geotechnical properties. They are often disposed of in either a slurry pond or co-disposed in a dyke formed by compacted coal discard. Coal washer fines are also very susceptible to erosion (CMSA, 1996). In many cases the washery fines and discard have economic value (Reddick et al., 2007) and their recovery must often be incorporated into the disposal plans.

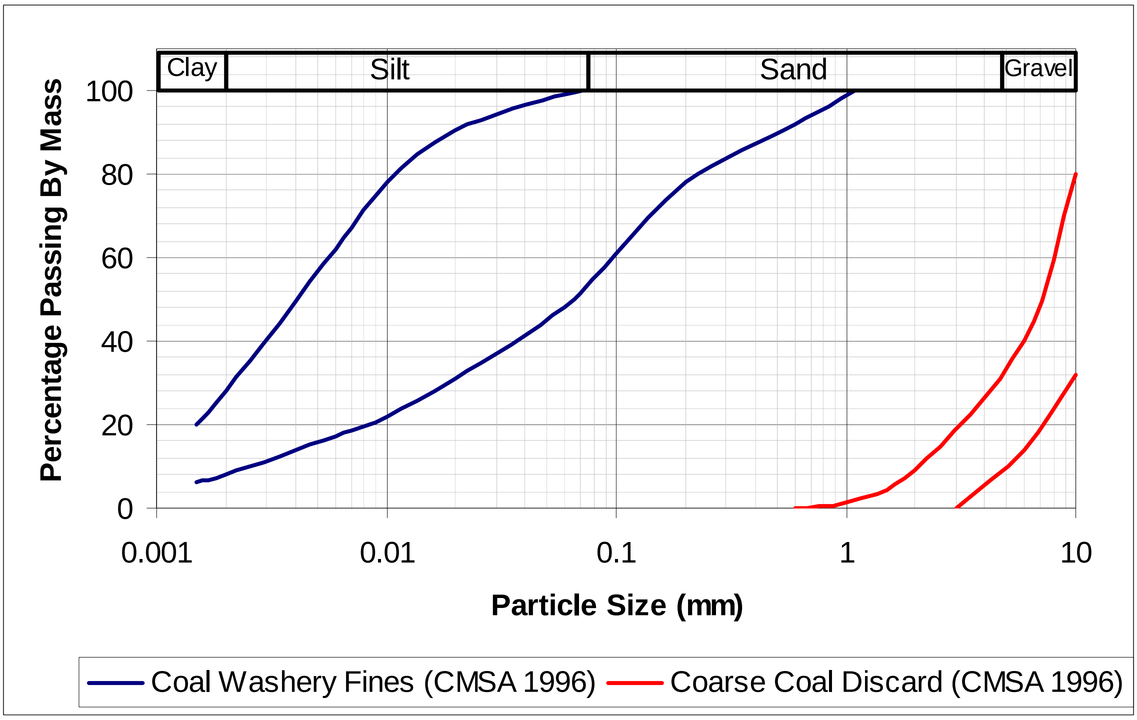

Figure B.7: Sample Coal tailings PSD

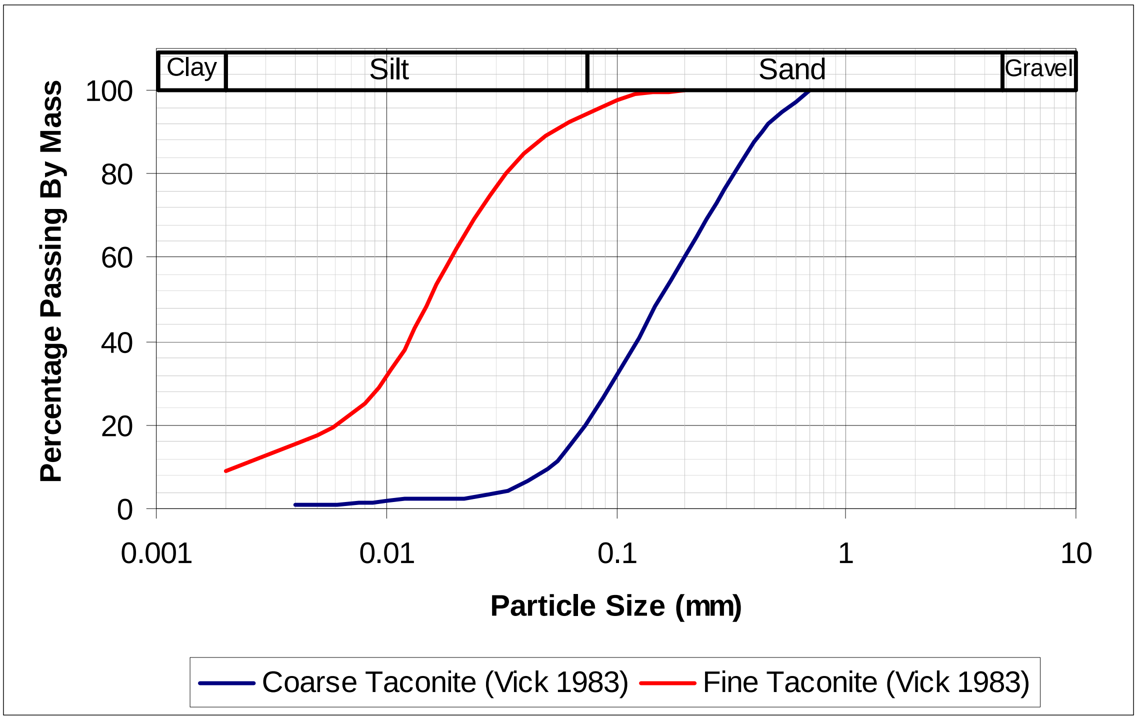

Figure B.8: Sample Iron Ore tailings PSD

Figure B.8 illustrates the typical particle size distribution of Taconite ore which is an iron ore body mined in the USA. This requires concentration by gravity separation, sometimes followed by magnetic separation resulting in coarse tailings. Non-magnetic low-grade ore requires crushing to very fine sizes followed by flotation. Mines that produce both coarse and fine discard usually produce far higher quantities of coarse waste (Vick, 1983). Processing in South Africa is similar in that crushing is kept to a minimum so as to reduce the quantity of fine produced in benefaction. Separation is undertaken by heavy-medium separation taking advantage of the high specific particle gravities of the hematite. Coarse fractions are separated in drums while the fine fractions are separated in heavy-medium cyclones (Voges, 1975). In South Africa the wastes produced from iron ore benefaction are disposed of with the spigotting method (Robinson, 2008).

Figure B.9 gives the particle size distribution for various other tailings found in the mining industry. Bauxite mud's are a by product of the extraction of aluminium oxide from bauxite ores. Ores are ground in hot caustic soda resulting in a particle size distribution in the silt range. Bauxite mud has extremely poor consolidation properties and is therefore generally disposed of within an impoundment. The extraction of diamonds from diamond ore bodies is a three stage process; crushing, washing and recovery. Primary concentration is done either in a pan plant or a heavy media separation plant. Uranium tailings are generally coarse however the clay content varies according to the nature of the ore. Furthermore the clay mineralogy can be altered if the extraction process involves acid leaching with montmorillonite forming kaolinite. Uranium can also be extracted in an alkaline process but requires finer grinding. The extraction of crude oil from oil sands generally produces a coarse waste but with a significant slimes fractions consisting of silt, clay and oil residue.

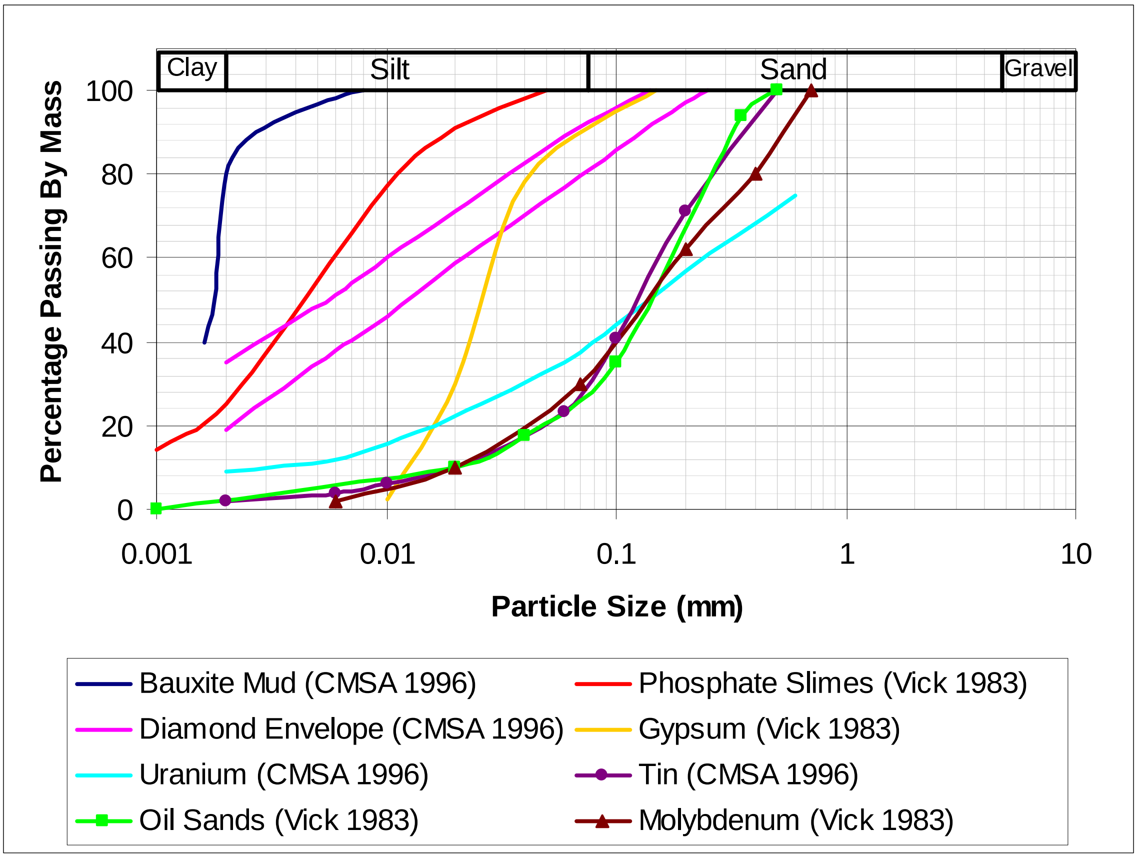

Figure B.9: Samples of various other tailings PSD

Particle Specific Gravity

The particle specific gravity (or density) is dependent on the type of ore mined as illustrate by Table B.1. Coal washery tailings generally have the lowest specific gravities however there is evidence that values vary regionally and careful reference to a particular mine needs to be made. The presence of pyrite in gold, copper and lead-zinc ore bodies and unrecovered iron minerals in iron ore bodies can also result in high specific gravities (Vick, 1983). For sub-aqueous deposition, the rate of sedimentation is affected by the specific value and particle size distribution. Given two particles of the same size, the one with a higher specific gravity will settle faster. For sub-aerial deposition, the beach angle and the hydraulic sorting that occurs on the beach is also dependent on the particle specific gravity. Heavier particles will behave coarser than they actually are settling at a steeper beach angle, with the opposite happening for particles with lower specific gravities (Robinson, 2008, Fahey and Newson, 1997). Some tailings have more than one material with different specific gravities this has a similar affect to being well graded and hence segregation along the beach can occur accordingly. It also has influence on the density or unit weight of the residue and hence on volume and mass calculations (CMSA, 1996).

Table B.1: Specific Gravity values quoted in literature

Tailings	Specific Gravity, G_s	Reference
Coal Washery Tailings	1.45 to 2.50	Fahey and Newson (1997)
	1.94	Qiu and Sego (2001)
	1.4 to 2.4	Vick (1983)
Gypsum	2.2 to 2.4	Vick (1983)
Platinum	2.24 to 2.30	Boshoff (2002)
	2.7 to 16.0 – 17.0	(Hochreiter et al., 1985).
Phosphate	2.5 to 2.8	Vick (1983)
Uranium	2.6 to 2.7	Vick (1983)
Molybdenum	2.6 to 2.8	Vick (1983)
Gold	2.6 to 3.1	Vick (1983)
	3.17	Qiu and Sego (2001)
Bauxite	2.6 to 3.3	Vick (1983)
Oil Sand	2.60	Qiu and Sego (2001)
Copper	2.75	Qiu and Sego (2001)
	2.72 to 2.98	Mittal and Morgenstern (1976)
Lead Zinc	2.8 to 3.6	Vick (1983)
Taconite (Iron Ore)	3.0 to 3.4	Vick (1983)

Mineralogy of the Clay-sized Fraction

Crushing and milling processes often results in fine-grained soils that are classified as clay sized particles. In many cases these clay sized particles do not behave in a similar manner to clay particles found in nature. Soil particle surfaces carry small electrical charges the magnitude of which depends on the mineral. The electrical charge is also proportional to the particle surface areas and inversely proportionate to the self weight of the particles. This electrical charge results in a bonding between particles, which affects the clays activity. Activity is a measure of a clays shrinking and swelling behaviour with changes in water content. Clays are usually formed last in geological erosional processes; such as glacially eroded particles carried slowly by rivers and eventually deposited in lakes. Three common highly active clay minerals are; Montmorillonite, Illite and Kaolinite. (Atkinson, 2007). Ore bodies are generally made up of hard rocks which have undergone very little weathering and do not contain these minerals.

Clay minerals are made up of two structural units; tetrahedrons and octahedrons that are joined up along a common base forming tetrahedral and octahedral sheets respectively. Different clay minerals are produced from the stacking of these sheets. Kaolinite is made up of alternating tetrahedral and octahedral sheets joined by strong hydrogen bonds. Illite is made up of several units of octahedral sheets sandwiched between two tetrahedral sheets held together by potassium ions. Montmorillonite has a similar atomic structure however units are held together by weak van der Waal forces. The activity of the clays is dependent on how easily water gets in between the units, which is dependent on the strength of inter unit bonds. Kaolinite has the strongest bonds, followed by Illite and lastly Montmorillonite. Thus Montmorillonite clays are the most expansive and reactive (Sivakugan and Das, 2010).

Clay can also have a positive effect on a soil in that the bonds provide cohesion between particles. This cohesion can improve soils shear strength, however this is not the case with many tailings. Strength between tailings particles is generally derived from the frictional forces between particles and suction forces developed during drying. When soils are progressively moistened they pass through distinct states known as brittle solid, semi-solid, plastic solid and liquid. Soils without any clay (mineralogy) particles will not exhibit any plastic solid behaviour as there is no cohesion. Atterberg limits are the water contents at which soils pass between the states, the Plastic Limit from semi-solid to plastic solid and the Liquid Limit from plastic solid to liquid. The Plastic Index, PI, is the difference between the Plastic Limit and Liquid Limit. Atterberg limits can be easily determined by standardised methods and thus can be used to test if a tailings sample has clay mineralogy particles. Atterberg limits are then used to determine the activity, A of a sample:

$$A = \frac{PI}{\%\ Clay\ Fraction}$$ **Equation B.9**

Table B.2 below gives the specific surfaces of the three important clay minerals and associated activities. Table B.3 summaries the plastic behaviour of various tailings.

Table B.2: Approximate values of specific surface and activity for clay minerals (Atkinson, 2007)

Clay Mineral	Specific Surface (m^2/g)	Activity
Montmorillonite	Up to 840	>5
Illite	65 – 200	≈0.9
Kaolinite	10 – 20	≈0.4

Table B.3: Sample of PI, clay fractions and activity (Vick, 1983)

Tailings	Location	PI (%)	% Clay Fraction	Activity
Coal Washery Fines	Eastern U.S.	0 – 13	50	0 – 0.26
	West Virginia, U.S.	2 – 12	35	0.06 – 0.34
	Great Britain	3 – 30	30 – 50	0.1 – 0.6
Copper	Western U.S.	13	45	0.29
	British Columbia	0 – 11	22	0 – 0.5
Phosphate Slimes	Florida	90 – 150	60	1.5 – 2.5

The behaviour of tailings containing clay minerals can significantly impact the depositional strategy. Relatively small percentages of Montmorillonite can severely affect the sedimentation rate, compressibility and permeability of tailings. Generally ore bodies that have undergone weathering, such as open cast mining operations where the ore body is close to the surface, can have significant percentages of clay. For example gold deposits within the Western Australia Kaolinite zone formed within a lateritic weathering profile and can have a clay content of 15 % to 30 % (Fahey and Newson, 1997). Shale deposits associated with coal bodies can also result in clay particles in the associated waste streams. Copper slimes can occasionally exhibit plastic behaviour. Florida phosphate slimes can have significant clay percentages; with active Montmorillonite, Kaolinite and Illite clays resulting in exceedingly slow consolidation characteristics This results in extremely high void ratios that do not decrease with time, resulting in deposits trapping considerable amounts of water and occupying enormous tracts of land. The exploitation of Nickel within highly weathered laterite deposits located in tropical environments is likely to result in tailings high in clay minerals (Vick, 1983). Diamonds are often recovered from kimberlite ores which are weathered and so exhibit plastic behaviour which results in poor consolidation behaviour (Robinson, 2008). Bauxite tailings, or red mud, in spite of low plastic limits and low clay contents have poor sedimentation and consolidation rates. The complex leaching process used to remove aluminium from the bauxite alters the mineralogy resulting in the unusual behaviour of the tailings (Vick, 1983). Thus the chemical extraction process needs to also be kept in mind when analysing tailings behaviour.

Shear strength characteristics

Deposited tailings in slurry form have no shear strength and simply flow. However as they settle, consolidate and desiccate they develop shear strength and no longer flow. A maximum shear strength is gained and if a tailings dam is loaded beyond this available strength failure can occur. The shear strength characteristics of tailings should be determined from either in-situ testing on similar tailings or by laboratory experimentation. In-situ tests include vane shear tests and pressuremeter tests; laboratory tests include triaxial shear tests and shear box tests. Strength characteristics need to be determined at the different stages of sedimentation, consolidation and desiccation to determine the maximum shear strength available at each stage. This then guides the manner in which a tailings impoundment is operated.

Permeability

The permeability properties of the deposited tailings have a controlling influence on both the stability of the dam and determining the anticipated seepage loses. The resulting phreatic surface from the water permeating through the tailings dam determines the pore pressure regime which then has an impact on the stability. Seepage loses can have a significant impact especially if toxic constituents are present. Mitigation and control of tailings impoundment seepage is rapidly becoming one of the key issues in environmental and regulatory evaluation of mining projects.

In most applications of determining the phreatic surface D'Arcy's assumptions of steady seepage and gravity flow are adopted. This often results in conservative estimates of pore pressures adding a degree of safety to stability analysis. However for seepage determination it may be necessary to adopt unsteady, transient, or unsaturated flow that occurs under capillary rather than gravity gradients (Vick, 1983).

Determination of the phreatic surface involves defining boundary conditions and then assuming a flow net. A flow net is required as the flow is not in one direction and is not uniform over the entire area perpendicular to the flow. Laplace's equation of continuity is used to determine the flow net between the upstream and downstream sides of the permeable tailings deposit. Flow lines, along which a water particle will follow, and equipotential lines, along which the potential head is constant, make up a flow net. Continuity dictates that flow lines and equipotential lines intersect at right angles and various well-established methods are available for drawing such lines. These involve either hand drawn methods (Donaldson, 1960) or numerical models (GeoStudio, 2007). Assumptions have to be made about the permeability of the tailings and foundation material. Simple flow nets assume homogeneous conditions and are factored depending on the ratio between the vertical and horizontal permeability. However such simple assumptions have been unable to predict the apparently depressed phreatic surface in many hydraulically deposited upstream tailings dams (Blight et al., 1985).

The common method of beaching tailings in a ring dyke fashion in South Africa results in a beach along which particle segregation occurs forming a relatively small pool with a much larger dam perimeter. As a result of particle sorting there is a tendency for coarser particles to settle away from the pool thus increasing permeability towards the toe of the dam. For continuity of flow to be maintained the flow rate must be constant throughout the distribution of permeabilities. Thus the flow gradient must progressively decrease progressively from the pool outwards. Added to this the radial flow from a relatively small pool further depresses the phreatic surface. Blight et al (1985) showed that using Hazen formula ($k = {D_{10}}^2$, where k is permeability (cm/s) and D_{10} is the particle size (mm) below which 10% by mass are smaller in size) the permeability along the beach as a result of particle segregation can be approximated by:

$$k = a\, e^{bH}$$ **Equation B.10**

where k is permeability
a and b are characteristics of the beach
H is the distance down the beach

This equation was then used in a finite element model and to determine the phreatic surface from the edge of the pool to the toe of the dam as illustrated by Figure B.10.

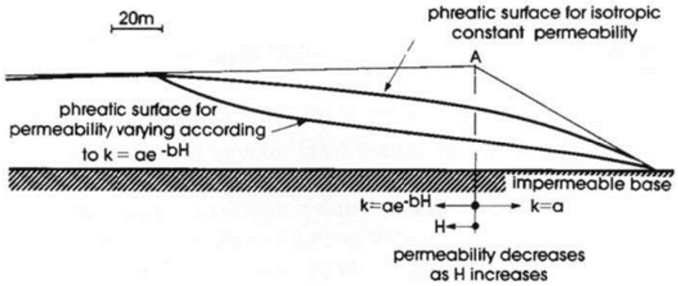

Figure B.10: Prediction of phreatic surface due to particle sorting along beach (Blight et al., 1985)

Although Hazen's formula was used by Blight et al (1985) this model was based primarily on the observations of permeabilities in loose, clean, filter sands. In a later paper Blight (1987) proposes that the equation proposed by Sherard et al (1984) should be used

$$k = 0.35 \times D_{15}^{\;2}$$ **Equation B.11**

where k, is permeability in cm/s

$D_{15,}$ is the particle size (mm) below which 15% by mass are smaller in size

Fourie (1988) investigated the permeability properties of tailings deposited in a flume by comparing the vertical permeability and horizontal permeability at the point of deposition and at the end of the beach. This research found that the difference in horizontal to vertical permeability is outweighed by the difference along the beach. Fourie (1988) concluded that this research agrees with the extensive finite element study by Kealy and Busch (1971). This finite element study found that the phreatic surface is virtually insensitive to the variation in the ratio of the horizontal to vertical permeability but rather dependent on the variation along the beach. However due to the dynamic nature of tailings beaching it is possible for sub-horizontal layering to occur. Horizontal layers with negligible vertical permeability can result in a series of perched water tables. The effect of these perched water tables on stability can be adverse with reports of failures in walls of heights of less than 3 m (Blight, 1988). Although not a concern in most warm arid locations the formation of ice layers can have a similar affect (Robertson, 1987).

The influence of void ratio (or dry density) has been extensively studied and shows that as the void ratio decreases the permeability likewise decreases. Figure B.11 is an example of such a study by Qiu and Sego (2001).

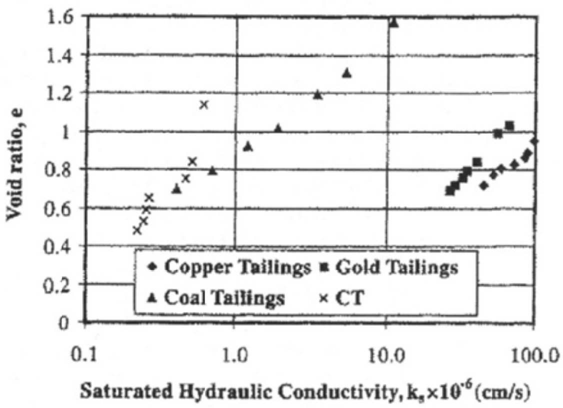

Figure B.11: Void ratio versus saturated hydraulic conductivity (Qiu and Sego, 2001)

Fahey and Toh (1992) proposed that this relationship between permeability and void ratio and can be defined for a particular tailings with the following equation:

$$k = A \times \left(\frac{e^B}{1+e} \right) \quad \textbf{Equation B.12}$$

Where k, is permeability
e, is the void ratio
A and B are characteristics of a tailings.

An additional source of seepage is the water that infiltrates the tailings at the point of deposition. Vick (1983) reports research by Nelson et al (1977) that suggests that the effects of infiltration can raise the phreatic surface 2 – 4 % of the embankment height near the active deposition point. Vick (1983) concludes that the most important factors in determining the phreatic surface for upstream embankments are the beach width, change in permeability due to particle sorting and the boundary flow conditions.

In most applications of downstream or centreline construction either a separate waste stream is used or the slurry is separated by a cycloning operation. In these cases the phreatic surface in the embankment determines the stability of the wall. As such the permeability properties of the deposited tailings are not the controlling factor but rather the material used for embankment construction. Material used to construct the embankment is often far more pervious than the deposited tailings. The tailings therefore perform a seepage-retarding function. Due to the necessity for continuity of flow the ratio between the permeabilities will have a significant effect on the phreatic surface. Figure B.12 reproduced by Vick (1983) from work by Wimpey (1972) illustrates the effect of the change in permeability on the phreatic surface. The condition illustrated in Figure B.12 only applies while the pool is not allowed to come into contact with the pervious embankment. Vick (1983) reports various authors indicating that should water be allowed to pond against the wall a phreatic surface equivalent to an embankment retaining water can develop. Should hydrological conditions or return water rates require the retention of significant depths of water an impervious core will be required between the ponded water and pervious embankment. Although cyclone underflows are generally more pervious and at lower water contents than the overflow they may introduce large quantities of water at localised portions of the wall. Therefore the cyclone operations and construction procedures may have a greater impact on the phreatic surface than the seepage from the contained overflow.

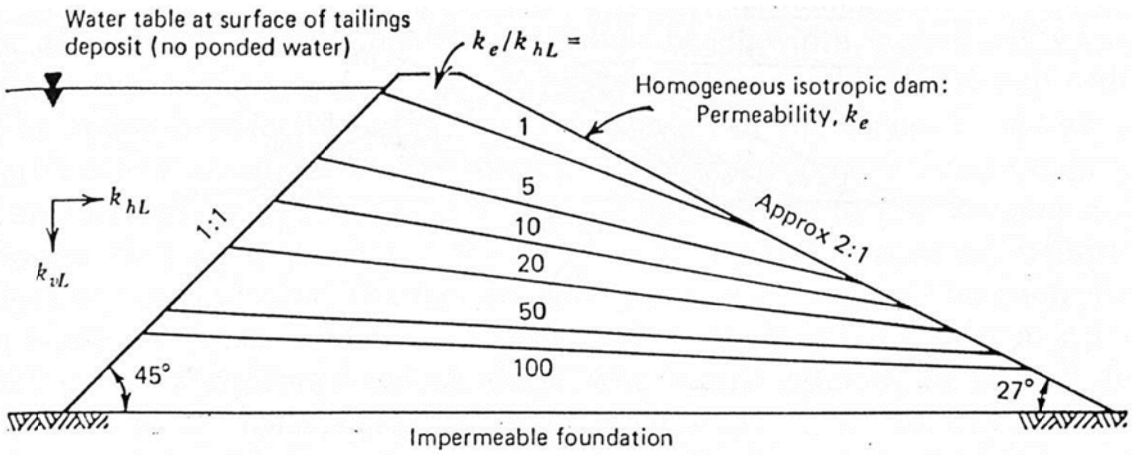

Figure B.12: Phreatic surface for down stream embankment (Vick, 1983)

Long Term Properties

In many cases the only geotechnical behaviour of a tailings deposit investigated is that during the operation of the facility. However, it should be remembered that after deposition many residues become subject to chemical and physical weathering with a consequent change in their geotechnical properties. Colliery residues are commonly made up of siltstones and mudstones, which may expand and slake on exposure to the weather reverting back to their original unconsolidated states as silty clays. Thus initially coarse, porous, free draining material may within a few years severely deteriorate. The resulting impervious material with reduced shear strength can be subject to severe settlement and piping erosion. Spontaneous combustion of coal deposits completely alters the geotechnical properties. Clay particles can become fused or semi-fused with better strength characteristics. However this is at the expense of the environment. Kimberlite and dolerite ore bodies are partly weathered igneous deposits and may undergo rapid deterioration on exposure to weather changing from granular material to clayey material within years. These examples highlight the necessity of investigating the long term changes in geotechnical properties. Further the tailings produced at the beginning of an operation may have very different geotechnical properties to when mining goes deeper into even less weathered ore bodies. (CMSA, 1996)

Appendix C: Failures

A paper by Perales (1998) on the media coverage following the Los Frailes tailings dam failure in Spain highlights the sever impacts failures can have on mining activities. Although the majority of the articles are a series of speculations, formed from both information and misinformation, they capture the sensationalism and sensitivity of the event. They also highlight the negative effects it had on Boliden, a relatively major mining company which owned the mine (Davies, 2002), and other mining operations in the Azanalcollar mining district.

A shallow foundation failure lead to the release of more than 5×10^6 m^3 of process water and tailings from one of the two adjacent ponds within an overall impoundment. A lack of understanding of the underlying foundation conditions lead to a design which contradicted site conditions. Rapid foundation movements created shear strains that triggered static liquefaction of the impounded tailings (Davies, 2002). The tailings stream was released into the Guadiamar river system which flows through the Doñana National Park. This park is the second biggest on the Iberian Peninsula and is classified as a Biosphere Reserve by UNESCO. As a result the potential impact of the spill on the National Park formed the paramount aspect of the media coverage. Considerable sensationalism was created with dramatic photographs of dead fish, illustrations of how food chains would be contaminated and impacts on birdlife migration patterns. Boliden’s local and international track record was reported on; such as the export of toxic waste from Swedish operations to Chile and resulting intoxication of local children.

Spanish and European officials placed the blame on Boliden, with environmental groups calling for criminal charges to be laid against Boliden. The Spanish Government and European Union covered compensation and rehabilitation costs with subsequent resolutions being passed requiring Boliden to repay these costs. Boliden however refused to make compensation payments, for the roughly 3500 Ha of agricultural land, until the Courts had evaluated the losses. Considerable impact on the mining industry was also apparent with many companies linked to Boliden initiating redundancy programs. This was in line with possible future restrictions on mining due to the increased scrutiny of environmental impacts. Newspapers also highlighted Boliden’s poor financial standings such as, deficits, received financial aid, potential losses from investments made in new mines and concerns regarding insurance policies. All these factors had a negative impact on the value of Boliden’s shares on the Toronto stock exchange. Within the space of five days the share price dropped by 28 % (Perales, 1998). The company eventually filled for bankruptcy in October 2002 (BBC, 2002). It is thus apparent that both the potential environmental impacts of a tailings dam failure and the associated financial implications on an operation can be severe.

It is fortunate that the Los Frailes disaster did not claim any lives unlike the Merriespruit and Stava disasters. The Merriespruit tailings dam operated by Harmony Gold in South Africa failed following a heavy rain storm on the evening of 22 February 1994. The rain water overtopped the embankment due to inadequate freeboard and began to erode the toe of the dam. The now steeper toe could no longer contain the fine essentially cohesionless tailings and triggered static liquefaction. More than 600 000 m^3 of tailings and 90 000 m^3 of water was released. The slurry travelled 2 km through the town of Merriespruit covering nearly 500 000 m^2 and claiming 19 lives. Two cross valley dams at a fluorite mine located near Stava in Northern Italy failed in a "domino fashion" on July 19, 1985. The design of the upstream constructed dams was not consistent with even the most elementary engineering principals available at this time. Based upon the likely state of the in-situ tailings, the curiosity of the failure was that the dams could attain such a height prior to failure. 240 000 m^3 of liquefied tailings travelled 4 km at 60 km/h obliterating the village of Stava and considerably damaging Tesero claiming 269 lives (Davies et al., 2000, Davies, 2002).

A common feature of the three described failures was the liquefaction of the tailings that occurred with a change in the stress regime at the time of failure. Liquefaction is not a new phenomenon, Terzaghi in 1947 stated that spontaneous liquefaction could occur if the original structure of the soil is "so loose and unstable that a slight disturbance causes its collapse." Further, the "sudden decrease of the shearing resistance…from its normal value to almost zero…is caused by a collapse of the structure of the sand, associated with a sudden but temporary increase of the pore water pressure." (Ulrich and Fourie, 2003). Prior to the failures recounted here the potential threat of static liquefaction to tailings dams was understood. Casagrande and MacIvor for example stated in 1970 that "the loose and saturated granular chemical wastes deposited behind a relatively thin shell of supporting material could cause failure of the tailings dam. While undisturbed tailings may adequately contribute to the stability of the dam, the strength of such a "shell" cannot possibly withstand liquefied tailings." One has to question why such disasters then occurred. Davies (2002) suggests that the classical soil mechanics as found in many textbooks still used today present a simplistic and erroneous view of the loading of saturated cohesionless particles and water systems – typical of most tailings. The simplistic view is that by defining the friction angle and pore water pressure of the sand we can predict the strength of the sand, the drained strength. The exception these references allow for sands is during earthquake when the sand may become 'liquefied'. Clays on the other-hand are deemed to be cohesive and have an undrained strength. He further goes on to state that these simplistic models need to be un-learned and replaced with a more rigorous understanding of the phenomenon.

A fundamental aspect of this more rigorous understanding is that the strength of cohesionless soil (sand and silts that make up most tailings) can like clay behave in an undrained fashion when rapidly loaded. Similarly like clay the strength can be stress path and strain path dependent. Tailings when deposited are a mass of loose sands and silts having very low strength and thus contract during shear like sensitive clays. Clays have a unique void ratio compression state whereas sands have a wide range in void ratio compression states. This combined with wide range of initial void ratios and material fabric as a result of field scale deposition makes predictions of undrained strength challenging. As a consequence of this any tailings impoundment that derives some of or all of its structural strength from the deposited material most be carefully analysed to ensure that the tailings are not contractant under any conceivable load. (Davies, 2002)

In many cases the contractant behaviour of the tailings is not the cause of the failure but rather result in dramatic flowing of the tailings once the impoundment is breached. However in many cases the tailings are impounded within tailings that have been deposited and managed in such away that they gain strength. A number of failure triggers have been highlighted in literature and include; seismic events, overtopping of decant water, increasing pore pressure, excessive rates of rise, poor control of slurry density. (Blight, 2010)

1. *Seismic Events*. Seismic events resulted in the catastrophic failure of the El Cobre and Barahona tailings in Chile in 1965 and 1928. Severe earthquakes can impose significant shear strains resulting in significant shear stresses causing finer partly consolidated tailings to strain soften. The tailings can then become liquefied and flow along with any water and become agitated. Upstream slopes may slide into the liquefied tailings and the agitated tailings flow over the impoundment. The erosive nature of many tailings exacerbates the situation such that any breach can progressively enlarge until the mass of tailings simply flow. The flow may only be stemmed once the shear strains imposed by the earthquake subside and a stable surface is formed (Blight, 2010). As a consequence any tailings impoundment that may potentially fail due to a seismic event needs to have a substantial impoundment structure. To this extent Davies (2002) states that earthquakes are of little consequence provided walls are constructed in a downstream fashion.
2. *Overtopping*. Management of tailings facilities is in many cases the main culprit for overtopping failures. The already mentioned Merriespruit disaster was an example of such a trigger as was the Bafokeng failure near the town of Rustenburg in 1974. Poor management of decant water on both facilities resulted in excess water building up. The remaining freeboard was insufficient to cater for storm water that accumulated shortly before the failures as a result of heavy rain fall. This water then found the most convenient route breaching the ring dyke walls. High susceptibility to erosion resulted in the breaches becoming progressively larger leaving very little support for the impounded tailings. As a result significant volumes of tailings flowed out of these breaches claiming the lives in its path.

3. *Pore Pressure*. The Simmergo dam was an impoundment that had been abandoned for 20 years when it was recommissioned. Prior to the recommissioning the phreatic surface had subsided to the level of the natural soil surface. After a month of operation the phreatic surface had risen to 20 m and this resulted in the almost immediate failure of the dyke. The hydrostatic suction that had provided the shear strength was lost once the phreatic surface rose.
4. *Rate of Rise.* The Saaiplaas tailings dam 5A was also recommissioned but was only intended as a short term solution. However deposition continued and soon the rate of deposition exceeded the time required for strength to be gained to form an impoundment. Short sighted mine management had also not approved underdrains and placed the penstock in the corner of the rectangular site rather than in the geometric centre. Decant water was however well managed and no overtopping occurred. The high rate of rise and lack of underdrainage resulted in an insufficiently consolidated wall that failed in shear in three separate areas between 18 and 22 March 1993.
5. *Slurry Control*. An unnamed small alluvial mining operation commissioned a new dam that was to be built up in an upstream manner by means of a spraybar system. Plant commissioning problems resulted in slurry being delivered at too high a slurry density for segregation to occur. As a consequence spraybar deposition was replaced with a cycloning operation to develop a coarse pervious outer wall. However the coarse pervious outer wall was underlain by a 5 m deposit of unsegregated material. When the wall had reached 15 m above the starter wall two separate rotational failures occurred 4 days apart. Piezocone testing revealed that the slip surface was most likely along the unsegregated material that acted as soft clay.

Appendix D: Factors Influencing Evaporation

Solar Radiation

The sun's energy is fundamental to the earth's climatology and meteorology. This energy is transferred by conduction, convection, advection and radiation. Conduction is the transfer of energy by the kinetic energy of colliding atoms and molecules. Convection involves the transfer of energy by the organised mixing of air. Similarly heat may be transferred horizontally by advection. Radiation is the means by which heat moves as an ensemble of waves through a vacuum. Vast quantities of energy are produced in the core of the sun through a fusion reaction between hydrogen to form helium. This energy is transferred through the various layers of the sun and from there into space. The amount of incoming radiation falling perpendicularly on unit area in unit time at the outer limit of the atmosphere, when the distance between the sun and the earth is at its mean value is the solar constant. This is estimated to be on average 1.37 kW/m^2 but can fluctuate by 1.5 %. Debate surrounds the possible short-term and long-term variation in the solar constant. Short-term fluctuations can be caused by sunspots blocking radiation to space. Long-term fluctuations are related to changes in the activity within the sun and the changing nature of the earth's orbit around the sun. The magnitudes of short-term fluctuations are inconclusive and long-term fluctuations are irrelevant to the time scope of the present study (Tyson and Preston-Whyte, 2004).

The longer the duration of daylight the greater the quantity of radiation received over a given portion of the earth. This is a function of the altitude of the sun which in turn varies according to the position of the earth as it orbits around the sun. Neat mathematical formula can therefore be developed to calculate the radiation reaching the outer surface of the atmosphere. Alternatively the incoming radiation can be determined from data captured by satellites such as the Earth Radiation Budget Satellite such information is displayed in Figure D.1 (Stickler, 1990). This incoming radiation is termed as Extraterrestrial Radiation.

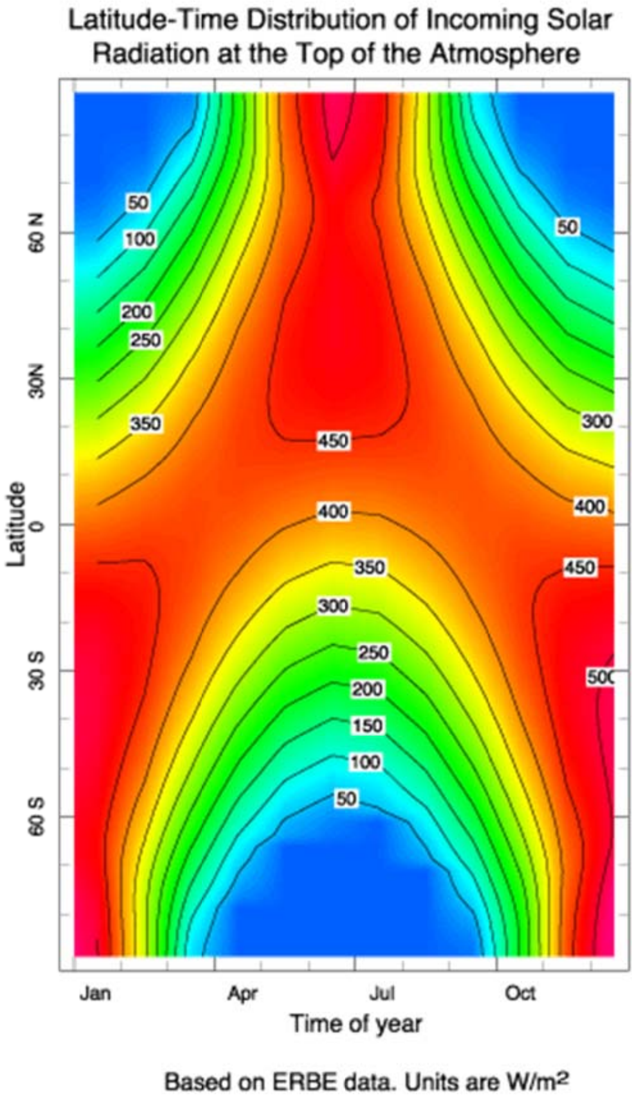

Figure D.1: Variation in solar radiation at the top of the atmosphere as a function of latitude and season (http://oso.tamucc.edu/labs/lab6/lab6.htm)

Radiation is attenuated in its passage through the atmosphere through adsorption, scattering and reflection. Further the energy absorbed during the daytime is radiated during the night. Radiation is conceived as constituting a continuous range of wavelengths, the totality of which is called the electromagnetic spectrum. However all bodies do not radiate in all parts of the spectrum. The sun for example radiates most of its energy in the 0.3 to 3 μm region and hence is called short-wave radiation. The earth-atmosphere system on the other hand radiates most of its energy in the 3 to 100 μm band and is known as terrestrial or long-wave radiation. Quantum theory holds that radiant energy exists in units called photons. These photons can be absorbed by electrons in atoms that make up gases. Atmospheric gases that are important in the absorption of radiant energy are oxygen, ozone, water vapour and carbon dioxide. Each gas absorbs energy in narrow wavelength intervals called spectral absorption lines. Ozone absorbs almost all the ultraviolet wavelengths (<0.29 µm) with water vapour absorbing in several bands between 2.5 and 13 µm. Little absorption occurs in the 0.3 to 0.8 µm band thus the atmosphere is transparent to the major portion of solar-radiation transmissions. Thus cloud cover does not absorb much solar-radiation; individual clouds may absorb 10 – 20 % but on average probably less than 3 %.

When the parallel beam of radiation pass through gases the impact between photons and air molecules causes them to be scattered. This scattering results in the different colours that are observed in the sky. The type of scattering is determined by the size of the scattering particles in relation to the wavelength of incident radiation as summarised by Table D.1. Refraction and reflection account for the majority of the attenuation in the atmosphere.

Table D.1: Types of scattering (after Tyson and Preston-Whyte, 2004)

Particle Radius	Scattering	Colour
Less than 1/10 of wavelength (Air Molecules)	Rayleigh	Blues and Red (Depending on depth of atmosphere penetrated)
Equal (Cloud droplets and pollution)	Mie	Grey to White
1/10 to 10 times wavelength	Diffraction	-
Greater than 10 times wavelength (Rain drops)	Refraction and Reflection	Rainbow

Solar radiation that passes through the atmosphere is further reflected by the incident surface. The fraction of incident radiation that is reflected by a surface is called its albedo, α and the fraction absorbed is called its absorptivity, a.

$$a = 1 - \alpha \qquad \textbf{Equation D.1}$$

Thus a strong absorber is a weak reflector and vice versa. Surface albedos can vary throughout the day and depend on the colour and texture of the incident surface. The albedo is greatest for solid surfaces early in the morning and late in the afternoon as the sun’s ray strike the surface at low angles. For water surfaces the opposite occurs with maximum albedo’s occurring during midday, as ripples prevent low angle sun rays being reflected (Blight, 2010). These daily fluctuations in albedo are often ignored and an aggregate value assumed for the entire day, Table D.2 gives some typical albedo values.

Table D.2: Some typical albedo values (after Tyson and Preston-Whyte, 2004 and Blight, 2010)

Surface Type		Albedo (%)
Fresh Snow		75-95
Desert		25-30
Deciduous Forest		10-20
Light grey fly ash	Wet (Darker)	22
	Dry (Lighter)	33
Dark brown tailings	Wet (Darker)	6
	Dry (Lighter)	14
Yellow gold tailings	Wet (Darker)	16
	Dry (Lighter)	33
Water over a light-coloured tailings surface		20

To account for the various energy attenuations due to absorption, scattering and reflection simplifications are made and a solar radiation balance, such as in Figure D.2, can be drawn up.

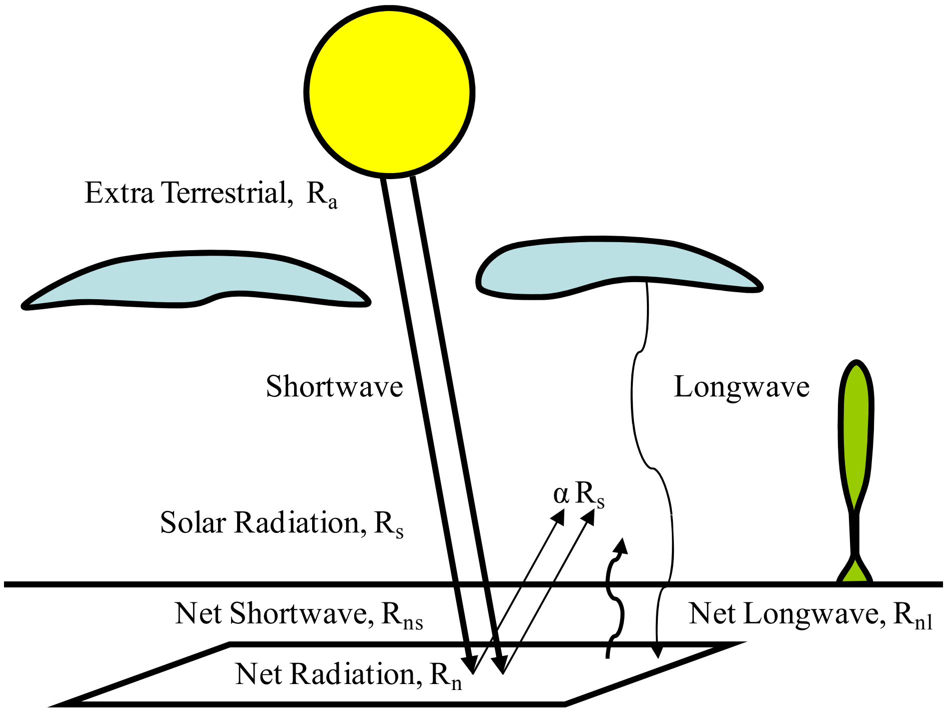

Figure D.2: Solar radiation balance (after Allen et al., 1998)

Solar radiation, R_s, is the amount of extraterrestrial radiation, R_a that passes through the atmosphere and reaches a horizontal plane. For a cloudless day, R_s is roughly 75% of extraterrestrial radiation whereas only 25% may reach the earth's surface with extremely dense cloud cover. Linked to R_s is the clear-sky solar radiation, R_{so} which is a calculated value for no cloud cover. R_s and R_{so} are often related to each other as relative shortwave radiation, R_s/R_{so}. Direct measurements of R_s can be made with pyranometers, radiometers and solarimeters. In cases when solar radiation is not directly measured formulas such as the Angstrom formula can be used.

The solar radiation absorbed by the earth is later released as heat energy. This energy is radiated at much longer wavelengths and is thus referred to as long wave radiation. Long wave radiation is either absorbed by the atmosphere or lost into space. A portion of this radiation is also reflected and thus again absorbed and released by the earth. The difference between the outgoing and incoming long wave radiation is called the net long wave radiation, R_{nl}, and can be determined by the Stefan-Boltzmann law.

Finally once all these values have been determined the net radiation, R_n can be determined. This is the difference between the incoming and outgoing short and long wave radiation. R_n is normally positive during the day and negative during the night time, and positive over 24 h except in extreme conditions at high latitudes.

Air Humidity

Air humidity is the amount of water vapour in the air and this has a fundamental role in regulating the heat transfer in the atmosphere. The amount of water present in the atmosphere as a gas is enormous and far exceeds that present as a liquid or solid. Unlike temperature and rainfall, there is no single measure of water vapour content of the atmosphere and different measures are used for different purposes.

Atmospheric pressure is the total pressure exerted by all the gases in the atmosphere. It is, therefore, the sum of the partial pressures of the constituent gases, of which evaporated water is one. The partial pressure exerted by the water vapour is called the vapour pressure, e_a. The amount of water vapour that can remain in a gaseous state is a function of temperature alone. Evaporation takes place initially from a plane water surface to the surrounding air. A state of equilibrium is reached when, at a particular temperature, no further exchange takes place between the air and water. At this stage the air is said to be saturated. The pressure exerted by this saturated air is called the saturation vapour pressure, e_s. The magnitude of the saturation vapour increases with temperature and can be determined by various relationships such as the Arden Buck equation (Buck, 1981). The difference between e_s and e_a is known as the saturation deficit and is a measure of the dryness of the air. Relative humidity, RH, is the ratio between the amount of water the ambient air actually holds and the amount it could hold at the same temperature expressed as a percentage. Although the actual vapour pressure might be relatively constant throughout the day, the relative humidity fluctuates between a maximum near sunrise and a minimum around early afternoon.

It is not possible to measure the actual vapour directly and thus it is derived from RH or dewpoint measurements. The dewpoint temperature is the temperature to which air at constant pressure and water vapour content must be cooled in order to become saturated and precipitate dew. The actual vapour pressure of the air is the saturation vapour pressure at the dewpoint temperature. Therefore, the drier the air the larger the difference between the air temperature and the dewpoint temperature. The dewpoint temperature is determined with a dewpoint meter. RH can be measured directly with hygrometers. These are based on the measurements of material such as hair that changes length in response to humidity or capacitance plates where the electrical capacitance changes with RH. Alternatively vapour pressure can be determined with psychrometers, the so-called dry and wet bulb thermometers. Dry-bulb temperature is determined from a ventilated or aspirated thermometer. Wet-bulb temperature is the temperature of a ventilated thermometer whose bulb is surrounded by water evaporating freely from a saturated wick dipped in distilled water. As evaporation of water vapour occurs, so the latent heat of vaporisation causes cooling. The wet-bulb temperature is defined, therefore, as the lowest temperature to which air can be cooled by evaporating water onto it. Relative humidity and dewpoint temperature data is notoriously plagued by measurement errors. This is common to both older hygrothermograph instruments and modern electronic devices. Dewpoint measurements should also be compared to computed values from daily minimum air temperatures which are frequently more reliable than relative humidity measurements (Allen et al., 1998).

Air Temperature

Temperature is a physical quantity characterising the mean random motion of molecules in a physical body. Temperature is characterised by the behaviour whereby two bodies in thermal contact tend to an equal temperature. Thus temperature represents the thermodynamic state of a body, and its value is determined by the direction of the net flow of heat between two bodies (WMO, 2008). Various different scales are used to define temperature requiring a fixed point and a unit of temperature. The unit is in most cases a linear increase from the given fixed point to another. For instance; for the Celsius scale water freezes at 0°C and boils at 100°C (Warner, 2004). The SI unit of temperature is the Kelvin with the triple point of water assigned as the fixed point with a value of 273.16 K. The magnitude of the Kelvin is equal to the unit of the Celsius scale. Air temperature is defined as the temperature indicated by a thermometer exposed to the air in a place sheltered from direct sunshine.

Solar radiation that reaches the earth surface and is absorbed provides the energy used in physical and biological processes. Usually a good linear relationship exists between the absorbed fraction and total incoming radiation. If we neglect the soil heat flux (which is near zero when averaged over a day), net radiation can be portioned between sensible heat and latent heat. Sensible heat is the heat that heats the air above the surface, and latent heat is consumed in evaporating water (Blight, 2002). Partitioning energy in this manner is commonly referred to as the Bowen ratio (sensible heat/latent heat). Sensible heat causes the daytime temperatures to rise above the night time temperatures. Under ideal night conditions the temperature will tend toward the dew point temperature, with the minimum just before sunrise. For a specific Bowen ratio, on a given day, the greater the net solar radiation, the greater the heating of the air will be. This will result in a larger difference between the daily maximum and minimum air temperatures. This relationship can be used to determine the daily incoming solar radiation from maximum and minimum daily temperatures (Bristow and Campbell, 1984).

The dew point temperature, T_{dew}, is the temperature at which air is saturated with water and hence no further evaporation occurs. The difference between T_{dew} and air temperature drives evaporation. Kimball et al (1997) report various authors showing that T_{dew} stays relatively constant throughout the day. Thus knowing the actual temperature and T_{dew} gives an indication of the evaporative potential. The gap between the air temperature and T_{dew} often decreases over night and often reaches T_{dew}. Thus the minimum daily temperature, T_{min}, can often be used as indication of T_{dew} from which humidity estimates can be made during the rest of the day. The main assumption in these relationships is that diurnal variation in vapour pressure is minimal. Bristow (1992) showed that vapour pressures at inland arid sites can vary considerably and T_{min} is not a good indicator of T_{dew}. However for humid coastal areas the relationship can be a good predictor. Kimball et al (1997) further investigated the relationship between T_{min} and T_{dew}. For arid sites they found large difference between T_{dew} and T_{min} over the entire year corresponding to differences between the daily vapour pressures. Semi-arid sites showed a large degree of seasonality with minimal differences between T_{dew} and T_{min} during wetter months and larger differences in warmer drier conditions. Other climatic regimes showed smaller differences and T_{min} was a better indicator of T_{dew}. Kimball et al (1997) developed a method to improve T_{min} based humidity estimates using daily air temperatures, annual precipitation and estimates of daily potential evapotranspiration for semi-arid and arid climates.

As shown daily temperature fluctuations are an indication of solar radiation and daily humidity. Thus empirical formulas have been proposed to determine potential evapotranspiration from mean air temperature. The premise for this is that daily temperatures are an indication of available energy for the latent heat required. However the main source of this energy is solar energy. During the course of the year air temperatures lag behind the changes in solar radiation. For instance the same solar intensity is experienced in spring and autumn however spring temperatures are lower than autumn temperatures. This mean air temperature solar radiation lag becomes more pronounced for continental climates due to the increasing aridity. As a result mean temperature based estimates of evapotranspiration can become less accurate for inland locations (Baier, 1963).

Various devices are used to measure temperature such; as liquid in glass thermometers, mechanical thermographs and electrical thermographs. Each has its advantages and disadvantages however these shall not be discussed here and readers are referred to WMO (2008). One common issue with temperature readings is the exposure and sitting of the device. Various sources of radiation can cause a thermometer to give a false reading of the air temperature. Thermometers therefore have to be shielded from direct radiation such as the sun to give an accurate indication of air temperature. Thus they are often contained within a Stevenson screen or behind ventilated radiation shields. These screens should be over level ground, freely exposed to sunshine and wind and not shielded by, or close to, trees, buildings and other obstructions. The World Meteorological Organization suggests that devices should be at an elevation of between 1.2 and 2 m for standardised results. Two types of temperature recordings can be made, either the prevailing temperature or the maximum and minimum temperature over a given time interval. Modern electronic devices record temperatures continually which can then be averaged and maximum and minimum temperatures determined. Older devices such as maximum and minimum mercury thermometers simply record the maximum and minimum temperatures between recordings which are then reset with a magnet.

Wind Speed

Wind is made up of random small-scale fluctuations in time and space that when superimposed are a large-scale organised flow. To fully describe the flow of air would require three-dimensional vectors however for all intensive purposes a two dimensional vector defined by the direction and wind speed is sufficient. This organised flow however is punctuated by gusts and depending on the accuracy of the device used to measure the wind these are either picked up or ignored (WMO, 2008). The process of vapour removal from an evaporating surface is to a large extent driven by the wind and ensuing turbulence above the surface. Vapour rising from a surface gradually saturates the air, if this is not removed saturation will be reached and no further evaporation will occur. It would follow that increasing wind speed would result in more evaporation however this is not the case.

The dryness and temperature of the air have a part to play in the evaporation process. Dry, hot air has ample capacity for vapour, with wind promoting the transport of vapour away from the surface. Humid, warm air has less capacity for vapour and increasing wind speed does not result in a matched increase in evaporation rate (Allen et al., 1998). Blight (2002) investigated the rate of evaporation from a bare soil surface under increasing wind speeds. Warm, humid air was passed over the specimens and a marked increase in evaporation rate was observed with a marginal increase in wind velocity from calm conditions. However the evaporation rate did not vary considerably after this initial increase. This indicates that a minimum amount of wind is likely required to remove the vapour and that only dry, hot winds will result in any further increase in evaporation rate.

Wind speed and direction are commonly measured with a cup and propeller set up and a wind direction vane. Wind speed increases considerably with height and it is recommended that measurements be taken at 10 m above ground level. Wind direction however does not vary as considerably with height (WMO, 2008). For agrometeorology purposes, such as determining potential evapotranspiration, wind speed is required at a height between 2 or 3 m however correction relationships have been developed. This takes into account the boundary layer that forms from the ground surface to the height at which the measurement is taken.

Not all weather stations record wind speed and direction in this cases it may be possible to import data. Variations may be considerable during the course of the day however over longer periods they can be similar. Air masses from the same origin or governed by similar weather fronts can be assumed to be similar between locations. However the main governing factors are relief and regional climate. Strong winds are associated with low relative humidity and light winds with high relative humidity. Thus the two sites need to have similar trends for daily maximum and minimum relative humidities. For mountainous areas data should not necessarily be from the nearest station but from a station with similar elevation and exposure to dominant winds. Imported data should only be used for determining evapotranspiration over several-day periods. When no information is available estimates can be made however this requires that the potential evaporation be determined for monthly periods.

Appendix E: FAO 56 Method

FAO 56 Penman-Monteith

The FAO Penman-Monteith equation is derived from the original Penman-Monteith equation and equations for aerodynamic and surface resistance and is presented below:

$$ET_o = \frac{0.408\Delta(R_n - G) + \gamma \frac{900}{T + 273} u_2 (e_s - e_a)}{\Delta + \gamma(1 + 0.34u_2)} \quad \textbf{Equation E.1}$$

where ET_o is the reference evapotranspiration in mm day^{-1}
R_n is the net radiation at the crop surface in MJ m^{-2} day^{-1}
G is the soil heat flux density in MJ m^{-2} day^{-1}
T is the air temperature at a height of 2 m in °C
u_2 is the wind speed at a height of 2 m in ms^{-1}
e_s is the saturation vapour pressure in kPa
e_a is the actual vapour pressure in kPa
$e_s - e_a$ is the vapour pressure deficit in kPa
Δ is the slope of the vapour pressure curve in kPa $°C^{-1}$
γ is the psychrometric constant in kPa $°C^{-1}$

FAO 56 outlines how this equation can be used to calculate the reference evapotranspiration for different time steps and includes procedures for applying the equation when climatic data is missing. Table E.1 outlines the various time steps that can be considered along with the assumptions that can be made and consequences on accuracy.

Table E.1: Reference Evapotranspiration for different time steps

Time Step	Data Requirements	Notes
Ten-day or Monthly	• Ten-day or monthly average daily maximum and average daily minimum temperature. • Ten-day or monthly averages of the actual vapour pressure. • Ten-day or monthly average of daily wind speed measured at 2 m. • Ten-day or monthly average of the daily net radiation	The FAO Penman-Monteith equation is non-linear and this can introduce some error for longer time steps. The soil heat flux should not be ignored during warming (spring) and cooling periods (autumn) and its value can be determined from mean monthly air temperatures

Daily	• Daily maximum and minimum air temperatures • Mean daily actual vapour pressure • Daily average wind speed at 2 m • Daily net radiation	Daily time steps generally provide accurate results. The daily soil heat flux is relatively small over a 24 h period and can be ignored without introducing significant error.
Hourly	• Average hourly air temperature • Average hourly wind speed measured at 2 m • Total hourly solar radiation with the determination of net shortwave and longwave radiation to give net solar radiation	Hourly time steps should be used when considerable daily changes in wind speed, humidity or cloudiness occur. The soil heat flux needs to be calculated for the hourly steps which can be done using the hourly temperatures. Precise hourly estimates can be difficult to obtain, and hourly steps should be summed to give 24 hour totals.

To calculate evapotranspiration using FAO 56 requires the calculation of various values which shall be outlined below (Allen et al., 1998):

1. *Atmospheric Parameters*. The atmospheric pressure, P in kPa, can be calculated at a point based on the positions elevation above sea level by adapting the ideal gas law:

$$P = 101.3\left(\frac{293 - 0.0065z}{293}\right)^{5.26} \qquad \textbf{Equation E.2}$$

where z is the elevation above sea level in meters.

The atmospheric pressure is used to determine the psychrometric constant, γ in kPa °C^{-1} for the site in question:

$$\gamma = \frac{C_a P}{\varepsilon\lambda} = 0.665 \times 10^{-3} P \qquad \textbf{Equation E.3}$$

where C_a is the specific heat of air at constant pressure, 1.013×10^{-3} MJ kg^{-1} °C^{-1}
λ is the latent heat of vaporisation, 2.45 MJ kg^{-1}
ε is the ratio of the molecular weight of water vapour to dry air, 0.622

2. *Air Temperature*. The average temperature over a 24 h period is taken as the mean of the daily maximum and minimum temperatures rather than the average of hourly values over a 24 h period:

$$T_{mean} = \frac{T_{max} + T_{min}}{2} \qquad \textbf{Equation E.4}$$

Some calculation procedures require temperature values in degrees Celsius whilst others required temperature values in Kelvin. The conversion is done by adding 273.16 to degrees Celsius values.

3. *Air Humidity*. Saturation vapour is related to air temperature and the relationship is expressed as:

$$e°(T) = 0.6108\, e^{\left(\frac{17.27T}{T+237.3}\right)} \qquad \textbf{Equation E.5}$$

where e°(T) is the vapour pressure at the air temperature T in kPa
T is temperature in °C
e is the base of the natural logarithm, 2.7183

As the above equation is not linear the average for the daily maximum and minimum temperatures should be calculated for the time interval under investigation:

$$e_s = \frac{e°(T_{max}) + e°(T_{min})}{2} \qquad \textbf{Equation E.6}$$

The slope of the relationship between temperature and saturation pressure is also required and this is given by:

$$\Delta = \frac{4098 \times \left(0.6108 e^{\left(\frac{17.27 T_{mean}}{T_{mean}+237.3}\right)}\right)}{(T_{mean} + 237.3)^2} \qquad \textbf{Equation E.7}$$

where Δ is the slope of the vapour pressure curve in kPa °C^{-1}
T_{mean} is the average air temperature in °C

Actual vapour pressure, e_a in kPa, can be calculated in a number of different ways depending on what data is available. If the dew point temperature can be accurately determined it can be used to determine the actual vapour pressure;

$$e_a = e°(T_{dew}) = 0.6108\, e^{\left(\frac{17.27 T_{dew}}{T_{dew}+237.3}\right)}$$ **Equation E.8**

where T_{dew} is the dew point temperature

This equation can also be used when no humidity data is available by assuming that T_{dew} is equal to T_{min}. However particularly for arid sites this may not be applicable. In these cases a local calibration can be determined from a nearby site with more extensive records or 2 – 3 °C subtracted from T_{min}.

A psychrometer can be used to determine vapour pressure. The two temperature readings from the dry and wet bulbs are used as follows:

$$e_a = e°(T_{wet}) - A \times P(T_{dry} - T_{wet})$$ **Equation E.9**

where T_{dry} is the dry-bulb temperature in °C
T_{wet} is the wet-bulb temperature in °C
$e°(T_{wet})$ is the saturation pressure at the wet-bulb temperature in kPa
A is an instrument specific psychrometric constant;
0.000662 - Ventilated Asmann type psychrometer with air movement of 5 m/s
0.000800 - Naturally ventilated psychrometer with air movement of 1 m/s
0.001200 - Non-ventilated psychrometer installed indoors

Depending on the availability of relative humidity data different equations should be used. When both the maximum and minimum daily relative humidities are known:

$$e_a = \frac{e°(T_{min})\frac{RH_{max}}{100} + e°(T_{max})\frac{RH_{min}}{100}}{2}$$ **Equation E.10**

where $e°(T_{min})$ is the saturation pressure at the daily minimum temperature in kPa
$e°(T_{max})$ is the saturation pressure at the daily minimum temperature in kPa
RH_{max} is the daily maximum relative humidity in %
RH_{min} is the daily minimum relative humidity in %

Weekly, ten-day or monthly averages should be averaged from the respective daily averages. For cases where there are errors in estimating RH_{min} only use RH_{max}:

$$e_a = e°(T_{min})\frac{RH_{max}}{100} \qquad \textbf{Equation E.11}$$

If the daily maximum and minimum relative humidities are unavailable the daily average can be used instead:

$$e_a = \frac{RH_{mean}}{100}\left[\frac{e°(T_{max}) + e°(T_{min})}{2}\right] \qquad \textbf{Equation E.12}$$

Once the saturation vapour pressure and actual vapour pressure have been determined the difference between the two values can be used to determine the reference evapotranspiration.

4. *Solar Radiation*. When the net solar radiation is not measured directly it can be calculated. The daily extraterrestrial radiation incident on a horizontal surface at the top of the atmosphere, R_a in MJ m^{-2} day^{-1}, can be determined from the solar constant, solar declination and time of the year:

$$R_a = \frac{24(60)}{\pi} S_o d_r \left(\omega_s \sin\Phi \sin\delta + \cos\Phi \cos\delta \sin\omega_s\right) \qquad \textbf{Equation E.13}$$

where S_o is the solar constant, 0.0820 MJ m^{-2} min^{-1}

Φ is the latitude in radians, negative in the southern hemisphere and positive in the northern hemisphere

d_r is the inverse relative Earth-Sun distance given by:

$$d_r = 1 + 0.033\cos\left(\frac{2\pi}{365}J\right) \qquad \textbf{Equation E.14}$$

δ is the solar declination given by:

$$\delta = 0.409\sin\left(\frac{2\pi}{365}J - 1.39\right) \qquad \textbf{Equation E.15}$$

J is the number of the day in the year between 1 (1 January) and 365 or 366 (31 December)

ω_s is the sunset hour angle given by:

$$\omega_s = \arccos(-\tan\Phi\tan\delta) \qquad \textbf{Equation E.16}$$

For hourly or shorter periods it is necessary to determine the solar time angle at the beginning and end period under consideration and finding the average value over the time. This value is then substituted for the sunset half hour in the above equation. The solar time angle takes into account the longitude and latitude of the station under consideration as well as necessary seasonal corrections.

To work out the net radiation it is necessary to determine the solar radiation, R_s in MJ m^{-2} day^{-1}, from the daily extraterrestrial radiation. If the actual sunshine hours are known the Angstrom equation can be used:

$$R_s = \left(a_s + b_s \frac{n}{N}\right) R_a \qquad \text{Equation } \mathbf{E}.17$$

where a_s is a regression constant, expressing the fraction of extraterrestrial radiation reaching the earth on overcast days, if no calibration is available it can be assumed to be 0.25

$a_s + b_s$ is the fraction of extraterrestrial radiation reaching the earth on clear days, if no calibration is available b_s can be assumed to be 0.50

n is the actual duration of sunshine in hours

N is the maximum possible duration of sunshine in hours in a day determined by:

$$N = \frac{24}{\pi} \omega_s \qquad \textbf{Equation E}.18$$

To compute the net longwave radiation it is necessary to determine the clear sky radiation value, R_{so} MJ m^{-2} day^{-1}:

$$R_{so} = (a_s + b_s) R_a \qquad \textbf{Equation E.19}$$

When no calibrated values of a_s and b_s are available the clear sky radiation can be determined with a relationship based on the sites elevation above sea level, z in m:

$$R_{so} = \left(0.75 + 2 \times 10^{-5} z\right) R_a \qquad \textbf{Equation E.20}$$

Net shortwave radiation, R_{ns} in MJ m^{-2} day^{-1}, is defined as the balance between the incoming and reflected solar radiation which is determined by the albedo of the surface, α which is 0.23 for the reference surface:

$$R_{ns} = (1 - \alpha) R_s \qquad \textbf{Equation E.21}$$

The difference between the outgoing and incoming long wave radiation is called the net long wave radiation, R_{nl}, and is determined by the Stefan-Boltzmann law:

$$R_{nl} = \sigma \left[\frac{T_{\max,K}{}^{4} + T_{\min,K}{}^{4}}{2} \right] \left(0.34 - 0.14\sqrt{e_a} \right) \left(1.35 \frac{R_s}{R_{so}} - 0.35 \right)$$ **Equation E.22**

where σ is the Stefan-Boltzmann constant (4.903 $MJK^{-4}m^{-2}day^{-1}$)
$T_{max,K}$ maximum 24 h temperature in Kelvin, K (K = °C +273.16)
$T_{min,K}$ minimum 24 h temperature in Kelvin, K (K = °C +273.16)
e_a is the actual vapour pressure

This equation takes into account the effects of humidity and cloudiness as these factors influence the net outgoing flux of longwave radiation. Measurements of incoming and outgoing longwave radiation can be used to calibrate the equation.

The net radiation, R_n in MJ m^{-2} day^{-1}, is the difference between the net incoming shortwave radiation, R_{ns}, and the net outgoing longwave radiation, R_{nl}:

$$R_n = R_{ns} - R_{nl}$$ **Equation E.23**

At many sites solar radiation is not measured directly and neither is the number of sunshine hours. It is possible to use data from a nearby station assuming the two sites are within the same region. Here a region is defined as; a small area, such that air masses governing rainfall and cloudiness are similar, and the regional physiography is almost homogeneous. As a consequence caution should be taken for importing data in mountainous and coastal areas where differences in altitude and exposure exists. Within a homogeneous region should the north-south distance between the station and site exceed 50 km the following correction can be made to determine the incoming solar radiation:

$$R_s = \frac{R_{s,\,reg}}{R_{a,\,reg}} \times R_a$$ **Equation E.24**

where $R_{s,\,reg}$ is the solar radiation at the regional location in MJ m^{-2} day^{-1}
$R_{a,\,reg}$ is the solar extraterrestrial radiation at the regional location MJ m^{-2} day^{-1}

The net longwave and shortwave radiation can then be calculated to give the net radiation. When the above adjustment for north-south distance is made, ET_o calculations should be restricted to monthly time periods. For daily intervals a comparison between the two sites maximum and minimum daily air temperature and humidity needs to be made. The difference between the maximum and minimum air temperatures gives an indication of a sites degree of cloudiness. Hargreaves and Samani (1982) used this principle to relate extraterrestrial radiation to solar radiation:

$$R_s = k_{rs}\sqrt{(T_{max} - T_{min})}R_a \quad \textbf{Equation E.25}$$

where R_s and R_a in MJ m^{-2} day^{-1}
T_{max} and T_{min} in °C
k_{rs} is an adjustment factor based on relative humidity, RH:

$$k_{rs} = 0.047 \times (100 - RH)^{1/3} \quad \textbf{Equation E.26}$$

If no relative humidity data is available k_{rs} can be assumed to be 0.16 for interior locations, where land mass dominates and air masses are not influenced by large water bodies. For coastal location, where air masses are influenced by large water bodies k_{rs} can be approximated as 0.19.

For island locations, where land mass is less than 20 km, so that air masses are influenced by adjacent water bodies in all directions, temperature methods are inappropriate. The following relationship can be used for low altitudes from 0 to 100 m:

$$R_s = 0.7R_a - b \quad \textbf{Equation E.27}$$

where b is an empirical constant equal to 4 MJ m^{-2} day^{-1} if no calibration is available.

Caution must be taken when using the above methods to estimate daily solar radiation, especially when relying on limited data sets. It is recommended that the values be either summed or average over a several day period to reduce any prediction error.

5. *Soil Heat Flux*. Complex models are available to calculate the soil heat flux, G is MJ m^{-2} day^{-1}; however the value is small compared to net radiation, particularly for well vegetated surfaces (as is the case for the reference surface) and calculation steps smaller than 24 h. For long time periods the soil temperature lags the air temperature and this can be used to estimate the soil heat flux for extended periods:

$$G = c_s \frac{T_i - T_{i-1}}{\Delta t} \Delta z \quad \textbf{Equation E.28}$$

where c_s is the soil heat capacity in MJ m^{-3} °C^{-1}
T_i is the temperature at time i °C
T_{i-1} is the temperature at time i-1 °C
Δt is the length of the time interval in days
Δz is the effective depth in m

The average temperature over the time interval should be considered. Effective depth is a function of the time interval under discussion. For a time interval of a few days the effective soil depth is only 0.10 – 0.20 m but for monthly periods may be up to 2 m. Soil heat capacity is a function of mineral and water content.

For one day or ten-day periods the soil flux beneath the grass reference surface is small and can be ignored. Temperatures correlations for hourly or shorter periods do not work as well and should be rather estimated from net radiation, R_n. For daylight periods:

$$G = 0.1R_n \quad \textbf{Equation E.29}$$

and during night periods:

$$G = 0.5R_n \quad \textbf{Equation E.30}$$

6. *Wind Speed*. For evapotranspiration wind direction is not necessary however the average wind speed over the time interval being calculated is required. Wind speed is slowest on a surface and increase with height. Wind speed is not always measured at a height of 2 m as required by the FAO Penman-Monteith equation and the following is used to adjust such readings:

$$u_2 = u_z \frac{4.87}{\ln(67{,}8z - 5.42)} \quad \textbf{Equation E.31}$$

where u_2 is the wind speed at 2 m above ground surface in m s^{-1}
u_z is the wind speed at z m above ground surface in m s^{-1}
z is the height of measurement above ground level in m

When no wind data is available for a particular site data from a station within the same region can be imported. Large variations in wind speed can exist during the course of the day however the variations can diminish when referring to longer periods or the total for the day. However trends in variation in other metrological parameters and relief should be compared. Should no wind data be available for a region; empirical estimates can be made from a general description of the wind using Table E.2.

Table E.2: General classes of monthly wind speed data

Description	Mean monthly wind speed at 2 m
Light Wind	≤1.0 m/s
Light to moderate wind	1 – 3 m/s
Moderate to strong wind	3 – 5 m/s
Strong wind	≥5.0 m/s

Where no data at all on wind speed is available a value of 2 m/s can be assumed as this is generally accepted as the average wind speed for stations around the globe. In general however wind speeds should be limited to about $u_2 \geq 0.5$ m/s for very low wind speeds to account for buoyancy affects at the surface.

FAO 56 A-Pan Correction Factors

The Pan Coefficient is determined by the pan type, the ground cover under the pan and the surroundings, as well as general wind and humidity conditions. Figure E.1 outlines the two cases that must be considered for the vegetation surrounding the pan.

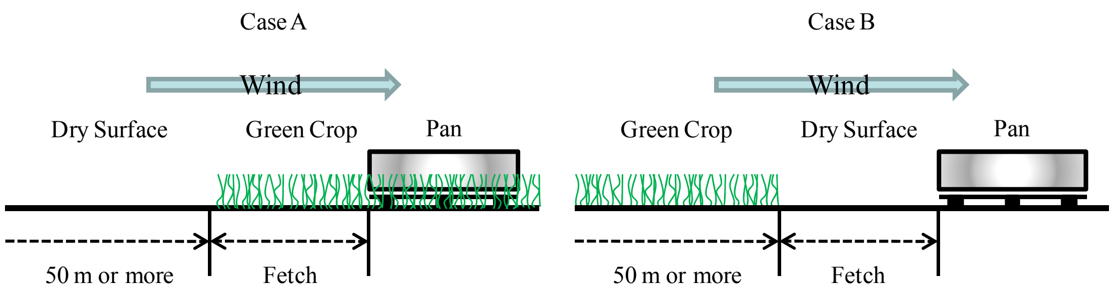

Figure E.1: Two cases of evaporation pan siting and their environment (after Allen et al., 1998)

The respective coefficient can be obtained from Table E.3 taking into account, pan siting with respect to environment and average relative humidity and wind conditions.

Table E.3: Pan coefficient for A-pan for different pan siting and environment and different levels of mean relative humidity and wind speed (after Allen et al., 1998)

Class A pan	Case A: Pan placed in short green cropped area				Case B: Pan placed in dry fallow area			
RH Mean (%) →		Low <40	Medium 40 – 70	High >70		Low <40	Medium 40 – 70	High >70
Wind speed (m s-1)	Windward side distance of green crop (m)				Windward side distance of dry fallow (m)			
Light <2	1	0.55	0.65	0.75	1	0.7	0.8	0.85
	10	0.65	0.75	0.85	10	0.6	0.7	0.8
	100	0.7	0.8	0.85	100	0.55	0.65	0.75
	1000	0.75	0.85	0.85	1000	0.5	0.6	0.7
Moderate 2 – 5	1	0.5	0.6	0.65	1	0.65	0.75	0.8
	10	0.6	0.7	0.75	10	0.55	0.65	0.7
	100	0.65	0.75	0.8	100	0.5	0.6	0.65
	1000	0.7	0.8	0.8	1000	0.45	0.55	0.6
Strong 5 – 8	1	0.45	0.5	0.6	1	0.6	0.65	0.7
	10	0.55	0.6	0.65	10	0.5	0.55	0.65
	100	0.6	0.65	0.7	100	0.45	0.5	0.6
	1000	0.65	0.7	0.75	1000	0.4	0.45	0.55
Very Strong >8	1	0.4	0.45	0.5	1	0.5	0.6	0.65
	10	0.45	0.55	0.6	10	0.45	0.5	0.55
	100	0.5	0.6	0.65	100	0.4	0.45	0.5
	1000	0.55	0.6	0.65	1000	0.35	0.4	0.45

Appendix F: Interpretation of Climatic Data

Site Records

Missing temperature data was interpolated by comparing available temperature data from Mogalakwena to the data obtained from the South African Weather Services station at Mokopane. Figure F.1 shows, as expected due to the sites being in a similar climatic zone, the close relationship between the daily maximum and minimum temperatures for the two sites. Figure F.2 illustrates the linear regression used to predict daily minimum and maximum temperatures for the Mogalakwena site based on the Mokopane data set. 10% of the Mogalakwena data set was in filled in this manner however during the depositions on Dam 2 a complete data set was available.

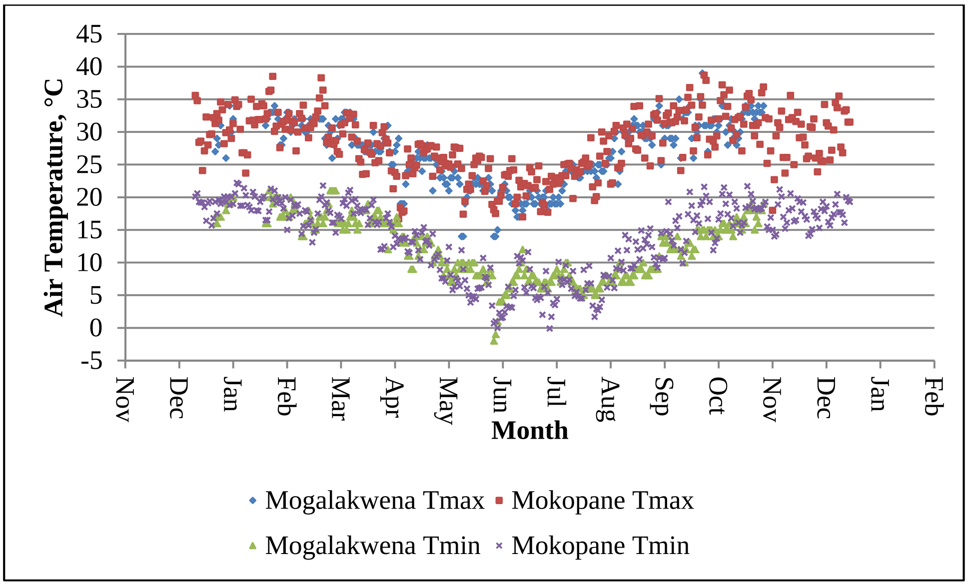

Figure F.1: Comparison of Mogalakwena and Mokopane air temperature data

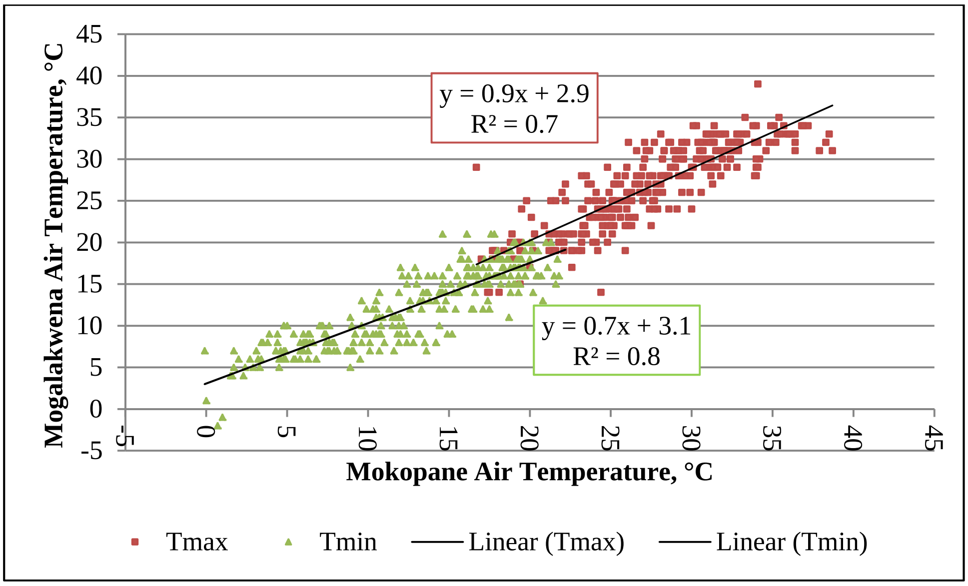

Figure F.2: Air temperature linear regression

South African Weather Service Records

Temperature and relative humidity data was missing for the 20th of April 2010 and therefore a moving average was used to interpolate the missing values. Figure F.3 and Figure F.4 illustrate how the in filled values closely related to the overall trend in values over the interval selected.

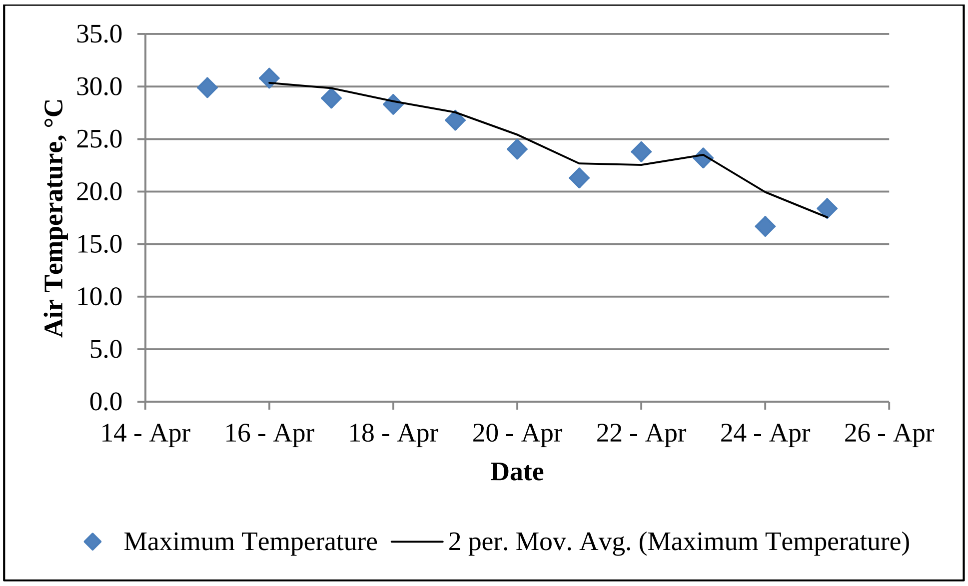

Figure F.3: Interpolation of maximum temperature

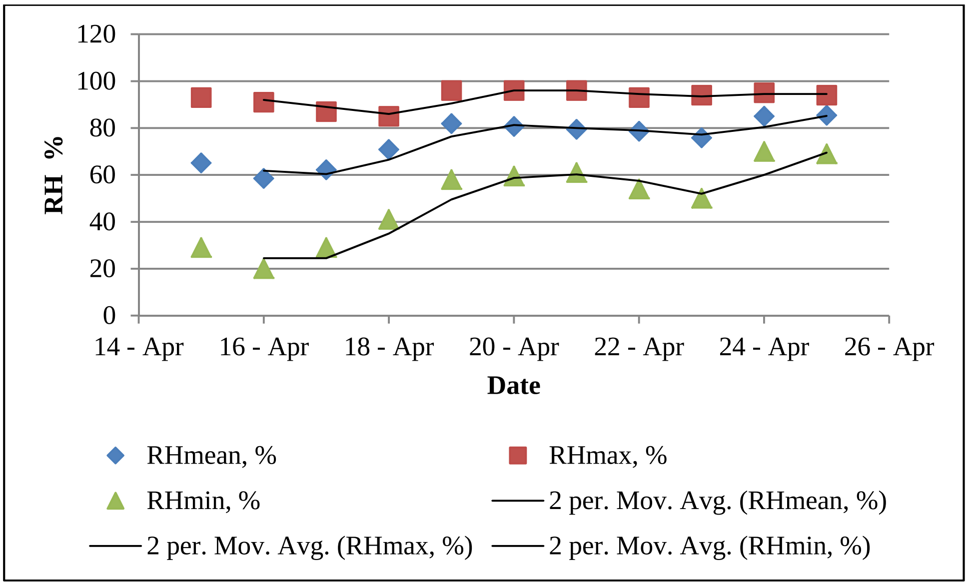

Figure F.4: Interpolation of relative humidity values

Class A-Pan

To operate a Class A-pan correctly the scale must be installed so that 1 unit on the scale should equal 0.5mm evaporation. This means that the scale must be installed at the correct angle. The evaporation pan has a thin vertical plate with a sharp point called the pointer. The purpose of the pointer is to help you install the gauge plate at the correct angle. The distance from the centre of the bolt to the pointer must be 85mm. The pan is then filled up with water up to the pointer. The scale must then be set to the correct slope by adjusting the nuts until you get a water level reading of 138 on the scale. If this is done then your scale is installed at the correct angle and 1 unit on the scale will be equal to 0.5mm evaporation.

Method of calculating the 85mm and the 138 units on the scale:

1 graduation on gauge plate = 3,048mm (On the incline)

1 graduation on gauge plate = 0,5mm evaporation (Vertical)

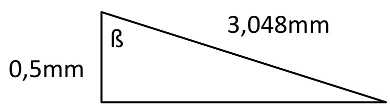

Cos ß = 0.5/3.048 ∴ ß = 80,558°

Refer to Fig. 1:

Sin 80,558° = 22,5/AB ∴AB = 22,809mm

BF = 85 -22,809 ∴BF = 62,191mm

Cos 80,558° = 62,191/BE ∴BE = 379,099mm

Tan 80,558° = 22,5/CB ∴CB = 3,742mm

DE = BE + CB + DC ∴DE = 420,841mm

On scale = 420,841/3,048 = 138,071

∴ Reading on scale when the water is at the level of the pointer should be 138.

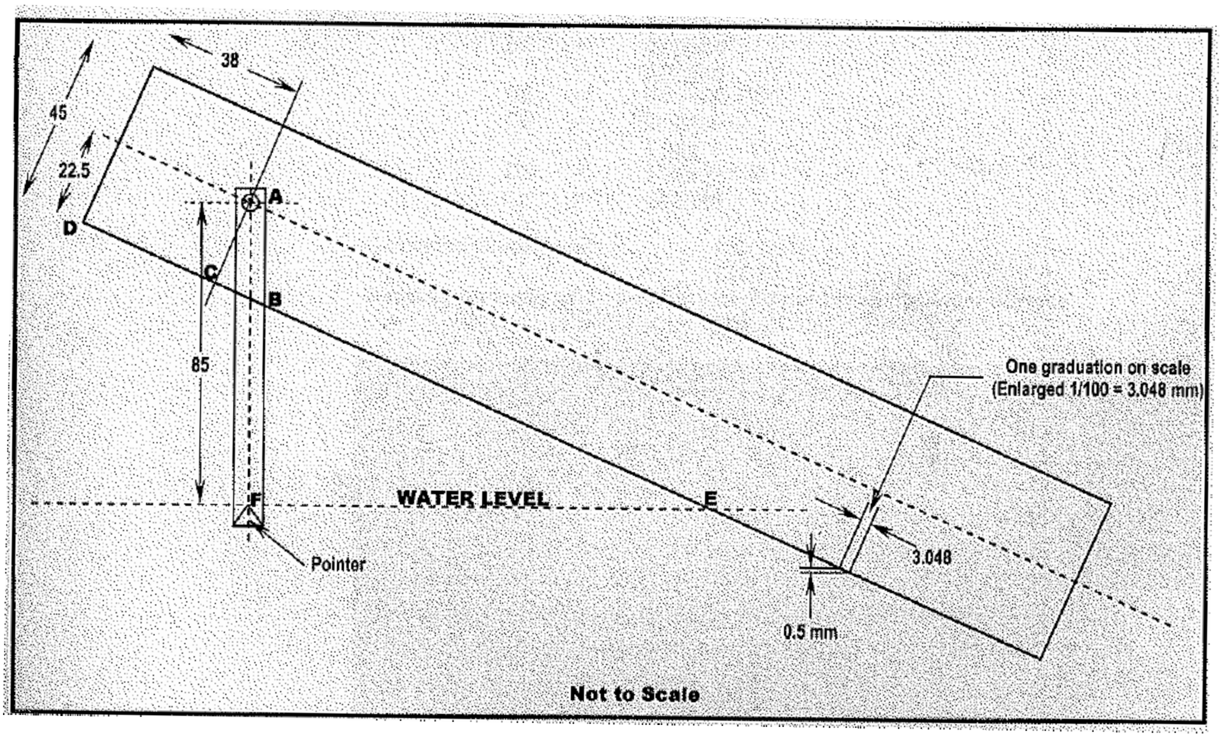

Fig. 1: Illustration sketch of A-Pan Scale.

Class A-Pan used at PPL

It was believed that the evaporation measured at PPL was under estimated. The following was measured afterwards to confirm if the evaporation was in fact under estimated:

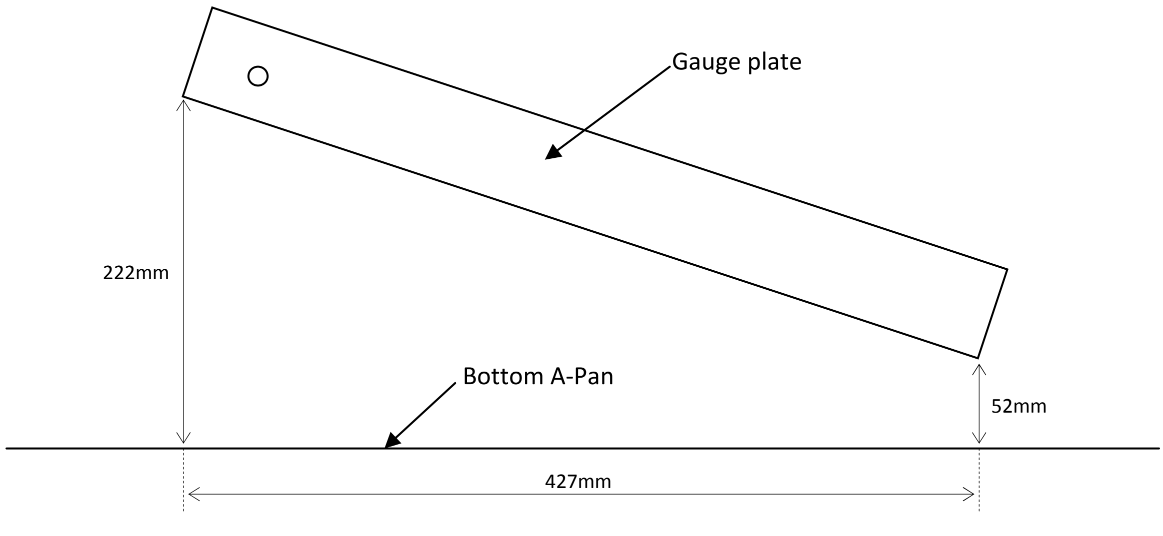

From the measurements the following was calculated:

AC = 222 – 52 = 170mm

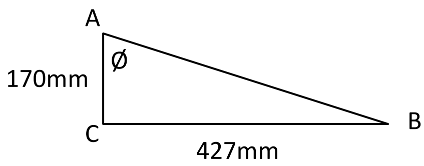

Tan Ø = 427/170 ∴ Ø = 68,291°

Evaporation:

1 graduation on gauge plate = 3,048mm (On the incline)

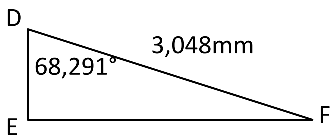

Cos 68,291° = DE/3,048 ∴ DE = 1,127mm

∴ 1 graduation on gauge plate = 1.127mm evaporation (Vertical)

The gauge plate was installed at the wrong angle. The evaporation was underestimated. The readings should have been multiplied by a factor of 1,127 and not 0,5.

Appendix G: Beach Profile Regression

Insurmountable safety obstacles prevented the surveying of the entire beach profile resulting in the need to estimate the last 130 m and 80 m of Dam 1 and Dam 2 respectively. An exponential regression line was plotted through the known data points and used to predict the elevation at the edge of the respective pools.

Figure G.1 below illustrates the incomplete surveyed beach profiles on Dam 1, Figure G.2 shows the regression curve used to predict the elevation at the pool for the second deposition on Dam 1. As a measure of fit the respective r^2 values were calculated and are here summarised in Table G.1. All the r^2 values are larger than 0.9 suggesting that the approximated profiles in Figure G.3 are statistically acceptable.

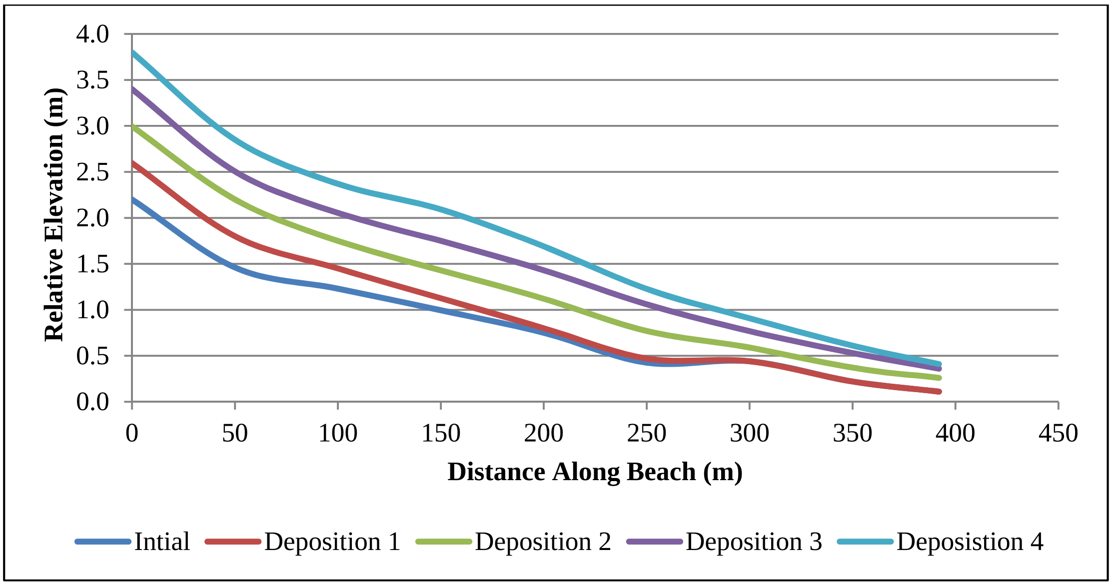

Figure G.1: Dam 1 surveyed beach profile

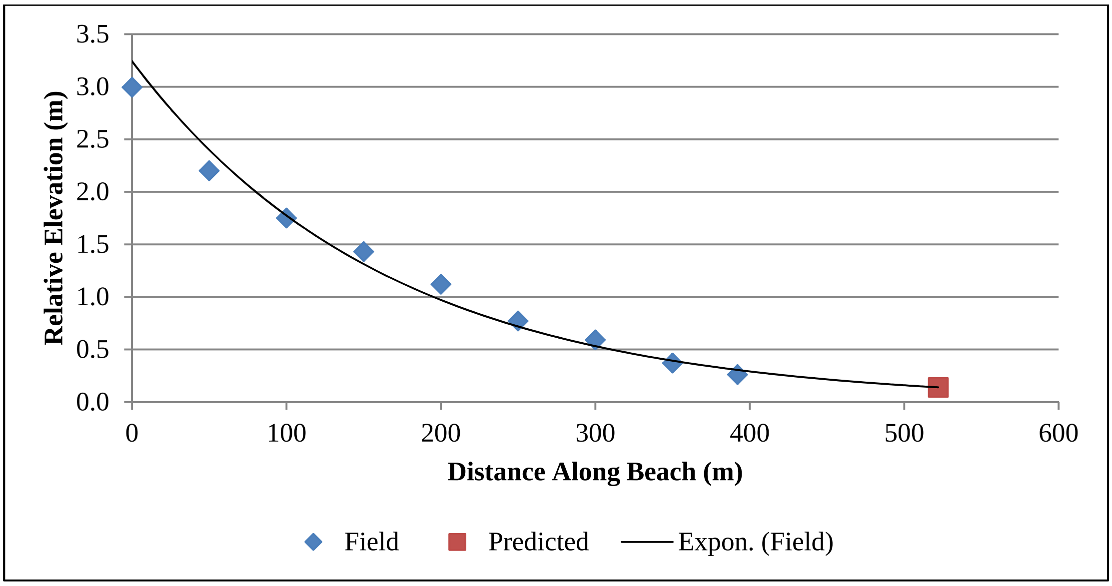

Figure G.2: Illustrative regression for Deposition 2 on Dam 1

Table G.1: Respective Dam 1 r^2 values

	Initial	Deposition 1	Deposition 2	Deposition 3	Deposition 4	Average
r^2	0.95	0.96	0.98	0.98	0.97	0.97

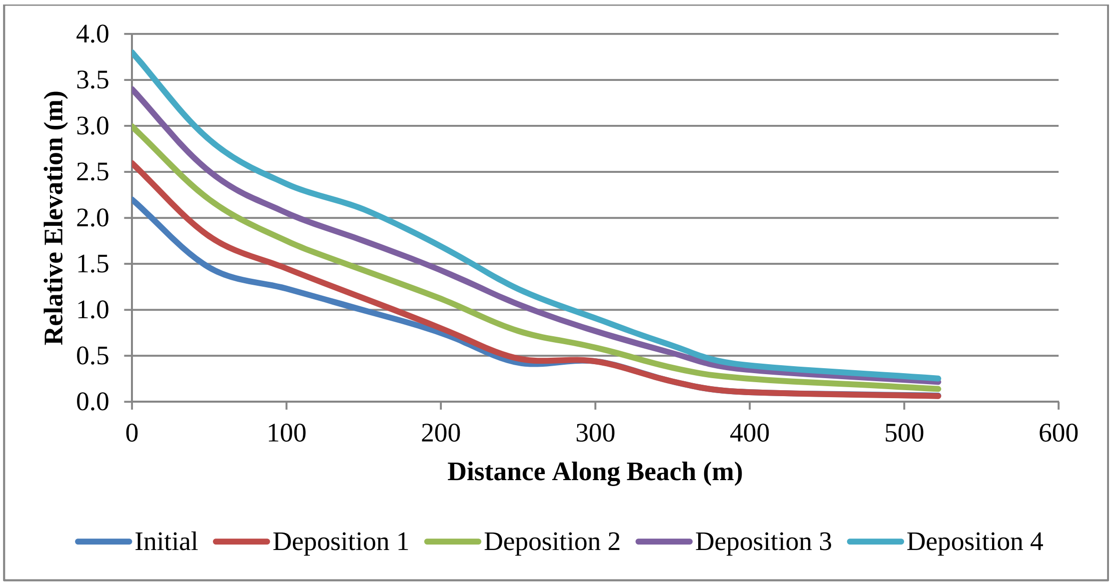

Figure G.3: Approximated Dam 1 beach profiles

Figure G.4 below illustrates the incomplete surveyed beach profiles on Dam 1, Figure G.5 shows the regression curve used to predict the elevation at the pool for the first deposition on Dam 2. As a measure of fit the respective r^2 values were calculated and are here summarised in Table G.2. All the r^2 values are larger than 0.9 suggesting that the approximated profiles in Figure G.6 are statistically acceptable.

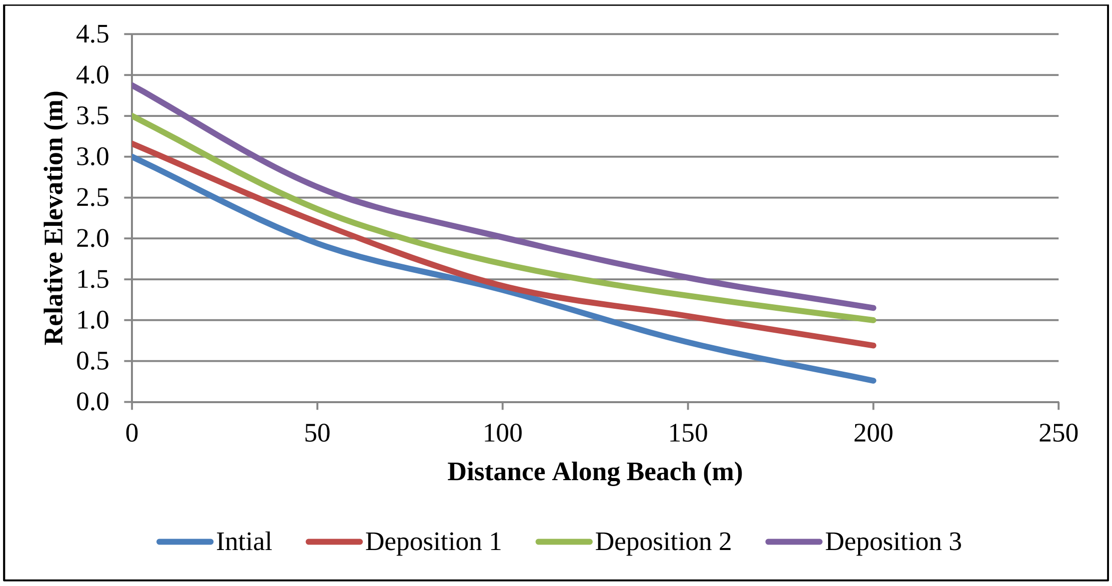

Figure G.4: Dam 2 surveyed beach profile

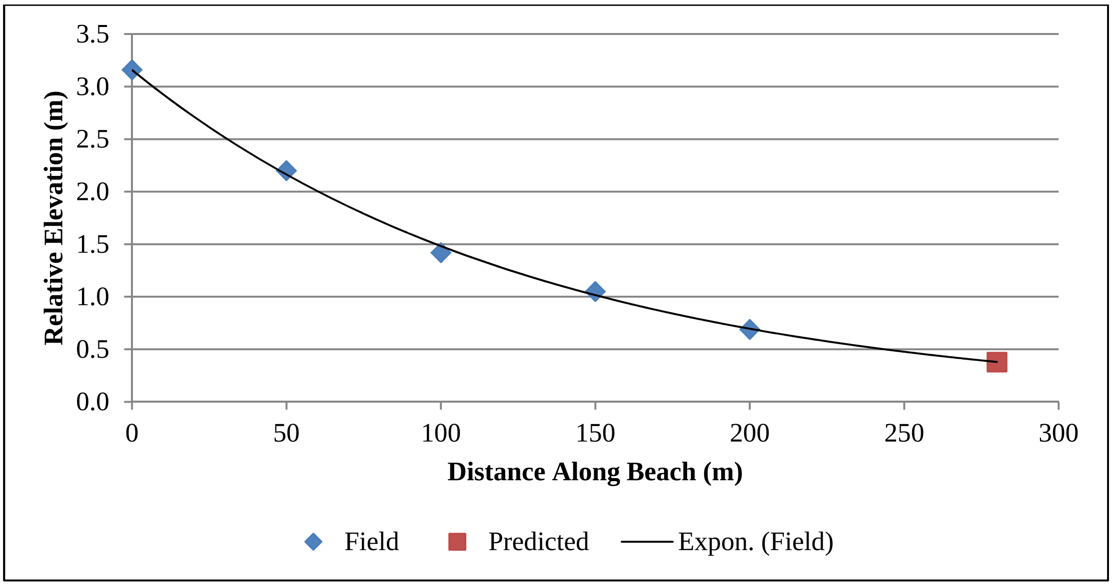

Figure G.5: Illustrative regression for Deposition 1 on Dam 2

Table G.2: Respective Dam 2 r^2 values

	Initial	Deposition 1	Deposition 2	Deposition 3	Average
r^2	0.95	1.00	0.99	0.99	0.98

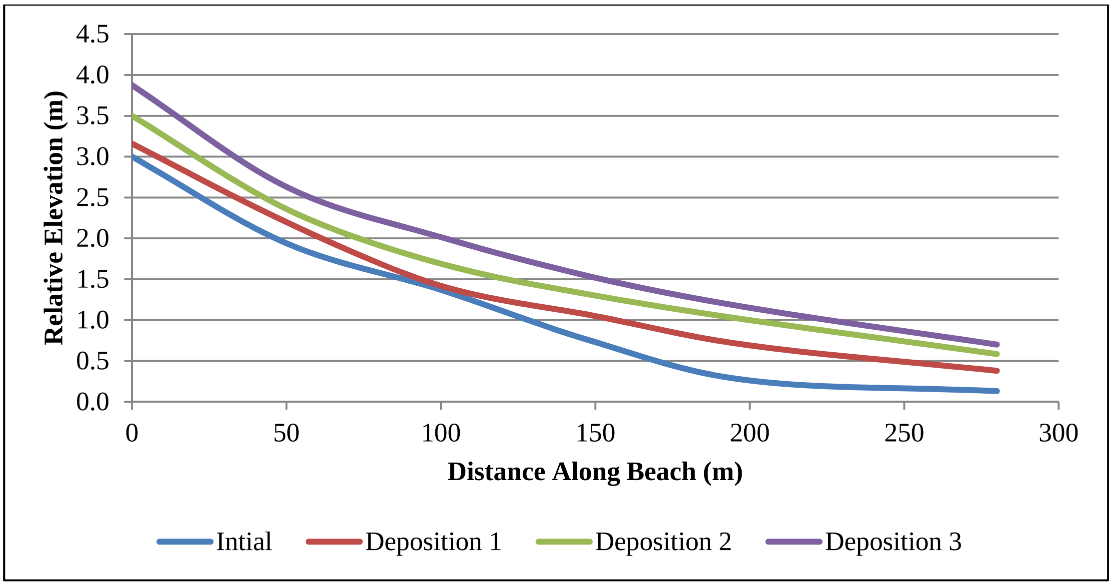

Figure G.6: Approximated Dam 2 beach profiles

Appendix H: Drying Iterative Regression Methodology

An iterative regression model was used to analyse the raw water contents determined from plant slurry densities, grab samples, and auger samples. Figure H.1 illustrates a sample data set for the first deposition at the head of the Dam 2 beach.

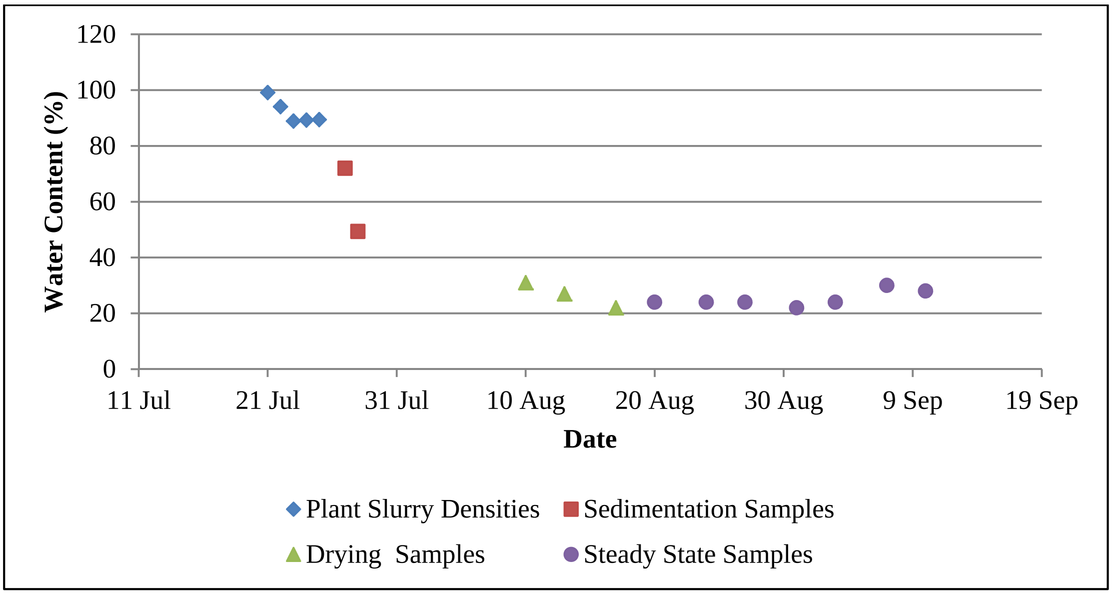

Figure H.1: Raw Data

Moisture loss due to sedimentation was determined from plant tails data and grab samples taken on the two days following cessation of deposition. Gravimetric water contents were determined from the grab samples. To account for the variation in slurry density over the deposition period the three quartile values of slurry water content were assumed to be the range of water contents during the final day of deposition. Figure H.2 below illustrates the five sets of sedimentation values used to determine the rate of sedimentation for the first deposition.

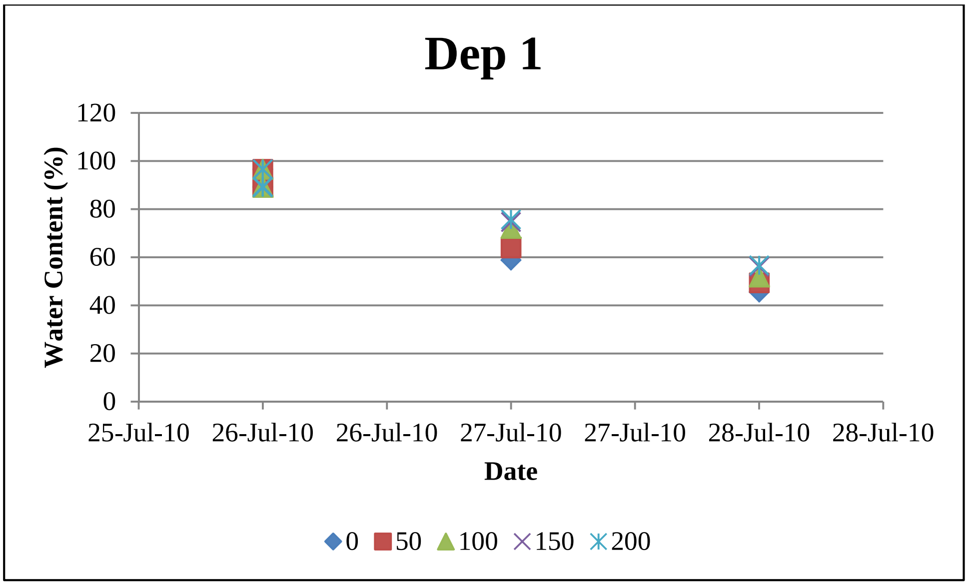

Figure H.2: Deposition 1 Sedimentation trend along Beach

Due to supernatant water flowing along the beach the rate of sedimentation decreases towards the pool. Figure H.3 below illustrates this trend along the beach clearly for Depositions 1 and 3; however the trend is not exhibited clearly by Deposition 2. A linear regression was plotted through the data to determine the sedimentation rate at each sampling point along the beach.

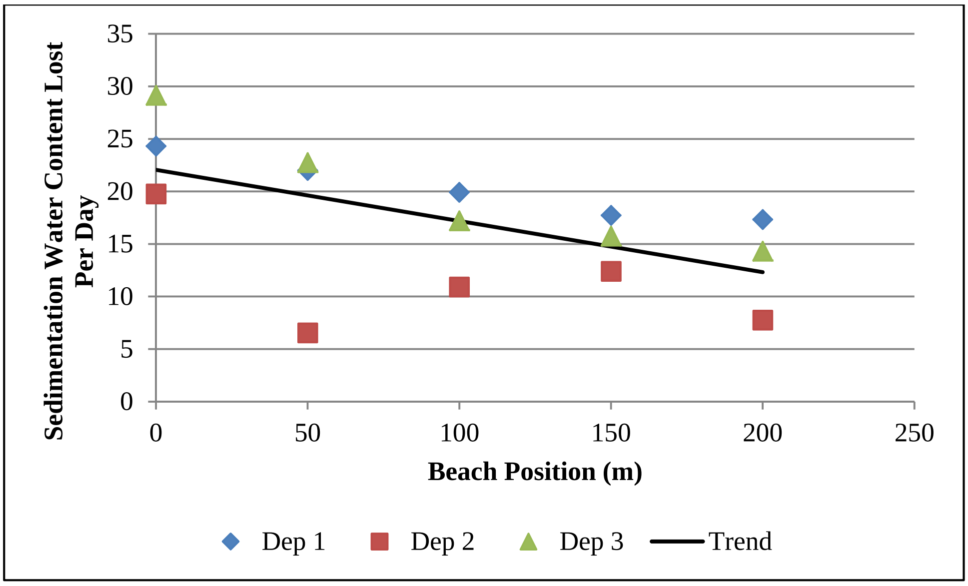

Figure H.3: Rate of Sedimentation along Beach

Figure H.4 illustrates the next iterative step which intersected two linear regressions through the first three surface auger water contents and the respective sedimentation curve from the previous step. This was to predict the range in final water contents after sedimentation shown in Table H.1.

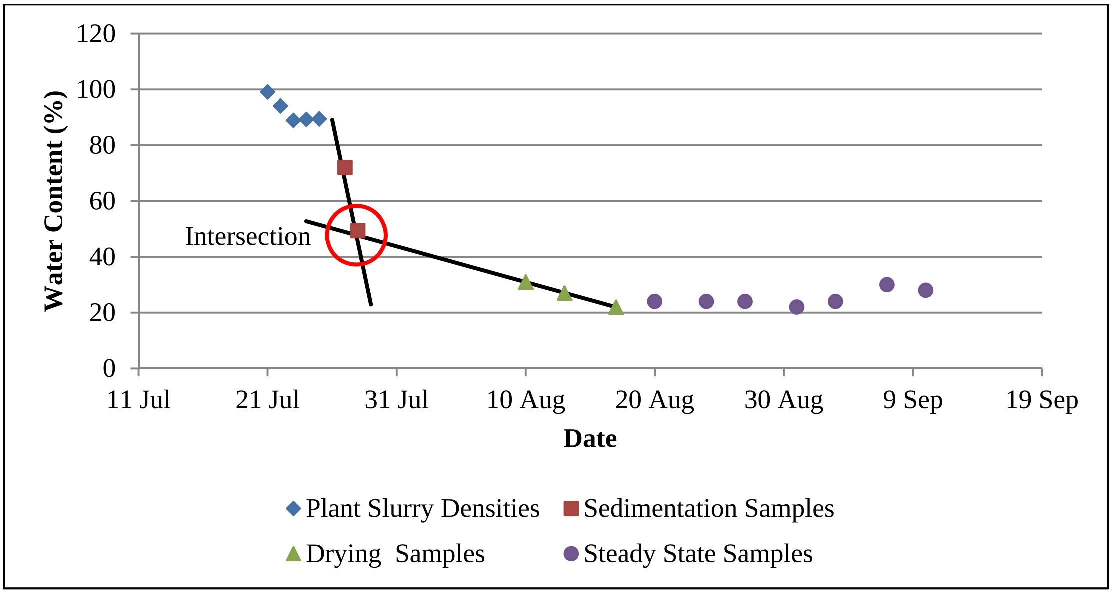

Figure H.4: Drying Iterative Step 1

Table H.1: Settled Water Contents for all Depositions

	Settled Water Content (%)
Upper Quartile	36.95
Median	42.65
Lower Quartile	46.81

Linear regression was carried out on the post evaporation surface water contents and the p-value of the slope was found to be greater than 0.05 in all cases. As such the steady state water content was assumed to be the linear trend of averages, at each sampling position, along the beach. Figure H.5 illustrates the steady state water content values used in the next iterative step to determine the number of days to reach the steady state water content. A linear regression through the quartile settled water contents and the first three surface auger water contents was intersected with the steady state water content as illustrated in Figure H.6. The number of days to reach this was plotted against beach position. Figure H.7 illustrates the trend in drying days along the beach for the first deposition. Although it appears that the drying period increased towards the pool it must be kept in mind that the final water content also increased towards the pool.

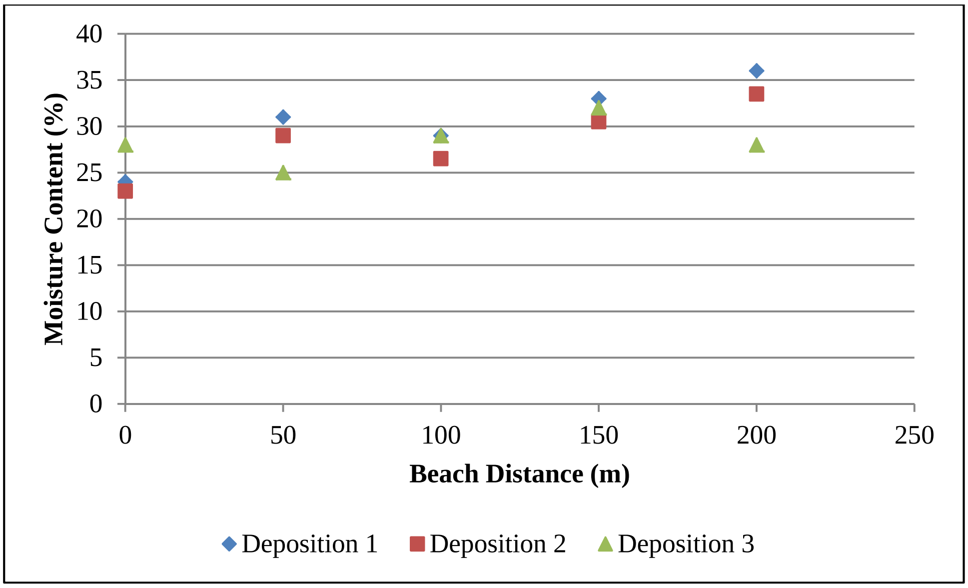

Figure H.5: Steady State Water Contents

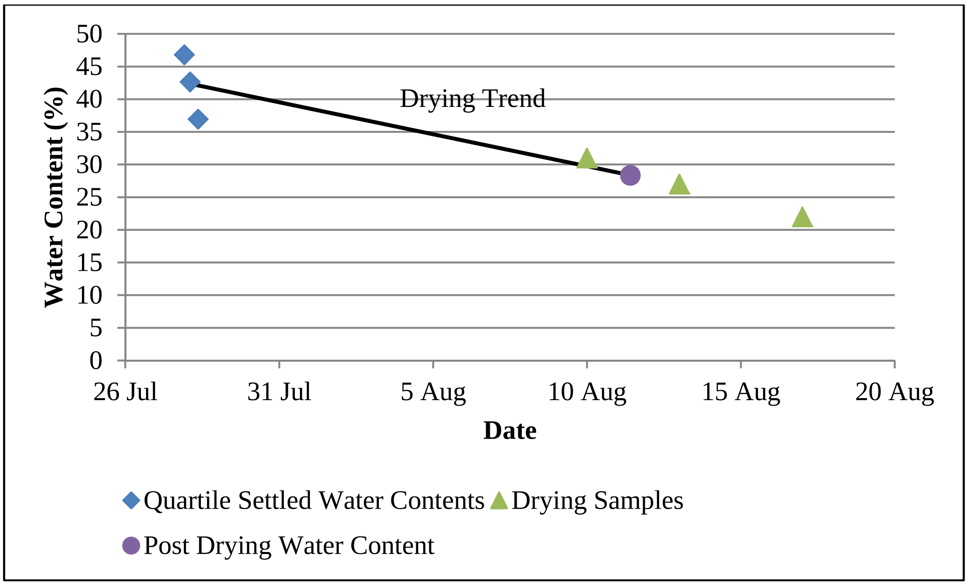

Figure H.6: Determination of Drying Period

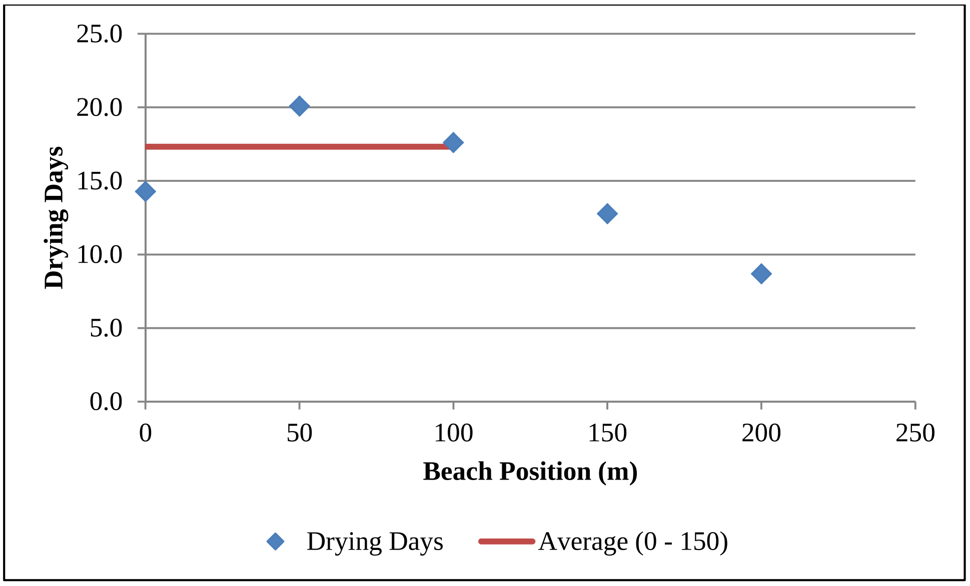

Figure H.7: Drying Period trend for Deposition 1

The final iteration determined the linear regression curve through the sedimentation and drying stages, by using both the predicted values from the previous two steps and the actual values. Figure H.8 illustrates the predicted lines for the sampling position at the head of the beach following the first deposition.

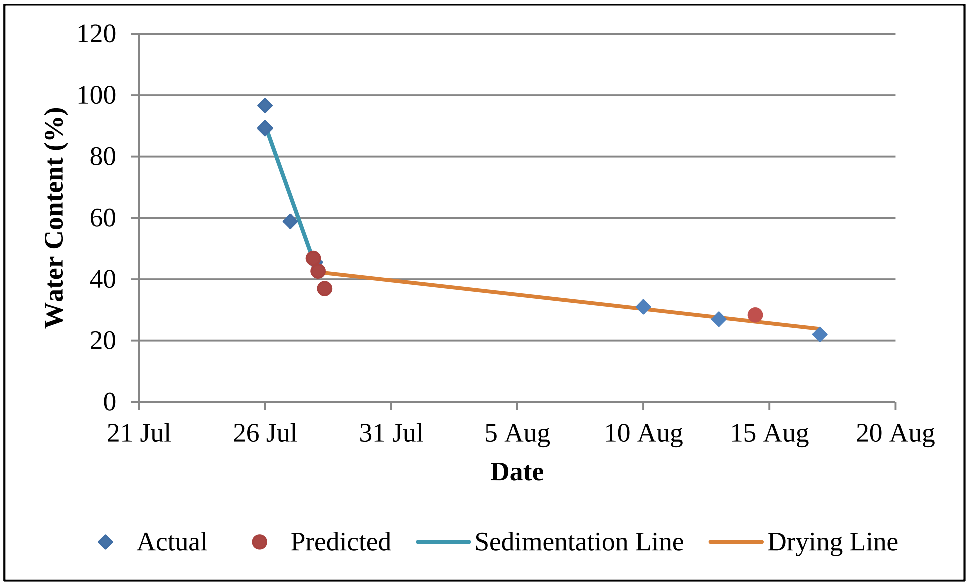

Figure H.8: Final Sedimentation and Drying Lines

Figure H.9 below illustrates the fitted model to the raw data presented in Figure H.1.

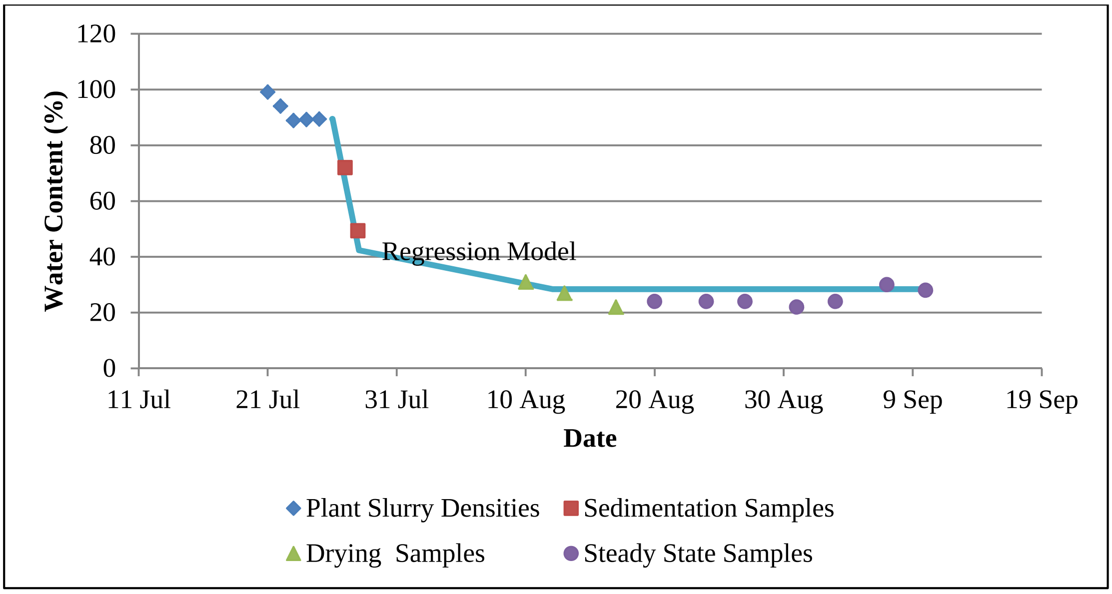

Figure H.9: Raw Data fitted with Regression Model